UNIVERSITY of CALIFORNIA
Santa Barbara

Pursuit Strategies for Autonomous Vehicles

A Dissertation submitted in partial satisfaction of the
requirements for the degree

Doctor of Philosophy
in
Mechanical Engineering

by

Shaunak Dattaprasad Bopardikar

Committee in charge:

Professor Francesco Bullo, Co-chair
Professor João P. Hespanha, Co-chair
Professor Bassam Bamieh
Professor Jeffrey Moehlis

March 2010

The dissertation of Shaunak Dattaprasad Bopardikar is approved.

Professor Bassam Bamieh

Professor Jeffrey Moehlis

Professor João P. Hespanha, Committee Co-chair

Professor Francesco Bullo, Committee Co-Chair

September 2009

Pursuit Strategies for Autonomous Vehicles

by

Shaunak Dattaprasad Bopardikar

To, my family

Acknowledgements

I consider myself really fortunate to have had the opportunity to do research under the joint tutelage of Prof. Francesco Bullo and Prof. João P. Hespanha. I would like to express my deepest words of gratitude to them for being mentors *par excellence*. I would also like to offer my thanks to Prof. Bassam Bamieh and Prof. Jeffrey Moehlis for having served as members of my doctoral committee. I would also like to thank the Mechanical Engineering and Electrical Engineering Departments' staff at UC Santa Barbara for their help from time to time.

I would like to thank Dr. Jacob and Dr. Joseph Yadegar, Dr. Anurag Ganguli and other co-workers of UtopiaCompression Corporation, Los Angeles for presenting to me a taste of industrial research in the form of an internship in the summer of 2008. I am thankful to all of the past and present members of Prof. Bullo and Prof. Hespanha's research groups for numerous insightful discussions. Special thanks go to Dr. Stephen L. Smith for a wonderful joint work.

I am very grateful to all my teachers for their guidance throughout this academic journey. I would like to acknowledge the support of numerous friends, past housemates and the Indian community in Goleta for making my stay memorable. Finally and most importantly, I am thankful to my family and relatives for their support, sacrifices and love bestowed upon me all this while.

Curriculum Vitæ

Shaunak Dattaprasad Bopardikar

Education

07/1999 – 08/2004 Dual Degree (Bachelor and Master of Technology) in Mechanical Engineering with Computer-Aided-Design and Automation, Indian Institute of Technology, Bombay

Experience

06/2008 – 08/2008 Summer Intern, UtopiaCompression Corporation, Los Angeles, CA, USA.

08/2004 – 05/2005 Engineer, General Electric India Technology Center, Bangalore, India.

Selected Publications

S. D. Bopardikar, F. Bullo and J. P. Hespanha, "On Discrete-time Pursuit-evasion Games with Sensing Limitations", in *IEEE Transactions on Robotics*, 24 (6), 2008.

S. D. Bopardikar, F. Bullo and J. P. Hespanha, "A cooperative Homicidal Chauffeur game", in *Automatica*, 45 (7), 2009.

S. D. Bopardikar, S. L. Smith, F. Bullo and J. P. Hespanha, "Dynamic vehicle routing for translating demands: Stability analysis and receding-horizon policies", To appear in the *IEEE Transactions on Automatic Control*, 2010. Note: (Submitted March 2009).

Abstract

Pursuit Strategies for Autonomous Vehicles

by

Shaunak Dattaprasad Bopardikar

Surveillance and continuous monitoring of the environment to provide security and protection against malicious mobile adversaries has attained utmost significance ever since ancient times. Assigning humans this task runs the risk of fatigue due to monotony and deception of the human. Recent growth in autonomous vehicle technology demonstrates tremendous potential worthy of delegation of these monotonous yet critical tasks. This assignment requires design of strategies, or a set of motion laws for these mobile autonomous vehicles that are both effective and efficient in mitigating adversarial threats, with provable correctness as a certificate of guarantee.

This thesis addresses design of strategies for one or many autonomous vehicles to pursue one or many targets via two prototype scenarios. The first scenario involves a single adversary and we design provably effective pursuit strategies under constraints on sensing as well as motion of the vehicles. Our approach towards the design of pursuer formations and the strategies has been partly inspired by ecological studies in predation. The second scenario involves multiple targets that sequentially arrive in a region and have predictable motion. We design provably efficient strategies and placements for the pursuing vehicles to reach them all. We borrow ideas from geometry, probability theory and stochastic processes, estimation and localization, combinatorial and receding-horizon optimization and convex analysis to establish our results.

Contents

List of Figures

Chapter 1

Introduction

Imagine going back in time to your childhood days, when games such as hide-and-seek or tag were a part of every evening's play. When you were the seeker, you surely would have designed ingenious ways to seek out your hiding friends. Or when you were the person wishing to tag your friend, then quick calculations would be running through your mind as to how to progressively advance towards your evading opponent. Unknowingly, you would have also established some "theorems", such as the faster you can move than your opponent, the quicker you would be tagging him or her. Designing pursuit strategies is not much different from these familiar childhood games, except that there is an increase in the level of complexity of the calculations.

Technological advances have led to the development of mobile robots that are equipped with high-precision sensors and computational resources to enable them to perform complex missions. One such complex mission for these robots is to detect, track and get close to or capture, one or many adversarial mobile robots. From the security point of view, there is a need to design effective as well as efficient strategies for the detecting robot(s) to capture the adversary. Although these missions arise primarily in surveillance applications such as border protection and security, these methods can be applied to civilian tasks such as search-and-rescue operations or towards collision avoidance among vehicles, and also in video games. Strategies to pursue targets moving in fixed directions and with fixed speed find industrial applications in robotic pick-and-place operations.

1.1 Pursuit Problems: A Brief History

The problems addressed in this thesis fall into the category of Pursuit-evasion which belong to the classic Theory of Games. A typical pursuit-evasion formulation is as follows [8]: given a system that is controlled by one or many pursuers and one or many evaders, a target set to which the system needs to be steered, determine the controls that the pursuers need to apply in order to steer the system to the target set in minimum time. Games of this type are known in the literature as *games of degree*. A classic method to solve these games, i.e., obtain the optimal controls for the pursuers and the evaders, is to solve the Hamilton-Jacobi-Bellman-Isaacs (HJBI) equation, which is a partial differential equation in the state variables and time. In general, for a non-linear system model and with constraints on the control inputs, the HJBI equation is difficult to solve in closed-form. Recently, [62] has presented an iterative approach based on limited look-ahead and successive improvements of a sub-optimal solution to determine optimal controls in multi-pursuer and evader problems. Additionally, numerous techniques to approximate the solutions to the HJBI equations have been proposed in [68, 9, 44] to cite a few. A computational approach based on evolution of forward reachability sets has been proposed in [30].

Another class of pursuit-evasion games that address the fundamental question of whether the target set can be reached are *games of kind*. These are games in which the goal is to design controls for the pursuers that ensure that capture takes place in finite time, as opposed to minimum time. A folklore game of kind is the classic Lion and Man problem posed as follows.

A lion and a man in a closed arena have equal maximum speeds. What tactics should the lion employ to be sure of his meal?

This problem was proposed by Rado and formally in [64]. For the case of capture with zero radius, it was shown that the man can avoid getting captured. However, for finite non-zero capture distance, [88] and more recently, [4] have presented lion strategies that lead to capture for a class of environments and from a set of favorable initial locations. Another classic pursuit game is the Homicidal Chauffeur game in which a faster pursuer that is constrained to move on trajectories with bounded curvature seeks to capture a slower evader which has simple motion [51].

When the environment in which the game is being played is complex, e.g., non-convex, a traditional method is to discretize the environment into simpler regions. Each simple region is a node of an underlying graph and we connect two nodes whenever two simple regions are neighbors. This approach was introduced in [76], and deterministic pursuit strategies were proposed in [2]. More recently, randomized strategies, where the solution is a probability distribution over a set of deterministic strategies have been addressed in [1, 52, 53, 98]. When there exist sensing constraints on the pursuers, the problem becomes related to optimal search [95, 6]. Another formulation in this context is *visibility-based pursuit-evasion* [97, 46], wherein the pursuers are assumed to be equipped with visibility (line-of-sight) sensors and the goal is to detect arbitrarily fast moving evaders.

1.2 Multiple Targets and Vehicle Routing

In this thesis, we also address the case in which there are multiple targets, slower than a pursuer. Treating this scenario as a game of degree tells us that in some finite time, which can be computed as a function of the initial distances, the pursuer captures all of the targets. The more challenging version of this problem is, in what order should the pursuer capture the targets so that the time taken to capture all of them is minimized? This is a difficult problem, belonging to the class of NP-hard problems in combinatorial optimization [58]. The NP-hard class of problems are those for which there does not exist any algorithm that can solve them with time complexity that grows at most as a polynomial in the size of the problem, which in our case is the number of targets.

However, if the motion of the targets has a certain structure, then one can design efficient algorithms to determine the order of capture. For example, if the targets are assumed to be translating, i.e., move with fixed speed in a given direction, then one can design an approximation scheme to determine the optimal sequence in which the targets much be captured [47].

If the targets were to arrive sequentially via a stochastic process in a region, and if they were to have predictable motion, then this problem amounts to a version of the dynamic vehicle routing problem. Vehicle routing refers to planning optimal vehicle routes for providing service to a given set of customers. In contrast, Dynamic Vehicle Routing (DVR) considers scenarios in which not all customer information is known *a priori*, and thus routes must be re-planned as new customer information becomes available. An early DVR problem is the Dynamic Traveling Repairperson Problem (DTRP) [13], in which customers, or demands arrive sequentially in a region and a service vehicle seeks to serve them by reaching each demand location. In [13], the authors propose a policy that is optimal in the case of low arrival rate, and several policies within a constant factor of the optimal in the case of high arrival rate. In [14], they also study multiple service vehicles, and vehicles with finite service capacity. In [75], a single policy is proposed which is optimal for the case of low arrival rate and performs within a constant factor of the best known policy for the case of high arrival rate. Recently, there has been an upswing in versions of DVR such as in [93] where different classes of demands have been considered; and in [78] which addresses the case of demand impatience. In [79], decentralized policies are developed for the multiple service vehicle versions, and in [92], a dynamic team-forming variation of the Dynamic Traveling Repairperson problem is addressed.

Vehicle routing with objects moving on straight lines was introduced in [29], in which a fixed number of objects move in the negative y direction with fixed speed, and the motion of the service vehicle is constrained to be parallel to either the x or the y axis. For a version of this problem wherein the vehicle has arbitrary motion, termed as the translational Traveling Salesperson Problem, a polynomial-time approximation scheme has been proposed in [47] to catch all objects in minimum time. Another variation of this problem with object motion on piece-wise straight line paths, and with different but finite object speeds has been addressed in [7]. Other variants of the Euclidean Traveling Salesperson Problem in which the points are allowed to move in different directions have been addressed in [48].

1.3 Statement of Contributions

In this thesis, we develop strategies, i.e., a set of rules for one or many vehicles termed as pursuers in order to capture one or many targets. We consider two types of target motions, which divides this thesis into two parts. In the first part, we assume that there is a single evading target and it moves adversarially, to avoid getting captured. We address pursuit games of kind under challenges such as limited sensing abilities and motion constraints. We follow an algorithmic approach in which the pursuers are specified what action to take under different conditions. For multiple pursuer problems, the design of the pursuer formations are inspired from formations observed in ecology. The distinguishing feature of this thesis is the characterization of conditions on the problem parameters under which our strategies provide guaranteed capture. We exploit geometry in the problem and our analysis techniques rely on showing that under certain favorable conditions, an appropriate cost function such as the distance between the pursuers and the evader decreases to the capture distance.

In the second part, we address the case when targets appear via a spatio-temporal stochastic process and upon arrival, move in a fixed direction with fixed speed. In this setting, we address problems such as where should one place the vehicles so that the average time taken to capture a target when it arrives is minimized?; and if the targets arrive at a high rate, what strategies should a pursuer follow so that the average number of targets in the environment does not grow unbounded? We use elements of convex analysis, stochastic processes and receding-horizon optimization in our analysis.

More specifically, the following are the contributions of this thesis:

Chapter 2 – Strategies under Sensing Limitations: We address discrete-time pursuit-evasion games in the plane where every player has identical sensing and motion ranges restricted to closed discs of given sensing and stepping radii. A single evader is initially located inside a bounded subset of the environment and does not move until detected. We propose a *Sweep-Pursuit-Capture* pursuer strategy to capture the evader and apply it to two variants of the game: the first involves a single pursuer and an evader in a bounded convex environment and the second involves multiple pursuers and an evader in a boundaryless environment. In the first game, we give a sufficient condition on the ratio of sensing to stepping radius of the players that guarantees capture. In the second, we determine the minimum probability of capture, which is a function of a novel pursuer formation and independent of the initial evader location. The Sweep and Pursuit phases reduce both games to previously-studied problems with unlimited range sensing, and capture is achieved using available strategies. We obtain novel upper bounds on the capture time and present simulation studies that address the performance of the strategies under sensing errors, different ratios of sensing to stepping radius, greater evader speed and different number of pursuers.

The work in this chapter is based on the journal article [19] and the conference articles [18] and [17].

Chapter 3 – Pursuit with Minimal Sensing Information: We address problems on pursuit using minimal information from the measurements. Based on the established *Grow-Intersect* estimation algorithm, we design pursuit strategies for (i) range-based sensing and (ii) bearing sensing formulations. For both formulations, we show that if the speed ratio of the evader to the pursuer is less than a certain threshold, then from any initial location, the pursuer can reduce the distance to the evader to a specified non-zero distance in finite time. Due to minimal information about the evader's location, at every instant, either the localization error increases but with reduction in the distance, or the localization error can be reduced but at the cost of increasing the distance to the evader. The central theme in the analysis of these problems is that at every alternate time instant, the distance to the evader strictly decreases if the speed ratio is less than a certain threshold.

The work in this chapter is based on the conference article [20].

Chapter 4 – Strategies under Motion Constraints: We address a pursuit-evasion problem involving an unbounded planar environment, a single evader and multiple pursuers moving along curves of bounded curvature. The problem amounts to a multi-agent version of the classic Homicidal Chauffeur problem; we identify parameter ranges in which a single pursuer is not sufficient to guarantee evader capture. We propose a novel multi-phase cooperative strategy in which the pursuers move in specific formations and confine the evader to a bounded region. The proposed strategy is inspired by hunting and foraging behaviors of various fish species. We characterize the required number of pursuers for which our strategy is guaranteed to lead to confinement.

The work in this chapter is based on the journal article [21] and the conference article [16].

Chapter 5 – Pursuing Sequentially-arriving and Translating Targets: We introduce a problem in which targets (or demands) arrive stochastically on a line segment, and upon arrival, move with a fixed velocity perpendicular to the segment. We design a receding horizon service policy for a pursuer, which is a simple vehicle with speed greater than that of the demands, based on the translational minimum Hamiltonian path (TMHP). We consider Poisson demand arrivals, uniformly distributed along the segment. For a fixed segment width and fixed vehicle speed, the problem is governed by two parameters; the demand speed and the arrival rate. We establish a necessary condition on the arrival rate in terms of the demand speed for the existence of any stabilizing policy. We derive a sufficient condition on the arrival rate in terms of the demand speed that ensures stability of the TMHP-based policy. When the demand speed tends to the vehicle speed, every stabilizing policy must service the demands in the first-come-first-served (FCFS) order; and of all such policies, the TMHP-based policy minimizes the expected time before a demand is serviced. When the demand speed tends to zero, the sufficient condition on the arrival rate for stability of the TMHP-based policy is within a constant factor of the necessary condition for stability of any policy. Finally, when the arrival rate tends to zero for a fixed demand speed, the TMHP-based policy minimizes the expected time before a demand is serviced. We numerically validate our analysis and empirically characterize the region in the parameter space for which the TMHP-based policy is stable.

The work in this chapter is based on the journal article [24] and the conference articles [23] and [91].

Chapter 6 – Vehicle Placement to Intercept Moving Targets: We address the problem of pursuing sequentially-arriving and translating targets posed above. We now consider the case when the arrival rate tends to zero, and the targets arrive as per a specified spatial probability density function on the line segment. We address the problem of optimally placing vehicles having simple motion in order to intercept a mobile target that arrives stochastically on a line segment. The optimality of vehicle placement is measured through a cost function, associated with intercepting the target. We consider both single and multiple vehicle scenarios. For the single vehicle case, we assume that the target either moves with fixed speed and in fixed direction or it moves to maximize the vertical height or intercept time. We show that each of the corresponding cost functions are convex, have smooth gradients and have unique minimizing locations, and so the optimal vehicle placement is obtained by any standard gradient-based optimization technique. For the multiple vehicle case, we assume that the target moves with fixed speed and in fixed direction. We present a partitioning and gradient-based algorithm in discrete time and we characterize conditions under which this algorithm asymptotically leads the vehicles to a set of critical configurations of the cost function.

The work in this chapter is based on the conference article [22].

1.4 Organization of this Thesis

This thesis is divided into two parts. Problems on pursuit and evasion are addressed in Chapters 2, 3 and 4. Chapter 2 considers pursuit-evasion games in which the evader and one or more pursuers have a limited range sensing ability. Chapter 3 considers pursuit problems that require minimalist sensing abilities for the pursuer. Chapter 4 addresses a pursuit problem in which multiple motion-constrained pursuers try to encircle a single slower-but-agile evader.

The second part of this thesis addresses a problem on designing pursuit strategies to efficiently capture multiple sequentially-arriving and translating targets. This problem is introduced and analyzed in Chapter 5. An extension of this problem that addresses vehicle placement is presented in Chapter 6. Finally, conclusions and future directions for this work are presented in Chapter 7.

Part I: Adversarial Target

Chapter 2

Pursuit under Sensing Limitations

2.1 Introduction

In this chapter, we study discrete-time pursuit-evasion games in which there are one or many pursuers and a single evader. Each player has identical speeds and sensing ability which is restricted to a disc, i.e., a pursuer can detect an evader perfectly and vice-versa only if the two are within a specified distance of each other. Our set-up is one of discrete-time-alternate-moves - the evader and the pursuer(s) move alternately with discrete steps. In this formulation, capture implies that the evader and the pursuer (some pursuer) meet at the same location after a finite time. This formulation is therefore equivalent to the continuous time formulation with capture within a non-zero radius.

Relevant Literature

Continuous time versions been studied in [50, 63, 72] to cite a few. Recently, discrete-time versions of the game has received significant attention. [88] has derived sufficient conditions and a strategy for a single pursuer to capture an evader in a semiopen environment. This strategy has been extended in [57] to the case of multiple pursuers in an unbounded environment, to capture a single evader which is inside their convex hull. [5] and [3] propose strategies so that the pursuer can reduce the distance between itself and the evader to a finite, non-zero amount after finite time steps. The game has also been studied in different types of bounded environments, e.g., circular environment [5], curved environments [61]. Visibility-based pursuit evasion has been studied in [46, 15] and in polygonal environments [52].

In the context of sensing limitations, in continuous time formulations, [40] deals with a version of visibility limited to an angle, instead of the entire region. [89] considers a successive pursuit of multiple evaders by a single faster pursuer in the plane with sensing range limited to a finite disc. [54] addresses the version of the Lion and Man problem in [88] for the case when the pursuer is equipped with a sensor that measures only the bearing angle (heading) of the evader's location with respect to the pursuer. [27] proposes a multi-phase pursuit strategy for groups of pursuers with limited range sensing and has demonstrated its capture properties in bounded environments via simulation without formal proof. In discrete time formulations, [53] considers the problem on a graph, with the visibility of the pursuer limited to nodes adjacent to the current node of a pursuer. A framework which uses probabilistic models for sensing devices for the agents is described in [49] and [100].

Contributions

We address the case of limited range sensing capability: a pursuer and an evader can sense each other only if the distance between them is less than or equal to a given sensing radius. We consider the discrete-time version with one or many pursuers and a single evader in a planar environment. The motion of each player is constrained to a stepping disc around it. The evader is initially located inside a bounded subset of the environment, which we term as the *field*. The players can leave the field but not the environment. The evader follows a *reactive rabbit* model, i.e., does not move until it senses a pursuer [53]. We present an algorithmic approach in the form of a *Sweep-Pursuit-Capture* strategy for the pursuer to capture the evader. We demonstrate this strategy using two variants of the pursuit-evasion game: the first involves a single pursuer and the evader in a bounded convex environment while the second considers multiple cooperating pursuers to capture the evader in a boundaryless environment.

In the first game, the pursuer *sweeps* the environment in a definite path until the evader is sensed, which must necessarily happen in finite time. This is analogous to the spanning-tree based coverage presented in [37]. We then establish how a GREEDY strategy of moving towards the *last-sensed* location of the evader, eventually reduces the present problem to a previously-studied one with unlimited sensing. The convexity assumption on the environment is required because otherwise, due to the limited sensing range, there exist environments similar to those considered in [52] and an evader strategy, such that the evader does not get detected again. Finally, we show how capture is achieved using the established LION strategy [88]. Our contributions are as follows: First, we present an analysis which provides a novel upper bound on the time required for the pursuit phase to terminate. Second, we obtain a sufficient condition on the ratio of sensing to stepping radius of the players for capture to take place in a given environment. Finally, we show that this condition is tight in the sense that if it is violated, then there exist sufficiently large environments, an evader strategy and initial positions for the players, that lead to evasion against the GREEDY strategy.

The second game is played with at least five cooperative pursuers in a boundaryless environment and the field is a bounded region known to the pursuers. Our contributions are as follows: First, we design a novel pursuer formation and a randomized SWEEP strategy for the pursuers to search the field. They *succeed* when they detect the evader inside a special *capture* region, which we characterize for the pursuer formation. We show that using our SWEEP strategy, the pursuers succeed with a certain probability which is a function of the pursuer formation and independent of the initial evader location. Next, we propose a cooperative pursuit strategy for the pursuers to confine the evader within their sensing discs. We show that using this pursuit strategy, the present problem is reduced to a previously-studied one with unlimited sensing. Finally, we show how capture is achieved using the established PLANES strategy [57]. We obtain novel upper bounds on the time for each phase in our strategy. Also, we present a simulation-based study of the performance of the strategies under sensing errors, different ratios of sensing to stepping radius, greater evader speed and different number of pursuers.

Ecological Motivation

The inspiration for the cooperative strategy proposed in this paper has been derived from aspects of animal behavior. It is well known that predators hunt as a conjoined group, when it is less efficient to hunt alone. This behavior is also observed when the prey is large or can move as fast as the predators [74]. Further, predators show an inclination towards specialized behavior by maintaining a fixed formation during search and capture of preys [38]. Such specializations suggest that there may be configurations that are preferred during group hunting. Also, in the presence of sensing limitations, groups tend to maintain spacing between each other that is regulated by their sensory capabilities [77]. These facts give us additional hints towards designing capture-conducive predator formations. In this context, our analysis sheds light on how the maximum group size of the predators varies with prey availability and with the prey's nutrition value in the present set-up.

Organization of this Chapter

This chapter is organized as follows: the problem's mathematical model and assumptions are presented in Section 2.2. The individual phases of the *sweep-pursuit-capture* strategies and the corresponding main results for both the problems are presented in Section 2.3. The proofs of the results are presented in Section 2.4. Simulation results are presented in Section 2.5. Finally, in Section 2.6, we study the relationship between pursuer group sizes and evader availability and its nutrition value in our set-up.

2.2 Problem Set-up

We assume a discrete-time model with alternate motion of the evader and the pursuers: the evader moving first. We assume that the players can sense each other precisely only if the distance between them is less than or equal to the sensing radius r_{sens}. Further, we assume that at each time instant, the players take measurements of each other before and after the evader's move, as shown in Figure 2.1. Define $\mathcal{E}_\phi := \mathcal{E} \cup \phi$, where $\mathcal{E} \subseteq \mathbb{R}^2$ denotes the environment and ϕ is the null element. The null element will be used to denote a lack of measurement in our limited range sensing model. Let $\mathcal{G} \subset \mathcal{E}$ denote the field, i.e., the region that initially contains the evader. The evader follows a *reactive rabbit* model - moves only after being detected for the first time. We assume that the pursuers know the field $\mathcal{G}$ and the environment $\mathcal{E}$. The goal of the pursuer(s) is to *capture* the evader, i.e., a pursuer and the evader are at the same position at some finite time. *Evasion* is said to occur if the pursuer cannot capture the evader. We describe the *Sweep-Pursuit-Capture* strategy for the following problems:

2.2.1 Single Pursuer Problem

We have a bounded convex environment $\mathcal{E} \subset \mathbb{R}^2$ and the field $\mathcal{G} = \mathcal{E}$. Let $e[t]$ and $p[t]$ denote the absolute positions of the evader and the pursuer respectively, at time

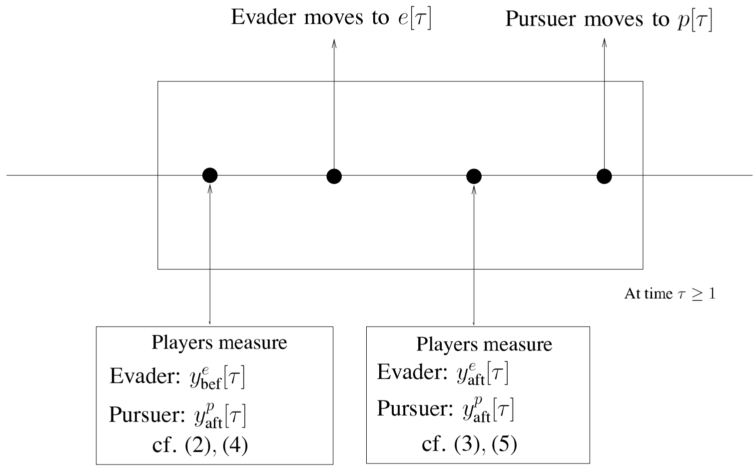

Figure 2.1. A snapshot of each time instant $\tau \in \{1, 2, \dots\}$ in our alternate motion model. The players take measurements before and after the evader's move.

$t \in \mathbb{Z}_{\geq 0}$. The discrete-time equations of motion are

$$\begin{aligned} e[t] &= e[t-1] + u^e\Big(e[t-1], \{y^e_{\text{bef}}[\tau]\}_{\tau=1}^{t}, \{y^e_{\text{aft}}[\tau]\}_{\tau=1}^{t-1}\Big), \\ p[t] &= p[t-1] + u^p\Big(p[t-1], \{y^p_{\text{bef}}[\tau]\}_{\tau=1}^{t}, \{y^p_{\text{aft}}[\tau]\}_{\tau=1}^{t}\Big), \end{aligned} \tag{2.1}$$

where at the τ-th time instant, $y^e_{\text{bef}}[\tau], y^e_{\text{aft}}[\tau] \in \mathcal{E}_\phi$ are the measurements of the pursuer's position taken by the evader before and after the *evader's* move, as shown in Figure 2.1. The parentheses notation $\{y^p_{\text{bef}}[\tau]\}_{\tau=1}^{t}$ denotes the set $\{y^p_{\text{bef}}[1], y^p_{\text{bef}}[2], \dots, y^p_{\text{bef}}[t]\}$. Due to limited range sensing model, for $\tau \in \{1, \dots, t\}$, we define

$$y^e_{\text{bef}}[\tau] = \begin{cases} p[\tau-1], & \text{if } \|p[\tau-1] - e[\tau-1]\| \leq r_{\text{sens}}, \\ \phi, & \text{otherwise.} \end{cases} \tag{2.2}$$

For notational convenience, we define $\{y^p_{\text{aft}}[\tau]\}_{\tau=1}^{t-1} = \phi$ for the initial time $t = 1$. For $t \geq 2$ and for $\tau \in \{1, \dots, t-1\}$, we have

$$y^e_{\text{aft}}[\tau] = \begin{cases} p[\tau-1], & \text{if } \|p[\tau-1] - e[\tau]\| \leq r_{\text{sens}}, \\ \phi, & \text{otherwise.} \end{cases} \tag{2.3}$$

Similarly, at the τ-th time instant , $y^p_{\text{bef}}[\tau], y^p_{\text{aft}}[\tau] \in \mathcal{E}_\phi$ are the measurements of the evader's position taken by the pursuer before and after the *evader's* move respectively, as shown in Figure 2.1. Due to limited range sensing model, for $\tau \in \{1, \dots, t\}$, we have

$$y^p_{\text{bef}}[\tau] = \begin{cases} e[\tau - 1], & \text{if } \|e[\tau - 1] - p[\tau - 1]\| \leq r_{\text{sens}}, \\ \phi, & \text{otherwise.} \end{cases} \tag{2.4}$$

For $\tau \in \{1, \dots, t\}$, we have

$$y^p_{\text{aft}}[\tau] = \begin{cases} e[\tau], & \text{if } \|e[\tau] - p[\tau - 1]\| \leq r_{\text{sens}}, \\ \phi, & \text{otherwise.} \end{cases} \tag{2.5}$$

The functions $u^e : \mathcal{E} \times \underbrace{\mathcal{E}_\phi \times \cdots \times \mathcal{E}_\phi}_{2t-1 \text{ times}} \to \mathcal{E}$ and $u^p : \mathcal{E} \times \underbrace{\mathcal{E}_\phi \times \cdots \times \mathcal{E}_\phi}_{2t \text{ times}} \to \mathcal{E}$ are termed as *strategies* for the evader and pursuer respectively. The apparent lack of symmetry between the number of arguments in the strategies of the evader and the pursuer is due to the alternate motion model. We assume that both players can move with a maximum step size of r_{step}, that is,

$$\|u^e\| \leq r_{\text{step}}, \quad \|u^p\| \leq r_{\text{step}}. \tag{2.6}$$

The sensing radius, r_{sens}, is κ times the motion radius, r_{step}. We assume κ is greater than 1, i.e., both players can sense further than they can move. From the reactive rabbit model for the evader, we have $u^e = 0$ until the evader is detected. After this happens, the single pursuer problem consists of *determining* u^p *that guarantees capture for any evader strategy,* u^e. This problem is described by two key parameters: the ratio of sensing to stepping radius κ and the ratio of the diameter of the environment to the stepping radius $\text{diam}(\mathcal{E})/r_{\text{step}}$.

2.2.2 Multiple Pursuer Problem

We have a total of $N \geq 5$ pursuers that can communicate among themselves the location of a sensed evader as well as their own position with respect to a fixed, global reference frame. The environment $\mathcal{E}$ is $\mathbb{R}^2$ and the field $\mathcal{G}$ is a bounded subset of $\mathbb{R}^2$. Define $\mathbb{R}^2_\phi := \mathbb{R}^2 \cup \phi$. Let $p_j[t]$ denote the absolute positions of the j-th pursuer at time t for every $j \in \{1, \ldots, N\}$. Analogous to (2.1), the discrete-time equations of motion are

$$\begin{aligned} e[t] &= e[t-1] + u^e\Big(e[t-1], \{y^e_{\text{bef}}[\tau]\}^t_{\tau=1}, \{y^e_{\text{aft}}[\tau]\}^{t-1}_{\tau=1}\Big), \\ p_j[t] &= p_j[t-1] + u^{p_j}\Big(\Big\{\{p_j[\tau]\}^N_{j=1}\Big\}^{t-1}_{\tau=1}, \big\{y^p_{\text{bef}}[\tau]\big\}^t_{\tau=1}, \big\{y^p_{\text{aft}}[\tau]\big\}^t_{\tau=1}\Big), \end{aligned} \tag{2.7}$$

where at the τ-th time instant, $y^e_{\text{bef}}[\tau], y^e_{\text{aft}}[\tau] \in \underbrace{\mathbb{R}^2_\phi \times \cdots \times \mathbb{R}^2_\phi}_{N \text{ times}}$ denote the sets of measurements of the pursuers' positions taken by the evader before and after its move. Similarly, $y^p_{\text{bef}}[\tau], y^p_{\text{aft}}[\tau] \in \mathbb{R}^2_\phi$ are the measurements of the evader's position taken by the pursuers before and after the evader's move. The measurements are given by expressions analogous to (2.2)-(2.5). Akin to the single pursuer problem, the functions $u^e : \mathbb{R}^2 \times \underbrace{\mathbb{R}^2_\phi \times \cdots \times \mathbb{R}^2_\phi}_{(2t-1)N \text{ times}} \to \mathbb{R}^2$ and $u^{p_j} : \underbrace{\mathbb{R}^2_\phi \times \cdots \times \mathbb{R}^2_\phi}_{(t-1)N \text{ times}} \times \underbrace{\mathbb{R}^2_\phi \times \cdots \times \mathbb{R}^2_\phi}_{2t \text{ times}} \to \mathbb{R}^2$ for every $j \in \{1, \ldots, N\}$, are strategies for the evader and pursuers respectively. The constraint on the maximum step size, given by (2.6), holds for the evader and every pursuer. Due to the reactive rabbit model for the evader, $u^e = 0$ until it is detected by the pursuers for the first time.

The multiple pursuer problem consists of *designing a pursuer formation and a corresponding strategy that guarantees capture of the evader*. This problem is described by the following key parameters: the ratio of sensing to stepping radius of the players κ, the ratio of the diameter of the field to the stepping radius $\text{diam}(\mathcal{G})/r_{\text{step}}$, and the number of pursuers N.

2.3 Strategies and Main Results

In this section, we describe the Sweep-Pursuit-Capture strategies for both the problems and the corresponding main results. The proofs are presented in Section 2.4.

We first introduce the following weak notion of capture.

Definition 2.3.1 (Trap) *The evader is* trapped within the sensing radius (resp. radii) *of the pursuer (resp. pursuers) if for any evader strategy u^e, the motion disc of the evader is completely contained within the sensing disc of the pursuer (resp. union of the sensing discs of the pursuers) after a finite time.*

To be specific, the evader is trapped at time instant T_{trap} if for any evader strategy,

$$y^p_{\text{bef}}[T_{\text{trap}}] = e[T_{\text{trap}} - 1], \quad \text{and} \quad y^p_{\text{aft}}[T_{\text{trap}}] = e[T_{\text{trap}}].$$

The idea behind our Sweep-Pursuit-Capture strategies is to detect the evader and pursue it so as to trap it. Next, we show that the evader remains trapped for all subsequent time instants and that capture is achieved by using strategies that were developed for the unlimited range sensing version of the respective game. This principle applies to both versions of the problem.

2.3.1 Single Pursuer Problem

We first present each phase of the strategy for the single pursuer problem.

Sweep Phase - Sweep Strategy

Let $\text{diam}(\mathcal{E})$ denote the diameter of $\mathcal{E}$. The Sweep strategy for the pursuer is to move with maximum step size along a path, as shown in Figure 2.2 such that the union of the sensing discs of the pursuer at the end of each step until the end of this phase contains $\mathcal{E}$. We term such a path a *sweeping path* for $\mathcal{E}$. Let t_{sweep} denote the time taken for this strategy to terminate. We have the following result.

Lemma 2.3.2 (Sweep strategy) *In the single pursuer problem with parameters* κ *and* $\mathrm{diam}(\mathcal{E})/r_{\mathrm{step}}$*, the time* t_{sweep} *taken by the* SWEEP *is at most*
$\left\lceil \mathrm{diam}(\mathcal{E}) \middle/ 2\kappa r_{\mathrm{step}} \right\rceil (\lceil \mathrm{diam}(\mathcal{E})/r_{\mathrm{step}} \rceil + \lceil \kappa \rceil)$ *steps.*

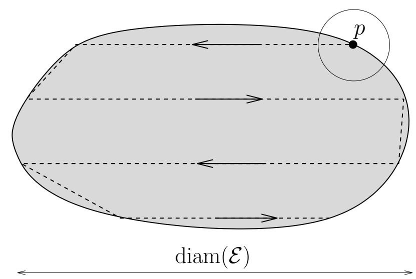

Figure 2.2. A sweeping path to detect the evader in the Single pursuer problem using the SWEEP strategy.

Pursuit Phase - Greedy Strategy

Once the evader is detected, the GREEDY strategy for the pursuer is to *move towards the last sensed position of the evader with maximum step size.* This strategy has the property that the pursuer senses the evader's position at every successive time instant. Let t_{trap} denote the *trapping time*, i.e., the time taken by the pursuer to trap the evader after detecting it. We now present our main result for the GREEDY strategy.

Theorem 2.3.3 (Greedy strategy) *In the single pursuer problem with parameters* κ *and*

$\mathrm{diam}(\mathcal{E})/r_{\mathrm{step}}$*, if* $\kappa > \sqrt{2 + 2\cos\beta_{\mathrm{c}}}$*, where*

$$\beta_{\mathrm{c}} := \frac{\sqrt{3}}{4\kappa} \left\lceil \frac{\mathrm{diam}(\mathcal{E})}{2\kappa r_{\mathrm{step}}} \right\rceil^{-1} \arctan \frac{1}{8\kappa}, \tag{2.8}$$

then the GREEDY strategy *has the following properties:*

1. the pursuer traps the evader within its sensing radius, and

2. the trapping time t_{trap} satisfies

$$t_{\text{trap}} \leq \left(\left\lceil \frac{\log(\sqrt{\kappa^2 - \sin^2 \beta_{\text{c}}} - \cos \beta_{\text{c}} - 1) - \log(\kappa - 1)}{\log(1 - (1 - \cos \beta_{\text{c}})/\kappa)} \right\rceil + 1 \right) \left\lceil \frac{\text{diam}(\mathcal{E})}{2\kappa r_{\text{step}}} \right\rceil. \quad (2.9)$$

Furthermore, if $\kappa > 2$, then as $(\text{diam}(\mathcal{E})/r_{\text{step}}) \to +\infty$, $t_{\text{trap}} \in O\left((\text{diam}(\mathcal{E})/r_{\text{step}})^3\right)$.

Theorem 2.3.3 is tight in the sense that if the condition on κ is violated then there exist sufficiently large environments, an evader strategy and initial positions for the players, that lead to evasion against the GREEDY pursuer strategy. This is described by the following result.

Proposition 2.3.4 (Evasion) *Given a single pursuer problem with parameters κ and $\text{diam}(\mathcal{E})/r_{\text{step}}$ such that $\kappa \leq \sqrt{2 + 2\cos\beta_{\text{c}}}$, where β_{c} is given by (2.8), and $\mathcal{E}$ contains a circle of radius $r_{\text{step}}/\sqrt{4 - \kappa^2}$, then there exist an evasion strategy and initial positions of the players for which the pursuer's* GREEDY *strategy fails to trap the evader.*

Figure 2.3 illustrates this evasion strategy under the conditions required by Proposition 2.3.4.

Capture Phase - Lion Strategy

Once the evader is trapped within the sensing range of the pursuer, the pursuer employs the LION strategy from [88] to complete the capture. For the sake of completeness, we now give a brief description of the LION strategy, adapted to the present problem setting.

The LION strategy can be applied to this phase as follows:

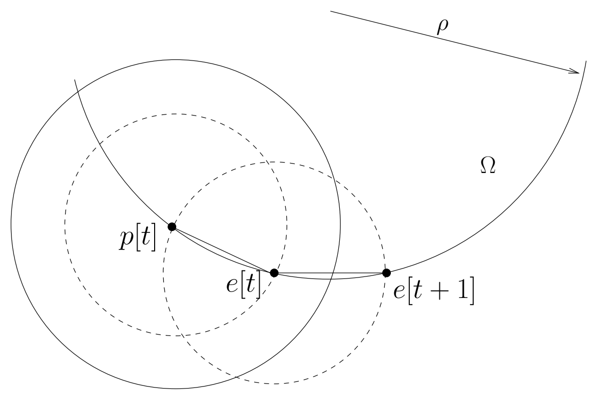

Figure 2.3. Illustrating evasion. The dotted circles are the player's motion discs and the solid circle is the pursuer's sensing disc. $e[t]$ and $p[t]$ are on the circle Ω described in Proposition 2.3.4 such that $\|e[t] - p[t]\| = r_{\text{step}}$. Evader chooses to move to $e[t+1]$ on Ω with full step size.

1. Prior to its $(t+1)$-th move, the pursuer constructs the line joining $e[t]$ and $p[t]$, as shown in Figure 2.4. Let this line intersect the boundary of the environment at a point $X[t]$ such that $p[t]$ lies between $e[t]$ and $X[t]$.

2. The pursuer then also constructs the line joining $e[t+1]$ and $X[t]$. It moves to the intersection of this line with the circle centered at $p[t]$ and of radius r_{step}. Of the two possible intersection points, the pursuer selects the one closer to $e[t+1]$.

This construction guarantees that the intersection point $X[t]$ remains the same as the point $X[t_{\text{sweep}} + t_{\text{trap}}]$, for every $t \geq t_{\text{sweep}} + t_{\text{trap}}$, where $t_{\text{sweep}} + t_{\text{trap}}$ is the time at the end of the pursuit phase. Denoting by t_{cap} the time taken by the pursuer to capture the evader after trapping it, we have the following result.

Theorem 2.3.5 (Lion strategy [88]) *In the single pursuer problem with parameters κ and $\text{diam}(\mathcal{E})/r_{\text{step}}$, after trapping the evader within the sensing radius and*

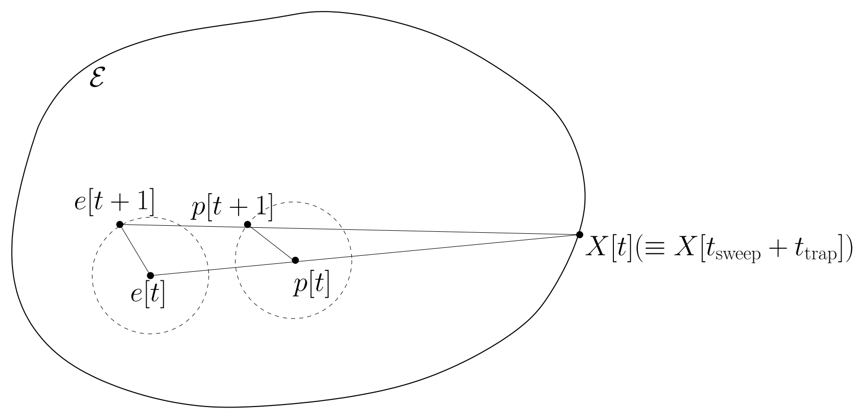

Figure 2.4. Single pursuer problem: Using the LION strategy to capture the evader. The dotted circles represent the motion discs of the players.

using the Lion strategy,

1. *the distance,* $\|p[t] - e[t]\|$*, is a non-increasing function of time,*

2. *the pursuer captures the evader,*

3. t_{cap} *is at most* $\left\lceil \left(\frac{\text{diam}(\mathcal{E})}{r_{\text{step}}}\right)^2 \right\rceil$ *steps.*

Thus, our problem with limited sensing is solved because once the evader is trapped within the pursuer's sensing radius, it remains trapped until capture, from part (i) of Theorem 2.3.5. We have also obtained an upper bound on the total time to capture, i.e., $t_{\text{sweep}} + t_{\text{trap}} + t_{\text{cap}}$.

2.3.2 Multiple Pursuer Problem

This section describes the sweep-pursuit-capture strategy for multiple pursuers and the corresponding results. We assume that $\kappa \geq 4$ and $N \geq 5$. We define the following formation for multiple pursuers.

Definition 2.3.6 (Trapping Chain) *A group of $N \geq 5$ pursuers $\{p_1, \ldots, p_N\}$ are said to be in a* trapping chain *formation if*

1. $p_2, \ldots, p_{N-1}$ *are placed counterclockwise on a semi-circle with diameter equal to* $\|p_2 - p_{N-1}\|$,

2. *for all* $j \in \{1, \ldots, N-1\}$

$$\|p_j - p_{j+1}\| = r_{\text{step}}\sqrt{4\kappa^2 - 25}, \qquad \textit{and,}$$

3. p_1, p_2, p_{N-1}, p_N *are on the vertices of a rectangle such that the polygon with vertices* $\{p_1, \ldots, p_N\}$*, in that order, is convex (cf. Figure 2.5).*

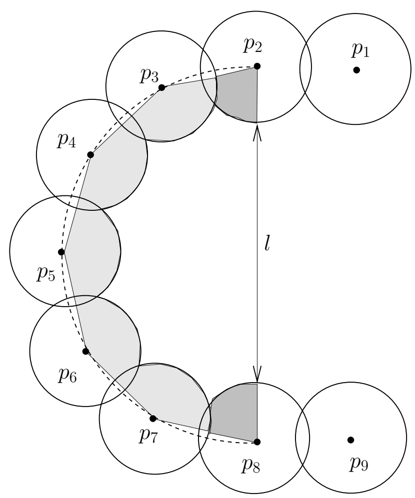

Figure 2.5. A trapping chain formation for $N = 9$ pursuers. The circles around the pursuers denote their sensing ranges. The lightly shaded region denotes the capture region and the darkly shaded region along with the lightly shaded one denotes the extended capture region.

We now describe the Sweep-Pursuit-Capture strategy for the multiple pursuer problem.

Sweep Phase - Sweep Strategy

The pursuers begin by placing themselves in a trapping chain formation. We define the *capture region* $\mathcal{S}$ for a trapping chain by

$$\mathcal{S} = \bigcup_{j\in\{3,\ldots,N-2\}} \mathcal{B}_{p_j}(r_{\text{sens}}) \cap \mathring{\text{Co}}\{p_2,\ldots,p_{N-1}\},$$

where $\mathcal{B}_{p_j}(r_{\text{sens}}) \subset \mathbb{R}^2$ denotes the sensing disc of pursuer p_j and $\mathring{\text{Co}}\{p_2,\ldots,p_{N-1}\} \subset \mathbb{R}^2$ denotes the interior of the convex hull of $\{p_2,\ldots,p_{N-1}\}$. The lightly shaded region in Figure 2.5 is the proposed capture region, $\mathcal{S}$, for the trapping chain. In the sweep phase, pursuers wish to detect the evader within the capture region. We consider a square region of length equal to diameter of the region $\mathcal{G}$, $\text{diam}(\mathcal{G})$ that contains the field $\mathcal{G}$. The pursuers sweep this square region in the direction of the normal to p_1p_N, outward with respect to the convex hull of the pursuers. For a trapping chain shown in Figure 2.5, we define the *effective* length l as

$$l := \|p_1 - p_N\| - 2r_{\text{sens}} = r_{\text{step}}\left(\frac{\sqrt{4\kappa^2 - 25}}{\sin(\frac{\pi}{2(N-3)})} - 2\kappa\right). \tag{2.10}$$

As the pursuers move in the direction described earlier, they clear a rectangular strip of length $\text{diam}(\mathcal{G})$ and width $l + 4r_{\text{sens}}$. The SWEEP strategy for the pursuers is as follows.

1. Choose the first rectangular strip at a random distance l_0 from one edge of the square region containing $\mathcal{G}$ and sweep it length-wise. The distance l_0 is a uniform random variable taking values in the interval $[-2r_{\text{sens}}, l + 2r_{\text{sens}}]$. Here, negative l_0 implies that some of the pursuers may begin sweeping from outside the region $\mathcal{G}$.

2. Form a sweeping path for the square region and sweep along adjacent strips as shown in Figure 2.6.

The shaded region in Figure 2.6 refers to the area that would fall in the proposed capture region $\mathcal{S}$. Now we are interested in determining the probability that an evader falls in the shaded region in Figure 2.6. That is given by the following result.

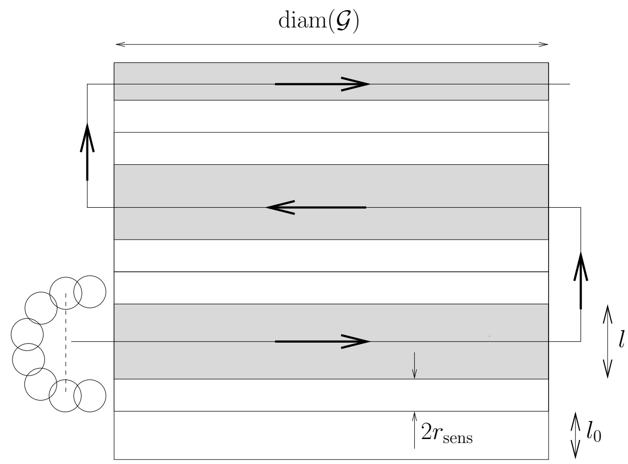

Figure 2.6. Multiple pursuer problem: SWEEP strategy. The shaded region represents the region swept by the capture region of the trapping chain.

Theorem 2.3.7 (Sweep strategy) *In the multiple pursuer problem with parameters* κ, $\mathrm{diam}(\mathcal{G})/r_{\text{step}}$ *and* N, *for any probability distribution for the initial position of the evader with support on* $\mathcal{G}$, *using the* SWEEP *strategy,*

1. *the probability* P *of detecting the evader inside* $\mathcal{S}$ *for a group of pursuers in a trapping chain, satisfies*

$$P \geq \frac{l}{l + 4r_{\text{sens}}} \geq 1 - \frac{2\pi\kappa}{\left(\sqrt{4\kappa^2 - 25}(N-3) + 2\pi\kappa\right)}, \qquad \textit{and}$$

2. *the time* t_{sweep} *taken by the* SWEEP *strategy to terminate satisfies*

$$t_{\text{sweep}} \leq \left\lceil \frac{\mathrm{diam}(\mathcal{G})}{r_{\text{step}}} \left(\frac{\pi/2}{\sqrt{4\kappa^2 - 25}(N-3) + \pi\kappa} \right) \right\rceil \times \left\lceil \frac{\mathrm{diam}(\mathcal{G})}{r_{\text{step}}} + 2\sqrt{4\kappa^2 - 25}N \right\rceil.$$

Remark 2.3.8 *The minimum probability P of the pursuers detecting the evader inside the capture region by using the* SWEEP *strategy is* independent *of the evader's location in $\mathcal{G}$. This means that the best that the evader can do in the present framework is to locate itself initially with a uniform probability in $\mathcal{G}$.*

We will see that the pursuers win when the evader is detected in $\mathcal{S}$ by the pursuers. Otherwise, there exists a path for the evader such that it can avoid being captured indefinitely.

Pursuit Phase - Circumcenter Strategy

If the evader is detected within the proposed capture region at time t_{sweep}, the pursuers need to ensure that they trap the evader within their sensing ranges. Before we describe the strategy for the pursuit phase, consider the following possibility: if the evader steps into the darkly shaded region of the sensing range of p_2 (or of p_{N-1}), then p_2 (resp. p_{N-1}) can use the GREEDY strategy (ref. Section 2.3.1). By moving towards the evader, the evader's motion disc gets contained inside that pursuer's sensing disc and thus the evader gets trapped. This motivates us to define an *extended capture region* $\mathcal{S}^e$ for the trapping chain by

$$\mathcal{S}^e = \bigcup_{j \in \{2,\ldots,N-1\}} \mathcal{B}_{p_j}(r_{\text{sens}}) \cap \mathring{\text{Co}}\{p_2, \ldots, p_{N-1}\}.$$

The darkly shaded region along with the lightly shaded region in Figure 2.5 is the extended capture region $\mathcal{S}^e$ for the trapping chain.

We now present the following pursuit strategy. At each time step $t \geq t_{\text{sweep}}$,

1. While $e[t+1] \notin \mathcal{S}^e[t]$, the pursuers $p_2, \ldots, p_{N-1}$ move towards the *circumcenter*[1]

[1] The circumcenter of a triangle is the unique point in the plane which is equidistant from all of its three vertices.

O of the triangle formed by $p_2[t_{\text{sweep}}]$, $e[t_{\text{sweep}}]$ and $p_{N-1}[t_{\text{sweep}}]$ with maximum step. Pursuers p_1 and p_N move parallel to p_2 and p_{N-1} respectively.

2. Otherwise, one of the pursuers which senses the evader directly, makes a GREEDY move (ref. Section 2.3.1) towards the evader and the others move parallel to that pursuer with the maximum step.

One such move is shown in Figure 2.7. In case (i) of the strategy, note that the pursuers may not sense the evader in every subsequent move. But they will encircle the evader by "closing" the trapping chain around it and then shrink the enclosed region around the evader. We thus have the following result.

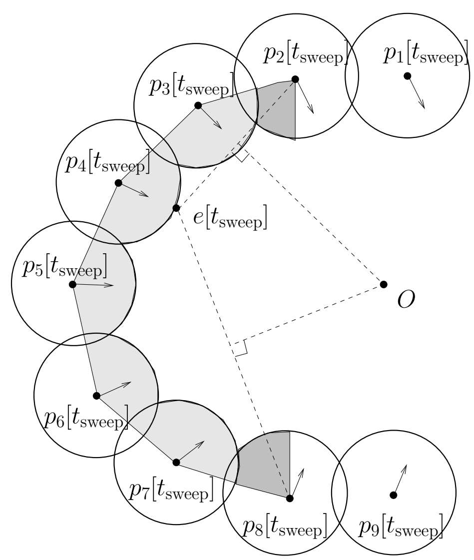

Figure 2.7. Multiple pursuer problem: CIRCUMCENTER strategy. At time t_{sweep}, the evader position is sensed by p_4. Pursuers $p_2, \ldots, p_8$ move towards O, the circumcenter of triangle formed by p_2, e and p_8. p_1 and p_9 move parallel to p_2 and p_8 respectively. The circles around the pursuers represent their sensing discs.

Theorem 2.3.9 (Circumcenter strategy) *In the multiple pursuer problem with parameters κ, $\operatorname{diam}(\mathcal{G})/r_{\text{step}}$ and N, starting from a trapping chain formation, if the* *evader is detected with* $e[t_{\text{sweep}}] \in \mathcal{S}[t_{\text{sweep}}]$*, then using the* Circumcenter *strategy,*

1. *the pursuers trap the evader within their sensing radii,*

2. *the* trapping time t_{trap} *satisfies*

$$t_{\text{trap}} \leq \sqrt{4\kappa^2 - 25}N\Big(1 + \frac{1}{2\sin\phi}\Big),$$

   where

$$\phi(\kappa) = \frac{\pi}{4} - \arctan\Big(\frac{\kappa}{\sqrt{3\kappa^2 - 25}}\Big), \qquad \textit{and}$$

3. *at that time, the evader is inside the pursuers' convex hull in such a way that*

$$\mathcal{B}_{\frac{r_{\text{step}}}{2}}(e[t_{\text{sweep}} + t_{\text{trap}}]) \subset \text{Co}\{p_1, \ldots, p_N\}[t_{\text{sweep}} + t_{\text{trap}}], \tag{2.11}$$

   where the notation $\mathcal{B}_r(a)$ *refers to the closed disc of radius* r *centered at point* a *in the plane.*

The Circumcenter strategy guarantees trapping of the evader even without pursuers p_1 and p_N. But in that case, the inclusion in (2.11), which will be required to establish an upper bound on the time for the capture phase that follows, is not guaranteed.

The Capture Phase - Planes Strategy

Once the evader is trapped within the sensing ranges of the pursuers, the pursuers use the Planes strategy from [57] to capture the evader. Before stating our results, we reproduce this strategy for completeness.

Let the time at the end of the pursuit phase be $t_{\text{sweep}}+t_{\text{trap}}$ and the evader be inside the convex hull of the pursuers as in (2.11) (cf. Figure 2.8(a)). For $t \geq t_{\text{sweep}} + t_{\text{trap}}$ and for every pursuer p_j:

- Draw the line $h_j[t+1]$ through $e[t+1]$, parallel to the line joining $e[t]$ and $p_j[t]$, as shown in Figure 2.8(b).

- Move to the point closest to $e[t+1]$ on the line $h_j[t+1]$ with maximum step size.

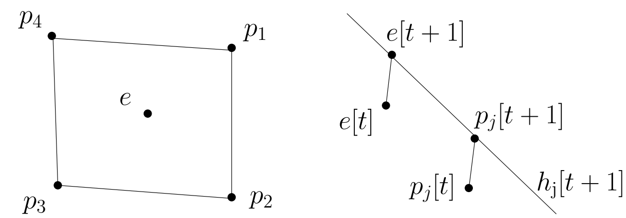

(a) Evader inside pursuers' convex hull

(b) PLANES strategy. Illustrating a pursuer move.

Figure 2.8. Algorithm PLANES

Theorem 2.3.9 shows that use of the CIRCUMCENTER strategy in the pursuit phase leads to the evader being trapped and inside the convex hull of the pursuers. Now capture follows from the following theorem, which was partly inspired by the results on the PLANES strategy in [57].

Theorem 2.3.10 (Planes strategy) *In the multiple pursuer problem with parameters κ, $\mathrm{diam}(\mathcal{G})/r_{\mathrm{step}}$ and N, let the evader be trapped inside the convex hull of the pursuers such that property (2.11) is satisfied. If every pursuer follows the* PLANES *strategy, then*

1. *the distances, $\|p_j[t] - e[t]\|$ for every $j \in \{1, \ldots, N\}$, are non-increasing functions of time,*

2. *the pursuers capture the evader and*

3. the time t_{cap} taken in the capture phase is at most $18\kappa\sqrt{4\kappa^2 - 25}N$.

Item (i) of Theorem 2.3.10 implies that once the evader is trapped within the sensing ranges of the pursuers, it remains trapped within their sensing ranges at the end of every pursuer move. The capture is now complete and we obtained a novel upper bound on the total time to capture, i.e., $t_{\text{sweep}} + t_{\text{trap}} + t_{\text{cap}}$.

2.4 Proofs of the Results

In this section, we formally prove the main results.

2.4.1 Single Pursuer Problem

Proof of Lemma 2.3.2: To determine an upper bound for t_{sweep}, consider placing $\mathcal{E}$ inside a square region of length $\text{diam}(\mathcal{E})$ and the pursuer moving along a hypothetical sweeping path for the square region, as shown in Figure 2.9. It is straightforward to show that to achieve coverage, this hypothetical sweeping path is between strips of width $2\kappa r_{\text{step}}$, parallel to the side. selection of width for the There are $\lceil(\text{diam}(\mathcal{E})/2\kappa r_{\text{step}})\rceil$ such strips and it takes at most $\lceil \text{diam}(\mathcal{E})/r_{\text{step}}\rceil + \lceil\kappa\rceil$ steps to sweep one strip completely and be positioned to sweep through a neighboring strip of this hypothetical sweeping path. ■

To prove Theorem 2.3.3, we need some preliminary definitions and results which we present now. In what follows, the notation $\angle ABC$ refers to the smaller of the two angles between segments AB and BC.

Definition 2.4.1 (Deviation and evasion angles) *Given evader and pursuer at positions $e[\tau]$, $p[\tau]$, for $\tau \in \{t, t+1\}$, define the* deviation angle $\alpha[t]$ *and the evasion*

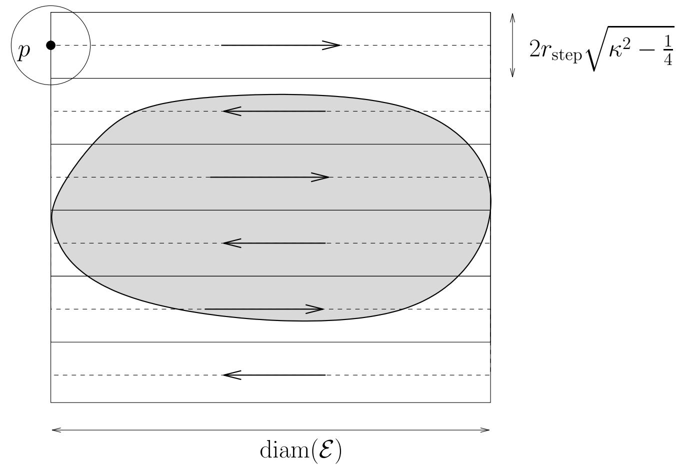

Figure 2.9. A hypothetical sweeping path to determine upper bound on number of steps to detect the evader.

angle $\beta[t]$ *by:*

$$\alpha[t] := \angle e[t+1]p[t+1]e[t],$$

$$\beta[t] := \alpha[t] + \angle p[t+1]e[t+1]e[t].$$

These angles are illustrated in Figure 2.10. The following result follows trivially.

Proposition 2.4.2 *When the pursuer uses the* GREEDY *strategy, for every instant of time* t*,*

$$|\beta[t]| \geq |\alpha[t]|. \tag{2.12}$$

Note that equality in (2.12) only holds when the evader moves away from the pursuer along the line $p[t]e[t]$.

It can be deduced that when the pursuer employs the GREEDY strategy, the distance between the pursuer and evader is a non-increasing function of time. We now define a geometric construction which is useful in the proof.

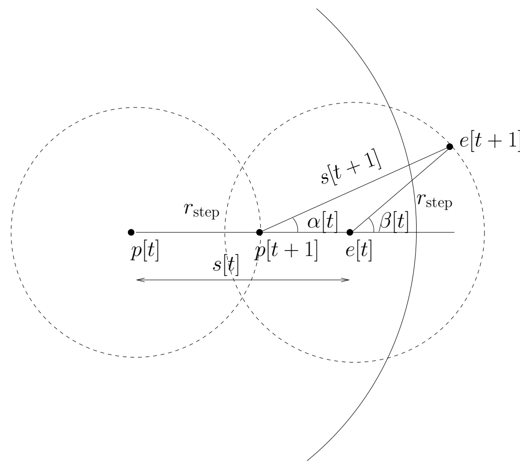

Figure 2.10. Relation between the deviation angle $\alpha[t]$ and the evasion angle $\beta[t]$. The dotted circles represent the motion discs of the players. The circle centered at $p[t]$ (shown partially here) is the pursuer's sensing range.

Definition 2.4.3 (Cone sector sequence) *Let t_0 denote the time at the end of the sweep phase. Given a time instant $k \in \mathbb{Z}_{\geq 0}$, the sequence $\mathcal{C}_k$ of cone sectors $\mathcal{C}_{k,i}$ for $i \in \mathbb{Z}_{\geq 0}$ is defined as follows:*

1. *Define the cone sector $\mathcal{C}_{k,0}$ with $p[t_\text{k}]$ as its vertex, angle bisector defined by the segment $e[t_\text{k}]p[t_\text{k}]$ and extended to a point X beyond $e[t_\text{k}]$ such that $L_{\text{cone}} := \|p[t_\text{k}] - X\| = 2\kappa r_{\text{step}}$, as shown in Figure 2.11. Let the segment YZ be of length $\frac{r_{\text{step}}}{2}$ and perpendicular to the segment $p[t_\text{k}]X$ with X as its midpoint. Accordingly, let $\theta := \angle Y p[t_\text{k}] Z = 2\arctan(1/8\kappa)$ be the* cone angle.

2. *For $k, i \geq 0$, denote by t^* the time when the evader leaves the cone sector $\mathcal{C}_{k,i}$. There are two possibilities:*

   (a) *the pursuer first constructs a new cone sector $\mathcal{C}_{k,i+1}$ which is a translation of $\mathcal{C}_{k,i}$ having vertex at $p[t^*]$. This is illustrated in Figure 2.12.*

(b) *If the evader is not inside $\mathcal{C}_{k,i+1}$, then we denote $t_{k+1} := t^*$. The pursuer constructs a new cone sector sequence $\mathcal{C}_{k+1}$.*

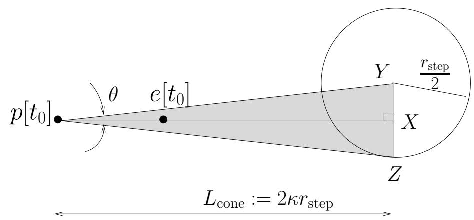

Figure 2.11. Construction of cone $\mathcal{C}_{0,0}$. Choose X on the line $e[t_0]p[t_0]$ such that $\|p[t_0] - X\| = 2\kappa r_{\text{step}}$. YZ has length $r_{\text{step}}/2$ and is perpendicular to segment $p[t_0]X$ with X as its midpoint. θ is the cone angle.

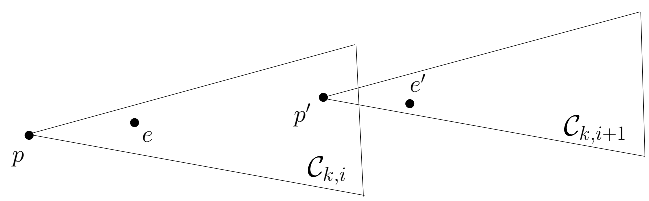

Figure 2.12. Construction of cone sector $\mathcal{C}_{k,i+1}$. Translate cone sector $\mathcal{C}_{k,i}$ to have its vertex at p'.

The cone sector sequence described above has the following property.

Proposition 2.4.4 (Cone sector sequence) *Given a cone sector sequence $\mathcal{C}_k$, the maximum number of steps M^* for which the evader can remain inside it without being captured satisfies*

$$M^* = \frac{4\kappa}{\sqrt{3}} \left\lceil \frac{\text{diam}(\mathcal{E})}{2\kappa r_{\text{step}}} \right\rceil . \tag{2.13}$$

Proof: We compute an upper bound on the number of steps a pursuer stays in any cone sector while using the Greedy strategy. From the definition of a cone sector, this is also an upper bound on the number of steps the evader can remain inside a cone sector. Construct a rectangle with length $L_{\rm cone}$ and width $r_{\rm step}/2$ such that it contains a cone sector, as shown in Figure 2.13. Orient a frame of reference such that its X axis is parallel to the angle bisector of the cone sector. Let $p[t_k] - P_1 - \cdots - P_5$ denote the path as a result of the pursuer's GREEDY strategy while in the cone sector $\mathcal{C}_{k,0}$.

We now construct a path with step size equal to $r_{\rm step}$ at each time instant, whose length is greater than or equal to that of any such greedy pursuer paths. Select a point P_1' between A and B such that $\|p[t_k] - P_1'\| = r_{\rm step}$. Then select another point P_2' on between C and D such that $\|P_1' - P_2'\| = r_{\rm step}$. Of the two possible points, select that point which is farther from $p[t_k]$ as P_2'. Selecting odd P_i''s between A and B and even P_i''s between A and B until it is not possible to select any more of the P_i''s on segments AB and CD. This is illustrated in Figure 2.13. This construction leads to the property that the X coordinates of the P_i''s are smaller than those of the corresponding P_i's. Thus the number of P_i''s is greater than or equal to the number of P_i's. Thus, the path $p[t_k] - P_1' - \cdots - P_5'$ has its length at least equal to that of $p[t_k] - P_1 - \cdots - P_5$. Since the length of segment AB is $L_{\rm cone}$, the number of steps of such a path is at most equal to $L_{\rm cone}$ divided by the difference in X coordinates of any two consecutive P_i''s, i.e., $\lceil (2/\sqrt{3}) L_{\rm cone}/r_{\rm step} \rceil$. Since $\mathcal{E}$ has a finite diameter, there can be at most $\lceil \mathrm{diam}(\mathcal{E})/L_{\rm cone} \rceil$ cone sectors in any cone sector sequence. Thus, the upper bound (2.13) is established. ■

We now state two additional results needed to prove Theorem 2.3.3.

Proposition 2.4.5 (Maximum evasion angle) *If the pursuer uses the* GREEDY *strategy and if* $(\kappa^2 - 1) r_{\rm step}^2 \geq s^2[t]$, *where* $s[t] = \|p[t] - e[t]\|$, *then define*

$$\beta_{\max}[t] := \arccos\left(\frac{(\kappa^2 - 1) r_{\rm step}^2 - s^2[t]}{2 s[t] r_{\rm step}}\right). \tag{2.14}$$

If at some time t, $\beta[t] \geq \beta_{\max}[t]$, *then the pursuer moves towards* $e[t+1]$ *and traps*

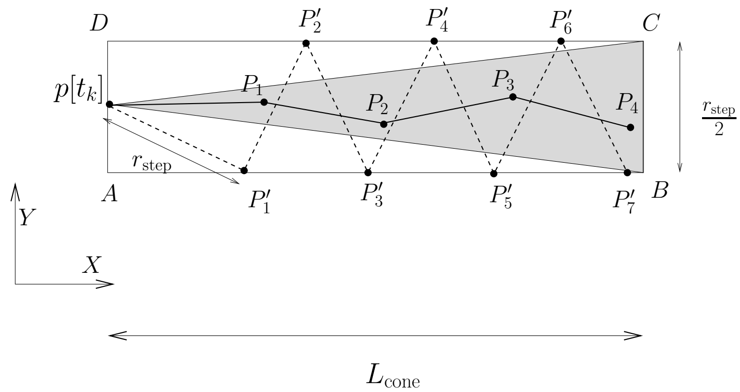

Figure 2.13. Upper bound on the number of steps a pursuer can be inside a cone sector. The cone sector $\mathcal{C}_{k,0}$ is illustrated here. The dotted path shows a hypothetical pursuer path that takes the maximum number of steps before leaving a cone sector.

the evader.

This result is obtained by applying the cosine rule to $\triangle p[t]e[t]e[t+1]$, where the notation $\triangle ABC$ stands for triangle formed by points A, B and C, as shown in Figure 2.14.

.

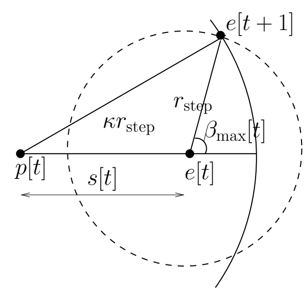

Figure 2.14. Constraint on maximum evasion angle. The dotted circle represent the evader's motion disc. The circle centered at $p[t]$ (shown partially here) is the pursuer's sensing range.

Lemma 2.4.6 (Constraint on maximum evasion angle) *For the evader to move out of a cone sector sequence $\mathcal{C}_k$, described in Definition 2.4.3, there exists a time in-*

stant $t \in [t_k, t_{k+1}[$ (ref. Definition 2.4.3) such that

$$|\beta[t]| > \frac{\theta}{2M^*} =: \beta_c, \tag{2.15}$$

where M^* is defined in Proposition 2.4.4.

Proof: For the evader to move out of the cone sector sequence $\mathcal{C}_k$, the sum of the angles of deviation for the pursuer must exceed half of the cone angle θ, i.e.,

$$\sum_{t=t_k}^{t_{k+1}} |\alpha[t]| > \frac{\theta}{2}.$$

Geometrically, this condition implies that the angle between the vectors $e[t_{k+1}] - p[t_{k+1}]$ and $e[t_k] - p[t_k]$ must be at least $\frac{\theta}{2}$. This is illustrated in Figure 2.15. From Proposition 2.4.2, it implies that

$$\sum_{t=t_k}^{t_{k+1}} |\beta[t]| > \frac{\theta}{2}.$$

Equation (2.15) now follows from the fact that $t_{k+1} - t_k \leq M^*$, for every k, since there exists a maximum number of time steps M^* for which the evader can remain inside any cone sector sequence, as derived in Proposition 2.4.4. ■

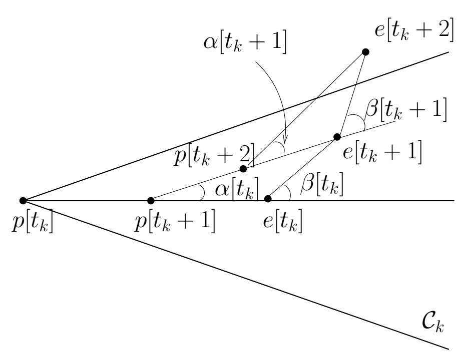

Figure 2.15. Illustrating Lemma 2.4.6. This is a case of the evader moving out of the cone sector sequence $\mathcal{C}_k$ by moving out of $\mathcal{C}_{k,0}$.

We are now ready to prove Theorem 2.3.3.

Proof of Theorem 2.3.3: Two cases need to be considered:

(i) *Evader does not move out of a cone sector sequence*: Capture follows from the construction of the cone sector sequence and from Proposition 2.4.4.

(ii) *Evader moves out of a cone sector sequence*: In this case, we seek to show that the evader cannot keep moving out of an arbitrarily large number of cone sector sequences. If the evader leaves the cone sector sequence $\mathcal{C}_k$, then for some $\tau \in \{t_k, \ldots, t_{k+1} - 1\}, \beta[\tau] > \beta_c$. Applying the cosine rule to $\triangle p[\tau]e[\tau]e[\tau+1]$, we obtain

$$
\begin{aligned}
& s^2[\tau+1] = r_{\text{step}}^2 + (s[\tau] - r_{\text{step}})^2 + 2r_{\text{step}}(s[\tau] - r_{\text{step}})\cos\beta[\tau], \\
\implies \quad & s^2[\tau] - s^2[\tau+1] = 2r_{\text{step}}(s[\tau] - r_{\text{step}})(1 - \cos\beta[\tau]).
\end{aligned}
$$

Using equation (2.15) and since

$$
s[\tau] + s[\tau+1] \leq 2\kappa r_{\text{step}},
$$

we obtain

$$
s[\tau+1] - r_{\text{step}} \leq \left(1 - \frac{(1 - \cos(\frac{\theta}{2M^*}))}{\kappa}\right)(s[\tau] - r_{\text{step}}). \tag{2.16}
$$

Defining $\chi_k := s[t_k] - r_{\text{step}}$, we conclude that

$$
\begin{aligned}
\chi_{k+1} \leq s[\tau+1] - r_{\text{step}} &\leq \left(1 - \frac{(1 - \cos(\frac{\theta}{2M^*}))}{\kappa}\right)(s[\tau] - r_{\text{step}}) \\
&\leq \left(1 - \frac{(1 - \cos(\frac{\theta}{2M^*}))}{\kappa}\right)\chi_k, \qquad (2.17)
\end{aligned}
$$

where the first and third inequalities follow from the fact that distance $s[t]$ is non-increasing in the Greedy strategy and the second inequality follows from equation (2.16). Recall that $\kappa > 1$ by assumption and hence the term in the parenthesis is positive and strictly less than 1. Thus, $\chi_k \to 0$ asymptotically, i.e., the distance between the pursuer and evader tends to r_{step} asymptotically. Moreover, for $\kappa > 2$, the distance reduces to $(\kappa - 1)r_{\text{step}}$ after a finite time. Thus, the motion disc of the evader will become completely contained within the sensing disc of the pursuer. Hence, the result follows.

The case of $\kappa = 2$: We have seen that the distance $s[t]$ between the pursuer and evader tends asymptotically to r_{step}. From Proposition 2.4.5, we obtain that as $s[t] \to r_{\text{step}}$, the angle $\beta_{\max} \to 0$. So, after some finite time,

$$\beta_{\max} < \frac{\theta}{2M^*} =: \beta_{\text{c}}.$$

Thus, the evader becomes confined to the present cone sector sequence according to Lemma 2.4.6 and from Proposition 2.4.4, and we can see from part (i) of this proof that the pursuer traps the evader within its sensing radius.

If $\kappa < 2$: We have seen that at each time step t, there is a maximum value $\beta_{\max}[t]$ of the evasion angle $\beta[t]$, so that the evader's next step $e[t+1]$ is not in the pursuer's sensing disc centered at $p[t]$. This is shown in Figure 2.16. The key idea of this part of the proof is that if we ensure that for all subsequent times after a certain time t^*, $\beta_{\max}[t]$ is less than the minimum value β_c (cf. Lemma 2.4.6) needed for the evader to leave a cone sector sequence, then the evader is forced to remain inside a final cone sector sequence and trapping follows from part (i). In previous cases, we have seen

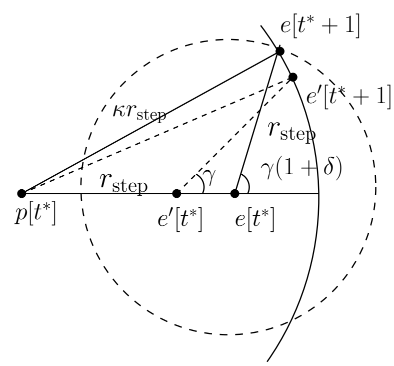

Figure 2.16. Illustrating parameters in Equation (2.18). $e'[t^*]$ is a point such that $\|p[t^*] - e'[t^*]\| = r_{\text{step}}$. γ is the value of the maximum evasion angle if the evader were at $e'[t^*]$. The circle of radius κr_{step} around the pursuer (shown partially here) is the pursuer's sensing disc which the dotted circle around $e[t^*]$ is the evader's motion disc.

that the Greedy strategy reduces the distance $s[t]$ asymptotically to r_{step}. Thus after a finite time t^*, $s[t^*]$ attains a value such that the maximum evasion angle is less than or equal to $(1+\delta)\gamma$, where γ is the maximum evasion angle if the evader is at $e'[t^*]$, which satisfies $\|p[t^*] - e'[t^*]\| = r_{\text{step}}$ and δ is a given positive number. At this time instant t_{final}, let the pursuer construct a new cone sector sequence, $\mathcal{C}_{\text{final}}$. So, if

$$(1+\delta)\gamma M^* = \frac{\theta}{2}, \tag{2.18}$$

where M^* and θ are defined in Proposition 2.4.4 and in the definition of a cone respectively, then for some $\tau \in \{t_{\text{final}}, \ldots, t_{\text{final}} + M^*\}$, $\beta[\tau] \geq (1+\delta)\gamma = \beta_{\text{c}}$ for the evader to leave $\mathcal{C}_{\text{final}}$. This means that the evader is forced to step inside the sensing disc of the pursuer or to remain inside the final cone $\mathcal{C}_{\text{final}}$. In both cases, the pursuer traps the evader within its sensing radius. From equation (2.18),

$$\gamma < \frac{\theta}{2M^*} = \beta_{\text{c}}.$$

Applying the cosine rule to $\triangle p[t]e'[t]e'[t+1]$,

$$\kappa = \sqrt{2 + 2\cos\gamma} > \sqrt{2 + 2\cos\beta_{\text{c}}}.$$

Thus, we have shown that if $\kappa > \sqrt{2 + 2\cos\beta_{\text{c}}}$, then the pursuer's Greedy strategy guarantees that the evader is trapped.

Computing an upper bound on the trapping time: We have seen that when the pursuer uses the Greedy strategy, the evader cannot leave an arbitrarily large number of cone sector sequences. Thus, to compute an upper bound on the trapping time, we compute an upper bound on the number of cone sector sequences that the evader can leave. We have seen that using the Greedy strategy, $\beta_{\max} \leq \beta_{\text{c}}$ after finite time. From (2.14), we can determine that distance s_{c} for which $\beta_{\max} = \beta_{\text{c}}$, so that subsequently, the evader is confined to the final cone sequence:

$$s_{\text{c}} = \left(\sqrt{\kappa^2 - \sin^2\beta_{\text{c}}} - \cos\beta_{\text{c}}\right) r_{\text{step}}.$$

If k is the final cone sequence index, then using equation (2.17),

$$s_{\text{c}} - r_{\text{step}} \leq \chi_k \leq \eta\chi_{k-1} \leq \cdots \leq \eta^k(\kappa - 1) r_{\text{step}},$$

where $\eta = 1 - (1 - \cos(\theta/2M^*))/\kappa$ and the worst-case $\chi_0 = (\kappa - 1)r_{\text{step}}$. Upon simplifying, we obtain

$$k \leq \left\lceil \frac{\log(\sqrt{\kappa^2 - \sin^2\beta_c} - \cos\beta_c - 1) - \log(\kappa - 1)}{\log(\eta)} \right\rceil.$$

The result now follows from the fact that for the case of $\kappa < 2$, we construct an extra final cone sequence and the maximum number of steps in each cone sequence can be at most M^*. The asymptotic result follows by routine simplifications. ■

Proof of Proposition 2.3.4: We prove this result by determining a set of initial conditions and an evader strategy that leads to evasion. Suppose at time t, the pursuer and the evader are on a circle Ω with radius $\rho = r_{\text{step}}/\sqrt{4 - \kappa^2}$, such that $\|e[t] - p[t]\| = r_{\text{step}}$ as shown in Figure 2.3. The evader is not trapped as its motion disc is not completely contained inside the pursuer's sensing disc. An evader strategy is to choose a point $e[t+1]$ on Ω such that $\|e[t] - e[t+1]\| = r_{\text{step}}$. Since $\rho = r_{\text{step}}/\sqrt{4 - \kappa^2}$, $e[t+1]$ lies outside the pursuer's sensing disc before its move at time $t+1$. By the GREEDY strategy, $p[t+1] = e[t]$. Thus, $\|e[t+1] - p[t+1]\| = r_{\text{step}}$ and the evader can avoid getting trapped. ■

2.4.2 Multiple Pursuer Problem

We first state a property of the effective length of the trapping chain.

Proposition 2.4.7 *The effective length of the trapping chain satisfies*

$$\frac{2(\sqrt{4\kappa^2 - 25}(N - 3) - \pi\kappa)}{\pi} < \frac{l}{r_{\text{step}}} < \sqrt{4\kappa^2 - 25}N - 2\kappa.$$

Proof: The left hand side of the inequality follows from the fact that the circumference of the circle passing through the vertices of the trapping chain is greater than the sum of the distances of neighboring vertices. The right hand side follows from repeated use of the triangle inequality. ■

Proof of Theorem 2.3.7: Let the evader be located at a point $Y_e \in \mathcal{G}$ and let its distance from the edge AB be y, as shown in Figure 2.17. Note that the distance of the evader from the edge AD does not play any role in what follows. The main idea behind this proof is as follows: Y_e would lie in the shaded region in Figure 2.17 if $l_0 + 2r_{\text{sens}} < y$ or $l_0 - 2r_{\text{sens}} > y$. This is equivalent to choosing a length equal to the effective length l of the trapping chain from a total length $l + 4r_{\text{sens}}$, if we let l_0 take a uniformly random value from $[-2r_{\text{sens}}, l + 2r_{\text{sens}}]$. Thus, the probability of success for the pursuers is at least the ratio of l to $l + 4r_{\text{sens}}$.

To be more specific, let the spatial probability density of the Y coordinate of the evader inside $\mathcal{G}$ be $p(y)$. Thus, $\int_0^{\operatorname{diam}\mathcal{G}} p(y)dy = 1$. The probability that the evader is detected inside the capture region $\mathcal{S}$ is given by

$$P(e \in \mathcal{S}) = \int_{-2r_{\text{sens}}}^{l+2r_{\text{sens}}} P(e \in \mathcal{S} | l_0 = k) P(l_0 = k) dl_0,$$

where $k \in [-2r_{\text{sens}}, l + 2r_{\text{sens}}]$. Assuming the pursuers have no information about the evader's location inside $\mathcal{G}$, l_0 is chosen uniformly randomly from $[-2r_{\text{sens}}, l + 2r_{\text{sens}}]$. Hence, we have

$$\begin{aligned}
P(e \in \mathcal{S}) &\geq \int_{-2r_{\text{sens}}}^{l+2r_{\text{sens}}} P(e \in \mathcal{S} | l_0 = k) \frac{1}{l + 4r_{\text{sens}}} dl_0 \\
&= \frac{1}{l + 4r_{\text{sens}}} \int_{-2r_{\text{sens}}}^{l+2r_{\text{sens}}} \Big(\sum_{j=0}^{n-1} \int_{l_0+2r_{\text{sens}}+j(l+2r_{\text{sens}})}^{l_0+2r_{\text{sens}}+j(l+2r_{\text{sens}})+l} p(y)dy \\
&+ \int_{l_0+2r_{\text{sens}}+n(l+4r_{\text{sens}})+l}^{\operatorname{diam}\mathcal{G}} p(y)dy \Big) dl_0,
\end{aligned}$$

where $n := \lceil \operatorname{diam}\mathcal{G}/(l + 4r_{\text{sens}}) \rceil$ is the number of times the pursuers sweep to clear the entire environment. Since the variables l_0 and y are independent (cf. Figure 2.18 for the region of integration), changing the order of integration gives

$$\begin{aligned}
P(e \in \mathcal{S}) &\geq \frac{1}{l + 4r_{\text{sens}}} \sum_{j=0}^{n-1} \int_{j(l_0+4r_{\text{sens}})}^{(j+1)(l_0+4r_{\text{sens}})} p(y) f(y, l) dy \\
&= \frac{1}{l + 4r_{\text{sens}}} \int_0^{n(l_0+4r_{\text{sens}})} p(y) f(y, l) dy,
\end{aligned}$$

where

$$f(y,l) := \begin{cases} \int_{-2r_{\text{sens}}}^{y-2r_{\text{sens}}} dl_0 + \int_{y+2r_{\text{sens}}}^{l+2r_{\text{sens}}} dl_0, & \text{for } y \le l, \\ \int_{y-2r_{\text{sens}}-l}^{y-2r_{\text{sens}}} dl_0, & \text{otherwise.} \end{cases}$$

In both cases, $f(y,l) = l$. Thus, the minimum probability of success is $l/(l + 4r_{\text{sens}})$, since $\int_0^{n(l_0+4r_{\text{sens}})} p(y)dy = \int_0^{\operatorname{diam}\mathcal{G}} p(y)dy + \int_{\operatorname{diam}\mathcal{G}}^{n(l_0+4r_{\text{sens}})} p(y)dy$, and $p(y) = 0$ outside of $\mathcal{G}$. The second inequality in part (i) follows by use of the left hand inequality in Proposition 2.4.7. The reason why this is a lower bound on the required probability is that if the pursuers had some information about the evader's location, then they could choose l_0 randomly from a smaller interval than the current one and thus increase the probability of detecting the evader in the capture region.

From the SWEEP strategy, the width of each strip swept is $l + 4r_{\text{sens}}$. So the maximum number of strips after which the sweep phase terminates is $\lceil \operatorname{diam}(\mathcal{G})/(l + 4r_{\text{sens}}) \rceil$. It takes at most $(\operatorname{diam}(\mathcal{G}) + 2(l + 2r_{\text{sens}}))/r_{\text{step}}$ time steps for the pursuers to clear a strip followed by aligning themselves parallel to the adjacent strip. The result now follows using Proposition 2.4.7. ■

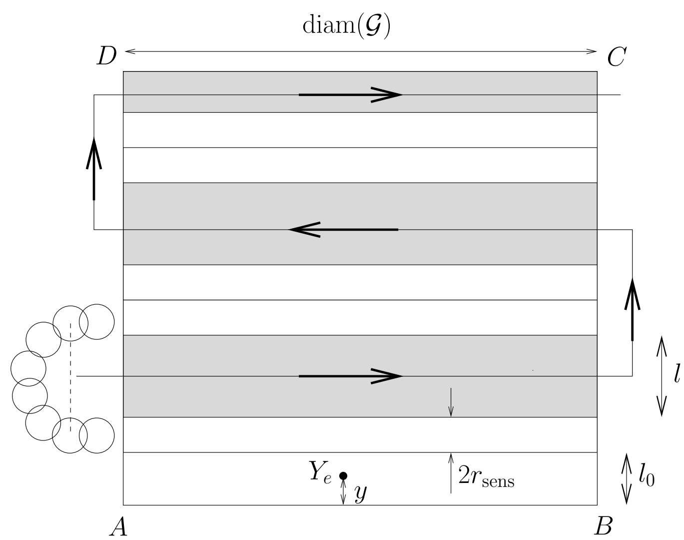

Figure 2.17. Illustrating the proof of Theorem 2.3.7.

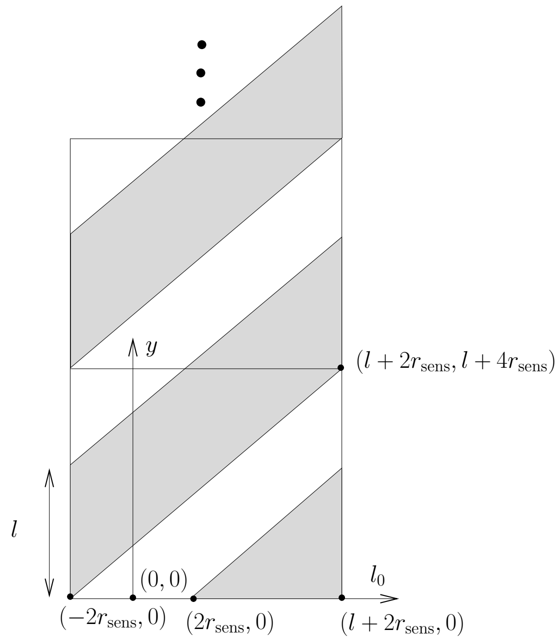

Figure 2.18. The region of integration in determining $P(e \in \mathcal{S})$ in the proof of Theorem 2.3.7. Fix a value of l_0 in the interval $(-2r_{\text{sens}}, l + 2r_{\text{sens}})$ to get the values of y that correspond to $P(e \in \mathcal{S})$.

To prove Theorem 2.3.9, we first establish the following properties of a trapping chain. In what follows, given points $a, b, c \in \mathbb{R}^2$, the notation $\text{dist}(a, bc)$ is the distance of point a from the line bc.

Lemma 2.4.8 (Trapping chain properties) *If $e[t] \in \mathcal{S}[t]$, then the following statements hold:*

1. *If* $\text{dist}(e[t], p_j[t]p_{j+1}[t]) > \frac{3}{2}r_{\text{step}}$, *for all* $j \in \{1, \ldots, N-1\}$, *then the evader cannot step outside* $\text{Co}\{p_1[t], \ldots, p_N[t]\}$ *at time* $t+1$ *by crossing* $p_j[t]p_{j+1}[t]$.

2. *If* $\text{dist}(e[t], p_j[t]p_{j+1}[t]) \leq \frac{3}{2}r_{\text{step}}$ *or* $\text{dist}(e[t+1], p_j[t]p_{j+1}[t]) \leq \frac{3}{2}r_{\text{step}}$, *for some* $j \in \{1, \ldots, N-1\}$, *then the evader is* trapped within the sensing radii *of pursuer* p_j *or* p_{j+1} *or of both* p_j *and* p_{j+1}.

3. There exists a $\phi > 0$, independent of N, such that for every point

$q \in \bigcup_{j\in\{3,\dots,\lfloor\frac{N}{2}\rfloor+1\}} \mathcal{B}_{p_j}(r_{\text{sens}}) \cap \mathring{\text{Co}}\{p_2,\dots,p_{N-1}\}$,

$$\angle qp_2p_{N-1} > \phi,$$

Proof: Parts (i) and (ii) follow from the definitions of trapping within sensing radii and from the construction of the trapping chain. For part (iii), we can see that for $j^* = \lfloor\frac{N}{2}\rfloor + 1$ if q (in the specified set) is the point of intersection of the tangent from p_2 to the sensing disc of p_{j^*}, then the angle $\angle qp_2p_{N-1}$ is minimized. This follows from the fact that the line $p_2p_{j^*}$ is parallel to $p_3 - p_{j^*-1}$. This angle is minimum when $N = 5$. Thus, given a $\kappa \geq 4$, from trigonometry, we obtain

$$\phi = \frac{\pi}{4} - \arctan\left(\frac{\kappa}{\sqrt{3\kappa^2 - 25}}\right).$$

■

The use of the Circumcenter strategy in the pursuit phase and the geometry of the trapping chain gives us the following result.

Lemma 2.4.9 *If the evader is trapped within the union of the sensing radii of pursuers at time t_{trap}, for every $j \in \{1,\dots,N-1\}$, then*

$$\text{dist}(e[t_{\text{trap}}], p_j[t_{\text{trap}}]p_{j+1}[t_{\text{trap}}]) > \frac{r_{\text{step}}}{2}.$$

Proof: Let the evader be trapped at time t_{trap} in the sensing radii of the pursuers. From part (ii) of Lemma 2.4.8, at time $t_{\text{trap}} - 1$ and for every $j \in \{1,\dots,N-1\}$,

$$\text{dist}(e[t_{\text{trap}} - 1], p_j[t_{\text{trap}} - 1]p_{j+1}[t_{\text{trap}} - 1]) > \frac{3}{2}r_{\text{step}}.$$

Thus, immaterial of where the evader decides to step, its distance from $p_j[t_{\text{trap}} - 1]p_{j+1}[t_{\text{trap}} - 1]$ is greater than $\frac{r_{\text{step}}}{2}$. Two cases are possible:

(a) *the evader steps inside the sensing disc of some pursuer p_j:* There are two further possibilities. If $\mathrm{dist}(e[t_{\mathrm{trap}}], p_j[t_{\mathrm{trap}}-1]p_{j+1}[t_{\mathrm{trap}}-1]) \leq \frac{3}{2}r_{\mathrm{step}}$, then the evader is trapped by part (ii) of Lemma 2.4.8 and the present lemma is proven. Else, we have $\mathrm{dist}(e[t_{\mathrm{trap}}], p_j[t_{\mathrm{trap}}-1]p_{j+1}[t_{\mathrm{trap}}-1]) > \frac{3}{2}r_{\mathrm{step}}$. Now, even in the case when p_j uses part (ii) of the CIRCUMCENTER strategy,
$\mathrm{dist}(e[t_{\mathrm{trap}}], p_j[t_{\mathrm{trap}}]p_{j+1}[t_{\mathrm{trap}}]) > \frac{r_{\mathrm{step}}}{2}$, for every $j \in \{1, \ldots, N-1\}$.

(b) *the evader steps outside the sensing disc of every pursuer:* In a trapping chain, the overlap between the sensing discs of any two neighboring pursuers has the property that length of the common chord of these discs is greater than $\frac{3}{2}r_{\mathrm{step}}$. This means that even if any two neighboring pursuers p_j and p_{j+1} happen to move parallel to each other, we have $\mathrm{dist}(e[t_{\mathrm{trap}}], p_j[t_{\mathrm{trap}}]p_{j+1}[t_{\mathrm{trap}}]) > \frac{r_{\mathrm{step}}}{2}$. ■

We now present the proof of Theorem 2.3.9.

Proof of Theorem 2.3.9:

We first look at a case in which $\mathrm{dist}(e[t_{\mathrm{sweep}}], p_j[t_{\mathrm{sweep}}]p_{j+1}[t_{\mathrm{sweep}}]) \leq \frac{3}{2}r_{\mathrm{step}}$ for some $j \in \{1, \ldots, N-1\}$. In this case, the evader is already trapped within the sensing radii of the pursuers, from part (ii) of Lemma 2.4.8 and the result holds.

Now let $\mathrm{dist}(e[t_{\mathrm{sweep}}], p_j[t_{\mathrm{sweep}}]p_{j+1}[t_{\mathrm{sweep}}]) > \frac{3}{2}r_{\mathrm{step}}$, for every $j \in \{1, \ldots, N-1\}$. There are two possibilities: if $e[t+1] \in \mathcal{S}^e[t]$, for any $t \geq t_{\mathrm{sweep}}$, then there is a pursuer p_j for which $y^e[t+1] = e[t+1]$. This pursuer uses part (ii) of the CIRCUMCENTER strategy and the evader is trapped within the sensing radius of p_j. Part (iii) of the result follows using Lemma 2.4.9.

So, let $e[t_{\mathrm{sweep}}+1] \notin \mathcal{S}[t_{\mathrm{sweep}}]$. Now, the pursuers compute the circumcenter O of $\triangle p_2[t_{\mathrm{sweep}}]e[t_{\mathrm{sweep}}]p_{N-1}[t_{\mathrm{sweep}}]$. Lemma 2.4.8 implies that the evader cannot step out of the pursuers' convex hull by crossing line $p_j[t]p_{j+1}[t]$, for any $j \in \{1, \ldots, N-1\}$. Thus, it suffices to show that the evader cannot leave the pursuers' convex hull by crossing line $p_1[t]p_N[t]$. In fact, we show that at the end of every pursuer move, the evader remains on the same side of p_2p_{N-1} until it gets trapped. We argue this as follows. As illustrated in Figure 2.19, any point on lines $p_2[t_{\text{sweep}}]O$ and $p_{N-1}[t_{\text{sweep}}]O$ is reached faster by p_2 and p_{N-1} respectively than by the evader. Thus, the motion of the evader is confined to the convex hull of $\{O, p_2, \ldots, p_{N-1}\}$, which reduces to the point O in a number of time steps upper bounded by

$$\max_{j \in \{2,\ldots,N-1\}} \left\lceil \frac{\|p_j[t_{\text{sweep}}] - O\|}{r_{\text{step}}} \right\rceil,$$

which is essentially the time taken by the furthest pursuer to reach O. Thus,

$$t_{\text{trap}} \leq \frac{R + l + 2\kappa r_{\text{step}}}{r_{\text{step}}},$$

where R denotes the circumradius of $\triangle p_2[t_{\text{sweep}}]e[t_{\text{sweep}}]p_{N-1}[t_{\text{sweep}}]$. From elementary geometry, at time t_{sweep} we have

$$R = \frac{\|p_2 - e\|\|p_{N-1} - e\|\|p_2 - p_{N-1}\|}{4\,\text{Area}(\triangle p_2 e p_{N-1})}, \leq \frac{l + 2\kappa r_{\text{step}}}{2\sin\angle e p_2 p_{N-1}}, \leq \frac{l + 2\kappa r_{\text{step}}}{2\sin\phi},$$

where the second and third inequalities follow from part (iii) of Lemma 2.4.8. Thus, part (ii) of the theorem follows from the use of right hand inequality in Proposition 2.4.7.

To prove part (iii), recall that pursuers p_1 and p_N move parallel to p_2 and p_{N-1}, respectively. Since the evader remains inside the convex hull of pursuers $p_2, \ldots, p_{N-1}$, the distance of the evader from line p_1p_N is always greater than $\frac{r_{\text{step}}}{2}$, until it gets trapped. From this fact and Lemma 2.4.9, part (iii) now follows. ■

Proof of Theorem 2.3.10: Part (i) follows from the Planes strategy. Thus, once the evader is trapped, it remains trapped at all successive time instants when the pursuers use the Planes strategy. Thus, the problem is reduced to one with unlimited sensing for the pursuers. To show that the algorithm leads to capture in finite time, we refer the reader to [57].

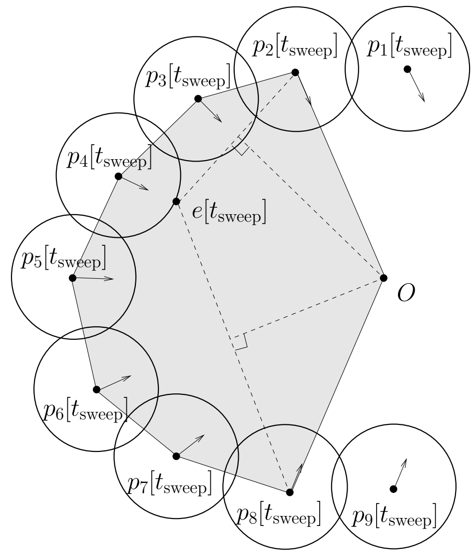

Figure 2.19. A move of the CIRCUMCENTER strategy. The evader is confined to the shaded region. The circles around the pursuers represent their sensing discs.

We now determine an upper bound on the time taken for the capture phase in terms of the trapping chain parameters. Referring back to the proof of correctness of the PLANES strategy, since the evader is in the convex hull of the pursuers, let v_j denote vectors of magnitude r_{step} in the direction of $p_j[t_{\mathrm{trap}}] - e[t_{\mathrm{trap}}]$. We now wish to seek a lower bound on the radius ϵ of the largest circle centered at the origin that can be inscribed inside the convex hull of the vectors v_j. This is equivalent to determining what is the largest of the angles $\angle p_i[t_{\mathrm{trap}}]e[t_{\mathrm{trap}}]p_j[t_{\mathrm{trap}}]$. Due to the property (2.11) and to the fact that the distance between any two adjacent pursuers in the trapping chain is non-increasing during the CIRCUMCENTER strategy, the angle $\angle p_i[t_{\mathrm{trap}}]e[t_{\mathrm{trap}}]p_j[t_{\mathrm{trap}}]$ is the greatest when i and j are adjacent and the evader is equidistant from both of them and at a distance of $\frac{r_{\mathrm{step}}}{2}$ from $p_i[t_{\mathrm{trap}}]p_j[t_{\mathrm{trap}}]$. This is shown in Figure 2.20. This gives, $\epsilon = r_{\mathrm{step}}\frac{r_{\mathrm{step}}/2}{\kappa r_{\mathrm{step}}} = \frac{r_{\mathrm{step}}}{2\kappa}$. Now, following [57], we observe that there exist three pursuers which contain the evader within their convex hull at the end of the pursuit phase, such that the sum of the distances of these pursuers to the evader decreases by at least $\frac{\epsilon}{3}$ at the end of every pursuer move.

The result now follows from the fact that the distance between any one of the three pursuers and the evader is at most $l + 2\kappa r_{\text{step}}$ at the end of the pursuit phase and the use of the right hand side inequality in Proposition 2.4.7. ■

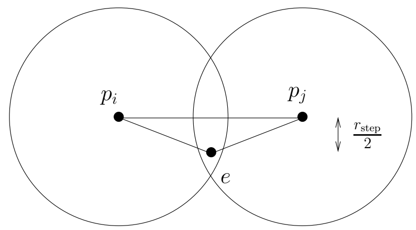

Figure 2.20. Illustrating proof of Theorem 2.3.10. Given the evader to be at a distance greater than $\frac{r_{\text{step}}}{2}$ from the line $p_i p_j$, the angle $\angle p_i[t_{\text{trap}}]e[t_{\text{trap}}]p_j[t_{\text{trap}}]$ is the greatest when the evader is equidistant from both of them

2.5 Simulation Results

We now present simulation studies to investigate the robustness of the algorithms to sensing errors. We study the performance of the algorithms in several cases such as different sensing to stepping radius ratio and faster evader. We also study the case of different number of pursuers in the multiple pursuer problem. All simulations were run using MATLAB®.

In the context of sensing errors, we assume two types of error models:

Gaussian errors: We assume zero-mean additive Gaussian measurement errors in the position of the evader with a standard deviation given by

$$\sigma_j[t] = \epsilon \|p_j[t] - e[t]\|,$$

for some constant $\epsilon \geq 0$. This means that the uncertainty in the location of the evader increases with its distance from a pursuer. The evader is defined to be captured if the probability of the evader being inside the motion disc of the pursuer before the pursuer's move is more than a certain threshold. In other words, for some t and for some pursuer p_j,

$$\mathcal{B}_{\sigma_j[t]}(y^p_{\text{bef}}[t]) \subset \mathcal{B}_{r_{\text{step}}}(p_j[t-1]),$$

where $\mathcal{B}_{\sigma_j[t]}(y^p_{\text{bef}}[t])$ denotes the circular region of radius $\sigma_j[t]$ centered at $y^p_{\text{bef}}[t]$.

Non-Gaussian errors: The measured distance is given by $(1+\epsilon^*)\|p_j[t]-e[t]\|$, where ϵ^* is a random variable uniformly distributed in the interval $[-\epsilon,\epsilon]$, where $\epsilon \geq 0$ is the specified error parameter. With respect to angular measurements, if θ_a is the actual angular location of the evader with respect to a local reference frame of a pursuer, then the measured angular location is given by $\theta_a+\epsilon_\theta$, where ϵ_θ is a random variable uniformly distributed in the interval $[-\Delta\theta,\Delta\theta]$, where the value of $\Delta\theta$ was chosen to be 1 degree. The evader is captured in this model if $y^p_{\text{bef}}[t] \in \mathcal{B}_{r_{\text{step}}}(p_j[t-1])$.

2.5.1 Single Pursuer Problem

Under the considered noisy sensor models:

- The Sweep strategy remains unchanged. It terminates when an evader measurement is available.
- For the Greedy and Lion strategies, the pursuer uses the noisy measurements of the evader position instead of the true position $e[t]$ to compute its next position.

For the evader's motion, we assume that it moves away from the pursuer with some randomization, while avoiding the boundary. Specifically,

- if the evader is not close to the boundary of the environment, then it chooses to move to a point on its motion circle, selected uniformly randomly in a sector with angle 0.2 radians. This sector is placed symmetrically along the line $e[t]p[t]$ and away from the pursuer.

- If the boundary is visible to the evader, then it chooses to move to a point $e[t+1]$ on its motion circle such that $\angle e[t+1]e[t]p[t] = \pi - 0.2$. Of the two points possible, the evader chooses that point which is further away from the boundary. In other words, when the evader reaches the boundary, it chooses to move to a point that is away from the pursuer as well as not very close to the boundary.

For our simulations, the environment is a circle with diameter 40 units. We assume $\kappa = 5$ units and $r_{\text{step}} = 1$ unit. The initial position of the evader was chosen uniformly randomly in the environment. An upper limit of $2,000$ time steps was set to decide whether the strategy terminated in a success.

The following is a summary of our findings:

(i) *Performance of the strategy with noisy measurements*: The plots of probability of success of the strategy and average capture times after detection (given that the strategy terminates with capture) for both noise models versus the respective error parameters ϵ are shown in Figure 2.21. We observe a similar trend in the performance of the strategy in both noise models.

(ii) *Different sensing to stepping radius ratios*: We repeated the simulations for the cases of the ratio of sensing to stepping ratio $\kappa = 7$ and $\kappa = 10$. We present the variation of probability of success in the Gaussian noise model in Figure 2.22.

(iii) *Faster evader*: We repeated the simulations for the case of faster evader. Assuming no noise, we present the variation of the probability of success in the top part of Figure 2.23. We observe that when the evader is at least $3/2$ times that of the pursuer, the proposed pursuer strategy is not efficient.

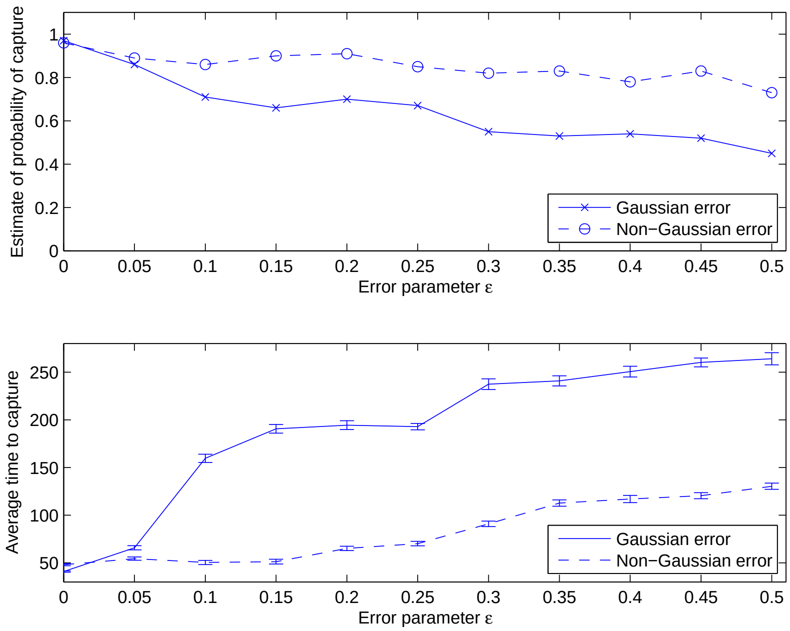

Figure 2.21. Effect of measurement noise in the single pursuer problem. For a particular evader strategy, we study how the capture probability and average capture time given that the strategy succeeds, vary with the noise parameter ϵ, under Gaussian and Non-gaussian error models. In the top figure, an interval of ± 0.1 (not shown to preserve clarity) about the probability estimates is the 95% confidence interval given by $\left[P(\epsilon) - 2\sqrt{\frac{0.25}{n}}, P(\epsilon) + 2\sqrt{\frac{0.25}{n}}\right]$, where $n = 100$ is the number of trials [101]. In the bottom figure, the vertical bars give a 95% confidence interval about the average capture time $T(\epsilon)$ which is given by $\left[T(\epsilon) - 2\sqrt{\frac{SD(\epsilon)}{nP(\epsilon)}}, T(\epsilon) + 2\sqrt{\frac{SD(\epsilon)}{nP(\epsilon)}}\right]$, where $SD(\epsilon)$ is the standard deviation in the capture time, $P(\epsilon)$ is the estimated probability of success and $n = 100$ is the number of trials [101].

2.5.2 Multiple Pursuer Problem

Under the considered noise models:

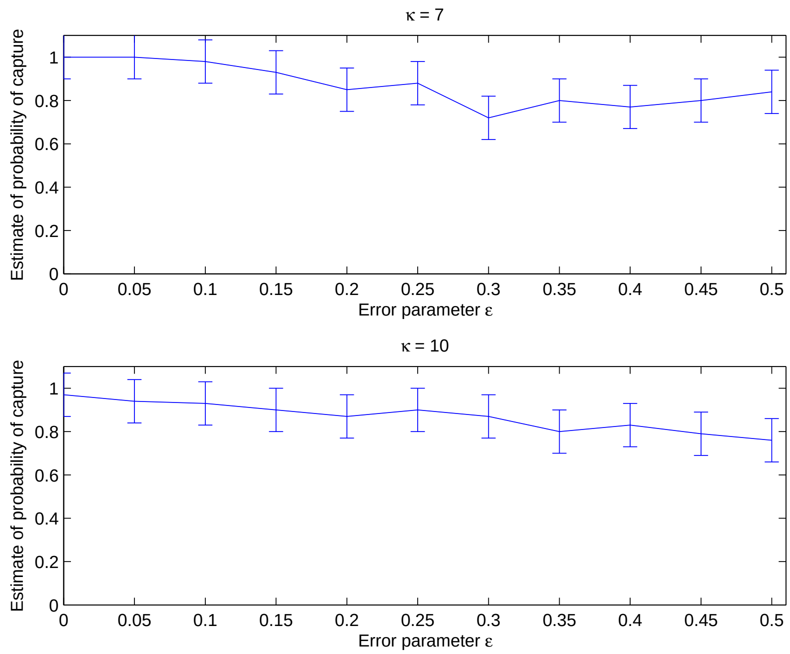

Figure 2.22. Effect of varying the sensing to stepping radius ratio κ in the single pursuer problem. For a particular evader strategy, we study how the capture probability varies for $\kappa = 7$ and $\kappa = 10$ with the noise parameter ϵ, under Gaussian noise model. The error bars are in accordance with Figure 2.21.

- The Sweep strategy remains unchanged. It terminates when an evader measurement is available.
- For the Circumcenter and Planes strategies, the team of pursuers use the average of the available evader measurements $\tilde{y}_{\text{t-1}}[t-1]$ and $\tilde{y}_{\text{t-1}}[t]$, to compute their next positions.

For the sake of simulations, we assume $N = 7$ pursuers with $\kappa = 5$ units and $r_{\text{step}} = 1$ unit. We assume a square field of edge length 100 units, where the evader is initially placed at a uniformly randomly selected location. Upon detection, we assume that the evader moves away from the closest pursuer with some randomization.

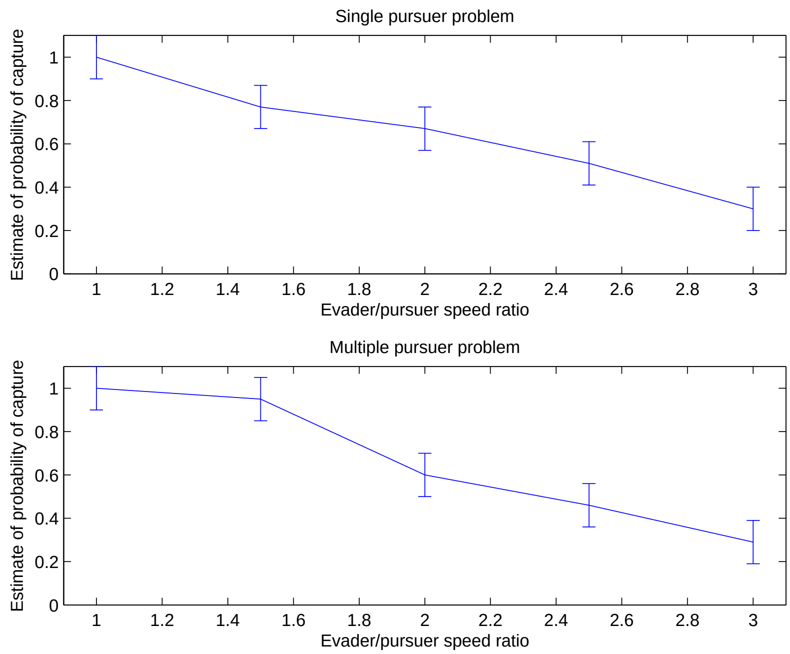

Figure 2.23. Performance of Sweep-Pursuit-Capture strategy against a faster evader. For a particular evader strategy, we study how the capture probability varies for higher evader speeds, assuming no measurement noise. The top figure presents the single pursuer case and the bottom figure presents the multiple pursuer case. The error bars are in accordance with Figure 2.21.

Specifically, it moves to a point on its motion circle, selected uniformly randomly in a sector of angle equal to 0.2 radians. This sector has its vertex at $e[t]$ and angle bisector parallel to the line $e[t_{\text{sweep}}]O$, where t_{sweep} is the time when the evader is detected and O is the circumcenter of the triangle $p_2[t_{\text{sweep}}]$, $p_6[t_{\text{sweep}}]$ and $e[t_{\text{sweep}}]$. We study how the average capture time after detection varies with ϵ. An upper limit of 1000 time steps was set to decide whether the strategy terminated in a failure.

The following is a summary of our findings:

(i) *Performance of the strategy with noisy measurements*: The plots of probability of success of the strategy and average capture times after detection (given that the strategy terminates with capture) for both noise models versus the respective error parameters ϵ are shown in Figure 2.24. We observe a similar trend in the performance of the strategy in both noise models.

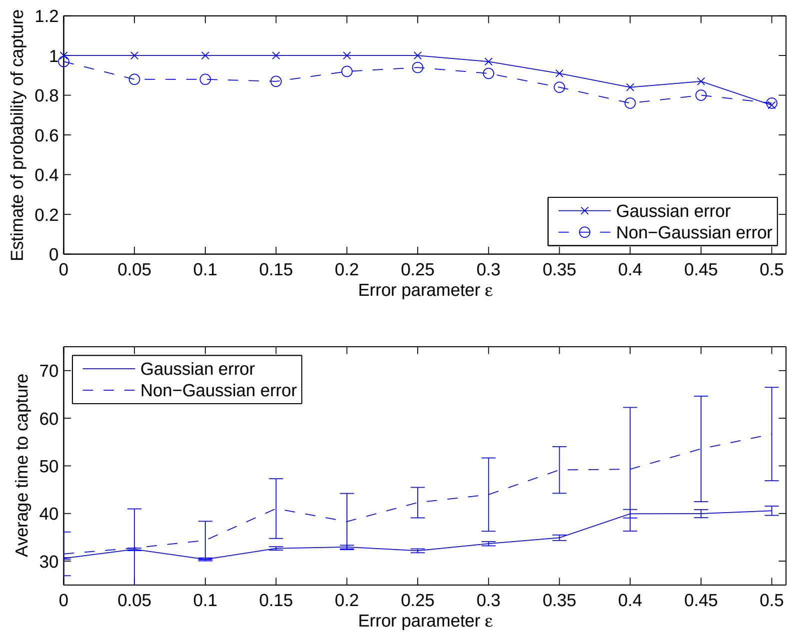

Figure 2.24. Effect of measurement noise in the multiple pursuer problem. For a particular evader strategy, we study how the capture probability (top figure) and average capture time (bottom figure) given that the strategy succeeds, vary with the noise parameter ϵ, under Gaussian and Non-gaussian error models. The error bars are in accordance with Figure 2.21.

(ii) *Different number of pursuers*: We repeated the simulations for the cases of the number of pursuers $N = 10$ and $N = 15$. We present the variation of probability of success in the Gaussian noise model in Figure 2.25.

(iii) *Faster evader*: We repeated the simulations for the case of faster evader. Assuming no noise, we present the variation of the probability of success in the bottom part of Figure 2.23. We observe that when the evader is at least 1.8 times

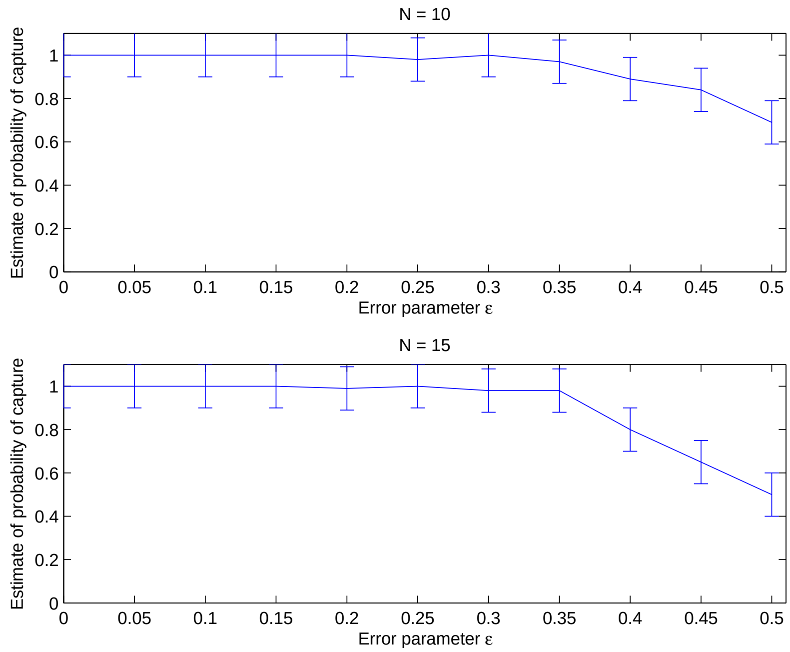

Figure 2.25. Effect of varying the number of pursuers N in the multiple pursuer problem. For a particular evader strategy, we study how the capture probability varies for $N = 10$ and $N = 15$ with the noise parameter ϵ, under Gaussian noise model. The error bars are in accordance with Figure 2.21.

that of the pursuers, the proposed pursuer strategy is not efficient.

2.6 Biological Interpretations

Our analysis in the previous sections can shed light on the trade-offs that predators face when deciding upon the group size. Based on our results from Section 2.3.2, we now study how the group size of the pursuers varies with the evader availability in the multiple pursuer problem.

For simplicity, we assume a square field where the evader is initially located and denote by $\delta := 1/\mathrm{diam}^2(\mathcal{G})$, the evader density. From the results in Section 2.3.2, an upper bound on the total time taken by the pursuers in all three phases of the strategy is given by

$$\frac{1}{\delta(aN+b)} + \frac{cN}{\sqrt{\delta}(aN+b)} + kN,$$

where $a := 2r_{\text{step}}^2\sqrt{4\kappa^2-25}/\pi$, $b := (2\pi\kappa - 6\sqrt{4\kappa^2-25})/\pi$, $c := 2r_{\text{step}}\sqrt{4\kappa^2-25}$ and $k := \sqrt{4\kappa^2-25}(1+1/\sin\phi) + 18\kappa\sqrt{4\kappa^2-25}$ are constants independent of the number of predators N or the evader density δ.

From part (i) of Theorem 2.3.7, we observe that when all other variables are kept constant, the lower bound on successful detection probability of the SWEEP strategy increases with N. However, a higher N results into a greater time to capture the evader. This suggests a trade-off on the group size N which we analyze as follows.

Let ν denote the nutritional content of the evader. We quantify the energy spent by each pursuer as the time taken to capture the evader. The energy gain from the pursuit is quantified as the amount of nutrition each participating pursuer receives from the evader. For a self-sustaining pursuit, we must have that the energy gained by each pursuer is at least equal to the energy spent during the hunt. Thus,

$$\frac{\nu}{N} \geq \frac{1}{\delta(aN+b)} + \frac{cN}{\sqrt{\delta}(aN+b)} + kN.$$

From this relation, we observe that for a given value of δ, there exists an upper limit on the number of pursuers in the group for which it is advantageous for the pursuers to engage in a pursuit with the prospect of gaining energy. A plot of the upper limit on the group size N versus the evader density δ is shown in Figure 2.26.

This analysis shows that for higher values of δ, a larger number of pursuers can be accommodated in the trapping chain. This is consistent with observations in the biology literature by Caraco and Wolf [28] that have reported higher group size in foraging lions during the wet season (prey abundance), than in the dry season, (prey scarcity). Further, from our analysis, it also follows that for a given evader density, the higher the prey nutrition value ν, the higher is the upper limit on the number of pursuers in the trapping chain. This is consistent with the observations reported by Griffiths [43] regarding how the size of hunting packs relate to the size of the prey relative to that of the predators.

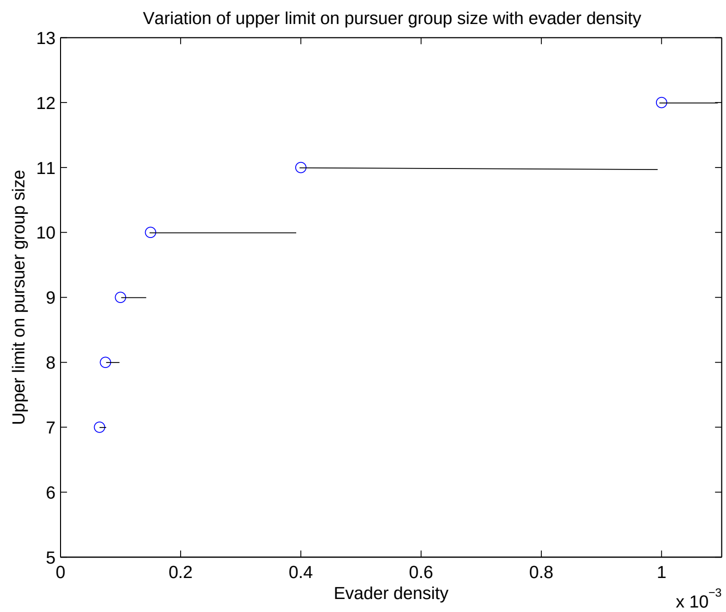

Figure 2.26. Plot of maximum group size of pursuers that can be sustained versus the evader density δ, for $\kappa = 5$, $r_{\text{step}} = 1$, $\nu = 10000$.

Summary

We have addressed discrete-time pursuit-evasion problems in the plane with sensing capabilities restricted to a finite disc. We considered two variants of the pursuit-evasion in discrete-time. The first involved a single pursuer and an evader in a bounded convex environment. The second was a formation design problem for multiple communicating pursuers to capture a single evader in a boundaryless environment. In both problems, the evader was initially located inside a bounded subset of the environment and moved only when detected.

We proposed a Sweep-Pursuit-Capture strategy for both problems. In the first problem, we gave sufficient conditions on the range of values taken by the ratio of sensing to stepping radius of the players so that the strategy of moving towards the last-sensed evader position lead to the evader being trapped within the pursuer's sensing disc and finally to capture. We also gave conditions under which there exist locations from which the evader can escape. In the second problem, we showed that the pursuers capture the evader with a certain probability that is independent of the initial evader location in a bounded region. We gave novel upper bounds on the total time taken to capture for both problems. We also presented simulation studies that suggest robustness with respect to sensing errors. Based on the upper bound on the capture time, we provided an upper bound on the pursuer group size for which the pursuit would be advantageous from the point of view of gaining energy. Our conclusions are consistent with observations reported in ecology literature.

Chapter 3

Pursuit with Minimalist Sensing

3.1 Introduction

Often pursuit strategies do not make use of the entire available information. For example, the GREEDY strategy from Chapter 2 requires only the bearing (relative heading) information of the evader location with respect to the pursuer. This motivates the question of whether it is possible to use only a part of the sensor information, such as bearing or relative distance and speeds, and still achieve capture. This would lead to design of sensors that provide a particular and relevant information more accurately rather than the entire data, and thus give rise to an efficient allocation and specialization of the system. In this chapter, we design pursuit strategies for problems in which only a part of the sensing information is needed.

The Grow-Intersect Algorithm and Related Work

At the heart of the problems presented in this chapter is Algorithm 1, which has been well-known in literature as the Grow-Intersect algorithm [87, 32], illustrated in Figure 3.1.

Algorithm 1: **The Grow-Intersect algorithm**

Assumes: The set $\hat{E}[t]$ that contains the evader at time t, and evader's maximum speed v .

1: **Grow** $\hat{E}[t]$ by an amount v in every possible direction.

2: **Intersect** the grown set with measurement $y[t+1]$.

3: **Output:** The set $\hat{E}[t+1]$ at time $t+1$.

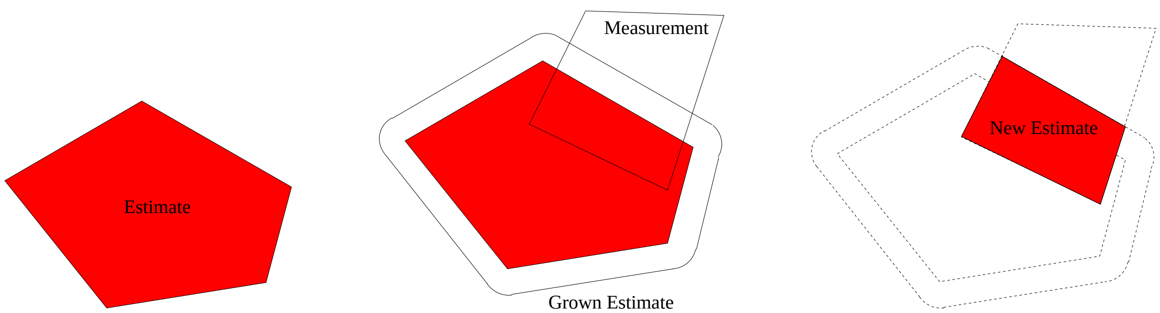

Figure 3.1. The Grow-Intersect Algorithm

Reducing sensor requirements to achieve certain tasks such as counting vertices in a polygonal environment or even capturing evaders has been considered in [96, 102]. With respect to pursuit under sensing constraints, [39] deals with a version of pursuer's visibility limited to a cone. [53] considers a graph environment, with the visibility limited to adjacent nodes, while [54] addresses a version of the Lion and Man problem in which the pursuer has only bearing information about the evader's location. [84] addresses the case in which the pursuer only knows an approximate location of the evader. [83] and [59] present a solution to the game under bounded measurement uncertainty in sensing the evader.

Other areas of research related to the problem we address, are target tracking and localization. Using distance-only measurements, [104] determines optimal motions for multiple mobile sensors to minimize the error in the posterior estimate of the target position. Using the Fisher Information Matrix, [94] characterizes a condition for local system observability of tracking a moving target in a plane with range-only measurements.

Contributions

We address discrete-time pursuit-evasion games played in the unbounded plane, between a pursuer and an evader. The pursuer wishes to reduce the distance between itself and the evader to 1 unit. We assume simple, first-order motion kinematics for both players. We normalize the speed of the pursuer unity and thus the evader's step size is upper bounded by $v < 1$. With respect to measurements, the pursuer is able to measure its distance from the evader before as well as after the evader's move, while the evader is assumed to have complete information of the pursuer's location. In continuous time, this is analogous to the pursuer being equipped with a sensor that measures the distance to the evader as well as the rate of change of this distance. [85] presents an example of one such sensor.

We present a pursuit strategy inspired by the *Grow-Intersect* algorithm and show that: (i) if the maximum evader step size $v < 0.5$, then the pursuer captures the evader in finite time, (ii) for the game played in $\mathbb{R}^3$: if $v < 0.5$, then two identical, cooperative pursuers capture the evader in finite time, and (iii) we provide upper bounds on the time taken to capture the evader in parts (i) and (ii). Finally, we present simulation studies in the planar case to address: (i) the case of $v \in [0.5, 1[$, (ii) the effect of additive, zero-mean Gaussian noise with variance proportional to the square of the distance between the evader and the pursuer on the outcome of the game, and (iii) a game with simultaneous moves.

We then consider a version of this problem in which the pursuer is equipped with a bearing-only sensor, i.e., it can detect the line through itself on which the evader lies, but without the orientation sense. An example of one such sensor is the emergency locator transmitter. We show that if the evader's speed is less than one-fourth of that of the pursuer, then our pursuit strategy leads to capture. We provide upper bounds on time taken to capture for both the formulations.

Organization

The problem formulation is described in Section 3.2. The capture strategy and main result is presented in Section 3.3. A cooperative pursuit version of this game is presented in Section 3.4. The proofs of the main results in Sections 3.3 and 3.4 are presented in Section 3.5. Simulations that address the case of evader speed $v \in [0.5, 1[$ and sensor noise are presented in Section 3.6. A version of the present game with simultaneous moves and a simulation study of the application of a modified capture strategy are presented in Section 3.6.3. The bearing-only formulation is presented in Section 3.7.

3.2 Problem Set-up

We assume a discrete-time model with alternate motion of the evader and the pursuer. The game is played in the unbounded plane. We assume simple, first-order motion kinematics for both players. The pursuer can move with a step size of at most 1 unit while the evader can move with a step size of $v < 1$. The pursuer is equipped with a range-only sensor that measures its distance from the evader. The evader is assumed to know exact information of the pursuer's location. Further, we assume that at each time instant, the players take measurements before and after the pursuer's move. Thus a *sequence* of the game consists of the following: (i) the evader moves, (ii) players take measurements, (iii) the pursuer moves, (iv) the players take measurements. This is shown in Figure 3.2. Capture is defined when the evader is not greater than a *unit* distance from the pursuer.

Let $e[t] \in \mathbb{R}^2$ and $p[t] \in \mathbb{R}^2$ denote the positions of the evader and the pursuer

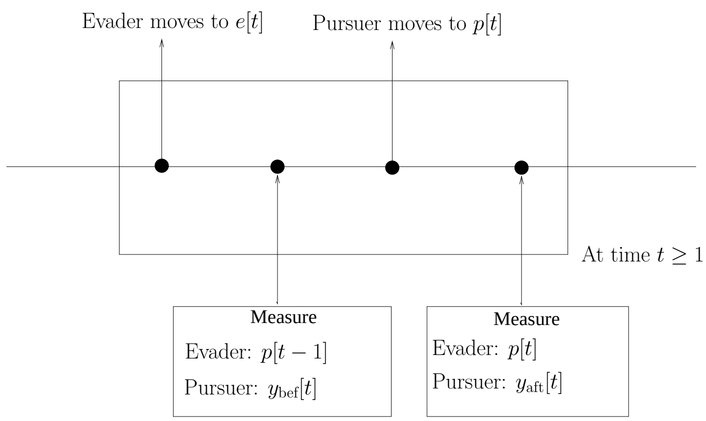

Figure 3.2. A *sequence* at each time instant $t \in \{1, 2, \dots\}$ in our alternate motion model. The players take measurements before and after the pursuer's move.

respectively, at time $t \in \mathbb{Z}_{\geq 1}$. The discrete-time equations of motion are

$$\begin{aligned} e[t] &= e[t-1] + u^e(e[t-1], \{p[\tau]\}_{\tau=0}^{t-1}), \\ p[t] &= p[t-1] + u^p(p[t-1], y_{\text{bef}}[t], y_{\text{aft}}[t]), \end{aligned} \tag{3.1}$$

where $\{p[\tau]\}_{\tau=1}^{t-1}$ denotes the set $\{p[0], p[1], \dots, p[t-1]\}$. For the pursuer, at the t^{th} time instant , $y_{\text{bef}}[t], y_{\text{aft}}[t] \in \mathbb{R}_{\geq 0}$ are the distances of the evader's position from the pursuer before and after the evader's move respectively. Thus, $y_{\text{bef}}[t] = \|e[t]-p[t-1]\|$ and $y_{\text{aft}}[t] = \|e[t] - p[t]\|$. The functions $u^e : \mathbb{R}^2 \times \underbrace{\mathbb{R}^2 \times \cdots \times \mathbb{R}^2}_{t \text{ times}} \to \mathbb{R}^2$ and $u^p : \mathbb{R}^2 \times \mathbb{R} \times \mathbb{R} \to \mathbb{R}^2$ are termed as *strategies* for the evader and pursuer respectively. Notice that in this formulation, we allow the evader the access to the entire history of the pursuer's motion, while we allow the pursuer the access to *only two* of the most recent evader measurements. The lack of symmetry between the number of arguments in strategies of the evader and the pursuer is due to the alternate motion model and due to the assumptions on the measurement models of the players.

Since the step sizes of each player are bounded, we have

$$\|u^e\| \leq v, \quad \text{and} \quad \|u^p\| \leq 1, \tag{3.2}$$

where $v < 1$. *Capture* takes place when for some $T_{\text{cap}} \in \mathbb{Z}_{\geq 0}$,

$$\|e[T_{\text{cap}}] - p[T_{\text{cap}} - 1]\| \leq 1 \quad \text{or} \quad \|e[T_{\text{cap}}] - p[T_{\text{cap}}]\| \leq 1. \tag{3.3}$$

The problem is *to determine a pursuer strategy u^p that guarantees capture for any evader strategy u^e.*

Remark 3.2.1 (Continuous-time analogy) *Such a model arises when one discretizes the continuous time pursuit-evasion game in which the pursuer is equipped with a sensor that continuously measures the distance to the evader as well as the rate of change of this distance.*

3.3 The Capture Strategy and Main Result

In this section, we describe our capture strategy and the corresponding main result. Our capture strategy has two phases: Initialization and Pursuit. These are described as follows.

3.3.1 Initialization phase

This phase lasts for only the first sequence. In the first sequence,

1. The evader moves to $e[1]$.
2. The pursuer gets the measurement $y_{\text{bef}}[1]$ and it constructs $\partial\mathcal{B}_{y_{\text{bef}}[1]}(p[0])$ which is a circle of radius $y_{\text{bef}}[1]$ around the point $p[0]$.
3. The pursuer randomly selects a direction to move and moves along it with unit step size.

4. The pursuer gets the measurement $y_{\text{aft}}[1]$ and it constructs $\partial\mathcal{B}_{y_{\text{aft}}[1]}(p[1])$ and computes the estimate

$$\hat{E}[1] := \partial\mathcal{B}_{y_{\text{aft}}[1]}(p[1]) \cap \partial\mathcal{B}_{y_{\text{bef}}[1]}(p[0]). \tag{3.4}$$

Since $\hat{E}[1]$ is an intersection of two non-concentric circles described in the right hand side of (3.4), we have the following result.

Proposition 3.3.1 (Initialization) $\hat{E}[1] = (\hat{e}_a[1], \hat{e}_b[1]) \in \mathbb{R}^2 \times \mathbb{R}^2$ *is an estimate of* $e[1]$.

If $\hat{e}_a[1] = \hat{e}_b[1]$, then the pursuer has accurately determined $e[1]$. In general, the pursuer is unable to distinguish between the two estimates.

3.3.2 Pursuit phase

We now present our pursuit strategy.

Until the evader is *not* captured, at time $t \geq 2$,

1. the pursuer selects a point $\hat{e}[t-1] \in \hat{E}[t-1]$ at random and moves towards it with full step size. Thus,

$$p[t] = p[t-1] + \frac{\hat{e}[t-1] - p[t-1]}{\|\hat{e}[t-1] - p[t-1]\|}. \tag{3.5}$$

2. The pursuer updates the estimate of the evader's position using

$$\hat{E}[t] := \partial\mathcal{B}_{y_{\text{bef}}[t]}(p[t-1]) \cap \Big(\hat{E}[t-1] \oplus \mathcal{B}_v(0)\Big) \cap \partial\mathcal{B}_{y_{\text{aft}}[t]}(p[t]), \tag{3.6}$$

   where $\mathcal{B}_v(0) \subset \mathbb{R}^2$ denotes the closed circular region of radius v around the origin $0 \in \mathbb{R}^2$ and the operation $\oplus$ denotes the Minkowski sum in the plane.

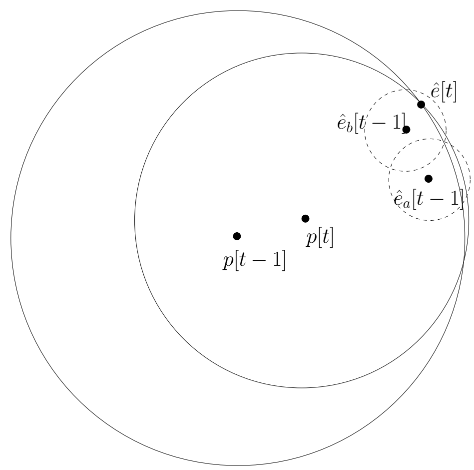

Figure 3.3. An instance of the pursuit strategy. The dotted circles have radii equal to v and denote the region where the evader can step at time t. This figure illustrates the case when the pursuer moves towards $\hat{e}_a[t-1]$ while the evader was actually at $\hat{e}_b[t-1]$ and consequently exactly localizes the evader at time t.

An instance of this strategy is shown in Figure 3.3. A simple induction argument gives the following result, the proof of which is presented in Section 3.5.

Lemma 3.3.2 (Evader estimate) *At every time instant $t \in \mathbb{Z}_{\geq 1}$,*

1. *The evader's position $e[t] \in \hat{E}[t]$, where $\hat{E}[t]$ is recursively defined using* (3.4) *and* (3.6)*.*

2. *The set $\hat{E}[t]$ contains at most two points $(\hat{e}_a[t], \hat{e}_b[t]) \in \mathbb{R}^2 \times \mathbb{R}^2$. Further, $\|\hat{e}_a[t] - p[t]\| = \|\hat{e}_b[t] - p[t]\|$, for every t.*

We now present the main result of this section.

Theorem 3.3.3 (Capture in $\mathbb{R}^2$) *If $v < 0.5$, then a single pursuer captures the evader using our capture strategy and in at most $\lceil (\|e[0]-p[0]\|+(1+2v))/(2(1-2v)) \rceil$*

time steps.

Remark 3.3.4 (Single pursuer in $\mathbb{R}^3$) *In $\mathbb{R}^3$, it is not clear whether it is possible to guarantee capture with a single pursuer using the proposed strategy. At each time instant t, the set of evader estimates $\hat{E}[t]$ in general contains more than just two points. This motivates the use of another cooperative pursuer in $\mathbb{R}^3$, which we address in the next section.*

3.4 Cooperative Pursuit in $\mathbb{R}^3$

We now present the pursuit problem in $\mathbb{R}^3$ played with two cooperative pursuers.

3.4.1 Problem Statement and Notation

The problem formulation is almost identical to the planar case except that now we have two identical pursuers which move simultaneously at their turn. The game is played in $\mathbb{R}^3$. Akin to (3.1), the equations of motion are given by

$$e[t] = e[t-1] + u^e(e[t-1], \{p[\tau]\}_{\tau=0}^{t-1}),$$
$$p_i[t] = p_i[t-1] + u^{p_i}(p_i[t-1], y^i_{\text{bef}}[t], y^i_{\text{aft}}[t]),$$

where for the i^{th} pursuer, $p_i[t] \in \mathbb{R}^3$ denotes its position at time t, $y^i_{\text{bef}}[t], y^i_{\text{aft}}[t] \in \mathbb{R}_{\geq 0}$ are the distances of the evader from it before and after the evader's move respectively and u^{p_i} is its strategy. The strategies satisfy (3.2) and capture is defined when for some $i \in \{1, 2\}$, (3.3) is satisfied.

The problem is *to design pursuer strategies u^{p_i} that guarantee capture for any evader strategy.*

3.4.2 Capture Strategy and Main result

We present our solution to the cooperative pursuit game played in $\mathbb{R}^3$. Again, our capture strategy has two phases: Initialization and Pursuit. These are described as follows.

Initialization phase

This phase lasts for only the first sequence. In the first sequence,

1. The evader moves to $e[1]$.

2. For $i = \{1, 2\}$, pursuer p_i gets the measurement $y^i_{\text{bef}}[1]$ and it constructs $\partial\mathcal{B}_{y^i_{\text{bef}}[1]}(p_i[0])$, i.e., the surface of a sphere of radius $y^i_{\text{bef}}[1]$ around $p_i[0]$.

3. Pursuer p_i selects a direction to move ensuring that $p_1[1] \neq p_2[1]$ and moves along it with unit step size.

4. Each pursuer p_i gets the measurement $y_{\text{aft}}[1]$ and it constructs $\partial\mathcal{B}_{y_{\text{aft}}[1]}(p_i[1])$ and computes the estimate

$$\hat{E}[1] := \bigcap_{i\in\{1,2\}} \Big(\partial\mathcal{B}_{y_{\text{aft}}[1]}(p_i[1]) \cap \partial\mathcal{B}_{y^i_{\text{bef}}[1]}(p_i[0])\Big). \tag{3.7}$$

For each $i \in \{1, 2\}$, the term in the outer parentheses in (3.7) is an intersection of the surfaces of two spheres in $\mathbb{R}^3$ and hence is a circle. Hence, $\hat{E}[1]$ is an intersection of two non-concentric circles and thus contains at most two points.

Pursuit phase

We now present our pursuit strategy.

Until the evader is *not* captured, at time $t \geq 2$,

(i) If $\hat{E}[t-1]$ contains only one point $\hat{e}[t-1]$, then the pursuer closer to it, say p_1 moves towards it with full step size. The other pursuer p_2 moves:

a) towards $\hat{e}[t-1]$ with maximum step size, if the three points $\hat{e}[t-1]$, $p_1[t-1]$ and $p_2[t-1]$ are not collinear.

b) anywhere inside except on the axis of a cone with vertex at $p_2[t-1]$, with $e[t-1]-p_2[t-1]$ as the axis and with half-angle equal to $\arcsin(v/\|e[t-1]-p_2[t-1]\|)$, with maximum step size, if the points $\hat{e}[t-1]$, $p_1[t-1]$ and $p_2[t-1]$ are collinear. Refer to Figure 3.6 for an illustration.

In case both pursuers are equidistant, then pursuer p_1 is the one that moves directly towards the evader. Otherwise, for $i = \{1, 2\}$, each pursuer p_i is assigned a unique point $\hat{e}_i[t-1]$ in $\hat{E}[t-1]$ and it moves towards it with full step size. Thus,

$$p_i[t] = p_i[t-1] + \frac{\hat{e}_i[t-1] - p_i[t-1]}{\|\hat{e}_i[t-1] - p_i[t-1]\|}. \tag{3.8}$$

(ii) The pursuer updates the estimate of the evader's position using

$$\hat{E}[t] := \Big(\hat{E}[t-1] \oplus \mathcal{B}_v(0)\Big) \bigcap_{i\in\{1,2\}} \Big(\partial\mathcal{B}_{y^i_{\mathrm{aft}}[t]}(p_i[t]) \cap \partial\mathcal{B}_{y^i_{\mathrm{bef}}[t]}(p_i[t-1])\Big). \tag{3.9}$$

where $\mathcal{B}_v(0) \subset \mathbb{R}^2$ denotes the closed sphere of radius v around the origin $0 \in \mathbb{R}^2$ and the operation $\oplus$ denotes the Minkowski sum in $\mathbb{R}^3$.

An instance of this strategy is shown in Figure 3.4. Akin to Lemma 3.3.2 in the single pursuer problem, we have the following result.

Lemma 3.4.1 (Evader estimate) *At every time instant $t \in \mathbb{Z}_{\geq 1}$,*

1. *Using the proposed cooperative pursuit strategy, both pursuers are at distinct locations in $\mathbb{R}^3$.*

2. *The set $\hat{E}[t]$ contains at most two points $(\hat{e}_1[t], \hat{e}_1[t]) \in \mathbb{R}^3 \times \mathbb{R}^3$. Further, for each $i \in \{1, 2\}$, $\|\hat{e}_1[t] - p_i[t]\| = \|\hat{e}_2[t] - p_i[t]\|$, for every t.*

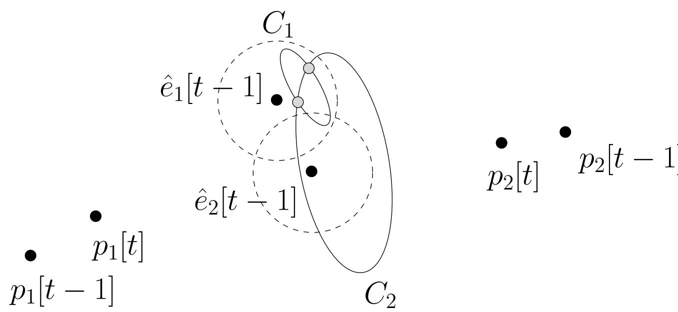

Figure 3.4. An instance of the cooperative pursuit in $\mathbb{R}^3$. The dotted circles have radii equal to v and denote the region where the evader can step at time t. Circles C_1 and C_2 (shown as ellipses here) are the intersections of the two spheres (not shown to preserve clarity) associated with each measurement for each pursuer. The lightly shaded dots is the set $\hat{E}[t]$.

3. *The evader's position $e[t] \in \hat{E}[t]$, where $\hat{E}[t]$ is recursively defined using* (3.7) *and* (3.9).

We now present the main result of this section.

Theorem 3.4.2 (Capture in $\mathbb{R}^3$) *If $v < 0.5$, then two pursuers capture the evader using the cooperative capture strategy and in at most $\lceil (\|e[0]-p_1[0]\| + \|e[0]-p_2[0]\| + 2(1+2v))/(1-2v) \rceil$ time steps.*

3.5 Proofs of the Main Results

In this section, we present the proofs of the main results presented in Sections 3.3 and 3.4.

3.5.1 Single pursuer in $\mathbb{R}^2$

We begin by proving Lemma 3.3.2.

Proof of Lemma 3.3.2:

We prove parts (i) using mathematical induction. Proposition 3.3.1 serves as the base of induction. Now assume $e[t-1] \in \hat{E}[t-1]$. Since the evader's step size is upper bounded by v, $e[t] \in \hat{E}[t-1] \oplus \mathcal{B}_v(0)$. From the definition of a sequence (ref. Section 3.2), $e[t]$ is contained in both $\partial\mathcal{B}_{y_{\text{bef}}[t]}(p[t-1])$ and $\partial\mathcal{B}_{y_{\text{aft}}[t]}(p[t])$. Thus, $e[t]$ is contained in the intersection of these three quantities and part (i) follows via the principle of induction.

By part (i) of this lemma, since both $\partial\mathcal{B}_{y_{\text{bef}}[t]}(p[t-1])$ and $\partial\mathcal{B}_{y_{\text{aft}}[t]}(p[t])$ contain $e[t]$, their intersection is non-empty and can contain at most two points due to the fact that they are non-concentric circles. The final statement follows from the fact that the intersection points of two circles are equidistant from their centers.

■

We also have the following useful result.

Lemma 3.5.1 *For every $t \in \mathbb{Z}_{\geq 2}$, $\|\hat{e}_a[t] - \hat{e}_b[t]\| \leq 2v$, where $\hat{e}_a[t]$ and $\hat{e}_b[t]$ are elements of the evader estimate set $\hat{E}[t]$.*

Proof: At time t, let the pursuer choose to move towards $\hat{e}_a[t]$ while executing part (i) of the pursuit strategy. From Lemma 3.3.2, $\hat{E}[t+1]$ contains at most two points, $\hat{e}_a[t+1]$ and $\hat{e}_b[t+1]$ and $e[t+1] \in \hat{E}[t] \oplus \mathcal{B}_v(0)$, which implies that $e[t+1] \in \mathcal{B}_v(\hat{e}_a[t]) \cup \mathcal{B}_v(\hat{e}_b[t])$. From geometry, the points $\hat{e}_a[t+1]$ and $\hat{e}_b[t+1]$ can be distinct *only if* both are contained inside $\mathcal{B}_v(\hat{e}_a[t])$. Thus, the result follows. ■

The last two lines of the proof of Lemma 3.5.1 lead to a useful corollary.

Corollary 3.5.2 *At the end of any sequence at time $t \in \mathbb{Z}_{\geq 2}$, if the evader estimates $\hat{e}_a[t]$ and $\hat{e}_b[t]$ are distinct, then they must be contained inside $\mathcal{B}_v(\hat{e}[t-1])$, where $\hat{e}[t-1]$ is the point the pursuer goes toward at the time step t.*

At each instant $t \in \mathbb{Z}_{\geq 2}$, recall that $y_{\text{aft}}[t] := \|e[t] - p[t]\| = \|\hat{e}_a[t] - p[t]\| = \|\hat{e}_b[t] - p[t]\|$. We have the following useful result.

Lemma 3.5.3 *If $v < 0.5$, then at every instant $t \in \mathbb{Z}_{\geq 2}$ for which $y_{\text{aft}}[t] > 1$, $y_{\text{aft}}[t+1] < y_{\text{aft}}[t] + v$.*

Proof: There are two possibilities: either $\hat{E}[t]$ contains only one point, i.e., $e(t)$ or $\hat{E}[t] = (\hat{e}_a[t], \hat{e}_b[t])$. In the first case, the pursuer moves towards $e[t]$ and on applying the triangle inequality, we have $y_{\text{aft}}[t+1] \leq y_{\text{aft}}[t] - (1-v) < y_{\text{aft}}[t] + v$, and the proposition is verified. In the second case, let us assume that the pursuer moves towards $\hat{e}_a[t]$. There are two possibilities now. If the evader was at $\hat{e}_a[t]$ at time t, then the result is verified to be true since this possibility is exactly similar to the first case. But if the evader was at $\hat{e}_b[t]$ at time t, then observe that since $y_{\text{aft}}[t] > 1$, $p[t+1]$ will lie somewhere between $p[t]$ and $\hat{e}_a[t]$. This is shown in Figure 3.5. By triangle inequality,

$$y_{\text{aft}}[t+1] = \|e[t+1] - p[t+1]\| \leq \|\hat{e}_b[t] - p[t+1]\| + \|e[t+1] - e[t]\|.$$

Since $v < 0.5$ and $y_{\text{aft}}[t] > 1$, $\|\hat{e}_b[t] - p[t+1]\| < \|\hat{e}_b[t] - p[t]\| =: y_{\text{aft}}[t]$. Thus, the result follows since $\|e[t+1] - e[t]\| \leq v$. ■

We present another important result.

Lemma 3.5.4 *For every time step $t \in \mathbb{Z}_{\geq 2}$, if $v < 0.5$ and as long as the evader is not captured,*

$$y_{\text{aft}}[t+2] < y_{\text{aft}}[t] - (1 - 2v).$$

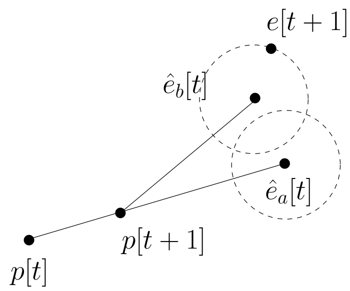

Figure 3.5. Illustration of a case in Lemma 3.5.3. The evader is at $\hat{e}_b[t]$ and the pursuer moves towards $\hat{e}_a[t]$.

Proof: At any time $t \in \mathbb{Z}_{\geq 2}$, there are two main possibilities:

(i) $\hat{e}_a[t] = \hat{e}_b[t] = e[t]$: In this case, the pursuer moves towards $e[t]$ at time $t+1$. Thus, by the triangle inequality at this step,

$$y_{\text{aft}}[t+1] \leq y_{\text{aft}}[t] - (1-v). \tag{3.10}$$

At time $t+1$, there are two further cases,

1) If $\hat{e}_a[t+1] \neq \hat{e}_b[t+1]$, then by Lemma 3.5.3, we have, $y_{\text{aft}}[t+2] < y_{\text{aft}}[t+1] + v$. This combined with (3.10) gives,

$$y_{\text{aft}}[t+2] < y_{\text{aft}}[t+1] + v < y_{\text{aft}}[t] - (1-2v).$$

Thus, the lemma holds for this case.

2) If $\hat{e}_a[t+1] = \hat{e}_b[t+1]$, then akin to (3.10), we have,

$$y_{\text{aft}}[t+2] \leq y_{\text{aft}}[t+1] - (1-v) < y_{\text{aft}}[t] - 2(1-v) < y_{\text{aft}}[t] - (1-2v).$$

Thus, the lemma holds for this case.

(ii) $\hat{e}_a[t] \neq \hat{e}_b[t]$: Let the pursuer choose to move towards $\hat{e}_a[t]$ at time $t+1$. Then, there are two further possibilities.

1) $\hat{e}_a[t+1] \neq \hat{e}_b[t+1]$: From Corollary 3.5.2, we know that $\hat{e}_a[t+1]$ and $\hat{e}_b[t+1]$

are contained in $\mathcal{B}_v(\hat{e}_a[t])$. So by triangle inequality,

$$y_{\text{aft}}[t+1] \leq y_{\text{aft}}[t] - (1-v). \tag{3.11}$$

At time step $t+2$, independent of which point in $\hat{E}[t+1]$ the pursuer decides to move toward, by Lemma 3.5.3, $y_{\text{aft}}[t+2] < y_{\text{aft}}[t+1] + v$. Combining this with (3.11), we get,

$$y_{\text{aft}}[t+2] \leq y_{\text{aft}}[t+1] - (1-v) + v < y_{\text{aft}}[t] - (1-2v).$$

Thus, the lemma holds for this case.

2) $\hat{e}_a[t+1] = \hat{e}_b[t+1] = e[t+1]$: Applying Lemma 3.5.3 at time step $t+1$, we get $y_{\text{aft}}[t+1] < y_{\text{aft}}[t] + v$. Before its move at time $t+2$, the pursuer knows the exact location $e[t+1]$. So at the end of time step $t+2$, by applying triangle inequality, akin to (3.10), we have,

$$y_{\text{aft}}[t+2] \leq y_{\text{aft}}[t+1] - (1-v) < y_{\text{aft}}[t] - (1-2v).$$

Thus, the lemma holds for this case.

We have verified that this lemma holds for all the possibilities. ■

The proof of Theorem 3.3.3 is almost immediate due to Lemma 3.5.4.

Proof of Theorem 3.3.3: If $v < 0.5$, then Lemma 3.5.4 states that for every time step $t \geq 2$ and as long as $y_{\text{aft}}[t] > 1$, the distance $y_{\text{aft}}[t]$ strictly decreases by a positive quantity $1-2v$ after every two time steps. Thus, after at most $(y_{\text{aft}}[2]-1)/(2(1-2v))$ time steps, we obtain $y_{\text{aft}}[t] \leq 1$, i.e., the evader is captured.

For the expression of the upper bound on the capture time, we seek an upper bound on $y_{\text{aft}}[2]$. In the initialization phase, it is possible that the pursuer and evader both move in a direction away from each other. Thus, $y_1[1] \leq \|e[0] - p[0]\| + (1+v)$. This can also take place at time step $t = 2$, since Lemma 3.5.3 does not hold at time step $t = 1$. Thus, $y_{\text{aft}}[2] \leq y_1[1] + (1+v)$. Thus, a conservative upper bound on $y_{\text{aft}}[2]$ is $\|e[0] - p[0]\| + 2(1+v)$. The result now follows. ■

3.5.2 Cooperative Pursuit in $\mathbb{R}^3$

We begin by proving Lemma 3.4.1.

Proof of Lemma 3.4.1: Observe that for each i, the set $\partial\mathcal{B}_{y^i_{\mathrm{aft}}[t]}(p_i[t]) \cap \partial\mathcal{B}_{y^i_{\mathrm{bef}}[t]}(p_i[t-1])$ is a circle with $p_i[t]$ located on its *axis*, i.e., the line passing through its center and perpendicular to the plane containing the circle. Thus, for each time instant t, the points in $\hat{E}[t]$ are equidistant from both pursuers.

We prove parts (i) and (ii) by mathematical induction. The lemma holds at time $t = 1$, as a consequence of the Initialization phase. Now assume that at some time t, the pursuers are at distinct locations and there are at most two points in $\hat{E}[t]$. Then there are two possibilities:

1) There are two distinct points $\hat{e}_1[t]$ and $\hat{e}_2[t]$ in $\hat{E}[t]$: If the four points $p_1[t], \hat{e}_1[t], p_2[t], \hat{e}_2[t]$ are co-planar, then $\hat{e}_1[t]$ and $\hat{e}_2[t]$ lie on opposite sides of the line joining $p_1[t]$ and $p_2[t]$. By the pursuit strategy, since each pursuer moves towards its respective $\hat{e}[t]$, the points $p_1[t+1]$ and $p_2[t+1]$ also lie on opposite sides of the line joining $p_1[t]$ and $p_2[t]$ and thus are distinct. If $p_1[t], \hat{e}_1[t], p_2[t], \hat{e}_2[t]$ are not co-planar, then the line joining $p_1[t]$ and $\hat{e}_1[t]$ and the line joining $p_2[t]$ and $\hat{e}_2[t]$ are skew in $\mathbb{R}^3$. Thus, any point on the first line is distinct from any on the second.

2) $\hat{e}_1[t] = \hat{e}_2[t] = e[t]$: If $e[t]$, $p_1[t]$ and $p_2[t]$ are not collinear, then by part (a) of item (i) in the pursuit strategy, the points $p_1[t+1]$ and $p_2[t+1]$ are distinct. If they are collinear, then the axis of the cone described in part (b) of item (i) of the pursuit strategy is the line l passing through $e[t]$, $p_1[t]$ and $p_2[t]$. The pursuer closer to the evader, say p_1 moves towards $e[t]$ and hence is still on the line l, while p_2 moves to a point not contained in l and thus $p_1[t+1]$ and $p_2[t+1]$ are distinct.

Thus, the pursuers are at distinct locations at time $t + 1$. For part (ii), observe that at time instant t, pursuer p_2 does not move towards $p_1[t-1]$. This means that the axes (defined in the first line of this proof) of the two circles $\partial\mathcal{B}_{y^i_{\mathrm{aft}}[t+1]}(p_i[t+1]) \cap \partial\mathcal{B}_{y^i_{\mathrm{bef}}[t+1]}(p_i[t])$ are never parallel to each other. Thus, their intersection and hence $\hat{E}[t+1]$ contains at most two points. Thus, the result holds by mathematical induction.

Proof of item (iii) is on similar lines as that of item (i) of Lemma 3.3.2. ■

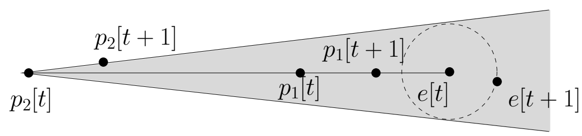

Figure 3.6. Illustration of case 2 in Lemma 3.4.1. The shaded region is the cone described in part (b) of item (i) of the Pursuit phase.

Lemma 3.5.5 *For every $t \in \mathbb{Z}_{\geq 2}$, $\|\hat{e}_1[t] - \hat{e}_2[t]\| \leq 2v$, where $\hat{e}_1[t]$ and $\hat{e}_1[t]$ are elements of the evader estimate set $\hat{E}[t]$.*

Proof: Let the evader be located at $\hat{e}_1[t-1]$ at time $t-1$. p_1 moves towards $\hat{e}_1[t-1]$ and hence $e[t]$ must be contained in $\left(\partial\mathcal{B}_{y^1_{\mathrm{aft}}[t]}(p_1[t]) \cap \partial\mathcal{B}_{y^1_{\mathrm{bef}}[t-1]}(p_1[t-1])\right) \bigcap \mathcal{B}_v(\hat{e}_1[t-1]) \subset \mathcal{B}_v(\hat{e}_1[t-1])$, which is a circle. The intersection points of this circle with the other circle due to p_2, must be contained inside $\mathcal{B}_v(\hat{e}_1[t-1])$ and thus the result follows. ■

Next, we observe that Lemma 3.5.3 holds for the cooperative pursuit strategy as well. This follows from Lemma 3.5.5 and the fact that only the triangle inequality was being used in the proof of Lemma 3.5.3. The only extra technicality is the possibility of occurrence of case 2 as in the proof of Lemma 3.4.1 (refer Figure 3.6). However, a simple calculation reveals that Lemma 3.5.3 still holds due to the motion as per part (b) of item (i) in the Pursuit strategy.

We now present a useful result.

Lemma 3.5.6 *For every time step $t \in \mathbb{Z}_{\geq 2}$, if $v < 0.5$ and as long as the evader is not captured,*

$$y^1_{\text{aft}}[t+1] + y^2_{\text{aft}}[t+1] < y^1_{\text{aft}}[t] + y^2_{\text{aft}}[t] - (1 - 2v).$$

Proof: At any instant t, by Lemma 3.4.1, it is clear that the evader is in $\hat{E}[t]$, which contains at most two points, $\hat{e}_1[t], \hat{e}_2[t]$. Let the evader be located at $\hat{e}_1[t]$. Then, by triangle inequality

$$y^1_{\text{aft}}[t+1] = \|e[t+1] - p_1[t+1]\| \leq \|e[t] - p_1[t]\| - (1 - v) = y^1_{\text{aft}}[t] - (1 - v).$$

From Lemma 3.5.3, we have $y^2_{\text{aft}}[t+1] < y^2_{\text{aft}}[t] + v$. Thus, adding the two inequalities, we get the required result. ■

Proof of Theorem 3.4.2: If $v < 0.5$ and if both $y^1_{\text{aft}}[t]$ and $y^2_{\text{aft}}[t]$ are greater than 1 for $t \in \mathbb{Z}_{\geq 2}$, then by Lemma 3.5.6, their sum $y^1_{\text{aft}}[t] + y^2_{\text{aft}}[t]$ strictly decreases by a positive quantity $(1-2v)$ at every instant of time. Thus, after at most $\lceil (y^1_2[2] + y^2_2[2] - 2)/(1 - 2v) \rceil$ time steps, $y^1_{\text{aft}}[t] + y^2_{\text{aft}}[t] \leq 2$, which means either $y^1_{\text{aft}}[t] \leq 1$ or $y^2_{\text{aft}}[t] \leq 1$, i.e., the evader is captured.

For the expression of the upper bound on the capture time, we seek an upper bound on $y^1_2[2] + y^2_2[2]$. On similar lines to the proof of Theorem 3.3.3, we have $y^i_2[2] \leq \|e[0] - p_i[0]\| + 2(1 + v)$. Thus, the result follows.

■

3.6 Simulation Studies

We now present simulation studies that address (i) the case of evader speed $v \in [0.5, 1[$; (ii) the case of the pursuer measurements being corrupted with additive, zero-mean Gaussian noise, with variance proportional to the square of the distance to the evader, and (iii) a version of this game with simultaneous moves. All simulations were run using MATLAB®.

3.6.1 The case of $v \in [0.5, 1[$

We ran simulations for $\|e[0]-p[0]\| = 20$, 30 and 40 units. An upper limit of 1000 time steps was set to decide whether the capture strategy terminated into capture or evasion.

It is unclear as to what is the optimal evader strategy in this problem. This is because if the evader decides to always move directly away from the pursuer with full step (i.e., *greedy* move), then it would reduce the uncertainty in its position for the pursuer. If it does not make a greedy move, then the distance from the pursuer may reduce. So we adopt the following reasonable evader strategy for simulations - with full step, move to a point selected uniformly randomly in a sector with angle 0.2 radians. This sector is placed symmetrically along the line $e[t]p[t]$ and away from the pursuer.

The plots of probability of success of the strategy versus the evader speed v are presented in Figure 3.7.

3.6.2 Noisy measurements

We assume that the pursuer measurements are corrupted with zero-mean, additive Gaussian noise whose variance proportional to the square of the distance to the evader. This implies $\sigma_{\text{bef}}[t] = \epsilon\|e[t]-p[t-1]\|$ and $\sigma_{\text{aft}}[t] = \epsilon\|e[t]-p[t]\|$, where $\epsilon > 0$ is the noise parameter. Thus, in the notation of Section 3.2, $y_{\text{bef}}[t] \sim \mathcal{N}(\|e[t]-p[t-1]\|, \sigma_{\text{bef}}[t])$ and $y_{\text{aft}}[t] \sim \mathcal{N}(\|e[t]-p[t]\|, \sigma_{\text{aft}}[t])$, where given $a, b \geq 0$, $\mathcal{N}(a, b)$ denotes the Gaussian distribution with mean a and standard deviation b.

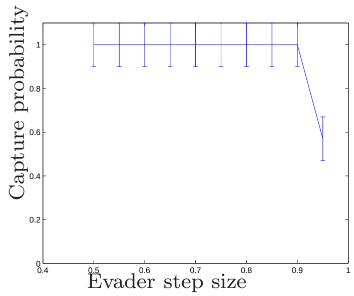

(a) Initial distance: 20 units

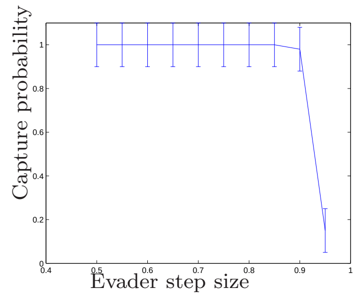

(b) Initial distance: 30 units

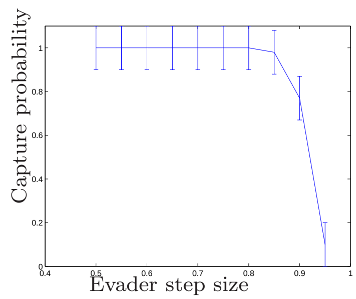

(c) Initial distance: 40 units

Figure 3.7. Estimate of capture probability versus evader step size v. The vertical bars give a 95% confidence interval about the probability estimate $P(v)$ which is given by $\left[P(v) - 2\sqrt{\frac{0.25}{n}}, P(v) + 2\sqrt{\frac{0.25}{n}}\right]$, where $n = 100$ is the number of trials [101]. For a particular evader strategy, we study how the capture strategy performs for evader step size $v \in [0.5, 1[$.

Since it is unclear as to what is the optimal evader strategy in this problem, we adopted the evader strategy in Section 3.6.1. We ran simulations for $\beta = 0.2$, 0.3 and 0.4 units. The initial distance was set to 20 units. An upper limit of 2000 time steps was set to decide whether the capture strategy terminated into capture or evasion. The plots of probability of success of the strategy versus the noise parameter ϵ are presented in Figure 3.8.

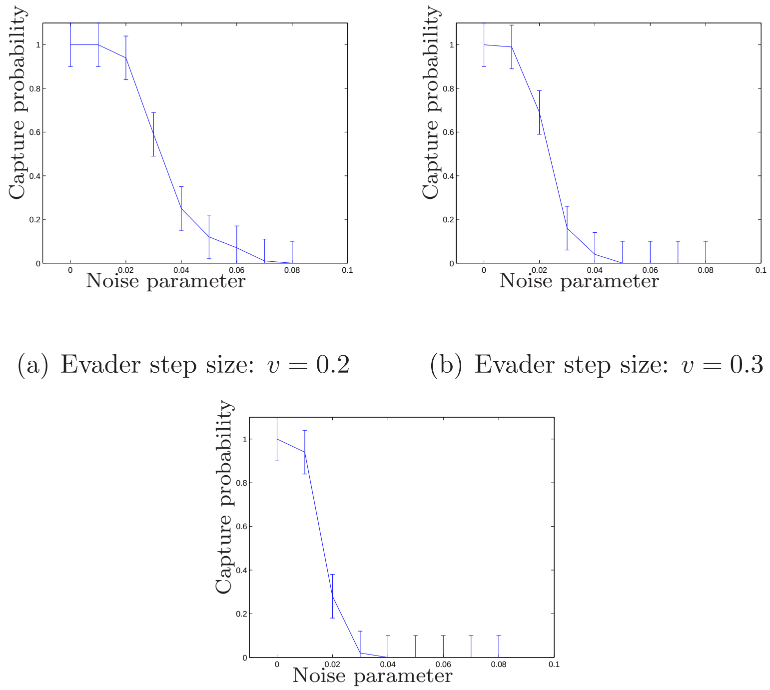

(a) Evader step size: $v = 0.2$

(b) Evader step size: $v = 0.3$

(c) Evader step size: $v = 0.4$

Figure 3.8. Estimate of capture probability versus noise parameter ϵ. The vertical bars give a 95% confidence interval about the probability estimate $P(\epsilon)$ computed as described in Figure 3.7. For a particular evader strategy, we study how the capture strategy performs under noisy measurements.

3.6.3 A Game with Simultaneous Moves: Simulation Study

We now consider a discrete-time version of the game in the plane in which the pursuer and the evader move simultaneously. In this version, at each instant of time, each player gets *only one* measurement of its opponent. This is equivalent to a game in which the pursuer receives *only* the distance to the evader at each instant in continuous time. Thus, (3.1) becomes

$$\begin{aligned} e[t] &= e[t-1] + u^e(e[t-1], \{p[\tau]\}_{\tau=0}^{t-1}), \\ p[t] &= p[t-1] + u^p(p[t-1], y[t-1]), \end{aligned} \tag{3.12}$$

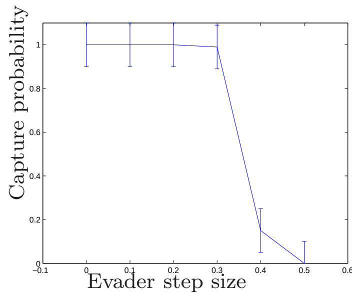

(a) Initial distance: 20 units

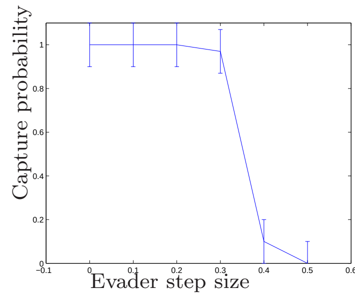

(b) Initial distance: 30 units

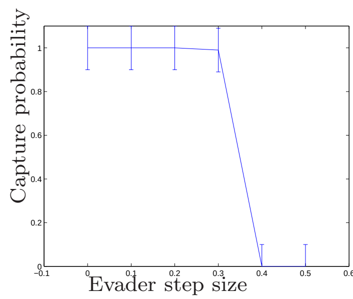

(c) Initial distance: 40 units

Figure 3.9. Estimate of capture probability versus evader step size v, in the game with simultaneous moves. The vertical bars give a 95% confidence interval about the probability estimate $P(v)$, computed as described in Figure 3.7. For a particular evader strategy, we study the performance of a modified capture strategy presented in Section 3.6.3.

We modify the capture strategy in Section 3.3 as follows.

Initialization phase: The following happens simultaneously for only the first time step:

(i) The evader moves to $e[1]$.

(ii) The pursuer randomly selects a direction to move and moves along it with unit step size.

(iii) The pursuer gets the measurement $y[1]$ and the evader estimate is given by

$$\hat{E}[1] := \partial\mathcal{B}_{y[1]}(p[1]).$$

Pursuit Phase: Until the evader is *not* captured, at time $t \geq 2$,

(i) If $\hat{E}[t-1]$ is a circle, then denote any point in it as $\hat{e}[t-1]$. Otherwise, denote as $\hat{e}[t-1]$ a point chosen uniformly randomly from one of the end points of the arcs in $\hat{E}[t-1]$. The pursuer moves towards $\hat{e}[t-1]$ with full step size.

(ii) The pursuer updates the estimate of the evader's position using

$$\hat{E}[t] := \left(\hat{E}[t-1] \oplus \mathcal{B}_v(0)\right) \cap \partial\mathcal{B}_{y[t]}(p[t]).$$

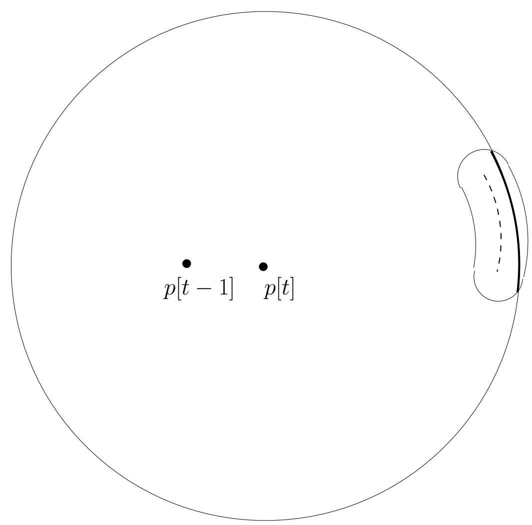

Figure 3.10. Illustration of the pursuit strategy in the game with simultaneous moves. The dotted line is the estimate $\hat{E}[t-1]$. The bean-shaped region around it is its Minkowski sum with $\mathcal{B}_v(0)$ and the darkly shaded arc is the estimate $\hat{E}[t]$.

The strategy is illustrated in Figure 3.10. Since it is unclear as to what is the optimal evader strategy in this problem, we adopted the same evader strategy as in Section 3.6.1. We ran simulations for $\|e[0] - p[0]\| = 20$, 30 and 40 units. An upper limit of 5000 time steps was set to decide whether the capture strategy terminated into capture or evasion. The plots of probability of success of the strategy versus the evader step size v are presented in Figure 3.9.

3.7 Bearing-only Formulation

In this section, we present another formulation in which the pursuer is equipped with a sensor that determines *only* the line that contains their positions. The equations of motion are identical to equation (3.12). The measurement $y[\tau]$ is the straight line passing through the pursuer and the evader at time τ. The sensing model assumed is different from bearing-only sensors in literature. In bearing-only sensors, the uncertainty associated with the evader's position is a semi-infinite line whereas that in the present scenario is an infinite line. Hence, although the evader is slower, a simple greedy strategy would fail as the pursuer would not know how it is to the evader.

3.7.1 The Capture Strategy and Main Result

We now present our capture strategy and the main result of this paper. Our strategy is as follows: Until the evader is captured and localized,

1. For $t = 2k+1$, where $k = 0, 1, 2, \ldots$, the pursuer moves to a point $p[2k+1]$ such that

$$p[2k+1] - p[2k] \perp y[2k], \quad \text{and } \|p[2k+1] - p[2k]\| = v + f_p[2k],$$

where $f_p[2k] \in]0, 1-v]$, for $k = 0, 1, \ldots$, is as per the pursuer's choice.

2. The pursuer computes the set $\hat{E}[t]$ recursively as follows.

$$\begin{aligned}\hat{E}[0] &= y[0],\\ \hat{E}[t] &= \left(\hat{E}[t-1] \oplus \mathcal{B}_v(0)\right) \cap y[t],\end{aligned}$$

   where $\mathcal{B}_v(0) \subset \mathbb{R}^2$ denotes the closed circular region of radius v around the origin $0 \in \mathbb{R}^2$ and the operation $\oplus$ denotes the Minkowski sum in the plane.

3. For $t = 2k$, where $k = 1, 2, \ldots,$ the pursuer moves toward the furthest point from it inside $\hat{E}[t-1]$, with maximum step size.

4. The pursuer repeats item 2 of this strategy.

The strategy is illustrated for at time instants $0, 1$ and 2 in Figure 3.11. From the definition of $\hat{E}[t]$ for $t \geq 1$, it can be shown that $\hat{E}[t]$ is a line segment and thus a compact set. Thus, the points in $\hat{E}[t]$ closest to and furthest from $p[t]$ exist. In the event that there exist two points which are furthest from $p[t]$, the pursuer selects any one among them at step (iii).

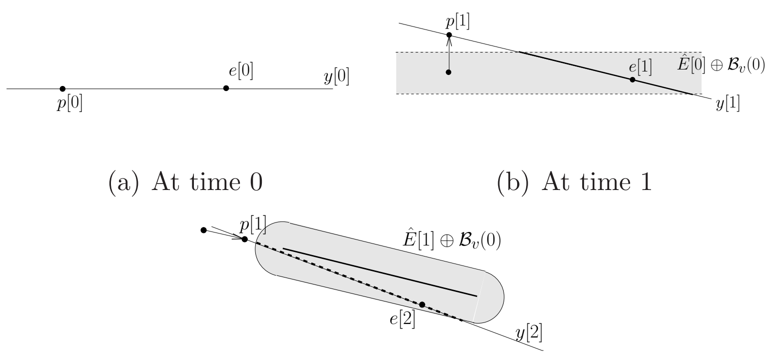

(a) At time 0

(b) At time 1

(c) At time 2

Figure 3.11. Illustration of the capture strategy for the bearing-only formulation at time instants 0, 1 and 2.

This strategy gives us the following result.

Theorem 3.7.1 (Capture with bearing-only sensor) *If $v < 0.25$, then the proposed pursuit strategy along with the choice of $f_p[2k] = v$, for every $k \in \{0, 1, 2, \ldots\}$ leads to*

1. *simultaneous localization and capture of the evader.*

2. *The number of time steps required upper bounded by*

$$\frac{3\sqrt{\|p[0] - e[0]\|^2 + 4v^2}}{1 - 4v} + 2.$$

3. *simultaneous localization and capture state maintained with periodicity of at most two time instants following the first time it is simultaneously localized and captured.*

Remark 3.7.2 (General strategy) *It turns out that the choice of $f_p[2k] = v$ has an inherent limitation that v needs to be no greater that 0.5, due to the move in step (i). In general, one can choose smaller values of f_p for step (i) and we were able to show that a sufficiently small value of f_p and a modification of step (iii), leads to capture under the same condition on v as given by Theorem 3.7.1. However, we are not able to comment upon the time taken for capture and whether property (iii) would be guaranteed.*

We present and prove some intermediate results before proving the main result.

Lemma 3.7.3 *For $t \geq 1$, let $d[t]$ denote the distance between $p[t]$ and the point furthest to it in $\hat{E}[t]$. The following statements are true:*

1. *For odd time instants $t \geq 1$, $d[t] \leq d[t-1] + 3v$.*

2. *At even time instants $t \geq 1$, the evader is localized and captured if $d[t-1] \leq 3/2$ and $v < 1/4$.*

3. *At even time instants $t \geq 1$, if $d[t-1] > 3/2$, then $d[t] \leq d[t-1] - (1-v)$.*

Proof: The proofs are based on application of the triangle inequality. Let $e_f[t] \in \hat{E}[t]$ denote the furthest point from $p[t]$ at time instant t.

1. At odd time instants t, applying triangle inequality to $\triangle p[t]p[t-1]e_f[t-1]$, as shown in Figure 3.12 we obtain,

$$\|p[t] - e_f[t]\| \leq d[t-1] + 2v.$$

Since the evader's maximum step size is upper bounded by v, from geometry $d[t] \leq \|p[t] - e_f[t-1]\| + v$. Combining these two inequalities, we obtain part (i). Observe that for odd time instants $t \geq 1$, $p[t] \notin \hat{E}[t]$.

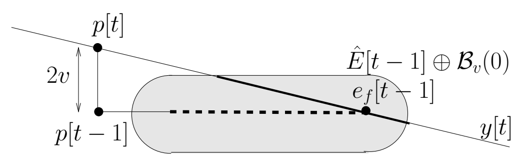

Figure 3.12. Illustration of proof of item (i) in Lemma 3.7.3. The broken line segment is $\hat{E}[t-1]$.

2. Let the positions of the players at the end of time $t-1$ be as shown in Figure 3.13. As per the strategy, the pursuer moves towards $e_f[t-1]$ with unit step. Let $e_c[t-1]$ denote the point inside $\hat{E}[t-1]$ that is closest to $p[t-1]$. We observe that for all possible positions of the evader, $\|e_c[t-1] - p[t]\| \leq 2/3$, where the right hand side value is due to the property of similar triangles. Equality occurs in the above inequality only if $e_f[t-1] = A$, as shown in Figure 3.13.

Thus, we obtain that $d[t] = \max\{\|e_c[t-1] - p[t]\| + v, d[t-1] - 1 + v\} = \max\{2/3 + v, 1/2 + v\} < 1$, if $v < 1/4$. This proves the result.

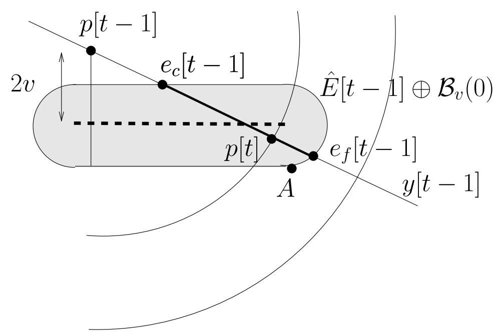

Figure 3.13. Illustration of proof of item (ii) in Lemma 3.7.3. The broken line segment is $\hat{E}[t-2]$, the dark solid line segment is $\hat{E}[t-1]$. The two circular arcs about $p[t-1]$ have radii 1 and 3/2 units respectively. Point A is the point of intersection of circle with unit radius around $p[t-1]$ and the straight portion of the boundary of the shaded region as shown. $e_c[t-1]$ and $e_f[t-1]$ are the closest and furthest points respectively inside $\hat{E}[t-1]$ from $p[t-1]$.

3. $d[t-1] > \frac{3}{2}$: This implies that the evader was not captured at time $t-1$. Thus, pursuer moves towards $e_f[t-1]$ with maximum step size. As in the previous case, we have $d[t] = \max\{\|e_c[t-1] - p[t]\| + v, d[t-1] - 1 + v\}$. However, the present case is feasible only if angle $\angle e_f[t-1]p[t-1]p[t-2] > \arccos(2v)$, as shown in Figure 3.14. This implies that the second argument in the max function for $d[t]$ dominates the first because under that inequality, $\|e_c[t-1] - p[t]\| < 1/2$. This proves the required result.

■

A combination of parts (i) and (iii) of Lemma 3.7.3 leads to the following corollary.

Corollary 3.7.4 *Let $t = 2k+1$ for some $k \in \{0, 1, 2, \dots\}$. If $d[2k+1] > 3/2$, then $d[2k+3] \leq d[2k+1] - (1-4v)$.*

We are now ready to prove Theorem 3.7.1

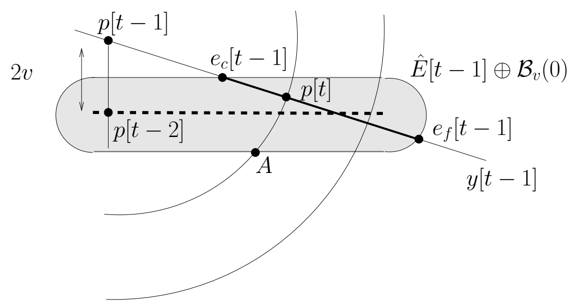

Figure 3.14. Illustration of proof of item (iii) in Lemma 3.7.3. The broken line segment is $\hat{E}[t-2]$, the dark solid line segment is $\hat{E}[t-1]$. The two circular arcs about $p[t-1]$ have radii 1 and 3/2 units respectively. Point A is the point of intersection of circle with unit radius around $p[t-1]$ and the straight portion of the boundary of the shaded region as shown. $e_c[t-1]$ and $e_f[t-1]$ are the closest and furthest points respectively inside $\hat{E}[t-1]$ from $p[t-1]$. This case is geometrically possible only when the intersection of $\hat{E}[t-1]$ and $\hat{E}[t-2]$ (possibly extended) does not lie inside the smaller circle as shown, i.e., the angle $\angle e_f[t-1]p[t-1]p[t-2] > \arccos 2v$.

Proof of Theorem 3.7.1:

1. Given any finite initial distance between the pursuer and evader, there exists a finite value for $d[1]$. If $v < 1/4$, then by Corollary 3.7.4, after a finite number of time steps, we obtain for some $k^* \in \{0, 1, 2, \dots\}$, $d[2k^*+1] \leq 3/2$. At time instant $2k^*+2$, applying item (ii) of Lemma 3.7.3, capture is ensured.

2. To compute an upper bound on the time taken to capture, we need to compute an upper bound on the number k^* in part (i) of this proof. Given any initial positions $p[0]$ and $e[0]$, by trigonometry we obtain

$$d[1] \leq \frac{3}{2}\sqrt{\|p[0]-e[0]\|^2 + 4v^2}.$$

Thus, an upper bound for k^* is given by

$$k^* \leq \frac{3}{2}\frac{\sqrt{\|p[0]-e[0]\|^2+4v^2}}{1-4v}.$$

Part (ii) of the theorem now follows.

3. This case is illustrated in Figure 3.15. Let the pursuer capture the evader at time $2k^*+2$. At time $2k^*+3$, by part (i) of Lemma 3.7.3, we obtain $d[2k^*+3] \leq d[2k^*+2]+3v$. The evader is captured again at time $2k^*+4$ if conditions of part (ii) of Lemma 3.7.3 hold. If they do not hold, then applying part (iii) of Lemma 3.7.3, $d[2k^*+4] \leq d[2k^*+3]-(1-v) \leq d[2k^*+2]-(1-4v) < 1$. Thus, part (iii) stands proved.

■

Summary

Inspired by the Grow-Intersect algorithm, we addressed discrete-time pursuit-evasion games in the plane in which the pursuer is equipped with (i) a range-only sensor that measures its distance from the evader, or with (ii) a bearing-only sensor that gives only the line containing the pursuer and the evader . We proposed pursuit strategies and showed that if the evader's speed is less than a critical value, then capture is achieved. We also provided upper bounds on the capture times. Simulation studies suggest good performance of the pursuit strategies for higher evader speeds as well as under noisy scenarios.

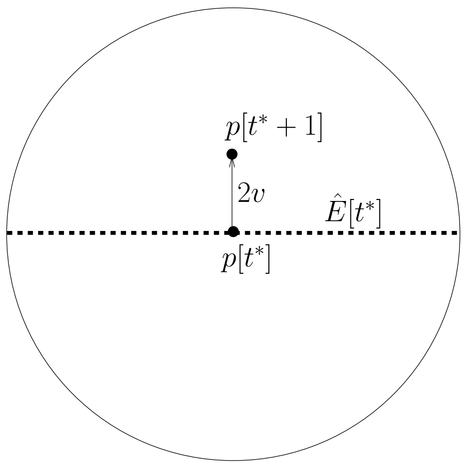

(a) At time $t^* := 2k^*$, the evader is simultaneously localized and captured.

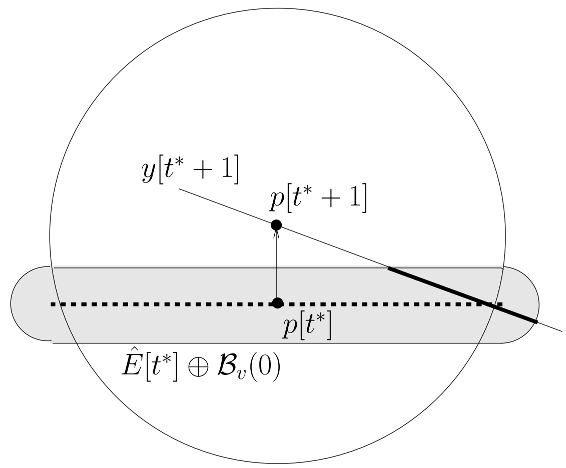

(b) At time $t^* + 1$. The pursuer checks whether the evader is still localized and captured.

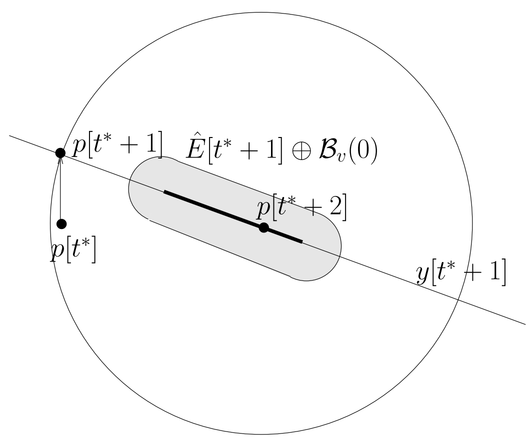

(c) At time $t^* + 2$, capture occurs again.

Figure 3.15. Illustration of part (iii) of the proof of Theorem 3.7.1.

Chapter 4

Pursuit under Motion Constraints

4.1 Introduction

In this chapter, we address a pursuit-evasion game of kind between a slower but agile evader and multiple faster but motion-constrained pursuers. We propose a cooperative pursuit strategy in order to achieve capture via confining the evader in a bounded region through which the evader cannot escape without being captured.

Related Literature

The Homicidal Chauffeur game, proposed originally in [51], involves a pursuer who wants to overrun an evader, both moving with fixed speeds. The pursuer has greater speed but has constraints on its turning radius, while the evader can make arbitrarily sharp turns. The evader is said to be *captured* when the distance between the pursuer and evader becomes less than a specified *capture radius*. The pursuer moves at fixed speed along planar paths with bounded curvature. The evader moves with a fixed speed lower than that of the pursuer and governed by a simple first-order-integrator dynamics. [51] gave a condition on the game parameters, i.e., the speed ratio between the players and the ratio of the capture radius to the minimum turning radius of the pursuer, such that the evader can evade indefinitely. Numerous variations of this problem have been studied, e.g., capture inside a cone sector [42], effects of stochastic noise [73] and a version without a priori assignment of the role of pursuer or evader [41] to cite a few.

Recent research attention has focused on cooperative control strategies for detection of targets. [66] have addressed the problem of cooperative rendezvous in which multiple UAVs are to arrive simultaneously at their targets. [82] have presented a cooperative target search using online learning and computing guidance trajectories for the agents. Recently, [99] have presented cooperative motion planning methods for first-order mobile sensing agents to detect a moving target that lies in a known initial region. [65] have proposed guaranteed strategies to search for mobile evaders in a plane. Recently, [55] and [11] have proposed schemes for agents with first-order dynamics to capture a target by arriving on a circle with specified radius around it.

Contributions

Based on the analysis of the Homicidal Chauffeur game, we identify regimes for the game parameters, i.e., the evader/pursuer speed ratio and the ratio of the capture radius to the pursuer's minimum turning radius, for which there exists a strategy for the evader to avoid capture. This motivates a multiple pursuer formulation of the game. We seek to confine the evader within a bounded region, for which we propose a multiple pursuer formation and a novel multi-phase, cooperative strategy for the pursuers. During all phases, the pursuers move in a specific formation, whereby some pursuer plays the role of "leader" and all other pursuers play the role of "followers." The strategy is partly decentralized, in the sense that it suffices to specify only the motion of the leader in each phase. For the followers, the only information required is the motion of the neighboring pursuer and the evader position. In the initial PRE-ALIGN and ALIGN phases of the strategy, the leader pursuer moves in such a way that the evader lies at a required distance directly ahead of the leader pursuer, while the followers move so as to maintain a straight line formation. In the remaining SWERVE, ENCIRCLE and CLOSE phases, the pursuers get into a "daisy-chain" formation and move to approach, encircle and finally close the chain around the evader. Independent of the evader motion, the final closed daisy-chain formation confines the evader within a bounded region, from which there exists no evader trajectory avoiding capture. Thus, given (i) the evader/pursuer speed ratio which is less than unity and (ii) the ratio of the capture radius to the pursuers' minimum turning radius, we characterize the required number of pursuers for which confinement is guaranteed.

Ecological Motivation

The inspiration for our strategy comes from certain aspects of fish behavior. [38] reported that in Cedar Key, Florida, USA, individual "driver" dolphins herd slower, more agile prey in circles as well as towards the tightly-grouped "barrier" dolphins. [81] reported a herd of killer whales imposing confinement on pantropical spotted dolphins. The whales cut out up to three dolphins from a school and proceeded to take turns chasing a single dolphin and keeping it within a confined area. The strategy proposed in this chapter bears similarities with foraging strategies observed recently among dolphins [12], as shown in Figure 4.1.

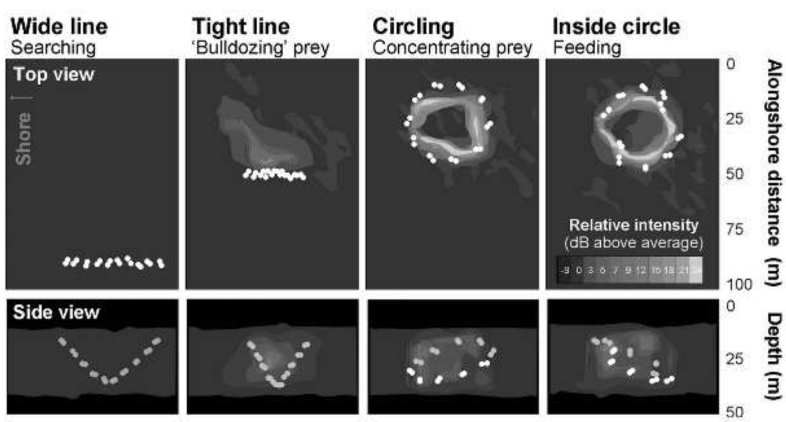

Figure 4.1. Cooperative multi-stage foraging observed among dolphins [12].

Organization of this Chapter

This chapter is organized as follows. The mathematical model and assumptions are presented in Section 4.2. The daisy-chain formation, the confinement strategy and the main analysis result are presented in Section 4.3. Section 4.4 contains proofs of some intermediate and the main results.

4.2 Problem Set-up

Our cooperative Homicidal Chauffeur game is played in an unbounded, planar environment between a single evader and multiple pursuers. The pursuers have identical motion abilities and possess greater speed than that of the evader. However, the evader can make arbitrarily sharp turns, while the pursuers are *Dubins* vehicles [34], i.e., fixed-speed non-holonomic vehicles constrained to move along paths of bounded curvature. We assume that the instantaneous position and velocity of the evader is available to all pursuers.

Let $e(t)$ and $p_k(t)$, for $k \in \{1, \dots, N\}$, denote the positions of the evader and the k-th pursuer in $\mathbb{R}^2$ at time t, as shown in Figure 4.2. Let v_{e} and v_{p} denote the speeds of the evader and of all pursuers, respectively. Given a *minimum turning radius* $\rho > 0$, the equations of motion are

$$
\begin{aligned}
\dot{p}_{k,x}(t) &= v_{\mathrm{p}} \cos\theta_{\mathrm{p},k}(t), \quad \dot{e}_x(t) = v_{\mathrm{e}} \cos\theta_{\mathrm{e}}(t), \\
\dot{p}_{k,y}(t) &= v_{\mathrm{p}} \sin\theta_{\mathrm{p},k}(t), \quad \dot{e}_y(t) = v_{\mathrm{e}} \sin\theta_{\mathrm{e}}(t), \\
\dot{\theta}_{\mathrm{p},k} &= \frac{v_{\mathrm{p}}}{\rho} u^{p_k},
\end{aligned}
\tag{4.1}
$$

where $\theta_{\mathrm{e}}(t)$ (resp. $\theta_{\mathrm{p},k}(t)$) is the angle between the velocity vector of the evader (resp. of the k-th pursuer) measured counterclockwise from a reference horizontal axis [51]. The control input for the evader is $\theta_{\mathrm{e}}(t) : [0, \infty[\, \to [0, 2\pi]$, which we assume is a measurable function of time. $u^{p_k} \in [-1, 1]$, is the control applied by the k-th pursuer. We define the *evader/pursuer speed ratio* $v := v_{\mathrm{e}}/v_{\mathrm{p}}$ and assume $v < 1$. Given a

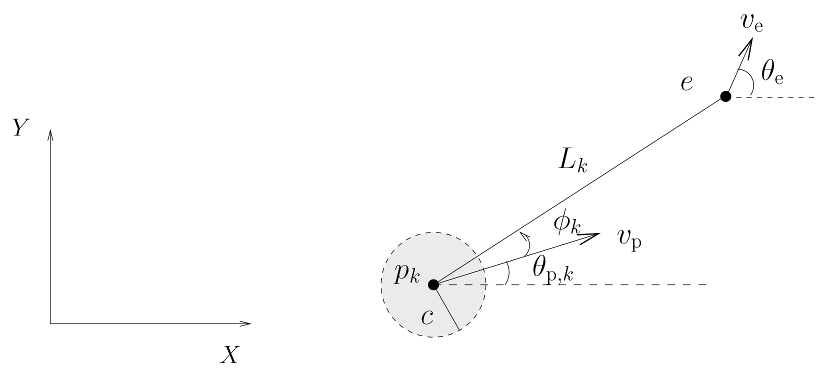

Figure 4.2. Intermediate variables in the Homicidal Chauffeur game: L_k is the distance between the evader and the k-th pursuer; $\phi_k \in [0, \pi]$ is the unsigned angle between the k-th pursuer's velocity vector and the vector $e - p_k$. The shaded region is the pursuer's capture disc.

capture radius $c > 0$, the evader is said to be *captured* if, at some time t and for some k, the evader is at a distance of at most c units from pursuer p_k. In what follows, without loss of generality, we set the capture radius c and the pursuers speed v_{e} to 1. In summary, our cooperative Homicidal Chauffeur game is described by the number of pursuers $N \in \mathbb{N}$, the minimum turning radius $\rho \in \mathbb{R}_{>0}$, and the evader/pursuers speed ratio $v \in]0, 1[$.

In the case of a single pursuer and single evader, it can be shown in that for $\rho \geq 5/2$, there exists an evasion policy if the evader/pursuer speed ratio satisfies $v \geq v_{\min}(\rho)$, where $v_{\min} : [5/2, +\infty[\to]0, 1[$ is the unique solution to

$$\frac{1}{x} = \sqrt{1 - v_{\min}(x)^2} + v_{\min}(x) \arcsin(v_{\min}(x)) - 1,$$

[51]. This motivates our cooperative version of the Homicidal Chauffeur game. The use of a game-theoretic approach to determine capture strategies involves solving the Hamilton-Jacobi-Bellman-Isaacs equation, which is difficult to solve in the present

context. Therefore, taking motivation from biology, we introduce the notion of evader confinement as follows.

Definition 4.2.1 (Confinement) *The evader is said to be* confined *to a bounded region $\mathcal{G} \subset \mathbb{R}^2$ at time t^* if $e(t^*) \in \mathcal{G}$ and there exist pursuer trajectories $p_k : [t^*, +\infty[\to \mathbb{R}^2$ solutions to equation* (4.1) *such that the evader cannot leave $\mathcal{G}$ without being captured. A set of functions $\{u^{p_k}\}$, for $k \in \{1, \dots, N\}$, leading to evader confinement is termed as a* confinement strategy.

In our cooperative Homicidal Chauffeur game with the evader/pursuer speed ratio $v < 1$, we seek deterministic multiple-pursuer strategies that guarantee evader confinement given any value of the pursuer's minimum turning radius $\rho > 0$.

4.3 A Confinement Strategy

In this section, we design a cooperative strategy for evader confinement and state our main analysis result. We begin by proposing two useful pursuer formations. We denote the velocity vector of the k-th pursuer by $\overline{v}_{\mathrm{p},k}$.

Definition 4.3.1 (Line formation) *The set $\{p_1, \dots, p_N, \overline{v}_{\mathrm{p},1}, \dots, \overline{v}_{\mathrm{p},N}\}$ is in a* line formation *if*

(i) $p_1, \dots, p_N$ are on a straight line with the velocity vectors $\overline{v}_{\mathrm{p},1}, \dots, \overline{v}_{\mathrm{p},N}$ parallel to one-another, and

(ii) For every $k \in \{1, \dots, N-2\}$, $\|p_k - p_{k+1}\| = \|p_{k+1} - p_{k+2}\| > 0$.

Figure 4.3 shows an example of a line formation. In what follows, we refer to pursuer p_1 as the *leader*, unless specified otherwise. A line formation has the property that,

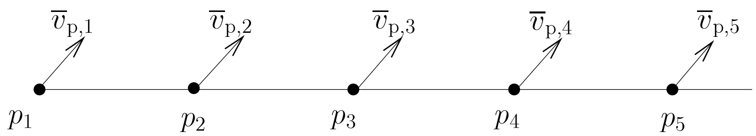

Figure 4.3. A pursuer line formation with $N = 5$ pursuers.

if all pursuers start in a line formation and use identical control inputs, then they remain in a line formation.

Definition 4.3.2 (Daisy-chain formation) *Given $s_{\mathrm{ip}} > 0$, the set $\{p_1, \ldots, p_N, \overline{v}_{\mathrm{p},1}, \ldots, \overline{v}_{\mathrm{p},N}\}$ is said to be in a* daisy-chain formation *at time t if, for every $k \in \{2, \ldots, N\}$, pursuer p_k can attain at time $t+s_{\mathrm{ip}}$, the position and orientation at time t of pursuer p_{k-1}. Formally, for every $k \in \{2, \ldots, N\}$, there exists a solution $\eta : [t, t + s_{\mathrm{ip}}] \to \mathbb{R}^2$ to equation* (4.1) *satisfying*

$$\eta(t) = p_k, \qquad \dot{\eta}(t) = \overline{v}_{\mathrm{p},k},$$

$$\eta(t + s_{\mathrm{ip}}) = p_{k-1}, \qquad \dot{\eta}(t + s_{\mathrm{ip}}) = \overline{v}_{\mathrm{p},k-1}.$$

The quantity s_{ip} in Definition 4.3.2 is also the *inter-pursuer separation* distance, since the pursuers' speed is normalized to unity. Figure 4.4 shows an example of a daisy-chain formation. A daisy-chain formation has the property that any time instant, a path taken by the leader pursuer can be exactly traversed by the k-th follower pursuer, for every $k \in \{2, \ldots, N\}$, in the daisy-chain after a time delay of $(k-1)s_{\mathrm{ip}}$.

Next, we characterize a possible evader motion. For $q \in \mathbb{R}^2$, let $\mathcal{B}_r(q) \subset \mathbb{R}^2$ denote the closed ball of radius r centered at q. Given $\{p_{k-1}, p_k, \overline{v}_{\mathrm{p},k-1}, \overline{v}_{\mathrm{p},k}\}$ in a daisy-chain formation at time t with inter-pursuer separation s_{ip}, let $\mathcal{C}^{k-1,k}_{\mathrm{left}}(t)$ and $\mathcal{C}^{k-1,k}_{\mathrm{right}}(t)$ be curves which are tangent to $\mathcal{B}_{\mathrm{c}}(\eta(\tau))$ for every $t \in [t, t + s_{\mathrm{ip}}]$. Here, η is a curve described in Definition 4.3.2. Then, the evader is said to *move between p_{k-1} and p_k* if $e(t) \in \mathcal{C}^{k-1,k}_{\mathrm{left}}(t)$ and $e(t + \overline{\tau}) \in \mathcal{C}^{k-1,k}_{\mathrm{right}}(t)$ or if $e(t) \in \mathcal{C}^{k-1,k}_{\mathrm{right}}(t)$ and $e(t + \overline{\tau}) \in \mathcal{C}^{k-1,k}_{\mathrm{left}}(t)$,

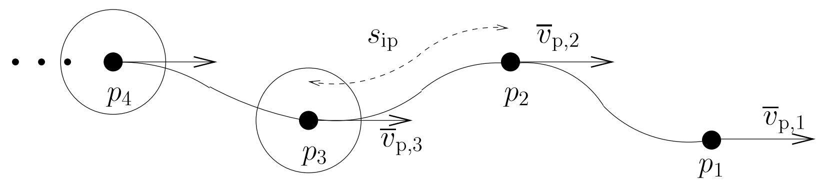

Figure 4.4. A daisy-chain formation with inter-pursuer separation s_{ip}. The curve between two consecutive pursuers is an example of a solution η as described in Definition 4.3.2. The discs around the pursuers represent their capture discs.

for some $\overline{\tau} < s_{\text{ip}}$. Figure 4.5 shows an example of such an evader trajectory.

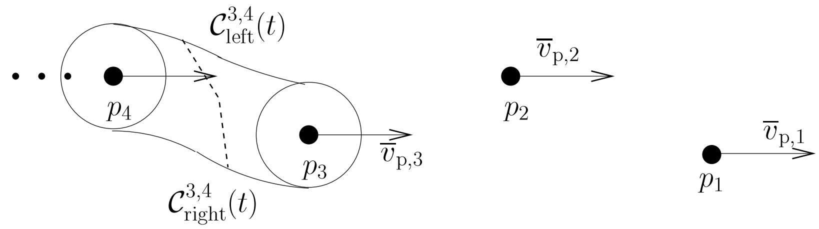

Figure 4.5. An example of the evader moving between pursuers p_3 and p_4. The dotted line between curves $\mathcal{C}^{3,4}_{\text{left}}(t)$ and $\mathcal{C}^{3,4}_{\text{right}}(t)$ shows one possible evader trajectory.

Given the pursuers' minimum turning radius ρ, for the evader/pursuers speed ratio v, we define the *critical inter-pursuer separation* as

$$s^*_{\text{ip}}(v,\rho) := \max\{2, \rho \cdot \Theta(v,\rho)\}, \quad \text{where} \tag{4.2}$$

$$\Theta(v,\rho) := \sqrt{\frac{(1+\rho)^2}{v^2\rho^2} - 1} - \arctan\sqrt{\frac{(1+\rho)^2}{v^2\rho^2} - 1} - \sqrt{\frac{1}{v^2} - 1} + \arctan\sqrt{\frac{1}{v^2} - 1}.$$

The quantity $s^*_{\text{ip}}(v,\rho)$ has the following property.

Lemma 4.3.3 (Critical inter-pursuer separation) *If $\{p_{k-1}, p_k, \overline{v}_{\text{p},k-1}, \overline{v}_{\text{p},k}\}$ are in a daisy-chain formation and the separation $s_{\text{ip}} \leq s^*_{\text{ip}}(v,\rho)$, then the evader cannot not move between p_{k-1} and p_k without being captured.*

Finally, we define two useful notions. First, a point $q \in \mathbb{R}^2$ is said to be *aligned* with $\{p_k, \overline{v}_{p,k}\}$ if the velocity vector $\overline{v}_{\mathrm{p},k}$ is parallel to $(q - p_k)$. Second, a daisy-chain formation with separation s_{ip} is said to be *closed* if there exists some $k \in \{2, \ldots, N\}$ and a path of length no more than s_{ip} that leads the leader pursuer to the position and orientation of the k-th pursuer. More specifically, a daisy-chain formation with separation s_{ip} is closed if for some $k \in \{2, \ldots, N\}$, there exists a $t_k \leq s^*_{\mathrm{ip}}(v, \rho)$ and a solution $\eta : [0, t_k] \to \mathbb{R}^2$ to equation (4.1) satisfying

$$\eta(0) = p_1, \qquad \dot{\eta}(0) = \overline{v}_{\mathrm{p},1},$$
$$\eta(t_k) = p_k, \qquad \dot{\eta}(t_k) = \overline{v}_{\mathrm{p},k}.$$

We now present our CONFINEMENT strategy. The pursuers begin in a line formation such that the distance between every two consecutive pursuers is $s^*_{\mathrm{ip}}(v, \rho)$. Pursuer p_1 is elected as leader of the line formation. We describe the strategy in the following five phases:

[Phase 1: PRE-ALIGN] The aim of the PRE-ALIGN phase is to ensure that the evader becomes aligned with $\{p_1, \overline{v}_{p,1}\}$ after some finite time, and that all the pursuers are in a line formation with the same initial separation $s^*_{\mathrm{ip}}(v, \rho)$. If the pursuers are already in this configuration, then proceed to Phase 2. Otherwise, pursuer p_1 performs the following maneuver: p_1 moves sufficiently far from the evader and turns on a tightest circle until the evader gets aligned with $\{p_1, \overline{v}_{p,1}\}$. All other pursuers move using identical control inputs to maintain the line formation.

More specifically, let l_{p} be the minimum of the roots of the quadratic equation:

$$(\gamma(l_{\mathrm{p}} + 2\pi\rho) + v\rho + \rho)^2 = (l_{\mathrm{p}} - L_0 \cos\psi_0)^2 + (\rho - L_0 \sin\psi_0)^2, \tag{4.3}$$

where ψ_0 is the angle between $\overline{v}_{\mathrm{p},1}(0)$ and $(e(0) - p_1(0))$ and $L_0 := \|p_1(0) - e(0)\|$. p_1 moves on a straight line path of length l_{p} and then moves on a circle of radius ρ and center on the side not containing $e(0)$ of the line along $\overline{v}_{\mathrm{p},1}(l_{\mathrm{p}})$. If $\phi_0 = 0$ or π, then the center of the circle of radius ρ can be chosen to be on either side of the line along $\overline{v}_{\mathrm{p},1}(l_{\mathrm{p}})$.

Lemma 4.4.1 shows that this phase terminates in finite time with the evader aligned with p_1 and at a distance greater than $v\rho$.

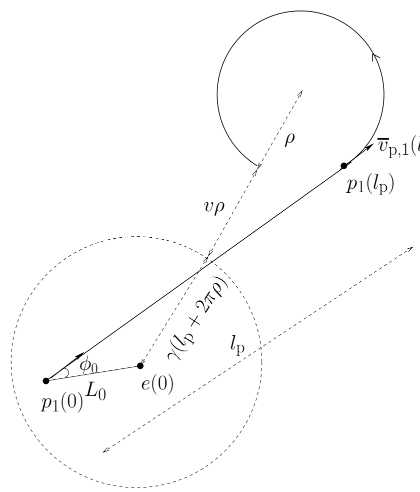

Figure 4.6. The Pre-Align phase: the bold line shows the trajectory followed by p_1.

[Phase 2: ALIGN] The aim of the ALIGN phase is to bring pursuer p_1 within distance $v\rho$ of the evader, that is, to achieve $\|e - p_1\| \leq v\rho$, while maintaining the evader aligned with $\{p_1, \overline{v}_{p,1}\}$ (this property was achieved by the PRE-ALIGN phase). During the ALIGN phase each pursuer p_k, $k \in \{1, \ldots, N\}$, moves according to

$$u^{p_k}(\theta_{\mathrm{e}}, e, \theta_{\mathrm{p},1}, p_1) = \frac{\rho v}{\|p_1 - e\|} \sin(\theta_{\mathrm{e}} - \theta_{\mathrm{p},1}). \tag{4.4}$$

We will show later that at the end of this phase, $\|p_1 - e\| \leq v\rho$, e is aligned with $\{p_1, \overline{v}_{p,1}\}$, and all pursuers are in a line formation, see Figure 4.7.

[Phase 3: SWERVE] This phase has two aims. First, the pursuers move into a straight-line daisy-chain formation with separation $s^*_{\mathrm{ip}}(v, \rho)$. Second, once the daisy-chain is formed, a new pursuer is elected as leader based on the relative position of the evader. These two steps are described as follows:

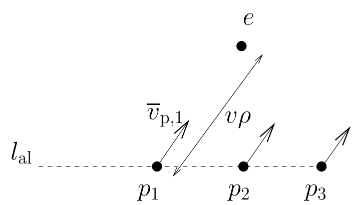

Figure 4.7. End of the ALIGN phase (beginning of the SWERVE phase); all pursuers are on a line formation. l_{al} denotes the line defining the line formation at the end of the ALIGN phase.

(i) **Form daisy-chain:** Each pursuer p_k, $k \in \{1, \ldots, N\}$, moves with maximal angular velocity $|u^{p_k}| = 1$ until all the pursuers are in a straight-line daisy-chain formation, as shown in Figure 4.8. This straight line through the pursuer positions is denoted by l_{sw}. The pursuers turn counterclockwise (resp. clockwise) if all other pursuers are on the right (resp. left) side of pursuer p_1 in the line formation.

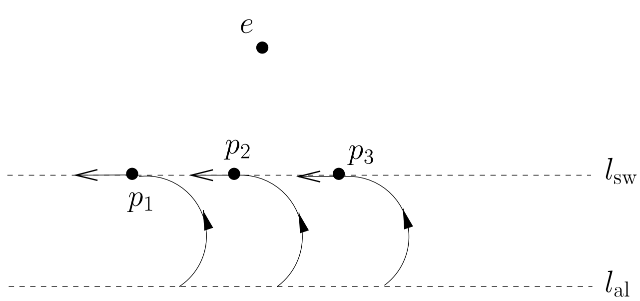

Figure 4.8. Forming a straight-line daisy-chain in the SWERVE phase. Starting from the configuration in Figure 4.7, the pursuers have turned counterclockwise and are now on the line l_{sw} with headings along l_{sw}.

(ii) **Re-elect leader:** Compute the angle $\phi_k(p_k, \overline{v}_{p,k}, e)$, for $k \in \{1, \ldots, N\}$, according to the definition in Figure 4.2. If there exists k for which $|\phi_k| \geq \frac{\pi}{2}$ (see Figure 4.9), then set $l := \max\left\{k \in \{1, \ldots, N\} \mid |\phi_k| \geq \frac{\pi}{2}\right\}$, discard from consideration the motion of the pursuers $p_1, \ldots, p_{l-1}$, and select pursuer p_l as the leader for the remaining daisy-chain formation. Otherwise, if $|\phi_k| < \frac{\pi}{2}$ for all $k \in \{1, \ldots, N\}$, then set $l = 1$, retain p_1 as the leader, and move p_l straight until $\phi_l = \pi/2$. Note that although the re-election is presented in a centralized way, there exist decentralized ways for the re-election, e.g., communicate ϕ_k with nearest neighbor, and then decide whether to stay in the daisy-chain or not.

We shall show later that with a sufficiently large number of pursuers, at the end of this step, there are more than one pursuer in the remaining daisy-chain formation.

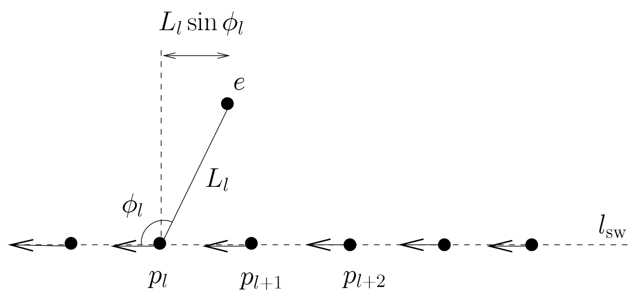

Figure 4.9. Election of the leader and the end of the SWERVE phase (beginning of the ENCIRCLE phase). All pursuers in front of p_l do not play any role in the subsequent phases.

[Phase 4: ENCIRCLE] The aim of the ENCIRCLE phase is to move to pursuers towards a closed shape and enclose the evader inside it. This is achieved via an alternating sequence of *turn* and *move straight* maneuvers. The strategy for the leader p_l is as follows:

(i) **Turn:** The pursuer p_l moves on a circular arc of appropriate radius and angle if the evader is "sufficiently behind" it. Specifically, if $|L_l \cos\phi_l| \geq \rho$ and $\phi_l \geq \pi/2$, then p_l moves on the circle with radius $R := \max\{L_l \sin\phi_l, \rho\}$ and with center in the half-plane that (i) is formed by the line along $\overline{v}_{\mathrm{p},l}$, and (ii) contains the evader. This maneuver lasts for a time interval $\Delta t := R \arctan(\sqrt{1-v^2}/v)$.

(ii) **Move straight:** If the evader is not "sufficiently behind" pursuer p_l, then p_l moves on a straight line to ensure that the evader gets "sufficiently behind" it, i.e., moves with $u_{\mathrm{p},l} = 0$, until $|L_l \cos\phi_l| \geq \rho$ and $\phi_l \geq \pi/2$.

The remaining pursuers follow the path of p_l, as shown in Figure 4.10. The ENCIRCLE phase ends when the velocity vector $\overline{v}_{p,l}$ has rotated by at least $3\pi/2$ with respect to its orientation at the start of the ENCIRCLE phase.

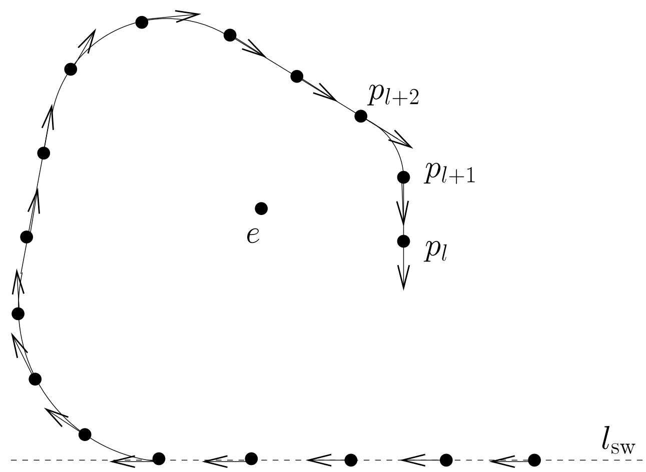

Figure 4.10. End of the ENCIRCLE phase (beginning of the CLOSE phase). The leader p_l keeps the evader on the same side of its velocity vector with the alternating turn-move straight maneuvers, until its velocity vector rotates by at least $3\pi/2$.

[Phase 5: CLOSE] The aim of the CLOSE phase is to close the daisy-chain around the evader in two steps:

(i) Pursuer p_l moves straight until it lies on the path between two pursuers in the daisy-chain, (cf. Figure 4.11).

(ii) Next, pursuer p_l moves on a circle C_1 of radius ρ centered at O_1, where O_1 is on the same side of the line along $\overline{v}_{\mathrm{p},l}$ as the evader. Then, it determines the location of center O_2 of circle C_2 of radius ρ which is tangent to C_1 and either l_{sw} or the path followed by p_l. Of the two possible locations for O_2, it selects the one which is further away from location of p_l at the end of part (i). Pursuer p_l moves along C_2 after reaching the tangency point until it closes the daisy-chain. This path is illustrated in Figure 4.11.

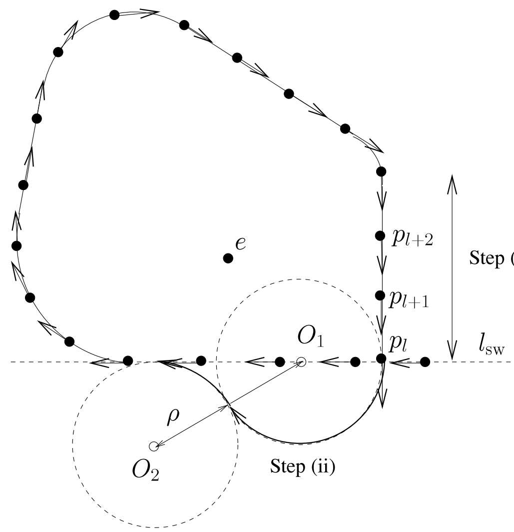

Figure 4.11. Maneuvers in the CLOSE phase for pursuer p_l. Step (i): move straight to intersect the daisy-chain. Step (ii): moves on the shortest path to close the daisy-chain.

This five-phase strategy gives us our main result.

Theorem 4.3.4 (Confinement) *Consider a cooperative Homicidal Chauffeur game with parameters $N \in \mathbb{N}$, $\rho > 0$, and $v < 1$. The proposed five-phase strategy guarantees evader confinement if the number of pursuers satisfies*

$$N \geq N_{\min}(v,\rho) := \lceil \rho(3+v\pi)/s^*_{\mathrm{ip}}(v,\rho) \rceil + \left\lceil \frac{2(1+v)\rho}{s^*_{\mathrm{ip}}(v,\rho)} \left(K^{i_{\max}} \left(\frac{4+v\pi}{1-v} \right) + \frac{i_{\max}}{1-v} + 2\pi \right) \right\rceil,$$

where $K := 1 + (1/v)\sqrt{(1+v)/(1-v)}$, $s^*_{\mathrm{ip}}(v,\rho)$ is as per equation (4.2) and the maximum number of turns in the ENCIRCLE *phase is*

$i_{\max} := \lceil 3\pi/(2\arctan(\sqrt{1-v^2}/v)) \rceil$.

Remark 4.3.5 (Asymptotic properties) *In the limit as* $v \to 1^-$, $N_{\min}(v, \rho) \to +\infty$, *as is expected. Moreover, for* v *very close to* 1 *and* $\rho \to +\infty$, *there exist constants* $c > 0$ *and* $\rho_0 > 0$ *such that* $N_{\min}(\rho) \leq c\rho$, $\forall \rho \geq \rho_0$.

Remark 4.3.6 (From Confinement to Capture) *Once the evader is confined in a region, one can achieve capture by means of additional pursuers placed in a line formation with spacing equal to twice the capture radius. These additional pursuers can then "sweep" through the region of confinement thus resulting into capture. This is illustrated in Figure 4.12. The additional number of agents required for this operation is proportional to the diameter of the confinement region, which by Remark 4.3.5, is proportional to the minimum turning radius.*

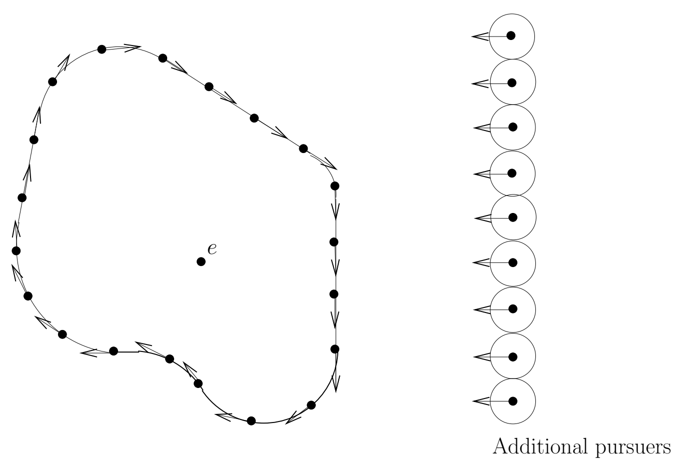

Figure 4.12. From confinement to capture using additional pursuers.

4.4 Proofs of the Main Results

In this section, we prove the main result from Section 4.3 along with certain intermediate results.

Proof of Lemma 4.3.3: Consider evader motion in a reference frame attached to the center O of the circle of radius ρ through pursuers p_{k-1} and p_k and rotating with angular speed $\frac{1}{\rho}$ in the direction of pursuer motion, as shown in Figure 4.13. The pursuers are stationary in this frame while the evader experiences an angular velocity of $1/\rho$ in the opposite direction. Let $r(t), \theta(t)$ denote the evader's polar coordinates, with $r(0) = \rho$. $\theta(t)$ is measured with respect to $p_{k-1} - O$. Let $\alpha_{\mathrm{e}}(t) \in [-\frac{\pi}{2}, \frac{\pi}{2}]$ denote the angle made by the evader's velocity in the ground frame with vector $N - e(t)$, where N is a point such that $e(t) - O \parallel N - e(t)$.

We determine the separation $s^*_{\mathrm{ip}}(v, \rho)$ which ensures that there does not exist any evader escape trajectory from arcs $p_{k-1}p_k$ to PQ, without entering any capture ball when pursuers p_{k-1} and p_k are placed on a circle of radius ρ as shown in Figure 4.13. The equations of motion for the evader in the present reference frame are

$$\dot{r}(t) = v \cos \alpha_{\mathrm{e}}(t),$$
$$\dot{\theta}(t) = v \sin \alpha_{\mathrm{e}}(t)/r(t) + 1/\rho.$$

The evader motion that maximizes θ at each r is given by $\alpha^*_{\mathrm{e}} = -\arcsin \frac{v\rho}{r(t)}$ [65]. Substituting in the differential equation for $r(t)$, we have

$$\dot{r}(t) = v\sqrt{1 - v^2\rho^2/r^2(t)}.$$

$$\text{Integrating, } r^2 = (vt + \rho\sqrt{1 - v^2})^2 + v^2\rho^2. \tag{4.5}$$

For the optimal evader motion considered, let T denote the time when $r(T) = \rho + 1$. Solving for T,

$$T = \sqrt{(1+\rho)^2/v^2 - \rho^2} - \rho\sqrt{1 - v^2}/v.$$

Substituting for r from equation (4.5) in

$$\dot{\theta}(t) = -v^2\rho/r^2 + 1/\rho,$$

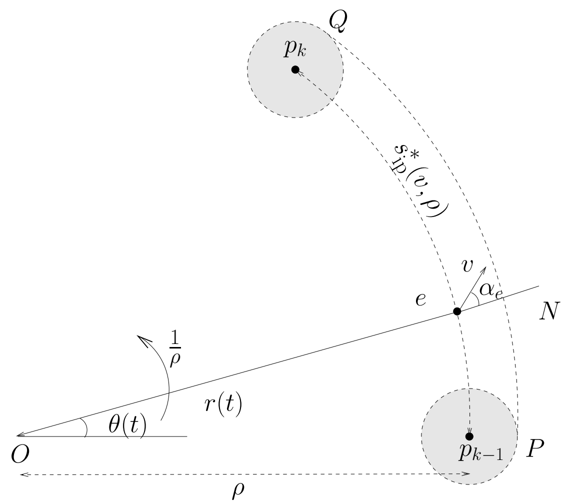

Figure 4.13. Illustrating proof of Lemma 4.3.3. We determine the critical inter-pursuer separation $s^*_{\rm ip}(v, \rho)$ which ensures the evader cannot move between p_{k-1} and p_k, without getting captured. The shaded regions are the capture discs of p_{k-1} and p_k.

and on integrating, we obtain

$$\begin{aligned}\theta(T) - \theta(0) &= -\int_0^T \frac{v^2\rho \mathrm{d}t}{(vt + \rho\sqrt{1-v^2})^2 + v^2\rho^2} + \frac{T}{\rho} \\ &= \sqrt{\frac{(1+\rho)^2}{v^2\rho^2} - 1} - \arctan\sqrt{\frac{(1+\rho)^2}{v^2\rho^2} - 1} \\ &- \sqrt{\frac{1}{v^2} - 1} + \arctan\sqrt{\frac{1}{v^2} - 1} =: \Theta.\end{aligned}$$

Thus, if the separation $s_{\rm ip}$ equals $\rho\cdot\Theta$, then there exists no evader trajectory from arc $p_{k-1}p_k$ to arc PQ that avoids capture. Now, if $\rho\cdot\Theta \le 2$, i.e., the capture balls of the two pursuers intersect, it suffices to have an inter-pursuer separation equal to 2 units. Further, it can be verified that given a value of $v < 1$, the quantity $\rho\cdot\Theta$ decreases monotonically with increasing ρ. This means that it suffices to design the inter-pursuer separation assuming that the pursuers are moving on the circle of smallest allowable radius. Thus, defining the critical separation $s^*_{\rm ip}$ as per equation (4.2) ensures that the evader cannot move between any two consecutive pursuers after the pursuers form a daisy-chain. ■

We now prove the following property of the Pre-Align phase.

Lemma 4.4.1 (Pre-Align phase) *The Pre-Align phase terminates in finite time with the evader aligned with* p_1 *at a distance greater than* $v\rho$.

Proof: The total time taken by p_1 to cover a distance l_p followed by distance of $2\pi\rho$ is $(l_\mathrm{p} + 2\pi\rho)$. In that time, the evader's reachability set is the dotted circle of radius $\gamma(l_\mathrm{p} + 2\pi\rho)$, centered at $e(0)$, as shown in Figure 4.6. Thus, to compute l_p, we impose the condition that the minimum distance between the evader's reachability set and the circular portion of the path of p_1 must be $v\rho$. Using elementary geometry, the equation (4.3) for l_p follows. ■

Lemma 4.4.2 (Align phase) *The* ALIGN *phase terminates after a finite time with the evader aligned with* $\{p_1, \overline{v}_{\mathrm{p},1}\}$ *and* $\|p_1 - e\| \leq v\rho$.

Proof: Consider the system as shown in Figure 4.2 with $k = 1$. Let α be the angle between the global X axis and the vector $e(t) - p_1(t)$ and $L_1 := \|e(t) - p_1(t)\|$. In the reference frame of the pursuer, the equations of motion are [42]

$$\dot{L}_1 = v_\mathrm{e}\cos(\theta_\mathrm{e} - \alpha) - v_\mathrm{p}\cos(\theta_{\mathrm{p},1} - \alpha), \tag{4.6}$$

$$\dot{\alpha} = \frac{1}{L_1}[v_\mathrm{e}\sin(\theta_\mathrm{e} - \alpha) - v_\mathrm{p}\sin(\theta_{\mathrm{p},1} - \alpha)], \tag{4.7}$$

$$\dot{\theta}_{\mathrm{p},1} = \frac{v_\mathrm{p} u^{p_1}}{\rho}. \tag{4.8}$$

Define $\phi_1 := \alpha - \theta_{\mathrm{p},1}$ and compute

$$\dot{\phi}_1 = \frac{1}{\rho}\left(\frac{\rho}{L_1}(v\sin(\theta_\mathrm{e} - \theta_{\mathrm{p},1} - \phi_1) + \sin\phi_1) - u^{p_1}\right).$$

As a result of the PRE-ALIGN phase, after evader is aligned with $\{p_1, \overline{v}_{p,1}\}$, i.e., $\phi_1 = 0$, pursuer p_1 seeks to ensure that $\dot{\phi}_1 = 0$, for all subsequent times. This is possible if

$u^{p_1} = \frac{\rho v}{L_1}\sin(\theta_{\rm e} - \theta_{\rm p,1})$. Substituting for u^{p_1}, existence of solutions to the system governed by equations (4.6)-(4.8) is guaranteed due to the measurability assumption on $\theta_{\rm e}$. The constraint on $\|u^{p_1}\|$ implies that the evader can be kept aligned with $\{p_1, \overline{v}_{p,1}\}$ as long as $L_1(t) \geq v\rho$. Further, observe that once $\phi_1 = 0$ and $\dot{\phi}_1 = 0$, $\dot{L}_1 \leq -(1-v)$. Thus, L_1 is reduced to $v\rho$ in finite time. ■

Lemma 4.4.3 (Swerve phase) *(i) A sufficient number of pursuers which ensures that after the leader re-election step, there are at least two pursuers in the remaining daisy-chain formation is* $\lceil \rho(3+v\pi)/s^*_{\rm ip}(v,\rho) \rceil$ *and,*

(ii) Let $d_{\rm sw}$ *be the distance of the evader from the line* $l_{\rm sw}$ *joining the pursuer positions at the end of the* SWERVE *phase, (cf. Figure 4.8). Then,* $d_{\rm sw} \leq \rho(3+v\pi)/(1-v)$.

Proof: In the SWERVE phase, let pursuer p_1 move on the circle of radius ρ centered at O as shown in Figure 4.14. The time taken for this phase is $\rho\beta$, where $\beta \in [0,\pi]$ is the angle between line $l_{\rm al}$ and the vector $\overline{v}_{\rm p,1}$ as shown in Figure 4.14. Let $d_{\rm x}$ (resp. $d_{\rm y}$) denote the magnitude of the component of the vector $p_l - e$ along (resp. perpendicular to) $l_{\rm sw}$ after re-election of the leader. To maximize $d_{\rm x}$, the evader must move parallel to $l_{\rm sw}$. From trigonometry,

$$d_{\rm x} = v\rho\beta + \|v\rho\cos\beta - \rho\sin\beta\| \leq \rho(3+v\pi),$$

where the first term is the radius of the evader's reachability set in time $\rho\beta$ and the second term in the right hand side equality is the x-component of the distance between e and p_1'. To ensure that at least two pursuers exist in the remaining daisy-chain, it suffices to have the length of the original straight-line daisy-chain equal to the upper bound on $d_{\rm x}$. This proves part (i).

On similar lines, to maximize d_{y}, the evader must move along the line perpendicular to l_{sw}. Thus, we obtain

$$d_{\mathrm{y}} = v\rho\beta + \|\rho(1-\cos\beta) - v\rho\sin\beta\| \leq \rho(3+v\pi).$$

If there exists k for which $|\phi_k| \geq \frac{\pi}{2}$ (see Figure 4.9), then $d_{\mathrm{sw}} = d_{\mathrm{y}}$ and part (ii) follows. Otherwise, if $|\phi_k| < \frac{\pi}{2}$ for all $k \in \{1, \ldots, N\}$, then pursuer p_1 (who is retained as the leader) moves straight for a time interval of at most $d_{\mathrm{x}}/(1-v)$, which then gives, $d_{\mathrm{sw}} \leq d_{\mathrm{y}} + d_{\mathrm{x}}v/(1-v)$. The result follows from the upper bounds on d_{x} and d_{y}. ■

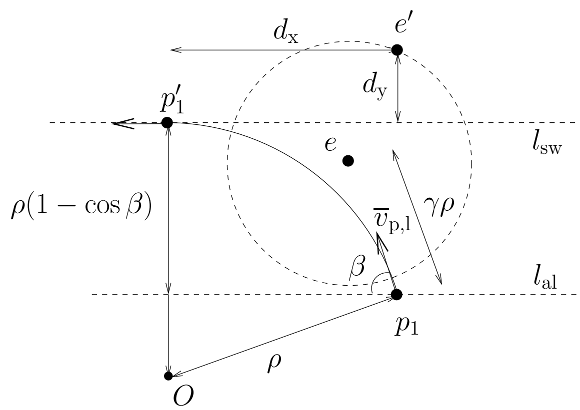

Figure 4.14. Illustrating the proof of Lemma 4.4.3. The primed notation refers to the positions of the players after the pursuers have formed a straight line daisy-chain. The dotted circle shows the reachability set of the evader in time interval $\rho\beta$.

Lemma 4.4.4 (Encircle and Close phases) *If the pursuers begin the* ENCIRCLE *phase at time t^*, then in the* ENCIRCLE *and part (i) of the* CLOSE *phases, there exists no evader trajectory such that the evader is aligned with $\{p_l, \overline{v}_{p,l}\}$ at any time $t \geq t^*$.*

To prove Lemma 4.4.4, we first introduce the following notation: let $\Sigma(t^*)$ denote the local coordinate system with origin at $p_l(t^*)$ and with the positive Y axis along its heading $\overline{v}_{p,l}$ at time t^*, as shown in Figure 4.15. Define

$$\mathcal{V}(p_l(t^*), \overline{v}_{p,l}(t^*)) := \Big\{(x^\Sigma, y^\Sigma) \in \Sigma(t^*) |\ x^\Sigma \geq 0, y^\Sigma \leq x^\Sigma\sqrt{1-v^2}/v\Big\}.$$

The set $\mathcal{V}$ possesses the following useful property.

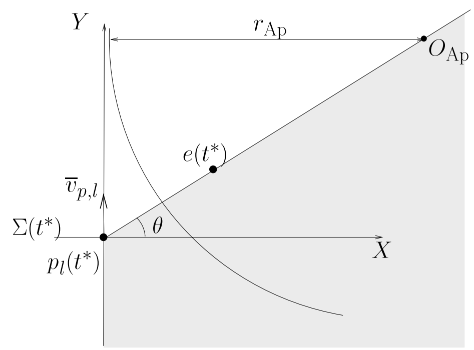

Figure 4.15. Proof of Lemma 4.4.5. For $\theta = \arctan(\sqrt{1-v^2}/v)$, the shaded region denotes the set $\mathcal{V}(p_l(t^*), \overline{v}_{p,l}(t^*))$.

Lemma 4.4.5 (Property of $\mathcal{V}$) *Given a time instant t^*, let pursuer p_l move with $u_{p,l} = 0$ for all subsequent time instants. If $e(t^*) \in \mathcal{V}(p_l(t^*), \overline{v}_{p,l}(t^*))$, then there exists no evader trajectory such that the evader is aligned with $\{p_l, \overline{v}_{p,l}\}$ at any time $t \geq t^*$.*

Proof: In the coordinate system $\Sigma(t^*)$, denote the point $e(t^*)$ by (x^{Σ}, y^{Σ}). Construct the Apollonius circle [51] of the points $p_l(t^*)$ and $e(t^*)$, as shown in Figure 4.15. This is the set of points that the evader can reach before pursuer p_l does, assuming that the pursuer does not possess turning constraints. The center O_{Ap} and radius r_{Ap} of the Apollonius circle are $O_{\mathrm{Ap}} = \frac{1}{1-v^2}(x^{\Sigma}, x^{\Sigma}\tan\theta)$ and $r_{\mathrm{Ap}} = \frac{vx^{\Sigma}\sec\theta}{1-v^2}$, respectively. Now, let the pursuer p_l move with $u_{p,l} = 0$ for all $t \geq t^*$. In the reference frame $\Sigma(t^*)$, if r_{Ap} does not exceed the X coordinate of O_{Ap}, then the pursuer reaches any point z on the Y axis before the evader can reach z. In other words, the evader cannot align itself with $\{p_l, \overline{v}_{p,l}\}$ at any subsequent time. Thus, $r_{\mathrm{Ap}} \leq x^{\Sigma}/(1-v^2)$ implies $\tan\theta \leq \sqrt{1-v^2}/v$. ■

Proof of Lemma 4.4.4: In the ENCIRCLE phase, let t^* be a time instant at which pursuer p_l is about to begin a move straight maneuver. It suffices to show that the evader is at a point $e(t^*)$ contained in the set $\mathcal{V}(p_l(t^*), \overline{v}_{p,l}(t^*))$. Two cases need to be considered:

Case 1: $R := L_l \sin\phi_l$. The angle through which pursuer p_l turns in a turn maneuver is $\arctan(\sqrt{1-v^2}/v)$ which is less than $\pi/2$. Figure 4.16 shows the positions of pursuer p_l and the evader just before a turn maneuver (at time instant t_{turn}) and just before the following move straight maneuver (at time instant t^*) in the ENCIRCLE phase. As per the strategy, we have $t^* = t_{\text{turn}} + \Delta t = t_{\text{turn}} + R\arctan(\sqrt{1-v^2}/v)$. Thus, in the time interval Δt, the evader's reachability set is the dotted circle, having radius upper bounded by $R\sqrt{1-v^2}$ as shown in Figure 4.16. By geometry, the pursuer's center of rotation O in the time interval Δt is precisely at a distance of $R\sqrt{1-v^2}$ from the boundary L defined in Figure 4.16, of the set $\mathcal{V}(p_l(t^*), \overline{v}_{p,l}(t^*))$. Since $\arctan(\sqrt{1-v^2}/v) < \pi/2$, it follows that the evader's reachability set in time Δt and hence $e(t^*)$ is contained in $\mathcal{V}(p_l(t^*), \overline{v}_{p,l}(t^*))$. Lemma 4.4.5 completes the proof.

Case 2: $R = \rho$. The proof of this case is on similar lines as that of case 1, with the additional property that one need not consider that part of the evader's reachability set which lies on the opposite side of the daisy-chain. ■

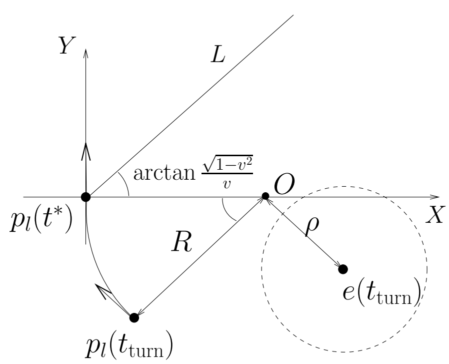

Figure 4.16. Case 1 in the proof of Lemma 4.4.4. The dotted circle is the evader's reachability set in time $R\arctan\sqrt{1-v^2}/v$. Pursuer p_l begins the turn and move straight maneuvers of the ENCIRCLE phase at times t_{turn} and t^*, respectively.

Proof of Theorem 4.3.4: It suffices to show that all five phases terminate in finite time. This partly follows from Lemmas 4.4.2 and 4.4.3. It remains to show that (a) the ENCIRCLE phase terminates in finite time and, (b) the evader is confined at the end of the CLOSE phase.

To show (a), we determine an upper bound T_{enc} on the time taken by the ENCIRCLE phase. From Lemma 4.4.4, we deduce that in the ENCIRCLE phase, the evader is always the same side of the line along $\overline{v}_{\text{p},l}$. Also, in each turn maneuver, pursuer p_l turns through an angle of at least $\arctan(\sqrt{1-v^2}/v))$. Thus, the turn maneuver is made at most $i_{\max} := \lceil 3\pi/(2\arctan(\sqrt{1-v^2}/v))\rceil$ times. This justifies the expression for $i_{\max}$ in this theorem.

Let t_0 be the time instant at the end of the SWERVE phase and $d_0 := d_{\text{sw}}$, i.e., the distance of the evader from the line l_{sw} at the end of the SWERVE phase. Let t_i denote the time instant when the pursuer begins the turn maneuver of the ENCIRCLE phase for the i-th time and let d_i denote the distance of the evader from the line along $\overline{v}_{\text{p},l}$ at the time instant t_i. We first determine an upper bound for d_i. Let p_l begin the turn maneuver at t_{i-1}, as shown in Figure 4.17. An upper bound for $t_i - t_{i-1}$ is

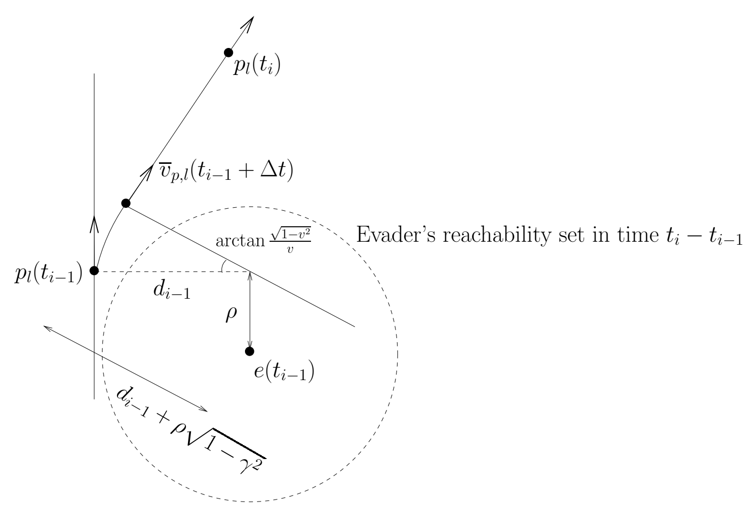

Figure 4.17. Determining an upper bound on the interval between two successive times in the ENCIRCLE phase, when the pursuer uses the turn maneuver.

obtained when the evader decides to move parallel to the line along $\overline{v}_{\mathrm{p},l}(t_{i-1}+\Delta t)$ in the interval $[t_{i-1}, t_i]$. Thus,

$$t_i - t_{i-1} \leq d_{i-1} \arctan \frac{\sqrt{1-v^2}}{v} + \frac{\rho + v d_{i-1} \arctan \frac{\sqrt{1-v^2}}{v}}{1-v} \leq \frac{d_{i-1}}{v}\sqrt{\frac{1+v}{1-v}} + \frac{\rho}{1-v},$$

where the first term in the first expression is the time for which p_l moves on a circular path and the second is an upper bound on the time taken for the following move straight maneuver, assuming that the evader moves parallel to $\bar{v}_{p,l}(t_{i-1}+\Delta t)$, (cf. Figure 4.17). The next inequality follows by using the fact that $\arctan(x) \leq x$, and upon simplification. An upper bound for d_i results when the evader moves normal to the line along $\overline{v}_{\mathrm{p},l}(t_{i-1}+\Delta t)$ in the time interval $[t_{i-1}, t_i]$. Thus,

$$\begin{aligned} d_i \leq d_{i-1} + \rho\sqrt{1-v^2} + v(t_i - t_{i-1}) &\leq d_{i-1}\Big(1 + \frac{1}{v}\sqrt{\frac{1+v}{1-v}}\Big) + \frac{\rho}{1-v} \\ &\leq K d_{i-1} + \frac{\rho}{1-v} \leq K^i\Big(d_0 + \frac{\rho}{1-v}\Big), \end{aligned}$$

where the second step follows from the upper bound on $t_i - t_{i-1}$ and the fact that $\sin x \leq 1$, and $K := 1 + (1/v)\sqrt{(1+v)/(1-v)}$. The last inequality follows from $K > 2$. Now, for $i \in \{1, \dots, i_{\max}\}$ where $i_{\max}$ equals $\lceil 3\pi/2(\arctan(\sqrt{1-v^2}/v))\rceil$, the time T_{enc} satisfies

$$T_{\mathrm{enc}} \leq \sum_{i=1}^{i_{\max}} t_i - t_{i-1} \leq \sum_{i=1}^{i_{\max}} \frac{d_{i-1}}{v}\sqrt{\frac{1+v}{1-v}} + i_{\max}\frac{\rho}{1-v}.$$

Using the upper bounds for d_{i-1}, and for d_0 (cf. part (ii) of Lemma 4.4.3),

$$T_{\mathrm{enc}} \leq K^{i_{\max}}\rho\Big(\frac{4+v\pi}{1-v}\Big) + \frac{i_{\max}\rho}{1-v}.$$

Note that T_{enc} is also the distance covered by pursuer p_l in the ENCIRCLE phase. So in part (i) of the CLOSE phase, p_l covers a distance of at most T_{enc}. Thus, we have shown that the ENCIRCLE phase and part (i) of the CLOSE phase terminate in finite time.

Pursuer p_l travels a distance of at most $4\pi\rho$ in part (ii) of the CLOSE phase before the daisy-chain gets closed. Thus, the total distance traveled by p_l in the ENCIRCLE and CLOSE phases is at most $2T_{\mathrm{enc}} + 4\pi\rho$. In the worst-case, to ensure closure of the daisy-chain, consider the distance between $p_l(t_0)$ and the point at which pursuer p_l intersects the daisy-chain. This distance can be at most $v(2T_{\mathrm{enc}} + 4\pi\rho)$, which is the distance covered by the evader if it moves with a fixed heading parallel to the line l_{sw} at the end of the SWERVE phase and in the direction opposite to the pursuers' velocity vectors at time t_0. Thus, a sufficient number of pursuers that ensures confinement in the ENCIRCLE and CLOSE phases is given by

$$\left\lceil \frac{2(1+v)}{s^*_{\mathrm{ip}}(v,\rho)} \Big(K^{i_{\max}} \rho \Big(\frac{4+v\pi}{1-v} \Big) + \frac{\rho i_{\max}}{1-v} + 2\pi\rho \Big) \right\rceil .$$

By Lemma 4.4.3, an additional $\lceil \rho(3+v\pi)/s^*_{\mathrm{ip}}(v,\rho) \rceil$ pursuers are sufficient for the leader re-election step in the SWERVE phase, and the result is proved. The evader is confined since the pursuers form a closed daisy-chain around it. ■

Summary

We addressed a cooperative Homicidal Chauffeur game in which a single pursuer is unable to capture an evader, given an arbitrary initial condition. We proposed a multi-phase partly-decentralized pursuer strategy that involved role specialization in the form of leader and followers, that guarantees confinement of an evader to a bounded region. We characterized the number of pursuers for which our strategy is guaranteed to lead to confinement.

Part II: Predictably-moving Targets

Chapter 5

Pursuing Translating Targets in Dynamic Environments

5.1 Introduction

So far we have addressed pursuit problems that involved a single evading target, and we designed strategies for one or many pursuers to capture it, under various sensing and motion constraints. We now focus our attention to designing strategies, or policies, to capture multiple targets that possess predictable motion. In this chapter, we introduce a problem involving multiple targets, referred to as demands, that arrive sequentially on a line segment, and upon arrival translate in a known direction and with known fixed speed. A single pursuer seeks to service the demands in a manner so that the average number of demands in the environment does not grow unbounded. The setup has similarities to the dynamic vehicle routing framework, with the novelty that the demands in our problem are in motion, in particular, translating with known speed.

Contributions

We introduce a dynamic vehicle routing problem in which demands arrive via a stochastic process on a line segment of fixed length, and upon arrival, translate with a fixed velocity perpendicular to the segment. A service vehicle, modeled as a first-order integrator having speed greater than that of the demands, seeks to serve these mobile demands. The goal is to design stable service policies for the vehicle, i.e., the expected time spent by a demand in the environment is finite. We propose a novel receding horizon control policy for the vehicle that services the translating demands as per a translational minimum Hamiltonian path (TMHP).

In this chapter, we analyze the problem when the demands are uniformly distributed along the segment and the demand arrival process is Poisson with rate λ. For a fixed length W of the segment and the vehicle speed normalized to unity, the problem is governed by two parameters; the demand speed v and the arrival rate λ. Our results are as follows. First, we derive a necessary condition on λ in terms of v for the existence of a stable service policy. Second, we analyze our novel TMHP-based policy and derive a sufficient condition for λ in terms of v that ensures stability of the policy. With respect to stability of the problem, we identify two asymptotic regimes: (a) *High speed regime*: when the demands move as fast as the vehicle, i.e., $v \to 1^-$ (and therefore for stability, $\lambda \to 0^+$); and (b) *Low speed regime*: when demand speed tends to zero, i.e., $v \to 0^+$ (and so a sufficiently high λ may still ensure stability). In the high speed regime, we show that: (i) for existence of a stabilizing policy, λ must converge to zero as $1/\sqrt{-\log(1-v)}$, (ii) every stabilizing policy must service the demands in the first-come-first-served (FCFS) order, and (iii) of all such policies, the TMHP-based policy minimizes the expected time to service a demand. In the low speed regime, we show that the sufficient condition on λ for the stability of the TMHP-based policy is within a constant factor of the necessary condition on λ for stability of any policy. Third, we identify another asymptotic regime, termed as the *low arrival regime*, in which the arrival rate $\lambda \to 0^+$ for a fixed demand speed. In this low arrival regime, we establish that the TMHP-based policy is optimal in terms of minimizing the expected time to service a demand. Fourth, for the analysis of the TMHP-based policy, we study the classic FCFS policy in which demands are served in the order in which they arrive. We determine necessary and sufficient conditions on λ for the stability of the FCFS policy. Fifth and finally, we validate our analysis with extensive simulations and provide an empirically accurate characterization of the region in the parameter space of demand speed and arrival rate for which the TMHP-based policy is stable.

A plot of the theoretically established necessary and sufficient conditions for stability in the v-λ parameter space is shown in Figure 5.1. The bottom figures are for the asymptotic regimes of $v \to 0^+$, and $v \to 1^-$, respectively.

Organization

This chapter is organized as follows. A short review of results on optimal motion and combinatorics is presented in Section 5.2. The problem formulation, the TMHP-based policy, and the main results are presented in Section 5.3. The FCFS policy is presented and analyzed in Section 5.4. Utilizing the results of Section 5.4, the main results are proven in Section 5.5. Finally, simulation results are presented in Section 5.6.

5.2 Preliminary Results

In this section, we provide some useful background results.

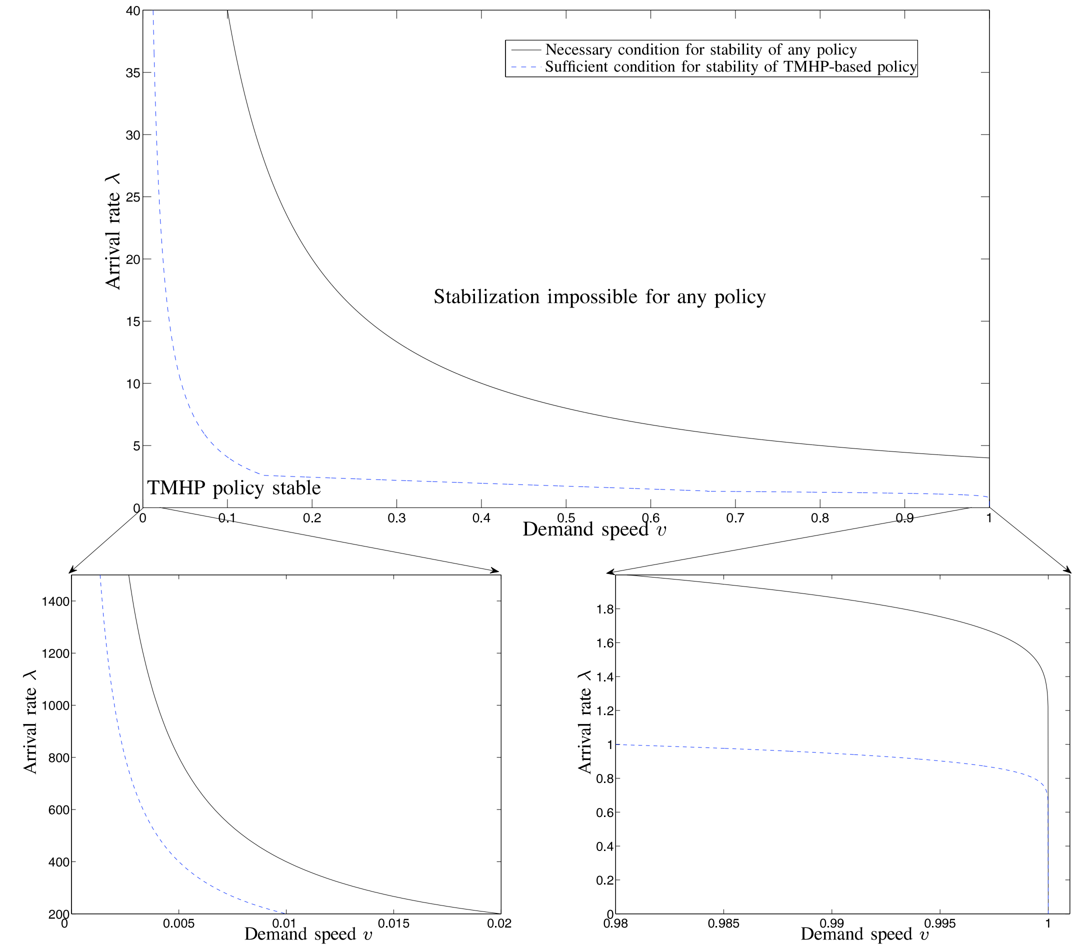

Figure 5.1. A summary of stability regions for the TMHP-based policy and the FCFS policy. Stable service policies exist only for the region under the solid black curve. In the top figure, the solid black curve is due to part (i) of Theorem 5.3.1 and the dashed blue curve is due to part (i) of Theorem 5.3.2. In the asymptotic regime shown in the bottom left, the dashed blue curve is described in part (ii) of Theorem 5.3.2, and is different than the one in the top figure. In the asymptotic regime shown in the bottom right, the solid black curve is due to part (ii) of Theorem 5.3.1, and is different from the solid black curve in the top figure.

5.2.1 Constant bearing control

We will use the following result on catching a moving demand in minimum time.

Definition 5.2.1 (Constant bearing control) *Given initial locations* $\mathbf{p} := (X, Y) \in \mathbb{R}^2$ *and* $\mathbf{q} := (x, y) \in \mathbb{R}^2$ *of the service vehicle and a demand, respectively, with the demand moving in the positive* y*-direction with constant speed* $v \in]0, 1[$, *the motion of the service vehicle towards the point* $(x, y + vT)$, *where*

$$T(\mathbf{p}, \mathbf{q}) := \frac{\sqrt{(1 - v^2)(X - x)^2 + (Y - y)^2}}{1 - v^2} - \frac{v(Y - y)}{1 - v^2}, \tag{5.1}$$

with unit speed is defined as the constant bearing control.

Constant bearing control is illustrated in Figure 5.2 and characterized in the following proposition.

Proposition 5.2.2 (Minimum time control, [51]) *The constant bearing control is the minimum time control for the service vehicle to reach the moving demand.*

5.2.2 Euclidean and Translational minimum Hamiltonian path (EMHP/TMHP) problems

Given a set of points in the plane, a Euclidean Hamiltonian path is a path that visits each point exactly once. A Euclidean minimum Hamiltonian path (EMHP) is a Euclidean Hamiltonian path that has minimum length. We also consider the problem of determining a constrained EMHP which starts at a specified start point, visits a set of points and terminates at a specified end point.

More specifically, the EMHP problem is as follows.

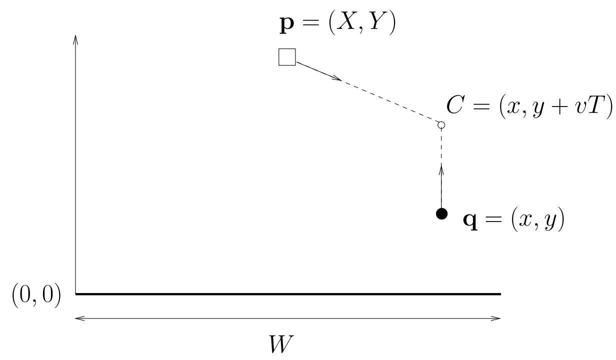

Figure 5.2. Constant bearing control. The vehicle moves towards the point $C := (x, y + vT)$, where x, y, v and T are as per Definition 5.2.1, to reach the demand.

Given n static points placed in $\mathbb{R}^2$, determine the length of the shortest path which visits each point exactly once.

An upper bound on the length of such a path for points in a unit square was given by Few [36]. Here we extend Few's bound to the case of points in a rectangular region.

Lemma 5.2.3 (EMHP length) *Given n points in a $1 \times h$ rectangle in the plane, where $h \in \mathbb{R}_{>0}$, there exists a path that starts from a unit length edge of the rectangle, passes through each of the n points exactly once, and terminates on the opposite unit length edge, having length upper bounded by*

$$\sqrt{2hn} + h + 5/2.$$

Proof: Suppose the rectangular region is given by $0 \leq x \leq 1$, $0 \leq y \leq h$. Let m be a positive integer (to be chosen later) and let the n points be denoted by $\{\mathbf{q}_1, \ldots, \mathbf{q}_n\}$. We now construct two paths through the points. The first consists of (a) the $m + 1$ lines $y = 0, h/m, 2h/m, \ldots, h$; (b) the n shortest distances from each of the n points to the nearest such line, each traveled twice, and (c) suitable portions of the lines $x = 0$, $0 \leq y \leq h$, and $x = 1$, $0 \leq y \leq h$. This is illustrated in Figure 5.3. The length of this path is

$$l_1 = m + 1 + 2\sum_{i=1}^{n} d_1(\mathbf{q}_i) + h,$$

where the notation $d_1(\mathbf{q}_i)$ denotes the shortest distance of point $\mathbf{q}_i$ from the nearest of the $m+1$ lines. The second path is constructed similarly using the m lines $y = h/2m, 3h/2m, \ldots, (2m-1)h/2m$. This path also commences on $y = h$, passes through the above m lines (visiting the points whenever they are at the shortest distance from these m lines) and ends on $y = 0$. The length of this path is

$$l_2 = (m+2) + 2\sum_{i=1}^{n} d_2(\mathbf{q}_i) + h,$$

where the notation $d_2(\mathbf{q}_i)$ denotes the shortest distance of point $\mathbf{q}_i$ from the nearest of the new m lines.

Observe that $d_1(\mathbf{q}_i) + d_2(\mathbf{q}_i) = h/2m$. Hence,

$$l_1 + l_2 = 2m + 3 + 2h + hn/m.$$

Now choose m to be the integer nearest to $\sqrt{hn/2}$, so that $n = 2(m+\theta)^2/h$, where $|\theta| \leq 1$. Thus,

$$\begin{aligned} l_1 + l_2 &= 2m + 3 + 2h + 2(m+\theta)^2/m \\ &= 4(m+\theta) + 2h + 3 + 2\theta^2/m \\ &\leq 2\sqrt{2hn} + 2h + 5. \end{aligned}$$

Thus, at least one of the two paths must have length upper bounded by $\sqrt{2hn} + h + 5/2$. ∎

Given a set $\mathcal{Q}$ of n points in $\mathbb{R}^2$, the Euclidean Traveling Salesperson Problem (ETSP) is to determine the shortest tour, i.e., a closed path that visits each point exactly once. Let ETSP($\mathcal{Q}$) denote the length of the ETSP tour through $\mathcal{Q}$. The following is the classic result by Beardwood, Halton, and Hammersly [10].

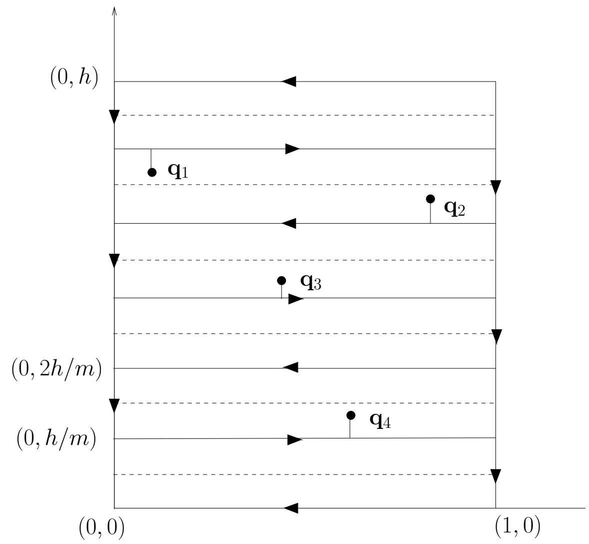

Figure 5.3. Illustration of the proof of Theorem 5.2.3. The dots indicate the locations of the points inside a rectangle of size $1 \times h$. The first of the two paths considered in the proof through the points begins at $(1, h)$ and follows the direction of the arrows, visiting a point whenever it is within a distance of $h/2m$ for a specific integer m from the solid horizontal lines.

Theorem 5.2.4 (Asymptotic ETSP length, [10]) *If a set $\mathcal{Q}$ of n points are distributed independently and uniformly in a compact region of area A, then there exists a constant β_{TSP} such that, almost surely,*

$$\lim_{n \to +\infty} \frac{\mathrm{ETSP}(\mathcal{Q})}{\sqrt{n}} = \beta_{\mathrm{TSP}} \sqrt{A}. \tag{5.2}$$

The constant β_{TSP} has been estimated numerically as $\beta_{\mathrm{TSP}} \approx 0.7120 \pm 0.0002$, [80].

Next, we describe the TMHP problem which was proposed and solved in [47]. This problem is posed as follows.

> Given initial coordinates; $\mathbf{s}$ of a start point, $\mathcal{Q} := \{\mathbf{q}_1, \ldots, \mathbf{q}_n\}$ of a set of points, and $\mathbf{f}$ of a finish point, all moving with the same constant speed v and in the same direction, determine a path that starts at time zero from point $\mathbf{s}$, visits all points in the set $\mathcal{Q}$ exactly once and ends at the finish point, and the length $\mathcal{L}_{T,v}(\mathbf{s}, \mathcal{Q}, \mathbf{f})$ of which is minimum.

In what follows, we wish to determine the TMHP through points which translate in the positive y direction. We also assume the speed of the service vehicle to be normalized to unity, and hence consider the speed of the points $v \in]0,1[$. A solution for the TMHP problem is the *Convert-to-EMHP* method:

1. For $v \in]0,1[$, define the conversion map $\mathrm{cnvrt}_v : \mathbb{R}^2 \to \mathbb{R}^2$ by
$$\mathrm{cnvrt}_v(x,y) = \Big(\frac{x}{\sqrt{1-v^2}}, \frac{y}{1-v^2}\Big).$$
2. Compute the EMHP that starts at $\mathrm{cnvrt}_v(\mathbf{s})$, passes through the set of points given by
$\{\mathrm{cnvrt}_v(\mathbf{q}_1), \dots, \mathrm{cnvrt}_v(\mathbf{q}_n)\}$ and ends at $\mathrm{cnvrt}_v(\mathbf{f})$.
3. Move between any two demands using the constant bearing control.

For the Convert-to-EMHP method, the following result is established.

Lemma 5.2.5 (TMHP length, [47]) *Let the initial coordinates* $\mathbf{s} = (x_\mathbf{s}, y_\mathbf{s})$ *and* $\mathbf{f} = (x_\mathbf{f}, y_\mathbf{f})$, *and the speed of the points* $v \in]0,1[$. *The length of the TMHP is*

$$\mathcal{L}_{T,v}(\mathbf{s}, \mathcal{Q}, \mathbf{f}) = \mathcal{L}_E(\mathrm{cnvrt}_v(\mathbf{s}), \{\mathrm{cnvrt}_v(\mathbf{q}_1), \dots, \mathrm{cnvrt}_v(\mathbf{q}_n)\}, \mathrm{cnvrt}_v(\mathbf{f})) + \frac{v(y_\mathbf{f} - y_\mathbf{s})}{1-v^2},$$

where $\mathcal{L}_E(\mathrm{cnvrt}_v(\mathbf{s}), \{\mathrm{cnvrt}_v(\mathbf{q}_1), \dots, \mathrm{cnvrt}_v(\mathbf{q}_n)\}, \mathrm{cnvrt}_v(\mathbf{f}))$ *denotes the length of the EMHP with starting point* $\mathrm{cnvrt}_v(\mathbf{s})$, *passing through the set of points* $\{\mathrm{cnvrt}_v(\mathbf{q}_1), \dots, \mathrm{cnvrt}_v(\mathbf{q}_n)\}$, *and ending at* $\mathrm{cnvrt}_v(\mathbf{f})$.

This lemma implies the following result: given a start point, a set of points and an end point all of whom translate in the positive vertical direction at speed $v \in]0,1[$, the order of the points followed by the optimal TMHP solution is the same as the order of the points followed by the optimal EMHP solution through a set of static locations equal to the locations of the moving points at initial time converted via the map cnvrt_v.

5.3 Problem Formulation and the TMHP-based Policy

In this section, we pose the dynamic vehicle routing problem with translating demands and present the TMHP-based policy along with the main results.

5.3.1 Problem Statement

We consider a single service vehicle that seeks to service mobile demands that arrive via a spatio-temporal process on a line segment with length W along the x-axis, termed the *generator*. The vehicle is modeled as a first-order integrator with speed upper bounded by one. The demands arrive uniformly distributed on the generator via a temporal Poisson process with intensity $\lambda > 0$, and move with constant speed $v \in \,]0, 1[$ along the positive y-axis, as shown in Figure 5.4. We assume that once the vehicle reaches a demand, the demand is served instantaneously. The vehicle is assumed to have unlimited fuel and demand servicing capacity.

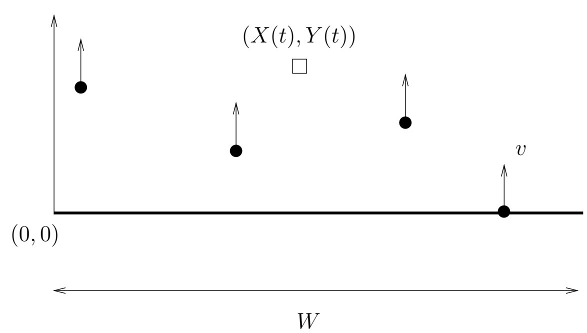

Figure 5.4. The problem set-up. The thick line segment is the generator of mobile demands. The dark circle denotes a demand and the square denotes the service vehicle.

We define the environment as $\mathcal{E} := [0, W] \times \mathbb{R}_{\geq 0} \subset \mathbb{R}^2$, and let $\mathbf{p}(t) = [X(t), Y(t)]^T$

$\in \mathcal{E}$ denote the position of the service vehicle at time t. Let $\mathcal{Q}(t) \subset \mathcal{E}$ denote the set of all demand locations at time t, and $n(t)$ the cardinality of $\mathcal{Q}(t)$. Servicing of a demand $\mathbf{q}_i \in \mathcal{Q}$ and removing it from the set $\mathcal{Q}$ occurs when the service vehicle reaches the location of the demand. A static feedback control policy for the system is a map $\mathcal{P} : \mathcal{E} \times \mathbb{F}(\mathcal{E}) \to \mathbb{R}^2$, where $\mathbb{F}(\mathcal{E})$ is the set of finite subsets of $\mathcal{E}$, assigning a commanded velocity to the service vehicle as a function of the current state of the system: $\dot{\mathbf{p}}(t) = \mathcal{P}(\mathbf{p}(t), \mathcal{Q}(t))$. Let D_i denote the time that the ith demand spends inside the set $\mathcal{Q}$, that is, the delay between the generation of the ith demand and the time it is serviced. The policy $\mathcal{P}$ is *stable* if under its action,

$$\limsup_{i \to +\infty} \mathbb{E}\left[D_i\right] < +\infty,$$

that is, the steady state expected delay is finite. Equivalently, the policy $\mathcal{P}$ is stable if under its action,

$$\limsup_{t \to +\infty} \mathbb{E}\left[n(t)\right] < +\infty,$$

that is, if the vehicle is able to service demands at a rate that is—on average—at least as fast as the rate at which new demands arrive. In what follows, our goal is to *design stable control policies* for the system.

To obtain further intuition into stability of a policy, consider the v-λ parameter space. In the asymptotic regime of high speed, where $v \to 1^-$, the arrival rate λ *must* tend to zero for stability, otherwise the service vehicle would have to move successively further away from the generator in expected value, thus making the system unstable. In the asymptotic region of low demand speed, where $v \to 0^+$, if $\lambda \to +\infty$, then we expect the system to be unstable; while for a sufficiently low λ, we expect to be able to stabilize the system. Thus, our goal is to characterize regions in the v-λ parameter space in which one can never design *any* stable policy, as well as those in which our policies are stable, with additional emphasis in the above two asymptotic regimes. In addition, for the asymptotic regime of low arrival, where for a fixed speed $v < 1$, the arrival rate $\lambda \to 0^+$, stability is intuitive as demands arrive very rarely. Hence, in this regime, we seek to minimize the steady state expected delay for a demand.

5.3.2 The TMHP-based policy

We now present a novel receding horizon service policy for the vehicle that is based on the repeated computation of a translational minimum Hamiltonian path through successive groups of outstanding demands. For a given arrival rate λ and demand speed $v \in]0, 1[$, let (X^*, Y^*) denote the vehicle location in the environment that minimizes the expected time to service a demand once it appears on the generator. The expression for the optimal location (X^*, Y^*) is postponed to Section 5.4.1. The TMHP-based policy is summarized in Algorithm 2, and an iteration of the policy is illustrated in Figure 5.5.

Algorithm 2: The TMHP-based policy

Assumes: The optimal location $(X^*, Y^*) \in \mathcal{E}$ is given.

1: **if** no outstanding demands are present in $\mathcal{E}$ **then**

2: Move to the optimal position (X^*, Y^*).

3: **else**

4: Service all outstanding demands by following a translational minimum Hamiltonian path starting from the vehicle's current location, and terminating at the demand with the lowest y-coordinate.

5: Repeat.

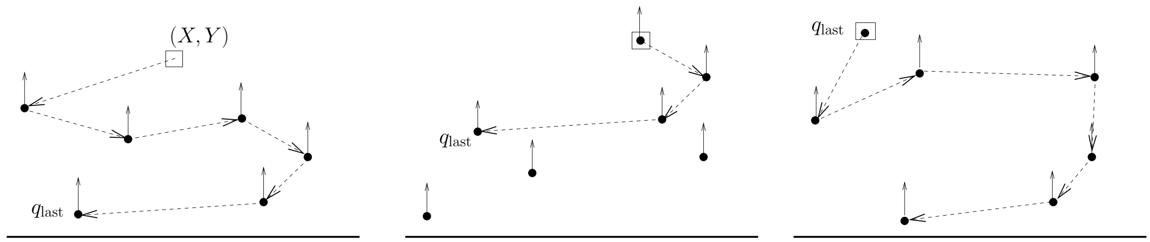

Figure 5.5. An iteration of a receding horizon service policy. The vehicle shown as a square serves all outstanding demands shown as black dots as per the TMHP that begins at (X, Y) and terminates at q_{last} which is the demand with the least y-coordinate. The first figure shows a TMHP at the beginning of an iteration. The second figure shows the vehicle servicing the demands through which the TMHP has been computed while new demands arrive in the environment. The third figure shows the vehicle repeating the policy for the set of new demands when it has completed service of the demands present at the previous iteration.

5.3.3 Main Results

The following is a summary of our main results and the locations of their proofs within the chapter. We begin with a necessary condition for stability, the proof of which is presented in Section 5.5.1. This result is primarily due to Mr. Stephen L. Smith.

Theorem 5.3.1 (Necessary condition for stability) *The following are necessary conditions for the existence of a stabilizing policy:*

1. *For* $v \in \,]0, 1[$,

$$\lambda \leq \frac{4}{vW}.$$

2. *For the asymptotic regime of high speed, where* $v \to 1^-$*, every stabilizing policy*

must serve the demands in the order in which they arrive and hence,

$$\lambda \leq \frac{3\sqrt{2}}{W\sqrt{-\log(1-v)}}.$$

Then, we derive a sufficient condition for stability of the TMHP-based policy, the proof of which is presented in Section 5.5.2. We introduce the following notation. Let

$$\lambda_{\text{FCFS}}(v, W) := \begin{cases} \frac{3}{W}\sqrt{\frac{1-v}{1+v}}, & \text{for } v \leq v^*_{\text{suf}}, \\ \frac{\sqrt{12v}}{W\sqrt{(1+v)\left(C_{\text{suf}} - \log\left(\frac{1-v}{v}\right)\right)}}, & \text{otherwise}, \end{cases}$$

where log(.) refers to the natural logarithm, $C_{\text{suf}} = \pi/2 - \log(0.5 \cdot \sqrt{3}/\sqrt{2})$, and v^*_{suf} is the solution to $\sqrt{12v^*} - 3\sqrt{(1-v^*)(C_{\text{suf}} - \log(1-v^*) + \log v^*)} = 0$, and is approximately equal to 2/3.

Theorem 5.3.2 (Sufficient condition for stability) *The following are sufficient conditions for stability of the TMHP-based policy.*

1. *For* $v \in \,]0, 1[$,

$$\lambda < \max\left\{\frac{(1-v^2)^{3/2}}{2vW(1+v)^2}, \lambda_{\text{FCFS}}(v, W)\right\}.$$

2. *For the asymptotic regime of low speed where* $v \to 0^+$,

$$\lambda < \frac{1}{\beta^2_{\text{TSP}} vW}, \qquad \textit{where } \beta_{\text{TSP}} \approx 0.7120.$$

A plot of the necessary and sufficient conditions is shown in Figure 5.1. In the asymptotic regime of high speed, the sufficient condition from part (i) of Theorem 5.3.2 simplifies to

$$\lambda < \frac{\sqrt{6}}{W\sqrt{-\log(1-v)}} =: \lambda^{1^-}_{\text{suf}},$$

and the necessary condition established in part (ii) of Theorem 5.3.1 simplifies to

$$\lambda \leq \frac{3\sqrt{2}}{W\sqrt{-\log(1-v)}} =: \lambda_{\text{nec}}^{1^-}.$$

In the asymptotic regime of low speed, the sufficient condition from part (ii) of Theorem 5.3.2 is $\lambda < 1/(\beta_{\text{TSP}}^2 vW) =: \lambda_{\text{suf}}^{0^+}$, and the necessary condition established in part (i) of Theorem 5.3.1 is $\lambda \leq 4/(vW) =: \lambda_{\text{nec}}^{0^+}$.

Theorems 5.3.1 and 5.3.2 immediately lead to the following corollary.

Corollary 5.3.3 (Constant factor sufficient condition) *In the asymptotic regime of*

1. *high speed, which is the limit as $v \to 1^-$, the ratio $\lambda_{\text{nec}}^{1^-}/\lambda_{\text{suf}}^{1^-} \to \sqrt{3}$.*

2. *low speed, which is the limit as $v \to 0^+$, the ratio $\lambda_{\text{nec}}^{0^+}/\lambda_{\text{suf}}^{0^+} \to 4\beta_{\text{TSP}}^2 \approx 2.027$.*

Finally, we state the following optimality property of the TMHP-based policy, the proof of which is presented in Section 5.5.2.

Theorem 5.3.4 (Optimality of TMHP-based policy) *The TMHP-based policy minimizes the expected time to service a demand in*

1. *the low arrival asymptotic regime, where $\lambda \to 0^+$ for a fixed $v \in]0,1[$, and*

2. *the high speed asymptotic regime, where $v \to 1^-$ (and therefore $\lambda \to 0^+$).*

In order to study the stability of the TMHP-based policy, we introduce and analyze a first-come-first-served (FCFS) policy in the next section.

5.4 The First-Come-First-Served (FCFS) Policy

In this section, we present the FCFS policy and establish some of its properties.

In the FCFS policy, the service vehicle uses constant bearing control and services the demands in the order in which they arrive. If the environment contains no demands, the vehicle moves to the location (X^*, Y^*) which minimizes the expected time to catch the next demand to arrive. This policy is summarized in Algorithm 3.

Algorithm 3: **The FCFS policy**

Assumes: The optimal location $(X^*, Y^*) \in \mathcal{E}$ is given.

1: **if** no outstanding demands are present in $\mathcal{E}$ **then**

2: Move toward (X^*, Y^*) until the next demand arrives.

3: **else**

4: Move using the constant bearing control to service the furthest demand from the generator.

5: Repeat.

Figure 5.6 illustrates an instance of the FCFS policy. The following lemma establishes the relationship between the FCFS policy and the TMHP-based policy.

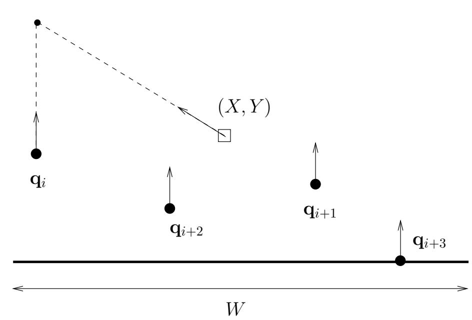

Figure 5.6. The FCFS policy. The vehicle services the demands in the order of their arrival in the environment, using the constant bearing control.

Lemma 5.4.1 (Relation between TMHP-based and FCFS policies) *Given an arrival rate λ and a demand speed v, if the FCFS policy is stable, then the TMHP-based policy is stable.*

Proof: Consider an initial vehicle position and a set of outstanding demands, all of which have lower y-coordinates than the vehicle. Let us compare the amount of time required to service the outstanding demands using the TMHP-based policy with the amount of time required for the FCFS policy. Both policies generate paths through all outstanding demands, starting at the initial vehicle location, and terminating at the outstanding demand with the lowest y-coordinate. By definition, the TMHP-based policy generates the shortest such path. Thus, the TMHP-based policy will require no more time to service all outstanding demands than the FCFS policy. Since this holds at every iteration of the policy, the region of stability of TMHP-based policy contains the region of stability for the FCFS policy. ∎

In the following subsections, we analyze the FCFS policy. We then combine these results with the above lemma to establish analogous results for the TMHP-based policy.

The first question is, how do we compute the optimal position (X^*, Y^*)? This will be answered in the following subsection.

5.4.1 Optimal Vehicle Placement

In this subsection, we study the FCFS policy when $v \in]0, 1[$ is fixed and $\lambda \to 0^+$. In this regime, stability is not an issue as demands arrive very rarely, and the problem becomes one of optimally placing the service vehicle (i.e., determining (X^*, Y^*) in the statement of the FCFS policy).

We seek to place the vehicle at location that minimizes the expected time to service a demand once it appears on the generator. Demands appear at uniformly random positions on the generator and the vehicle uses the constant bearing control to reach the demand. Thus, the expected time to reach a demand generated at position $\mathbf{q} = (x, 0)$ from vehicle position $\mathbf{p} = (X, Y)$ is given by

$$\mathbb{E}\left[T(\mathbf{p}, \mathbf{q})\right] = \frac{1}{W(1-v^2)} \int_0^W \left(\sqrt{(1-v^2)(X-x)^2 + Y^2} - vY\right) dx. \tag{5.3}$$

The following lemma characterizes the way in which this expectation varies with the position $\mathbf{p}$.

Lemma 5.4.2 (Properties of the expected time) *The expected time* $\mathbf{p} \mapsto \mathbb{E}\left[T(\mathbf{p}, \mathbf{q})\right]$ *is convex in* $\mathbf{p}$*, for all* $\mathbf{p} \in [0, W] \times \mathbb{R}_{>0}$*. Additionally, there exists a unique point* $\mathbf{p}^* := (W/2, Y^*) \in \mathbb{R}^2$ *that minimizes* $\mathbf{p} \mapsto \mathbb{E}\left[T(\mathbf{p}, \mathbf{q})\right]$*.*

Proof: Regarding the first statement, it suffices to show that the integrand in equation (5.3), $T(\mathbf{p}, (x, 0))$ is convex for all x. To do this we compute the Hessian of $T((X, Y), (x, 0))$ with respect to X and Y. Thus, for $Y > 0$,

$$\begin{bmatrix} \frac{\partial^2 T}{\partial X^2} & \frac{\partial^2 T}{\partial X \partial Y} \\ \frac{\partial^2 T}{\partial Y \partial X} & \frac{\partial^2 T}{\partial Y^2} \end{bmatrix} = \frac{1}{\left((1-v^2)(X-x)^2 + Y^2\right)^{3/2}} \begin{bmatrix} Y^2 & Y(X-x) \\ Y(X-x) & (X-x)^2 \end{bmatrix}.$$

The Hessian is positive semi-definite because its determinant is zero and its trace is non-negative. This implies that $T(\mathbf{p}, \mathbf{q})$ is convex in $\mathbf{p}$ for each $\mathbf{q} = (x, 0)$, from which the first statement follows.

Regarding the second statement, since demands are uniformly randomly generated on the interval $[0, W]$, the optimal horizontal position is $X^* = W/2$. Thus, it suffices to show that $Y \mapsto \mathbb{E}\left[T((W/2, Y), \mathbf{q})\right]$ is strictly convex. From the $\partial^2 T/\partial Y^2$ term of the Hessian we see that $T(\mathbf{p}, \mathbf{q})$ is strictly convex for all $x \neq W/2$. But, letting $\mathbf{p} = (W/2, Y)$ and $\mathbf{q} = (x, 0)$ we can write

$$\mathbb{E}\left[T(\mathbf{p}, \mathbf{q})\right] = \frac{1}{W(1-v^2)} \int_{x \in [0,W] \setminus \{W/2\}} T(\mathbf{p}, \mathbf{q}) dx.$$

The integrand is strictly convex for all $x \in [0, W] \setminus \{W/2\}$, implying that $\mathbb{E}[T(\mathbf{p}, \mathbf{q})]$ is strictly convex on the line $X = W/2$, and that the point $(W/2, Y^*)$ is the unique minimizer. ■

Lemma 5.4.2 tells us that there exists a unique point $\mathbf{p}^* := (X^*, Y^*)$ which minimizes the expected travel time. In addition, we know that $X^* = W/2$. Obtaining a closed form expression for Y^* does not appear to be possible. Computing the integral in equation (5.3), with $X = W/2$, one can obtain

$$\mathbb{E}[T(\mathbf{p}, \mathbf{q})] = \frac{Y}{a}\left(\frac{1}{2}\sqrt{1 + \frac{aW^2}{4Y^2}} - \frac{Y}{\sqrt{a}W}\log\left(\sqrt{1 + \frac{aW^2}{4Y^2}} - \sqrt{\frac{aW^2}{4Y^2}}\right) - v\right),$$

where $a = 1 - v^2$. For each value of v and W, this convex expression can be easily numerically minimized over Y, to obtain Y^*. A plot of Y^* as a function of v for $W = 1$ is shown in Figure 5.7.

For the optimal position $\mathbf{p}^*$, the expected delay between a demand's arrival and its service completion is

$$D^* := \mathbb{E}[T(\mathbf{p}^*, (x, 0))].$$

Thus, a lower bound on the steady-state expected delay of any policy is D^*. We now characterize the steady-state expected delay of the FCFS policy D_{FCFS}, as λ tends to zero.

Lemma 5.4.3 (FCFS optimality) *Fix any $v \in]0, 1[$. Then in the limit as $\lambda \to 0^+$, the FCFS policy minimizes the expected time to service a demand, i.e., $D_{\mathrm{FCFS}} \to D^*$.*

Proof: We have shown how to compute the position $\mathbf{p}^* := (X^*, Y^*)$ which minimizes equation (5.3). Thus, if the vehicle is located at $\mathbf{p}^*$, then the expected time to service the demand is minimized. But, as $\lambda \to 0^+$, the probability that demand $i + 1$ arrives before the vehicle completes service of demand i and returns to $\mathbf{p}^*$ tends to zero. Thus, the FCFS policy is optimal as $\lambda \to 0^+$. ■

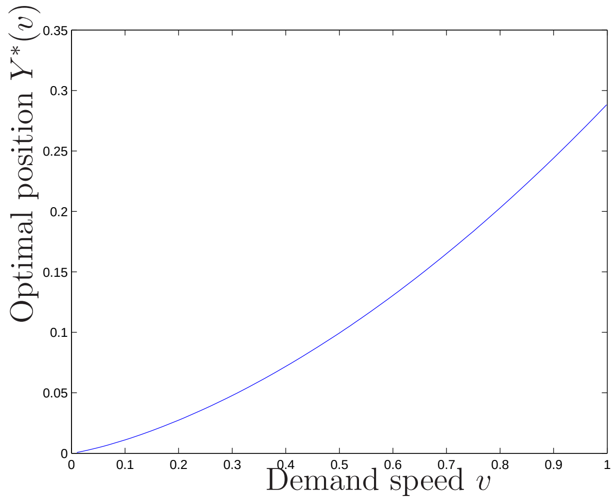

Figure 5.7. The optimal position Y^* of the service vehicle which minimizes the expected distance to a demand, as a function of v. In this plot, the generator has length $W = 1$.

Remark 5.4.4 (Minimizing the worst-case time) *Another metric that can be used to determine the optimal placement (X^*, Y^*) is the worst-case time to service a demand. Using an argument identical to that in the proof of Lemma 5.4.3, it is possible to show that for fixed $v \in \,]0, 1[$, and as $\lambda \to 0^+$, the FCFS policy, with $(X^*, Y^*) = (W/2, vW/2)$, minimizes the worst-case time to service a demand.* □

5.4.2 A Necessary Condition for FCFS Stability

In the previous subsection, we studied the case of fixed v and $\lambda \to 0^+$. In this subsection, we analyze the problem when $\lambda > 0$, and determine necessary conditions on the magnitude of λ that ensure the FCFS policy remains stable. To establish these conditions we utilize a standard result in queueing theory (cf. [56]) which states that a necessary condition for the existence of a stabilizing policy is that $\lambda \mathbb{E}[T] \leq 1$, where $\mathbb{E}[T]$ is the expected time to service a demand (i.e., the travel time between demands). We begin with the following result.

Proposition 5.4.5 (Special case of equal speeds) *For $v = 1$, there does not exist a stabilizing policy.*

Proof: When $v = 1$, each demand and the service vehicle move at the same speed. If a demand has a higher vertical position than the service vehicle, then clearly the service vehicle cannot reach it. The same impossibility result holds if the demand has the same vertical position and a distinct horizontal position as the service vehicle. In summary, a demand can be reached only if the service vehicle is above the demand. Next, note that the only policy that ensures that a demand's y-coordinate never exceeds that of the service vehicle (i.e., that all demands remain below the service vehicle at all time) is the FCFS policy. In what follows, we prove the proposition statement by computing the expected time to travel between demands using the FCFS policy. First, consider a vehicle location $\mathbf{p} := (X, Y)$ and a demand location with initial location $\mathbf{q} := (x, y)$, the minimum time T in which the vehicle can reach the demand is given by

$$T(\mathbf{p}, \mathbf{q}) = \frac{(X - x)^2 + (Y - y)^2}{2(Y - y)}, \quad \text{if } Y > y, \tag{5.4}$$

and is undefined if $Y \leq y$. Second, assume there are many outstanding demands below the service vehicle, and none above. Suppose the service vehicle completed the service of demand i at time t_i and position $(x_i(t_i), y_i(t_i))$. Let us compute the expected time to reach demand $i+1$, with location $(x_{i+1}(t_i), y_{i+1}(t_i))$. Since arrivals are Poisson it follows that $y_i(t_i) > y_{i+1}(t_i)$. To simplify notation we define $\Delta x = |x_i(t_i) - x_{i+1}(t_i)|$ and $\Delta y = y_i(t_i) - y_{i+1}(t_i)$. Then, from equation (5.4)

$$T(\mathbf{q}_i, \mathbf{q}_{i+1}) = \frac{\Delta x^2 + \Delta y^2}{2\Delta y} = \frac{1}{2}\left(\frac{\Delta x^2}{\Delta y} + \Delta y\right).$$

Taking expectation and noting that Δx and Δy are independent,

$$\mathbb{E}\left[T(\mathbf{q}_i, \mathbf{q}_{i+1})\right] = \frac{1}{2}\left(\mathbb{E}\left[\Delta x^2\right]\mathbb{E}\left[\tfrac{1}{\Delta y}\right] + \mathbb{E}\left[\Delta y\right]\right).$$

Now, we note that $\mathbb{E}[\Delta y] = 1/\lambda$, that $\mathbb{E}[\Delta x^2]$ is a positive constant independent of λ, and that

$$\mathbb{E}\left[\tfrac{1}{\Delta y}\right] = \int_{y=0}^{+\infty} \frac{1}{y}\lambda \mathrm{e}^{-\lambda y} dy = +\infty.$$

Thus $\mathbb{E}[T(\mathbf{q}_i, \mathbf{q}_{i+1})] = +\infty$, and for every $\lambda > 0$,

$$\lambda \mathbb{E}[T(\mathbf{q}_i, \mathbf{q}_{i+1})] = +\infty.$$

This means that the necessary condition for stability, i.e., $\lambda \mathbb{E}[T(\mathbf{q}_i, \mathbf{q}_{i+1})] \leq 1$, is violated. Thus, there does not exist a stabilizing policy. ■

Next we look at the FCFS policy and give a necessary condition for its stability. This lemma is primarily due to Mr. Stephen L. Smith.

Lemma 5.4.6 (Necessary stability condition for FCFS) *A necessary condition for the stability of the FCFS policy is*

$$\lambda \leq \begin{cases} \dfrac{3}{W}, & \text{for } v \leq v^*_{\text{nec}}, \\[2ex] \dfrac{3\sqrt{2v}}{W\sqrt{(1+v)\left(C_{\text{nec}} - \log\left(\frac{\sqrt{1-v^2}}{v}\right)\right)}}, & \text{otherwise,} \end{cases}$$

where $\log(.)$ *refers to the natural logarithm,* $C_{\text{nec}} = 0.5 + \log(2) - \gamma$*, where* γ *is the Euler constant; and* v^*_{nec} *is the solution to the equation* $2v - (1+v)(C_{\text{nec}} - 0.5 \cdot \log(1 - v^2) + \log v) = 0$*, and is approximately equal to* $4/5$*.*

Proof: Suppose the service vehicle completed the service of demand i at time t_i at position $(x_i(t_i), y_i(t_i))$, and demand $i+1$ is located at $(x_{i+1}(t_i), y_{i+1}(t_i))$. Define $\Delta x := |x_i(t_i) - x_{i+1}(t_i)|$ and $\Delta y := y_i(t_i) - y_{i+1}(t_i)$. For $v \in]0, 1[$, the travel time between demands is given by

$$T = \frac{1}{1-v^2}\left(\sqrt{(1-v^2)\Delta x^2 + \Delta y^2} - v\Delta y\right). \tag{5.5}$$

Observe that the function T is convex in Δx and Δy. Jensen's inequality leads to

$$\mathbb{E}\left[T\right] \geq \frac{1}{1-v^2}\Big(\sqrt{(1-v^2)(\mathbb{E}\left[\Delta x\right])^2 + (\mathbb{E}\left[\Delta y\right])^2} - v\mathbb{E}\left[\Delta y\right]\Big).$$

Substituting the expressions for the expected values, we obtain

$$\mathbb{E}\left[T\right] \geq \frac{1}{1-v^2}\Big(\sqrt{(1-v^2)\frac{W^2}{9} + \frac{v^2}{\lambda^2}} - \frac{v^2}{\lambda}\Big).$$

From the necessary condition for stability, we must have

$$\lambda\mathbb{E}\left[T\right] \leq 1 \qquad \Longleftrightarrow \qquad \lambda\frac{1}{1-v^2}\Big(\sqrt{\frac{(1-v^2)W^2}{9} + \frac{v^2}{\lambda^2}} - \frac{v^2}{\lambda}\Big) \leq 1.$$

By simplifying, we obtain

$$\lambda \leq \frac{3}{W}. \tag{5.6}$$

This provides a good necessary condition for low v. Next, we obtain a much better necessary condition for large v.

Since T is convex in Δx, we apply Jensen's inequality to equation (5.5) to obtain

$$\mathbb{E}\left[T|\Delta y\right] \geq \frac{1}{1-v^2}\left(\sqrt{(1-v^2)W^2/9 + \Delta y^2} - v\Delta y\right), \tag{5.7}$$

where $\mathbb{E}\left[\Delta x\right] = W/3$. Now, the random variable Δy is distributed exponentially with parameter λ/v and probability density function

$$f(y) = \frac{\lambda}{v}\mathrm{e}^{-\lambda y/v}.$$

Un-conditioning equation (5.7) on Δy, we obtain

$$\mathbb{E}\left[T\right] = \int_0^{+\infty}\mathbb{E}\left[T|y\right]f(y)dy \geq \frac{\lambda}{v(1-v^2)}\int_0^{+\infty}\left(\sqrt{\frac{(1-v^2)W^2}{9} + y^2} - vy\right)\mathrm{e}^{-\frac{\lambda y}{v}}dy. \tag{5.8}$$

The right hand side can be evaluated using the software Maple® and equals

$$\frac{\pi W}{2\cdot 3\sqrt{1-v^2}}\left[\mathbf{H}_1\left(\frac{\lambda W\sqrt{1-v^2}}{3v}\right) - \mathbf{Y}_1\left(\frac{\lambda W\sqrt{1-v^2}}{3v}\right)\right] - \frac{v^2}{\lambda(1-v^2)},$$

where $\mathbf{H}_1 : \mathbb{R} \to \mathbb{R}$ is the 1st order Struve function and $\mathbf{Y}_1 : \mathbb{R} \to \mathbb{R}$ is 1st order Bessel function of the 2nd kind [69]. Using a Taylor series expansion of the function

$\mathbf{H}_1(z) - \mathbf{Y}_1(z)$ about $z = 0$, followed by a subsequent analysis of the higher order terms, one can show that

$$\mathbf{H}_1(z) - \mathbf{Y}_1(z) \geq \frac{1}{\pi}\left(\frac{2}{z} + C_{\text{nec}} z - z\log(z)\right), \quad \forall z \geq 0,$$

where $\log(.)$ refers to the natural logarithm, $C_{\text{nec}} = 1/2 + \log(2) - \gamma$, and γ is the Euler constant. This inequality implies that equation (5.8) can be written as

$$\mathbb{E}[T] \geq \frac{v}{\lambda(1+v)} + \frac{\lambda W}{18v}\left(C_{\text{nec}} - \log\left(\frac{\lambda W\sqrt{1-v^2}}{3v}\right)\right),$$

where we have used the fact that

$$\frac{v}{\lambda(1-v)^2} - \frac{v^2}{\lambda(1-v^2)} = \frac{v}{\lambda(1+v)}.$$

To obtain a stability condition on λ we wish to remove λ from the log term. To do this, note that from equation (5.6) we have $\lambda W/3 < 1$, and thus

$$\begin{aligned}\mathbb{E}[T] &\geq \frac{v}{\lambda(1+v)} + \frac{\lambda W}{18v}\left(C_{\text{nec}} - \log\frac{W\lambda}{3} - \log\frac{W\sqrt{1-v^2}}{3v}\right)\\ &\geq \frac{v}{\lambda(1+v)} + \frac{\lambda W}{18v}\left(C_{\text{nec}} - \log\left(\frac{\sqrt{1-v^2}}{v}\right)\right).\end{aligned}$$

The necessary stability condition is $\lambda\mathbb{E}[T] \leq 1$, from which a necessary condition for stability is

$$\frac{\lambda^2 W}{18v}\left(C_{\text{nec}} - \log\left(\frac{\sqrt{1-v^2}}{v}\right)\right) \leq 1 - \frac{v}{1+v} = \frac{1}{1+v}.$$

Solving for λ when $\log(\sqrt{1-v^2}/v) < C_{\text{nec}}$, we obtain that

$$\lambda \leq \frac{3\sqrt{2v}}{W\sqrt{(1+v)\left(C_{\text{nec}} - \log\left(\frac{\sqrt{1-v^2}}{v}\right)\right)}}, \tag{5.9}$$

The condition $C_{\text{nec}} > \log(\sqrt{1-v^2}/v)$, implies that the above bound holds for all $v > 1/\sqrt{1+\mathrm{e}^{2C_{\text{nec}}}}$. We now have two bounds; equation (5.6) which holds for all $v \in\,]0,1[$, and equation (5.9) which holds for $v > 1/2$. The final step is to determine the values of v for which each bound is active. To do this, we set the right-hand side of equation (5.6) equal to the right-hand side of equation (5.9) and denote the solution by v^*_{nec}. Thus, the necessary condition for stability is given by equation (5.6) when $v \leq v^*_{\text{nec}}$, and by equation (5.9) when $v > v^*_{\text{nec}}$. ∎

5.4.3 A Sufficient Condition for FCFS stability

In Section 5.4.2, we determined a necessary condition for stability of the FCFS policy. In this subsection, we will derive the following sufficient condition on the arrival rate that ensures stability for the FCFS policy. To establish this condition, we utilize a standard result in queueing theory (cf. [56]) which states that a sufficient condition for the existence of a stabilizing policy is that $\lambda \mathbb{E}[T] < 1$, where $\mathbb{E}[T]$ is the expected time to service a demand (i.e., the travel time between demands).

Lemma 5.4.7 (Sufficient stability condition for FCFS) *The FCFS policy is stable if*

$$\lambda < \begin{cases} \dfrac{3}{W}\sqrt{\dfrac{1-v}{1+v}}, & \text{for } v \leq v^*_{\text{suf}}, \\ \dfrac{\sqrt{12v}}{W\sqrt{(1+v)\left(C_{\text{suf}} - \log\left(\frac{1-v}{v}\right)\right)}}, & \text{otherwise,} \end{cases}$$

where $\log(.)$ *refers to the natural logarithm,* $C_{\text{suf}} = \pi/2 - \log(0.5 \cdot \sqrt{3}/\sqrt{2})$*, and* v^*_{suf} *is the solution to* $\sqrt{12v^*} - 3\sqrt{(1-v^*)(C_{\text{suf}} - \log(1-v^*) + \log v^*)} = 0$*, and is approximately equal to* $2/3$*.*

Proof: We begin with the expression for the travel time between two consecutive demands using the constant bearing control (cf. Definition 5.2.1),

$$T = \frac{\sqrt{(1-v^2)\Delta x^2 + \Delta y^2}}{1-v^2} - \frac{v\Delta y}{1-v^2} \leq \frac{|\Delta x|}{\sqrt{1-v^2}} + \frac{\Delta y}{1-v^2}, \tag{5.10}$$

where we used the inequality $\sqrt{a^2+b^2} \leq |a| + |b|$. Taking expectation,

$$\mathbb{E}[T] \leq \frac{W}{3\sqrt{1-v^2}} + \frac{v}{\lambda(1-v^2)},$$

since the demands are distributed uniformly in the x-direction and Poisson in the y-direction. A sufficient condition for stability is

$$\lambda \mathbb{E}[T] < 1 \quad \Longleftrightarrow \quad \lambda < \frac{3}{W}\sqrt{\frac{1-v}{1+v}}. \tag{5.11}$$

The upper bound on T given by equation (5.10) is very conservative except for the case when v is very small. Alternatively, taking expected value of T conditioned on Δy, and applying Jensen's inequality to the square-root part, we obtain

$$\mathbb{E}\left[T|\Delta y\right] \leq \frac{1}{1-v^2}\left(\sqrt{(1-v^2)W^2/6+\Delta y^2} - v\Delta y\right),$$

since $\mathbb{E}\left[\Delta x^2\right] = W^2/6$. Following steps which are similar to those between equation (5.7) and equation (5.8), we obtain

$$\mathbb{E}\left[T\right] \leq \frac{\pi W}{2\cdot\sqrt{6}\sqrt{1-v^2}}\left[\mathbf{H}_1\left(\frac{\lambda W\sqrt{1-v^2}}{\sqrt{6}v}\right) - \mathbf{Y}_1\left(\frac{\lambda W\sqrt{1-v^2}}{\sqrt{6}v}\right)\right] - \frac{v^2}{\lambda(1-v^2)}. \tag{5.12}$$

In [69], polynomial approximations have been provided for the Struve and Bessel functions in the intervals $[0,3]$ and $[3,+\infty)$. We seek an upper bound for the right-hand side of (5.12) when v is sufficiently large, i.e., when the argument of $\mathbf{H}_1$ and $\mathbf{Y}_1$ is small. From [69], we know that

$$\mathbf{H}_1(z) \leq \frac{z}{2}, \quad \mathbf{Y}_1(z) \geq \frac{2}{\pi}\left(\mathbf{J}_1(z)\log\frac{z}{2} - \frac{1}{z}\right), \quad \text{and } \mathbf{J}_1(z) \leq \frac{z}{2}, \quad \text{for } 0 \leq z \leq 3,$$

where $z := \lambda W\sqrt{1-v^2}/(\sqrt{6}v)$, and $\mathbf{J}_1 : \mathbb{R} \to \mathbb{R}$ denotes the Bessel function of the first kind. To obtain a lower bound on $\mathbf{Y}_1(z)$, we observe that if $0 \leq z \leq 2$, then due to the log term in the above lower bound for $\mathbf{Y}_1(z)$, we can substitute $z/2$ in place of $\mathbf{J}_1(z)$. Thus, we obtain

$$\mathbf{H}_1(z) \leq \frac{z}{2}, \quad \mathbf{Y}_1(z) \geq \frac{2}{\pi}\left(\frac{z}{2}\log\frac{z}{2} - \frac{1}{z}\right), \quad \text{for } 0 \leq z \leq 2. \tag{5.13}$$

Substituting into equation (5.12), we obtain

$$\begin{aligned}\mathbb{E}\left[T\right] \leq \frac{\pi W}{2\cdot\sqrt{6}\sqrt{1-v^2}}\Big[&\frac{\lambda W\sqrt{1-v^2}}{2\sqrt{6}v} + \frac{2}{\pi}\Big(\frac{\sqrt{6}v}{\lambda W\sqrt{1-v^2}} \\ &- \frac{\lambda W\sqrt{1-v^2}}{2\sqrt{6}v}\log\frac{\lambda W\sqrt{1-v^2}}{2\sqrt{6}v}\Big)\Big] - \frac{v^2}{\lambda(1-v^2)},\end{aligned}$$

which yields

$$\mathbb{E}\left[T\right] \leq \frac{\lambda W^2}{12v}\left(\frac{\pi}{2} - \log\frac{\lambda W}{3} - \log\frac{\sqrt{3}\sqrt{1-v^2}}{2\sqrt{2}v}\right) - \frac{1}{\lambda(1+v)}. \tag{5.14}$$

Now, let λ^* be the least upper bound on λ for which the FCFS policy is unstable, i.e., for every $\lambda < \lambda^*$, the FCFS policy is stable. To obtain λ^*, we need to solve $\lambda^*\mathbb{E}[T] = 1$. Using equation (5.14), we can obtain a lower bound on λ^* by simplifying

$$\frac{\lambda^{*2}W^2}{12v}\left(\frac{\pi}{2} - \log\frac{\lambda^* W}{3} - \log\frac{\sqrt{3}\sqrt{1-v^2}}{2\sqrt{2}v}\right) - \frac{1}{1+v} \geq 1.$$

From the condition given by equation (5.11), the second term in the parentheses satisfies

$$\frac{\lambda^* W}{3} > \sqrt{\frac{1-v}{1+v}}.$$

Thus, we obtain,

$$\lambda^* \geq \frac{\sqrt{12v}}{W\sqrt{(1+v)\left(C_{\text{suf}} - \log\left(\frac{1-v}{v}\right)\right)}},$$

where $C_{\text{suf}} = \pi/2 - \log(0.5 \cdot \sqrt{3}/\sqrt{2})$. Since $\lambda < \lambda^*$ implies stability, a sufficient condition for stability is

$$\lambda < \frac{\sqrt{12v}}{W\sqrt{(1+v)\left(C_{\text{suf}} - \log\left(\frac{1-v}{v}\right)\right)}}. \tag{5.15}$$

To determine the value of the speed v^*_{suf} beyond which this is a less conservative condition than equation (5.11), we solve

$$\frac{\sqrt{12v^*_{\text{suf}}}}{W\sqrt{(1+v^*_{\text{suf}})\left(C - \log\left(\frac{1-v^*_{\text{suf}}}{v^*_{\text{suf}}}\right)\right)}} = \frac{3}{W}\sqrt{\frac{1-v^*_{\text{suf}}}{1+v^*_{\text{suf}}}}.$$

For $v > v^*_{\text{suf}}$, one can verify that the numerical value of the argument of the Struve and Bessel functions is less than 2, and so the bounds given by equation (5.13) used in this analysis are valid. Thus, a sufficient condition for stability is given by equation (5.11) for $v \leq v^*_{\text{suf}}$, and by equation (5.15) for $v > v^*_{\text{suf}}$. ■

Remark 5.4.8 (Tightness in low speed regime) *As $v \to 0^+$, the sufficient condition for FCFS stability becomes $\lambda < 3/W$, which is exactly equal to the necessary*

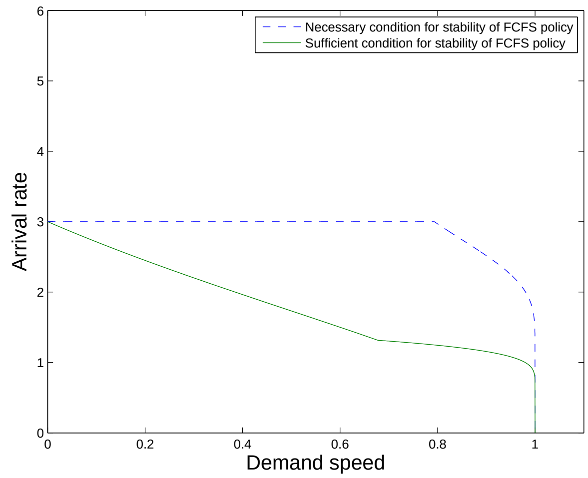

Figure 5.8. The necessary and sufficient conditions for the stability for the FCFS policy. The dashed curve is the necessary condition for stability as established in Lemma 5.4.6; while the solid curve is the sufficient condition for stability as established in Lemma 5.4.7.

condition given by part (ii) of Lemma 5.4.6. Thus, the condition for stability is asymptotically tight in this limiting regime.

Figure 5.8 shows a comparison of the necessary and sufficient stability conditions for the FCFS policy. It should be noted that λ *converges to* 0^+ *extremely slowly as* v *tends to* 1^-*, and still satisfy the sufficient stability condition in Lemma 5.4.7. For example, with* $v = 1 - 10^{-6}$*, the FCFS policy can stabilize the system for an arrival rate of* $3/(5W)$. $\square$

5.5 Proofs of the Main Results

In this section, we present the proofs of the main results which were presented in Section 5.3.3.

5.5.1 Proof of Theorem 5.3.1

We first present the proof of part (i). We begin by looking at the distribution of demands in the service region.

Lemma 5.5.1 (Distribution of outstanding demands) *Suppose the generation of demands commences at time* 0 *and no demands are serviced in the interval* $[0, t]$. *Let* $\mathcal{Q}$ *denote the set of all demands in* $[0, W] \times [0, vt]$ *at time* t. *Then, given a measurable compact region* $\mathcal{R}$ *of area* A *contained in* $[0, W] \times [0, vt]$,

$$\mathbb{P}[|\mathcal{R} \cap \mathcal{Q}| = n] = \frac{\mathrm{e}^{-\bar{\lambda} A} (\bar{\lambda} A)^n}{n!}, \quad \textit{where } \bar{\lambda} := \lambda/(vW).$$

Proof: Let $\mathcal{R} = [\ell, \ell + \Delta\ell] \times [h, h + \Delta h]$ be a rectangle contained in $[0, W] \times [0, vt]$ with area $A = \Delta\ell\Delta h$. Let us calculate the probability that at time t, $|\mathcal{R} \cap \mathcal{Q}| = n$ (that is, the probability that $\mathcal{R}$ contains n points in $\mathcal{Q}$). We have

$$\mathbb{P}[|\mathcal{R} \cap \mathcal{Q}| = n] = \sum_{i=n}^{\infty} \mathbb{P}\left[i \text{ demands arrived in } \left[\frac{h}{v}, \frac{h + \Delta h}{v}\right]\right] \times$$
$$\mathbb{P}[n \text{ of } i \text{ are generated in } [\ell, \ell + \Delta\ell]].$$

Since the generation process is temporally Poisson and spatially uniform the above equation can be rewritten as

$$\mathbb{P}[|\mathcal{R} \cap \mathcal{Q}| = n] = \sum_{i=n}^{\infty} \mathbb{P}\left[i \text{ demands arrived in } [0, \Delta h/v]\right] \times \mathbb{P}[n \text{ of } i \text{ are in } [0, \Delta\ell]]. \tag{5.16}$$

Now we compute

$$\mathbb{P}\left[i \text{ demands arrived in } [0, \Delta h/v]\right] = \frac{\mathrm{e}^{-\lambda \Delta h/v}(\lambda \Delta h/v)^i}{i!},$$

and

$$\mathbb{P}[n \text{ of } i \text{ are in } [0, \Delta\ell]] = \binom{i}{n}\left(\frac{\Delta\ell}{W}\right)^n\left(1 - \frac{\Delta\ell}{W}\right)^{i-n},$$

so that, substituting these expressions and adopting the shorthands $L := \Delta\ell/W$ and $H := \Delta h/v$, equation (5.16) becomes

$$\mathbb{P}[|\mathcal{R} \cap \mathcal{Q}| = n] = \mathrm{e}^{-\lambda H} L^n \sum_{i=n}^{\infty} \frac{(\lambda H)^i}{i!}\binom{i}{n}(1 - L)^{i-n}. \tag{5.17}$$

Rewriting $(\lambda H)^i$ as $(\lambda H)^n(\lambda H)^{i-n}$, and using the definition of binomial $\binom{i}{n} = \frac{i!}{n!(i-n)!}$, equation (5.17) reads

$$\mathbb{P}[|\mathcal{R} \cap \mathcal{Q}| = n] = \mathrm{e}^{-\lambda H}\frac{(\lambda L H)^n}{n!}\sum_{j=0}^{\infty}\frac{(\lambda H(1-L))^j}{j!} = \mathrm{e}^{-\lambda L H}\frac{(\lambda L H)^n}{n!}.$$

Finally, since $LH = A/(vW)$, we obtain

$$\mathbb{P}[|\mathcal{R} \cap \mathcal{Q}| = n] = \mathrm{e}^{-\bar{\lambda} A}\frac{(\bar{\lambda} A)^n}{n!},$$

where $\bar{\lambda} := \lambda/(vW)$. Thus, the result is established for rectangles. However, every measurable, compact region can be written as a countable union of rectangles, and thus the result follows. ■

Remark 5.5.2 (Uniformly distributed demands) *Lemma 5.5.1 shows us that the number of demands in an unserviced region with area A is Poisson distributed with parameter $\lambda A/(vW)$, and conditioned on this number, the demands are distributed uniformly.* □

Lemma 5.5.3 (Travel time bound) *Consider the set $\mathcal{Q}$ of demands that are uniformly distributed in $\mathcal{E}$ at time t. Let T_d be a random variable giving the minimum* *amount of time required to travel to a demand in $\mathcal{Q}$ from a vehicle position selected* a priori*. Then*

$$\mathbb{E}\left[T_d\right] \geq \frac{1}{2}\sqrt{\frac{vW}{\lambda}}.$$

Proof: Let $\mathbf{p} = (X, Y)$ denote the vehicle location selected *a priori*. To obtain a lower bound on the minimum travel time, we consider the best-case scenario, when no demands have been serviced in the time interval $[0, t]$, and when the set $\mathcal{Q}$ contains many demands (i.e., t is very large). Consider a demand in $\mathcal{Q}$ with position (x, y) at time t. Using Proposition 5.2.2, we can write the travel time T from $\mathbf{p}$ to $\mathbf{q} := (x, y)$ implicitly as

$$T(\mathbf{p}, \mathbf{q})^2 = (X - x)^2 + ((Y - y) - vT(\mathbf{p}, \mathbf{q}))^2. \tag{5.18}$$

Next, define the set S_T as the collection of demands that can be reached from (X, Y) in T or fewer time units. From equation (5.18) we see that when $v < 1$, the set S_T is a disk of radius T centered at $(X, Y - vT)$. That is,

$$S_T := \{(x, y) \in \mathcal{E} \mid (X - x)^2 + ((Y - vT) - y)^2 \leq T^2\},$$

where we have omitted the dependence of T on $\mathbf{p}$ and $\mathbf{q}$. The area of the set S_T, denoted $\operatorname{area}(S_T)$, is upper bounded by πT^2, and the area is equal to πT^2 if the S_T does not intersect a boundary of $\mathcal{E}$. Now, by Lemma 5.5.1 the demands in an unserviced region are uniformly randomly distributed with density $\bar{\lambda} = \lambda/(vW)$. Let us compute the distribution of $T_d := \min_{\mathbf{q} \in \mathcal{Q}} T(\mathbf{p}, \mathbf{q})$. For every vehicle position $\mathbf{p}$ chosen before the generation of demands, the probability that $T_d > T$ is given by

$$\mathbb{P}[T_d > T] = \mathbb{P}[|S_T \cap \mathcal{Q}| = 0] \geq \mathrm{e}^{-\bar{\lambda}\operatorname{area}(S_T)} \geq \mathrm{e}^{-\lambda\pi T^2/(vW)}.$$

Hence we have

$$\mathbb{E}\left[T_d\right] \geq \int_0^{+\infty} \mathbb{P}[T_d > T] dT \geq \int_0^{+\infty} \mathrm{e}^{-\lambda\pi T^2/(vW)} dT = \frac{\sqrt{\pi}}{2\sqrt{\lambda\pi/(vW)}} = \frac{1}{2}\sqrt{\frac{vW}{\lambda}}.$$

■

We can now prove part (i) of Theorem 5.3.1.

Proof: [Proof of part (i) of Theorem 5.3.1] A necessary condition for the stability of any policy is

$$\lambda \mathbb{E}[T] \leq 1,$$

where $\mathbb{E}[T]$ is the steady-state expected travel time between demands i and $i+1$. For every policy $\mathbb{E}[T] \geq \mathbb{E}[T_d] \geq \frac{1}{2}\sqrt{\frac{vW}{\lambda}}$. Thus, a necessary condition for stability is that

$$\lambda \frac{1}{2}\sqrt{\frac{vW}{\lambda}} \leq 1 \quad \iff \quad \lambda \leq \frac{4}{vW}.$$

■

Remark 5.5.4 (Constant fraction service) *A necessary condition for the existence of a policy which services a fraction $c \in]0,1]$ of the demands is that*

$$\lambda \leq \frac{4}{c^2 vW}.$$

Thus, for a fixed $v \in]0,1[$ no policy can service a constant fraction of the demands as $\lambda \to +\infty$. This follows because in order to service a fraction c we require that $c\lambda \mathbb{E}[T_d] < 1$.

In order to service a fraction c of the demands, we consider a subset of the generator having length cW, with the arrival rate on that subset being equal to $c\lambda$. The use of the TMHP-based policy on this subset and with the arrival rate $c\lambda$ gives a sufficient condition for stability analogous to Theorem 5.3.2, but with an extra term of c^2 in the denominator. □

For the proof of part (ii) of Theorem 5.3.1, we first recall from Lemma 5.4.6 that for stability of the FCFS policy, although λ must go to zero as $v \to 1^-$, it can go very slowly to 0. Specifically, λ goes to zero as

$$\frac{1}{\sqrt{-\log(1-v)}}.$$

This quantity goes to zero more slowly than any polynomial in $(1-v)$. We are now ready to complete the proof of Theorem 5.3.1.

Proof: [Proof of part (ii) of Theorem 5.3.1] Observe that the condition on λ in the statement of part (ii) is the expression given by the necessary condition for FCFS stability in the asymptotic regime as $v \to 1^-$, from Lemma 5.4.6. Therefore, suppose there is a policy P that does not serve demands FCFS, but can stabilize the system with

$$\lambda = B(1-v)^p,$$

for some $p > 0$, and $B > 0$. Let t_i be the first instant at which policy P deviates from FCFS. Then, the demand served immediately after i is demand $i+k$ for some $k > 1$. When the vehicle reaches demand $i+k$ at time t_{i+1}, demand $i+1$ has moved above the vehicle. To ensure stability, demand $i+1$ must eventually be served. The time to travel to demand $i+1$ from any demand $i+j$, where $j > 1$, is

$$\begin{aligned} T(\mathbf{q}_{i+j}, \mathbf{q}_{i+1}) &= \sqrt{\left(\frac{\Delta x}{\sqrt{1-v^2}}\right)^2 + \left(\frac{\Delta y}{1-v^2}\right)^2} + \frac{v\Delta y}{1-v^2} \\ &\geq \frac{\Delta y}{1-v^2} + \frac{v\Delta y}{1-v^2} = \frac{\Delta y}{1-v}, \end{aligned}$$

where Δx and Δy are now the minimum of the x and y distances from $\mathbf{q}_{i+j}$ to the $\mathbf{q}_{i+1}$. The random variable Δy is Erlang distributed with shape $j-1 \geq 1$ and rate λ, implying

$$\mathbb{P}[\Delta y \leq c] \leq 1 - \mathrm{e}^{-\lambda c/v}, \quad \text{for each } c > 0\text{, and in particular, for } c = (1-v)^{1/2-p}.$$

Now, since $\lambda = B(1-v)^p$ as $v \to 1^-$, almost surely $\Delta y > (1-v)^{1/2-p}$. Thus

$$T(\mathbf{q}_{i+j}, \mathbf{q}_{i+1}) \geq (1-v)^{-(p+1/2)},$$

almost surely as $v \to 1^-$. Thus, the expected number of demands that arrive during $T(\mathbf{q}_{i+j}, \mathbf{q}_{i+1})$ is

$$\lambda T(\mathbf{q}_{i+j}, \mathbf{q}_{i+1}) \geq B(1-v)^p (1-v)^{-(p+1/2)} \geq B(1-v)^{-1/2} \to +\infty,$$

as $v \to 1^-$. This implies that almost surely the policy P becomes unstable when it deviates from FCFS and that any deviation must occur with probability zero as $v \to 1^-$. Thus, a necessary condition for a policy to be stabilizing with $\lambda = B(1-v)^p$ is that, as $v \to 1^-$, the policy must serve demands in the order in which they arrive. But this needs to hold for every p and, by letting p go to infinity, $B(1-v)^p$ converges to zero for all $v \in (0, 1]$. Thus, a non-FCFS policy cannot stabilize the system no matter how quickly $\lambda \to 0^+$ as $v \to 1^-$. Hence, as $v \to 1^-$, every stabilizing policy must serve the demands in the order in which they arrive. Additionally, notice that the definition of the FCFS policy is that it uses the minimum time control (i.e., constant bearing control) to move between demands, thus the expression in part (ii) of Theorem 5.3.1 is a necessary condition for all stabilizing policies as $v \to 1^-$. ■

5.5.2 Proofs of Theorem 5.3.2 and Theorem 5.3.4

We first present the proof of Theorem 5.3.2. We begin with the proof of part (i).

Proof: [Proof of part (i) of Theorem 5.3.2] If there are any demands "above" the vehicle initially, at the end of the first iteration of the TMHP-based policy, all outstanding demands have their y-coordinates less than or equal to that of the vehicle, and hence would be located "below" the vehicle as shown in the first of Figure 5.5. Hence at the end of every iteration of the TMHP-based policy, all outstanding demands would be located "below" the vehicle.

Let the vehicle be located at $\mathbf{p}(t_i) = (X(t_i), Y(t_i))$ and $\mathbf{q}_{\text{last}}$ denote the demand with the least y-coordinate at time instant t_i. Let $|\mathcal{Q}|$ denote the number of demands in the set $\mathcal{Q}$. If there exists a non-empty set of unserviced demands $\mathcal{Q}$ below the vehicle at time t_i, then for $k \in \mathbb{Z}_{\geq 1}$, we have

$$Y(t_{i+1}) = v\mathcal{L}_{T,v}(\mathbf{p}(t_i), \{\mathbf{q}_1(t_i), \ldots, \mathbf{q}_{\text{last}-1}(t_i)\}, \mathbf{q}_{\text{last}}(t_i)) + y_{\text{last}}(t_i), \text{ w.p. } \mathbb{P}(|\mathcal{Q}| = k),$$

where $y_{\text{last}}(t_i)$ is the y-coordinate of $\mathbf{q}_{\text{last}}(t_i)$ and $\mathcal{L}_{T,v}(\mathbf{p}(t_i), \{\mathbf{q}_1(t_i), \ldots, \mathbf{q}_{\text{last}-1}(t_i)\}, \mathbf{q}_{\text{last}}(t_i))$ is the time taken for the vehicle as per the TMHP that begins at $\mathbf{p}(t_i)$, serves all demands in $\mathcal{Q}$ other than $\mathbf{q}_{\text{last}}$ and ends at the demand $\mathbf{q}_{\text{last}}$.

We seek an upper bound for the length $\mathcal{L}_{T,v}$ of the TMHP for which we use the Convert-to-EMHP method (cf. Section 5.2.2). Invoking Lemma 5.2.5 for $\mathcal{Q} = \{\mathbf{q}_1, \ldots, \mathbf{q}_{\text{last}-1}\}$, and writing $Y_i := Y(t_i)$ for convenience, we have

$$\begin{aligned}
&\mathcal{L}_{T,v}(\mathbf{p}(t_i), \{\mathbf{q}_1(t_i), \ldots, \mathbf{q}_{\text{last}-1}(t_i)\}, \mathbf{q}_{\text{last}}(t_i)) \\
&= \mathcal{L}_E(\text{cnvrt}_v(\mathbf{p}(t_i)), \{\text{cnvrt}_v(\mathbf{q}_1(t_i)), \ldots, \text{cnvrt}_v(\mathbf{q}_{\text{last}-1}(t_i))\}, \text{cnvrt}_v(\mathbf{q}_{\text{last}}(t_i))) \\
&+ \frac{v(y_{\text{last}}(t_i) - Y_i)}{1 - v^2} \\
&\leq \sqrt{\frac{2W(Y_i - y_{\text{last}}(t_i))|\mathcal{Q}|}{(1 - v^2)^{3/2}}} + \frac{Y_i - y_{\text{last}}(t_i)}{1 + v} + \frac{5W}{2\sqrt{1 - v^2}} \\
&\leq \sqrt{\frac{2WY_i|\mathcal{Q}|}{(1 - v^2)^{3/2}}} + \frac{Y_i}{1 + v} + \frac{5W}{2\sqrt{1 - v^2}},
\end{aligned}$$

where the first inequality is obtained using Lemma 5.2.3, and the second inequality follows since $y_{\text{last}}(t_i) \geq 0$.

If $\mathcal{Q}$ is empty at time t_i, then the vehicle moves towards the optimal location (X^*, Y^*). When a new demand arrives, the vehicle moves towards it. If $Y_i \leq W$, then in the worst-case, the vehicle is very close to an endpoint of the generator and the next demand arrives at the other endpoint. In this case, the vehicle moves with a vertical velocity component equal to v and horizontal component equal to $\sqrt{1 - v^2}$. So in the worst-case, the vehicle is at a height $vW/\sqrt{1 - v^2}$ at the beginning of the next iteration. The other possibility is if $Y_i > W$. In this case, to get an upper bound on the height of the vehicle at the next iteration, we consider the vehicle motion when it first moves horizontally so that the x-coordinate equals that of the demand, and then moves vertically down to meet the demand. This gives an upper bound on the height of the vehicle at the next iteration as $v(Y_i - vW)/(1+v)$. Thus, if $\mathcal{Q}$ is empty, then the sum of these two upper bounds is trivially an upper bound on the height of the vehicle at the beginning of the next iteration. Thus, if $\mathcal{Q}$ is empty, then

$$Y_{i+1} \leq \frac{vW}{\sqrt{1-v^2}} + \frac{v}{1+v}(Y_i - vW) \leq \frac{vW}{\sqrt{1-v^2}} + \frac{vY_i}{1+v}.$$

Conditioned on Y_i, we have

$$\begin{aligned}\mathbb{E}\left[Y_{i+1}\middle|Y_i\right] \leq &\Big(\frac{vW}{\sqrt{1-v^2}} + \frac{vY_i}{1+v}\Big)\mathbb{P}(|\mathcal{Q}| = 0|Y_i)+ \\ &v\sum_{k=1}^{\infty}\Big(\sqrt{\frac{2WY_ik}{(1-v^2)^{3/2}}} + \frac{Y_i}{1+v} + \frac{5W}{2\sqrt{1-v^2}}\Big)\mathbb{P}(|\mathcal{Q}| = k|Y_i) + \mathbb{E}\left[y_{\text{last}}(t_i)\middle|Y_i\right].\end{aligned}$$

It can be shown that $\mathbb{E}\left[y_{\text{last}}(t_i)\middle|Y_i\right] \leq v/\lambda$. Collecting the terms with $vY_i/(1+v)$ together and on further simplifying, we obtain

$$\begin{aligned}\mathbb{E}\left[Y_{i+1}\middle|Y_i\right] \leq &\frac{vW}{\sqrt{1-v^2}}\mathbb{P}(|\mathcal{Q}| = 0|Y_i) + \frac{vY_i}{1+v} \\ &+ \sum_{k=1}^{\infty}\Big(\sqrt{\frac{2v^2WY_ik}{(1-v^2)^{3/2}}} + \frac{5vW}{2\sqrt{1-v^2}}\Big)\mathbb{P}(|\mathcal{Q}| = k|Y_i) + \frac{v}{\lambda} \\ \leq &\frac{vW}{\sqrt{1-v^2}} + \frac{vY_i}{1+v} + \sqrt{\frac{2v^2W}{(1-v^2)^{3/2}}}\mathbb{E}\left[\sqrt{|\mathcal{Q}|Y_i}\middle|Y_i\right] \\ &+ \frac{5vW}{2\sqrt{1-v^2}}\sum_{k=1}^{\infty}\mathbb{P}(|\mathcal{Q}| = k|Y_i) + \frac{v}{\lambda} \\ \leq &\frac{vY_i}{1+v} + \sqrt{\frac{2v^2W}{(1-v^2)^{3/2}}}\sqrt{Y_i}\mathbb{E}\left[\sqrt{|\mathcal{Q}|}\middle|Y_i\right] + \frac{7vW}{2\sqrt{1-v^2}} + \frac{v}{\lambda}.\end{aligned} \tag{5.19}$$

Applying Jensen's inequality to the conditional expectation in the second term in the right hand side of equation (5.19), we have

$$\mathbb{E}\left[\sqrt{|\mathcal{Q}|}\middle|Y_i\right] \leq \sqrt{\mathbb{E}\left[|\mathcal{Q}|\middle|Y_i\right]} = \sqrt{\lambda\frac{Y_i}{v}},$$

where the equality follows since the arrival process is Poisson with rate λ and for a time interval Y_i/v. Substituting into equation (5.19), we obtain

$$\mathbb{E}\left[Y_{i+1}\middle|Y_i\right] \leq \left(\frac{v}{1+v} + \sqrt{\frac{2v\lambda W}{(1-v^2)^{3/2}}}\right) Y_i + \frac{7vW}{2\sqrt{1-v^2}} + \frac{v}{\lambda}.$$

Using the law of iterated expectation, we have

$$\mathbb{E}\left[Y_{i+1}\right] = \mathbb{E}\left[\mathbb{E}\left[Y_{i+1}|Y_i\right]\right] \leq \left(\frac{v}{1+v} + \sqrt{\frac{2v\lambda W}{(1-v^2)^{3/2}}}\right) \mathbb{E}\left[Y_i\right] + \frac{7vW}{2\sqrt{1-v^2}} + \frac{v}{\lambda}, \quad (5.20)$$

which is a linear recurrence in $\mathbb{E}\left[Y_i\right]$. Thus, $\lim_{i\to+\infty} \mathbb{E}\left[Y_i\right]$ is finite if

$$\frac{v}{1+v} + \sqrt{\frac{2Wv\lambda}{(1-v^2)^{3/2}}} < 1 \quad \iff \quad \lambda < \frac{(1-v^2)^{3/2}}{2Wv(1+v)^2}.$$

Thus, if λ satisfies the above condition, then expected number of demands in the environment is finite and the TMHP-based policy is stable.

Finally, from Lemma 5.4.1, the region of stability for the FCFS policy is contained in the region of stability for the TMHP-based policy. Thus, the TMHP-based policy is stable for all arrival rates the FCFS policy is contained in the region of stability for the TMHP policy. Thus, the TMHP-based policy is stable for all arrival rates satisfying the bound in Lemma 5.4.7. This gives us the desired result. ■

Remark 5.5.5 (Upper bound on expected delay) *Since equation* (5.20) *is a linear recurrence in* $\mathbb{E}\left[Y_i\right]$, *we can easily obtain an upper bound for* $\lim_{i\to+\infty} \mathbb{E}\left[Y_i\right]$. *Moreover, we may upper bound the expected delay for a demand by*

$$\frac{7W}{2\sqrt{1-v^2}}\left(\frac{1}{1/(1+v) - \sqrt{2Wv\lambda/(1-v^2)^{3/2}}}\right). \quad \bullet$$

Proof: [Proof of part (ii) of Theorem 5.3.2] In this part, we make use of the following two facts. First, as $v \to 0^+$, the length of the TMHP constrained to start at the vehicle location and end at the lowest demand, is equal to the length of the EMHP in the corresponding static instance under the map cnvrt_v, as described in

Lemma 5.2.5. Second, consider a set $\mathcal{Q}$ of n points which are uniformly distributed in a region with finite area. Then, in the limit as $n \to +\infty$, the length of a constrained EMHP through $\mathcal{Q}$ tends to the length of the ETSP tour through $\mathcal{Q}$.

More specifically, consider the ith iteration of the TMHP-based policy, and let $Y_i > 0$ be the position of the service vehicle. In the limit as $\lambda \to +\infty$, the number of outstanding demands in that iteration $n_i \to +\infty$, and in addition, conditioned on n_i, the demands are uniformly distributed in the region $[0, W] \times [0, Y_i]$ (cf. Remark 5.5.2). Now using the above two facts, we can apply Theorem 5.2.4 to obtain an expression for the length of the TMHP constrained to start at the vehicle location and ending at the lowest demand. As $\lambda \to +\infty$, the position of the vehicle at the end of the ith iteration is given by

$$Y_{i+1} = v\beta_{\mathrm{TSP}}\sqrt{n_i A} = v\beta_{\mathrm{TSP}}\sqrt{n_i Y_i W},$$

where $A := Y_i W$ is the area of the region below the vehicle at the ith iteration. Thus, conditioned on Y_i being bounded away from 0, we have

$$\mathbb{E}\left[Y_{i+1}|Y_i\right] = v\beta_{\mathrm{TSP}}\sqrt{Y_i}\mathbb{E}\left[\sqrt{W n_i}\right] \le v\beta_{\mathrm{TSP}}\sqrt{W Y_i \mathbb{E}\left[n_i\right]},$$

where we have applied Jensen's inequality. Using Lemma 5.5.1, $\mathbb{E}\left[n_i\right] = W Y_i \lambda/(vW)$ and thus

$$\mathbb{E}\left[Y_{i+1}|Y_i\right] \le v\beta_{\mathrm{TSP}}\sqrt{W^2 Y_i^2 \frac{\lambda}{vW}} = \beta_{\mathrm{TSP}}\sqrt{\lambda v W}Y_i.$$

Thus, the sufficient condition for stability of the TMHP-based policy as $\lambda \to +\infty$ (and thus $v \to 0^+$) is

$$\lambda < \frac{1}{\beta_{\mathrm{TSP}}^2 vW} \approx \frac{1.9726}{vW}.$$

∎

Finally, we present the proof of Theorem 5.3.4.

Proof: [Proof of Theorem 5.3.4] The proof of part (i) of Theorem 5.3.4 follows from Lemma 5.4.3 and Lemma 5.4.1. The proof of part (ii) follows from part (ii) of

Theorem 5.3.1 and Lemma 5.4.1 along with the fact that the TMHP-based policy spends the minimum amount of time to travel between demands. ■

5.6 Simulations

In this section, we present a numerical study of the TMHP-based policy. We numerically determine the region of stability of the TMHP-based policy, and compare it with the theoretical results from the previous sections.

In the actual implementation of the TMHP-based policy, the computational complexity increases undesirably as the values of the problem parameters (λ, v) approach the instability region. Therefore, we adopt a different procedure to characterize the stable/unstable region boundary, which is based upon the following central idea. For a given value of (λ, v) and a sufficiently high value of the height of the vehicle, if the policy is stable, then after one iteration of the policy, the vehicle's height must decrease. In particular, the following procedure was adopted.

1. For a collection of instructive pairs of the demand speed v and λ in the region of interest, we set the generator width $W = 1$ and we set the initial height h_0 of the environment of interest so that the expected number of demands in the environment are 1000. Thus, $h_0 = 1000v/\lambda$.

2. We repeated 10 times the following procedure. The vehicle is placed at the height h_0 and at a uniformly random location in the horizontal direction. A Poisson distributed number n_0 with parameter λ/v, of outstanding demands are uniformly randomly placed in the environment (cf. Lemma 5.5.1). The vehicle uses the TMHP-based policy to serve all outstanding demands and we store the height h_1 of the vehicle at the end of the single iteration of the policy. Finally, we compute the average height $\bar{h}_1$ of the 10 iterations.

3. If $\bar{h}_1 \leq h_0$, then the policy is deemed to be stable for the chosen value of (v, λ). Otherwise the policy is deemed to be unstable.

The `linkern`[1] solver was used to generate approximations to the TMHP at every iteration of the policy. The linkern solver takes as an input an instance of the Euclidean traveling salesperson problem. To transform the constrained EMHP problem into an ETSP, we replace the distance between the start and end points with a large negative number, ensuring that this edge is included in the linkern output.

The results of this numerical experiment are presented in Figure 5.9. For the purpose of comparison, we overlay the plots for the theoretical curves, which were presented in Figure 5.1. We observe that the numerically obtained stability boundary for the TMHP-based policy falls between the necessary and the sufficient conditions which were established in parts (i) of Theorems 5.3.1 and 5.3.2 respectively. Further, although the sufficient condition characterized in part (ii) of Theorem 5.3.2, is theoretically an approximation of the stability boundary in the asymptotic regime of high arrival, our numerical results show that the condition serves as a very good approximation to the stability boundary, for nearly the entire range of demand speeds.

Summary

We introduced a dynamic vehicle routing problem with translating demands. We determined a necessary condition on the arrival rate of the demands for the existence of a stabilizing policy. In the limit when the demands move as fast as the vehicle, we showed that every stabilizing policy must service the demands in the FCFS order. We proposed a novel receding horizon policy that services the moving demands as per a translational minimum Hamiltonian path. In the asymptotic regime when

[1]The TSP solver `linkern` is freely available for academic research use at `http://www.tsp.gatech.edu/concorde.html`.

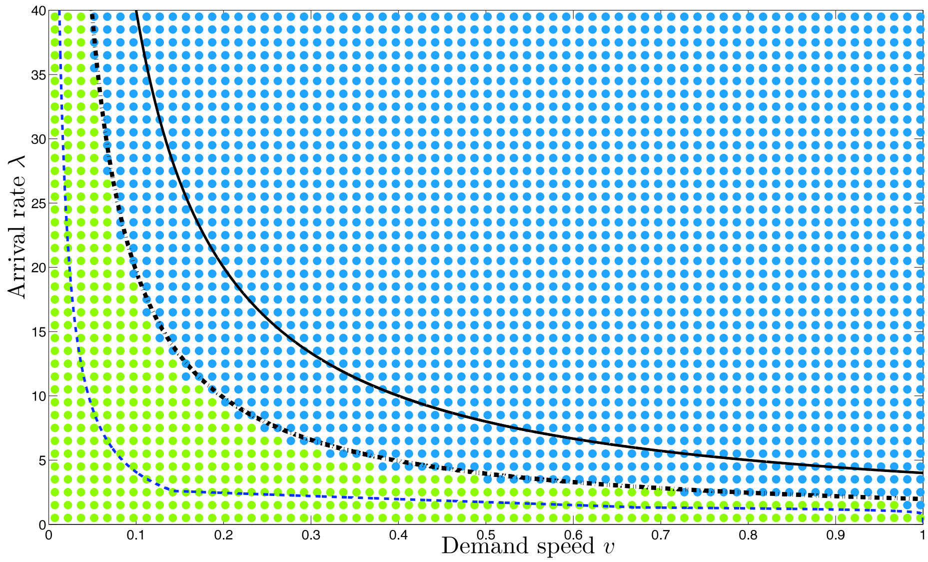

Figure 5.9. Numerically determined region of stability for the TMHP-based policy. A lightly shaded (green-coloured) dot represents stability while a darkly shaded (blue-coloured) dot represents instability. The uppermost (thick solid) curve is the necessary condition for stability for any policy as derived in Theorem 5.3.1. The lowest (dashed) curve is the sufficient condition for stability of the TMHP-based policy as established by Theorem 5.3.2. The broken curve between the two curves is the sufficient stability condition of the TMHP-based policy in the low speed regime as derived in part (ii) of Theorem 5.3.2. The environment width is $W = 1$.

the demands move as fast as the vehicle, we showed that the TMHP-based policy minimizes the expected time to service a demand. We derived a sufficient condition for stability of the TMHP-based policy, and showed that in the asymptotic regime of low demand speed, the sufficient condition is within a constant factor of the necessary condition for stability. In a third asymptotic regime when arrival rate tends to zero for a fixed demand speed, we showed that the TMHP-based policy is optimal in terms of minimizing the expected time to service a demand. Finally, a numerical implementation, we observed that the sufficient condition for the asymptotic regime of low demand speeds serves as a good approximation to the boundary of the stability region for a significantly large interval of values of demand speed.

Chapter 6

Vehicle Placement to Intercept Moving Targets

6.1 Introduction

In chapter 5, we introduced a problem in which a single pursuer seeks to capture sequentially arriving and translating targets. For the case when the target (or demand) arrival rate is low, we saw in Section 5.4.1 in Chapter 5 that the problem becomes one of providing optimal coverage, i.e., where should the vehicle be placed so that the expected time to reach a demand is minimized? In this chapter, we address this placement problem for multiple pursuers and for general spatial arrival density for the demands.

Contributions

We consider a line segment on which a mobile target appears via a known spatial probability density and one or multiple vehicles seek to intercept it. The goal is to determine vehicle placements that minimize a cost function associated with the target motion. This work is an extension of Section 5.4.1 in Chapter 5, where we introduced the placement problem for target motion with fixed speed and in fixed direction, and for a uniform target arrival density.

We address the following cases.

1. Single vehicle and targets that move with fixed speed and in fixed direction.

2. Single vehicle with the target seeking to maximize the vertical distance from the line or the intercept time.

3. Multiple vehicles and targets that move with fixed speed and in fixed direction.

For the first two cases, we consider a class of cost functions and establish properties such as convexity, smoothness and the existence and uniqueness of a globally minimizing vehicle location. Next, we derive expressions for the cost functions related to both types of target motion. We show that the cost functions associated with the target moving with fixed speed and in a fixed direction, and with the target seeking to maximize the distance from the segment, fall in the class of cost functions that we have analyzed. The cost function for target motion that maximizes the intercept time is proportional to the continuous 1–median function.

For the third case, we first provide an algorithm to partition the line segment among the vehicles and characterize its properties. With the expected intercept time as the cost function, we propose a Lloyd descent algorithm in which every vehicle computes its partition and moves along the gradient of the expected time computed over its partition. We characterize conditions under which the vehicles asymptotically reach a set of critical configurations. We also present simulations of the algorithm with different probability densities, and with different numbers of vehicles.

Related Work

In static environments, vehicle placement problems are analogous to geometric location problems such as in [67], and in [103], where given a set of static points, the goal is to find supply locations that minimize a cost function of the distance from each point to its nearest supply location. For a single vehicle, the average distance to a random point, generated according to a probability density function is given by the Weber or the continuous 1–median function, for which there exists a global minimizer as shown in [35], termed as the *median*. This property has been used in [13] to minimize average time to reach targets when they appear via a stochastic arrival process with very low arrival rates.

For the case of multiple distinct vehicle locations, the expected distance between a random point generated according to a probability density and one of the locations is known in literature as the continuous Weber or the continuous multi-median function, e.g., see [33]. For more than one location, the multi-median function is non-convex, and thus determining locations that minimize the multi-median function is hard in the general case. It is of interest to characterize the set of critical points of the multi-median function. In [31], the authors have characterized the set of critical points for the problem of deploying a group of robots in a region to optimize a multi-median cost function. This work has been extended in [86] to enable robots to approximate the function from sensor measurements. More recently, [60] have presented a coverage algorithm for vehicles in a river environment.

For scenarios that involve motion of targets, the cost for the vehicle is typically a function of relative locations, speeds and motion constraints considered. For the case when the targets appear uniformly on a segment and are constrained to move perpendicular to the segment, we have derived the optimal placement for a single vehicle [24]. If a target is allowed to move adversarially, then the optimal vehicle motion is obtained by solving a min-max pursuit-evasion game [51], in which the target seeks to maximize while the vehicle seeks to minimize a certain cost function. In the presence of constraints such as a wall in the playing space or non-zero capture distance, optimal player motions with respect to the intercept time have been derived in [51, 71].

Organization

This paper is organized as follows. The problem formulation and useful background results are presented in Section 6.2. Single vehicle scenarios are presented in Section 6.3. The multiple vehicle scenario is addressed in Section 6.4.

6.2 Problem Formulation and Background

We first present the problem and some background results.

6.2.1 Problem statement

We consider vehicles with simple motion and speed upper bounded by unity. A target arrives at a random position $(x, 0)$ on the segment $G := [0, W] \times \{0\}$, termed the *generator*, via a specified probability density function $\phi : [0, W] \to \mathbb{R}_{\geq 0}$. We assume that the density function ϕ is bounded, i.e., there exists an $M > 0$ such that $\phi(x) \leq M, \forall x \in [0, W]$. The target moves with bounded speed less than that of the vehicles. It is intercepted or captured if a vehicle and the target are at the same point. The goal is to determine vehicle placements that minimize a certain cost function based on the maneuvering abilities of the target.

More specifically, we consider the following scenarios.

Single vehicle case

The goal is to determine a vehicle location $\mathbf{p}^* \in \mathbb{R} \times \mathbb{R}_{\geq 0}$ so as to minimize

$$C_{\text{exp}}(\mathbf{p}) := \int_0^W C(\mathbf{p}, x)\phi(x)dx,$$

where $C : \mathbb{R}^2 \to \mathbb{R}_{\geq 0}$ is an appropriately defined cost of the vehicle position $\mathbf{p}$. In what follows, we seek to minimize the following different cost functions.

(i) *Expected constrained travel time:* We assume that the target arriving at $(x, 0)$ translates in the positive Y-direction with speed $v < 1$. From [24], the cost function for this formulation is

$$T(\mathbf{p}, x) = \frac{\sqrt{(1-v^2)(X-x)^2 + Y^2}}{1-v^2} - \frac{vY}{1-v^2}, \tag{6.1}$$

which is the time taken for the vehicle to intercept the constrained target.

(ii) *Expected vertical height:* The cost function for this formulation is the vertical height $H(\mathbf{p}, x)$ which the target seeks to maximize before being intercepted.

(iii) *Expected intercept time*: The cost function for this formulation is the intercept time $\mathbf{Ti}(\mathbf{p}, x)$ which the target seeks to maximize.

Figure 6.1 illustrates the vertical height and intercept time.

Multiple vehicles case

We assume that the target translates in the positive Y-direction with speed $v < 1$. As shown in Figure 6.2, given $m \geq 2$ vehicles having complete communication, the goal is to determine vehicle locations $\mathbf{p}_i \in [0, W] \times \mathbb{R}_{\geq 0}$, for every $i \in \{1, \ldots, m\}$, that minimize the expected constrained travel time given by

$$T_{\text{exp}}(\mathbf{p}_1, \ldots, \mathbf{p}_m) := \int_0^W \min_{i \in \{1,\ldots,m\}} T(\mathbf{p}_i, x)\phi(x)dx, \tag{6.2}$$

where $T(\mathbf{p}_i, x)$ is given by equation (6.1).

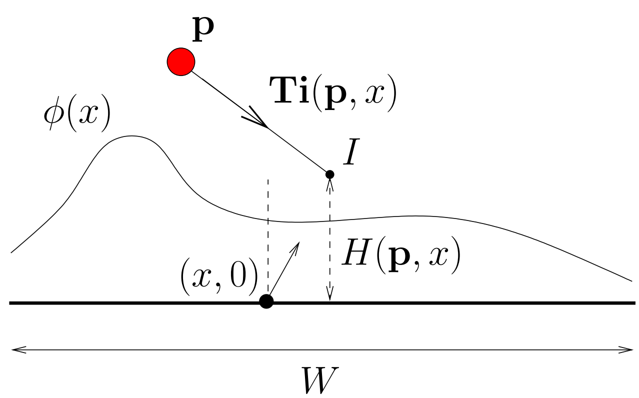

Figure 6.1. Intercepting a target that seeks to maximize either the vertical height H or the time $\mathbf{Ti}$ until intercept (which is also the distance travelled by the vehicle.

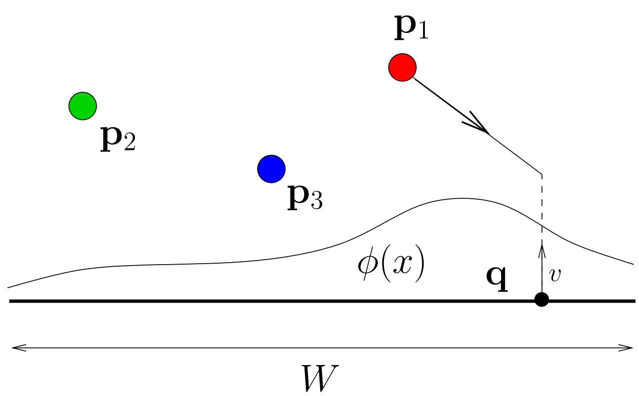

Figure 6.2. Intercepting a target that moves with fixed speed in the positive Y-direction with multiple vehicles.

6.2.2 Background: Appolonius circle and Multiplicative Voronoi partition

Given an ordered pair of distinct points $\{\mathbf{q}_1, \mathbf{q}_2\}$ in a plane and a scalar $\lambda \in [0, 1[$, the set $\mathcal{C}_{\mathrm{App}}(\mathbf{q}_1, \mathbf{q}_2, \lambda)$ of all points $\mathbf{w}$ in the plane that satisfy $\|\mathbf{q}_2 - \mathbf{w}\| = \lambda \|\mathbf{q}_1 - \mathbf{w}\|$, is known as the *Appolonius circle*. [51]. Define,

$$\mathbf{q}_{\mathrm{int}} := (\mathbf{q}_2 + \lambda \mathbf{q}_1)/(1 + \lambda), \;\; \mathbf{q}_{\mathrm{ext}} := (\mathbf{q}_2 - \lambda \mathbf{q}_1)/(1 - \lambda).$$

The following property is well known.

Proposition 6.2.1 (Appolonius circle center and radius) *The Appolonius circle* $\mathcal{C}_{\text{App}}$ *is centered at the point* $(\mathbf{q}_{\text{int}} + \mathbf{q}_{\text{ext}})/2$ *and has radius* $\|\mathbf{q}_{\text{int}} - \mathbf{q}_{\text{ext}}\|/2$.

Given two points $\mathbf{q}_1$ and $\mathbf{q}_2$ in a region, the multiplicative Voronoi partition [70] of $\mathbf{q}_1$ (resp. $\mathbf{q}_2$) for the parameter λ is set of all points $\mathbf{w}$ that satisfy

$$\|\mathbf{q}_1 - \mathbf{w}\| \le \lambda\|\mathbf{q}_2 - \mathbf{w}\|, \text{ (resp. } \|\mathbf{q}_1 - \mathbf{w}\| \ge \lambda\|\mathbf{q}_2 - \mathbf{w}\|).$$

6.2.3 Background: Pursuit-evasion in the plane

Given a pursuer and a slower evader (target), both with simple motion in the plane, the optimal strategy [51] for the pursuer is to select its velocity vector based on the target's velocity vector so as to ensure

1. that the line joining the target to the pursuer remains parallel to the line joining their initial locations, and
2. that the distance to the target monotonically decreases.

This strategy is a version of the classic proportional navigation guidance law [45]. We refer to this strategy as *constant bearing control*.

If the pursuer's speed is unity and the evader's speed is $v < 1$, then the Appolonius circle is the boundary of the set of all points which the evader can reach without being captured [51]. Letting the pursuer position $(X, Y) =: \mathbf{q}_1$ and the evader position $(x, y) =: \mathbf{q}_2$ and $v =: \lambda$, Proposition 6.2.1 yields the center and the radius of the Appolonius circle as

$$\begin{aligned} O &= \Big(\frac{x - v^2X}{1 - v^2}, \frac{y - v^2Y}{1 - v^2}\Big), \\ R &= \frac{v}{1 - v^2}\sqrt{(X - x)^2 + (Y - y)^2}, \end{aligned} \tag{6.3}$$

respectively. The Appolonius circle possesses the following geometrical fact given in [51], illustrated in Figure 6.3.

Proposition 6.2.2 (Appolonius circle during pursuit) *If the pursuer and the evader both travel straight toward a point U on the Appolonius circle, then any new such circle, obtained from a pair of simultaneous intermediate positions of the pursuer and the evader, is tangent to the original circle at U, and is contained in the original circle.*

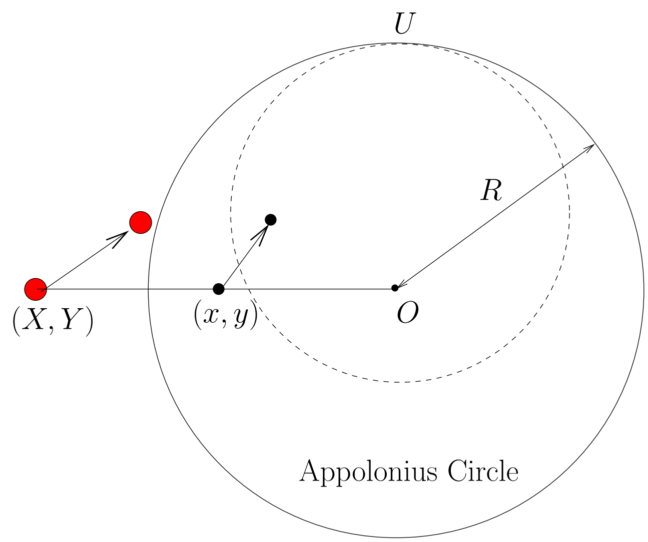

Figure 6.3. The Appolonius circle for a pursuer at (X, Y) moving with unit speed and the evader at (x, y) moving with speed $v < 1$. The dotted circle is the Appolonius circle with respect to the new positions of the players and is contained inside the original one, by Proposition 6.2.2.

6.3 Single Vehicle Scenarios

We now analyze the single vehicle scenarios.

6.3.1 A class of cost functions

We first analyze a class of cost functions. We will see that this form appears in two distinct scenarios, the expected constrained travel time and the expected vertical height.

We assume that the cost function is given by

$$C_{\text{exp}}(X,Y) := \int_0^W C(X,Y,x)\phi(x)dx,$$

where the function C has the form

$$C(X,Y,x) := a\sqrt{b(X-x)^2 + Y^2} - cY, \tag{6.4}$$

and a, b, and c are positive constants, with $a > c$.

The partial derivatives of $C_{\text{exp}}(X,Y)$ with respect to X and Y can be computed as follows.

$$\frac{\partial C_{\text{exp}}}{\partial X} = ab\int_0^W \frac{(X-x)\phi(x)}{\sqrt{b(X-x)^2+Y^2}}dx, \tag{6.5}$$

$$\frac{\partial C_{\text{exp}}}{\partial Y} = aY\int_0^W \frac{\phi(x)}{\sqrt{b(X-x)^2+Y^2}}dx - c. \tag{6.6}$$

We have the following results.

Lemma 6.3.1 (Convexity of expected cost) *The expected cost $C_{\text{exp}}(X,Y)$ is a convex function of X and Y.*

Proof: The Hessian of the function C with respect to X and Y, for $Y > 0$ is given by

$$\frac{ab}{(b(X-x)^2+Y^2)^{3/2}}\begin{bmatrix} Y^2 & -Y(X-x) \\ -Y(X-x) & (X-x)^2 \end{bmatrix} \geq 0.$$

The Hessian is positive semi-definite, for $Y > 0$, and hence the quantity $C(X,Y,x)$ is a convex function of X and Y. Since the expectation operator preserves convexity [25], the cost function C_{exp} is convex in X and Y. ■

Lemma 6.3.2 (Existence of Minima) *There exists a vehicle location* $(X^*, Y^*) \in]0, W[\times\mathbb{R}_{>0}$ *that minimizes the expected cost* C_{exp}.

Proof: We show that a minima cannot lie on the boundary of the region $[0, W] \times \mathbb{R}_{\geq 0}$. We begin by showing that Y^* exists and is finite. We take the limit of $C_{\text{exp}}(X, Y)$ as $Y \to +\infty$. Thus,

$$\liminf_{Y\to+\infty} C_{\text{exp}}(X, Y) \geq \liminf_{Y\to+\infty} (a - c)Y \int_0^W \phi(x)dx = +\infty,$$

since by assumption, $a > c$. Thus, Y^* exists and is finite.

Finally, to show that a minima lies in $(0, W) \times \mathbb{R}_{>0}$, we need to prove two statements: (a) $Y^* \neq 0$, and (b) $X^* \in]0, W[$. We first show (a). For that, we consider the partial derivative of the expected cost with respect to Y,

$$\frac{\partial C_{\text{exp}}}{\partial Y} = aY \int_0^W \frac{\phi(x)}{\sqrt{b(X - x)^2 + Y^2}} dx - c.$$

Let $M > 0$ be such that $\phi(x) \leq M$, for every $x \in [0, W]$. Observe that

$$\frac{\partial C_{\text{exp}}}{\partial Y} \leq MYa \int_0^W \frac{dx}{\sqrt{b(X - x)^2 + Y^2}} - c.$$

which on simplifying yields,

$$\frac{\partial C_{\text{exp}}}{\partial Y} \leq \frac{MYa}{\sqrt{b}} (\log(W + \sqrt{W^2 + Y^2/b}) - \log(Y/\sqrt{b})) - c.$$

Thus, $\limsup_{Y\to 0^+} \partial C_{\text{exp}}/\partial Y \leq -c$. Thus, for Y near zero the gradient of C_{exp} points in the negative Y-direction, implying that $Y^* \neq 0$.

To show (b), we first observe that for a given Y, in the limit as $X \to \pm\infty$, $C_{\text{exp}} \to +\infty$, and therefore X^* must be bounded. Finally, the claim follows since the partial derivative of C_{exp} with respect to X is strictly negative at $X = 0$ and is strictly positive at $X = W$.

These statements coupled with the convexity of C_{exp} with respect to X and Y imply the existence of a minima in the region $]0, W[\times\mathbb{R}_{>0}$. ■

Next, we prove the following uniqueness result.

Lemma 6.3.3 (Uniqueness) *There exists a unique vehicle location* (X^*, Y^*) *that minimizes the expected cost* C_{exp}.

Proof: Let there be two locations (X_1, Y_1) and (X_2, Y_2) that minimize the expected cost. From Lemma 6.3.1, since the expected cost C_{exp} is convex in X and Y, a convex combination of (X_1, Y_1) and (X_2, Y_2) also minimizes the expected time. Thus, the necessary conditions for minima are satisfied by $(\bar{X}(\alpha), \bar{Y}(\alpha)) := (\alpha X_1 + (1-\alpha)X_2, \alpha Y_1 + (1-\alpha)Y_2)$, for every $\alpha \in [0,1]$. Thus,

$$\int_0^W \frac{(\bar{X}(\alpha) - x)\phi(x)}{\sqrt{(b\bar{X}(\alpha) - x)^2 + \bar{Y}(\alpha)^2}} dx = 0,$$
$$\int_0^W \frac{\bar{Y}(\alpha)\phi(x)}{\sqrt{b(\bar{X}(\alpha) - x)^2 + \bar{Y}(\alpha)^2}} dx = \frac{c}{a}.$$

Since the above conditions hold for every $\alpha \in [0,1]$, the partial derivatives of the above conditions evaluated at $\alpha = 0$, must equal zero. Thus, upon simplifying, we obtain,

$$\int_0^W \frac{(X_2 - x)Y_2(Y_1 - Y_2) - Y_2^2(X_1 - X_2)}{(b(X_2 - x)^2 + Y_2^2)^{3/2}} \phi(x) dx = 0,$$
$$\int_0^W \frac{(X_2 - x)Y_2(X_1 - X_2) - (Y_1 - Y_2)(X_2 - x)^2}{(b(X_2 - x)^2 + Y_2^2)^{3/2}} \phi(x) dx = 0,$$

where $\phi(x)/(b(X_2 - x)^2 + Y_2^2)^{3/2} =: f(X_2, Y_2, x)$ is non-negative for $Y_2 > 0$. Multiplying the first equation by $(X_1 - X_2)$, the second by $(Y_1 - Y_2)$, and on adding the resulting equations, we obtain

$$\int_0^W f(X_2, Y_2, x)(Y_2(X_1 - X_2) - (X_2 - x)(Y_1 - Y_2))^2 dx = 0.$$

Now, if f is zero on any subset of G, then we can discard that subset on which f is zero, and consider only the subset on which f is strictly positive. This implies that $Y_2(X_1 - X_2) - (X_2 - x)(Y_1 - Y_2) = 0$, and this is true *for every* x. This is feasible only if $X_1 - X_2 = 0$ and $Y_1 - Y_2 = 0$, thus completing the proof. ■

We now present the main result for this section.

Theorem 6.3.4 (Minimizing expected cost) *Starting from an initial location in* $\mathbb{R}\times\mathbb{R}_{>0}$ *and by using a gradient optimization technique, the vehicle reaches the unique point that minimizes the expected cost* $C_{\exp}$.

Proof: The gradient of $C_{\exp}$ with respect to X and Y is a continuous function of X and Y in the region $\mathbb{R} \times \mathbb{R}_{>0}$. The function $C_{\exp}$ is convex in X and Y (cf. Lemma 6.3.1) and has a unique minima in $]0, W[\times\mathbb{R}_{>0}$ (cf. Lemmas 6.3.2 and 6.3.3). Thus, a gradient optimization technique [25] leads the vehicle to the unique global minimizer of $C_{\exp}$. ■

6.3.2 Optimal placement for constrained target motion

We now address the problem of minimizing the expected value of T, given by equation (6.1). Comparing equation (6.1) with the definition of C in equation (6.4), we have $a := 1/(1-v^2)$, $b := (1-v^2)$ and $c := v/(1-v^2)$, and $a > c$. Thus, by applying Theorem 6.3.4, the following result holds.

Theorem 6.3.5 (Minimizing expected time) *Starting from an initial location in* $\mathbb{R}\times\mathbb{R}_{>0}$ *and by using a gradient optimization technique, the vehicle reaches the unique point that minimizes the expected constrained travel time* $T_{\exp}$.

In general, it is difficult to provide closed form expressions for the vehicle location that minimizes the expected time. A special case is described in Remark 6.3.6.

Remark 6.3.6 (The limiting case of $v = 1$) *In this case, we can obtain closed form expressions for the optimal placement by solving the necessary conditions, given* *by*

$$X^* = \int_0^W \phi(x)x dx;\ Y^* = \sqrt{\int_0^W \phi(x)(X^* - x)^2 dx}. \quad \square$$

6.3.3 Optimal placement for adversarial target

We now address the case when the target is an evader possessing adversarial motion. We consider two types of cost functions that the evader tries to maximize; the vertical height and the intercept time.

Minimizing the expected vertical height

Here we address the problem of minimizing the cost function H_{exp}. We first present the solution to the differential game with payoff equal to the vertical height.

Since the pursuer's optimal strategy is governed by the evader's strategy, it suffices to determine the optimal evader strategy. We propose the following strategy for the evader.

Algorithm 4: **Move towards top-most**

Assumes: Pursuer at (X, Y). Evader at $(x, 0)$.

1: Find (cf. equation (6.3)) the Appolonius center and radius

$$O := (O_x, O_y) = \Big(\frac{x - v^2 X}{1 - v^2}, \frac{-v^2 Y}{1 - v^2}\Big),$$
$$R := \frac{v}{1 - v^2}\sqrt{(X - x)^2 + Y^2}.$$

2: Move towards the point $(O_x, O_y + R)$ with speed v.

This strategy is illustrated in Figure 6.4. We obtain the following result, which is immediate from Proposition 6.2.2.

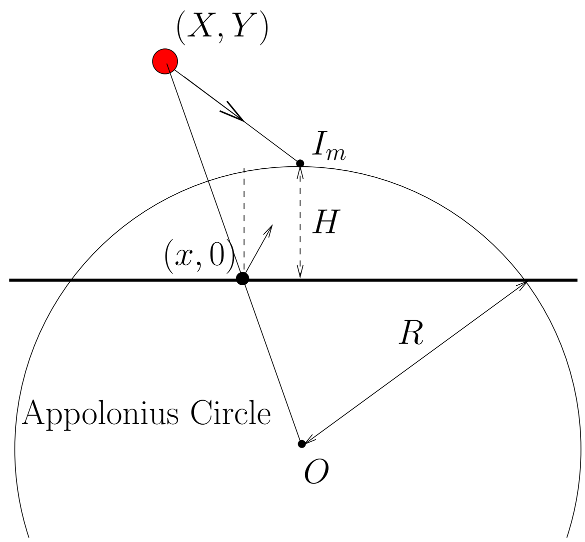

Figure 6.4. Move towards top-most strategy for the evader.

Lemma 6.3.7 (Move towards top-most is optimal) *The strategy* move towards top-most *is the evader's optimal strategy and the resulting optimal vertical height of the intercept point is*

$$H(X, Y, x) = \frac{v}{1 - v^2}\sqrt{(X - x)^2 + Y^2} - \frac{v^2 Y}{1 - v^2}.$$

Comparing the expression for H given by Lemma 6.3.7 with the definition of C in equation (6.4), we have $a := v/(1 - v^2)$, $b := 1$ and $c := v^2/(1 - v^2)$, and $a > c$ since $v < 1$. Thus, by applying Theorem 6.3.4, we obtain the following result.

Theorem 6.3.8 (Minimizing expected height) *Starting from an initial location in* $\mathbb{R} \times \mathbb{R}_{>0}$ *and by using a gradient optimization technique, the vehicle reaches the unique point that minimizes the expected height* H_{exp}.

Minimizing the expected intercept time

Here we address the problem of minimizing the cost function $\mathbf{Ti}_{\text{exp}}$. In this formulation, we assume that the evader is constrained to remain above or on the X-axis.

Thus, the underlying differential game in this set up is the classic *wall pursuit* game, originally proposed and solved in [51]. For the sake of completeness, we present the main result.

Lemma 6.3.9 (Wall pursuit game) *The evader strategy that maximizes the intercept time is to move towards the furthest point of the Appolonius circle on the X-axis.*

This optimal evader strategy is illustrated in Figure 6.5.

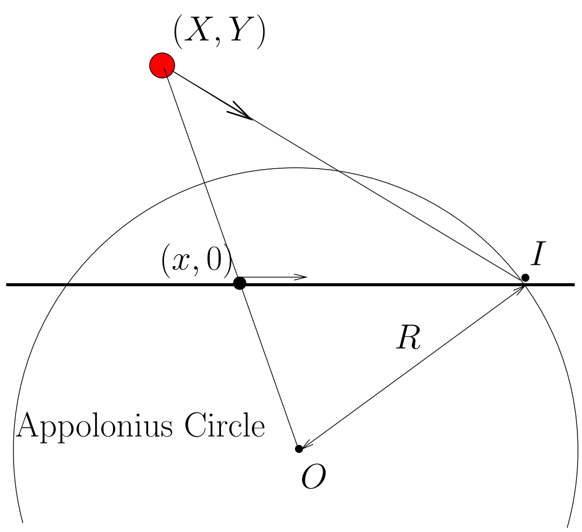

Figure 6.5. Illustrating Lemma 6.3.9.

We recall the following definition from [35]. Given a convex region $\mathcal{S} \subset \mathbb{R}$ and a density function $\psi : \mathcal{S} \to \mathbb{R}_{\geq 0}$, the *median* p_{med} is the unique global minimum of

$$\int_{\mathcal{S}} |p - z|\psi(z)dz.$$

We now present the main result of this section.

Theorem 6.3.10 (Optimal point is the median) *The median point of the region $[0, W] \times \{0\}$ with the density function ϕ uniquely minimizes the expected intercept time.*

Proof: Using Lemma 6.3.9 and the Pythagoras theorem, we can write the expression for the intercept time.

$$\mathbf{Ti}(X, Y, x) = \sqrt{R^2 - \left(\frac{vY}{1-v}\right)^2} + \left|\frac{x - vX}{1-v} - x\right|,$$

where R is the radius of the Appolonius circle drawn at the initial instant. Substituting the expression for R and from the fact that placing the pursuer on the X-axis, i.e., $Y = 0$, results into decreasing the intercept time $\mathbf{Ti}$, we have

$$\mathbf{Ti}_{\text{exp}}(X) = \frac{v^2 + 3v}{1 - v^2} \int_0^W |X - x| \phi(x) dx,$$

which is minimized uniquely by the median of the region $[0, W] \times \{0\}$ with the density function ϕ. ■

6.4 A Multiple Vehicle Scenario

We now address the multi-vehicle placement problem.

6.4.1 Dominance region partition

We first introduce a partitioning procedure for the generator by defining the concept of dominance region for each pair of vehicles.

Definition 6.4.1 (Pairwise dominance region) *For $i, j \in \{1, \ldots, m\}$, the pairwise dominance region $U_{ij} \subseteq [0, W]$ of $\mathbf{p}_i$ with respect to $\mathbf{p}_j$ is the set of target locations for which vehicle $\mathbf{p}_i$ takes* lesser *time to intercept the target than $\mathbf{p}_j$:*

$$U_{ij} := \{x \in [0, W] \,|\, T(\mathbf{p}_i, x) \leq T(\mathbf{p}_j, x)\}.$$

In what follows, we describe a procedure to determine U_{ij}, which is summarized in Algorithm 5. Without loss of generality, assume that $X_i < X_j$. If $Y_i = Y_j$, i.e., the vehicles are at the same distance from the generator, then U_{ij} is the piece of G that lies in the half-plane that is formed by the perpendicular bisector of the segment joining $\mathbf{p}_i$ and $\mathbf{p}_j$ and which contains $\mathbf{p}_i$. Now if $Y_i < Y_j$, then we look for points $(x, 0)$ in G for which $T(\mathbf{p}_i, x) \leq T(\mathbf{p}_j, x)$. By setting $(1 - v^2) =: b$, equation (6.1) gives

$$\sqrt{b(X_i - x)^2 + Y_i^2} - vY_i \leq \sqrt{b(X_j - x)^2 + Y_j^2} - vY_j. \tag{6.7}$$

On simplifying, one can show that Eq. (6.7) is quadratic in x having real roots, which provides at most two points for the boundary between U_{ij} and U_{ji}. To determine the boundary points, consider the perpendicular bisector of the segment joining $\mathbf{p}_i$ and $\mathbf{p}_j$, as shown in Figure 6.6. We look for points A_1 and A_2 on this bisector such that

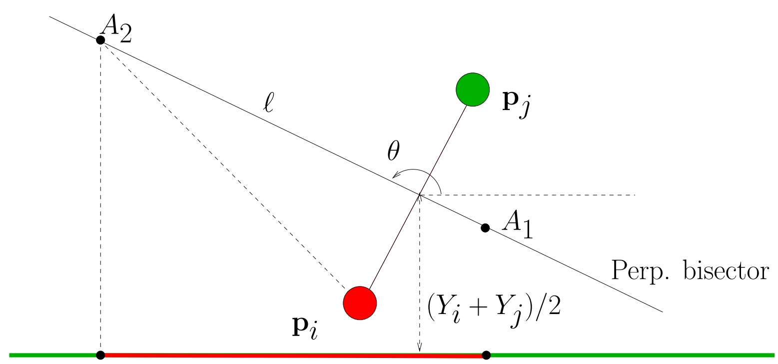

Figure 6.6. To determine pairwise dominance regions.

the distances of A_1 and A_2 from the real line is v times their respective distances from the vehicles. This gives rise to the following quadratic equation in the variable ℓ

$$4(\sin^2\theta - v^2)\ell^2 + 4(Y_i + Y_j)\sin\theta\ell = -(Y_i + Y_j)^2 + v^2\|\mathbf{p}_i - \mathbf{p}_j\|^2,$$

where ℓ and $\theta := \arctan_2((Y_i - Y_j), (X_i - X_j)) + \pi/2$ are as shown in Figure 6.6. Let ℓ_1 and ℓ_2 be the roots of the above quadratic. Then the Y-coordinates of the candidate boundary points A_1 and A_2 are given by

$$[y_1,\, y_2]^T = [1,\, 1]^T(Y_i + Y_j)/2 + [\ell_1,\, \ell_2]^T \sin\theta.$$

Now, A_1 and A_2 are both boundary points if and only if both have positive Y-coordinates. It can be shown that there exists at least one among them which has positive Y-coordinate. There arise two cases:

(i) If there are two candidate points A_1 and A_2 (as in Figure 6.6), then we look at their corresponding X coordinates, (x_1, x_2) given by Step 7. For $(x, 0) \in G \cap [x_1, x_2] \times \{0\}$, we have $T(\mathbf{p}_i, x) \leq T(\mathbf{p}_j, x)$, and thus U_{ij} is $G \cap [x_1, x_2] \times \{0\}$.

(ii) If there is only one candidate point A_1, then we look at its X coordinates, x_1 given by Step 9. By assumption $X_i < X_j$, and hence for $(x, 0) \in G \cap [-\infty, x_1] \times \{0\}$, we have $T(\mathbf{p}_i, x) \leq T(\mathbf{p}_j, x)$ and thus U_{ij} is $G \cap [-\infty, x_1] \times \{0\}$.

Thus, we have established the following property.

Proposition 6.4.2 (Pairwise dominance region) *Given distinct locations* $\mathbf{p}_i = (X_i, Y_i)$, $\mathbf{p}_j = (X_j, Y_j)$, *if a target arrives at* $(x, 0)$, *where* $x \in U_{ij}$ *generated by Algorithm 5, then* $T(\mathbf{p}_i, x) \leq T(\mathbf{p}_j, x)$.

Let $\mathcal{E}$ be the region $[0, W] \times \mathbb{R}_{\geq 0}$, let $\mathcal{P}([0, W])$ denote the set of all subsets of $[0, W]$ and let $\mathcal{B}(r)$ be the closed ball of radius r around the origin. The domain of a set-valued map $F : X \rightrightarrows Z$ is the set of all $\mathbf{q} \in X$ such that $F(\mathbf{q}) \neq \emptyset$. F is said to be upper (resp. lower) semi-continuous in its domain if, for every $\mathbf{q}$ in its domain and for every $\epsilon > 0$, there exists a $\delta > 0$ such that for every $\mathbf{z} \in \mathbf{q} + \mathcal{B}(\delta)$, $F(\mathbf{z}) \subset F(\mathbf{q}) + B(\epsilon)$ (resp. $F(\mathbf{q}) \subset F(\mathbf{z}) + B(\epsilon)$). F is continuous in its domain if it is both upper and lower semi-continuous.

The roots of equation (6.7) which is a quadratic in x, vary continuously with $\mathbf{p}_i$ and $\mathbf{p}_j$. Thus, the pairwise dominance region between $\mathbf{p}_i$ and $\mathbf{p}_j$ is a set valued function $U_{ij} : \mathcal{E}^2 \setminus \mathcal{S}_{ij} \rightrightarrows \mathcal{P}([0, W])^2$, where $\mathcal{S}_{ij} \subset \mathcal{E}^2$ is the set of coincident locations for $\mathbf{p}_i$ and $\mathbf{p}_j$.

Proposition 6.4.3 (Continuity properties of U_{ij}) *For every distinct i and j in the set $\{1, \dots, m\}$, the set valued map U_{ij} is continuous in $\mathcal{E}^2 \setminus \mathcal{S}_{ij}$.*

Similar to pairwise dominance regions, we introduce the concept of *dominance region* $\mathcal{V}_i \in \mathcal{P}([0, W])$ for the ith vehicle, for every $i \in \{1, \dots, m\}$, which is the set of X-coordinates of target locations for which $\mathbf{p}_i$ takes the *minimum* time to intercept of all vehicles.

Assuming complete communication between vehicles, Algorithm 5 is extended to determine the dominance region for a vehicle by (i) determining pairwise dominance regions between vehicles and, (ii) taking intersection of all pairwise dominance regions, as presented in Algorithm 6.

Algorithm 6: **Dominance region**

Assumes: Distinct locations $\{\mathbf{p}_1, \dots, \mathbf{p}_m\}$.

1: **foreach** vehicle $j \in \{1, \dots, m\} \setminus \{i\}$, **do**

2: Determine U_{ij} using Algorithm 5.

3: $\mathcal{V}_i = \bigcap_{j=1,\dots,m, j \neq i} U_{ij}$.

Algorithm 6 has the following property.

Proposition 6.4.4 (Optimality of dominance regions) *Given distinct vehicle positions and a target arrival location,*

1. *the dominance regions generated by Algorithm 6 form a partition of the generator.*

2. *The time taken to reach the target is minimized by the vehicle whose dominance region contains the target arrival location.*

Proof: Part (i) follows since the union of all dominance regions is the generator, and any two dominance regions have disjoint interior. Part (ii) follows by Proposition 6.4.2, and is due to the fact that in Step 4 of Algorithm 6, we take the intersection of all pairwise dominance regions for a vehicle. ∎

It is possible for the dominance region of a vehicle to be empty. For instance, when one of the vehicles is very far from the generating line (cf. first part of Figure 6.10). However, one condition under which every vehicle has a non-empty dominance region is when all vehicles have the same Y-coordinate. For a general set of locations, Figure 6.7 illustrates a dominance region partition induced by three vehicles.

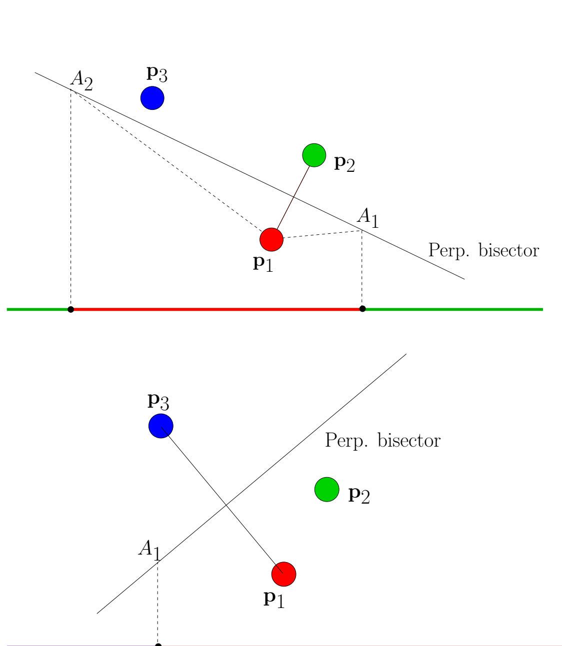

Figure 6.7. Dominance region partition induced by vehicles $\mathbf{p}_1$, $\mathbf{p}_2$ and $\mathbf{p}_3$.

Akin to U_{ij}, we can also represent the dominance region partition for vehicle i as a set-valued map $\mathcal{V}_i : \mathcal{E}^m \setminus \mathcal{S}_i \rightrightarrows \mathcal{P}([0, W])^{2(m-1)}$, where $\mathcal{S}_i \subset \mathcal{E}^m$ is the set of vehicle locations in which at least one other vehicle is coincident with $\mathbf{p}_i$.

Proposition 6.4.5 (Continuity properties of $\mathcal{V}_i$) *For each vehicle $i \in \{1, \ldots, m\}$, the set valued map $\mathcal{V}_i$ is continuous on its domain.*

Proof: The domain of $\mathcal{V}_i$ is contained in the domain of U_{ij} for every $j \neq i$. By Proposition 6.4.3, for every $j \neq i$, the set-valued map U_{ij} is upper semi-continuous in $\mathcal{E}^2$. Thus, for every $j \neq i$, at every $\mathbf{q}$ in the domain of $\mathcal{V}_i$ and for every $\epsilon > 0$, there exist $\delta_{ij} > 0$ such that for every $\mathbf{z} \in \mathbf{q} + \mathcal{B}(\delta_{ij})$, $U_{ij}(\mathbf{z}) \subset U_{ij}(\mathbf{q}) + B(\epsilon)$. Given an $\epsilon > 0$, by the choice of $\delta_i = \min\{\delta_{ij}, \forall j \neq i\}$, we obtain that for every $\mathbf{z} \in \mathbf{q} + \mathcal{B}(\delta_i)$, $\mathcal{V}_i(\mathbf{z}) \subset \mathcal{V}_i(\mathbf{q}) + B(\epsilon)$. Thus $\mathcal{V}_i$ is upper semi-continuous. Lower semi-continuity of $\mathcal{V}_i$ is established similarly and the result follows. ■

6.4.2 Minimizing the expected constrained travel time

For distinct vehicle locations, equation (6.2) can be written as

$$T_{\text{exp}}(\mathbf{p}_1, \ldots, \mathbf{p}_m) = \sum_{i=1}^{m} \int_{\mathcal{V}_i} T(\mathbf{p}_i, x)\phi(x)dx, \tag{6.8}$$

where $\mathcal{V}_i$ is the dominance region of the ith vehicle. We say that $\mathbf{p}_j$ is a *neighbor* of $\mathbf{p}_i$, i.e., $j \in \text{neigh}(i)$, if $\mathcal{V}_i \cap \mathcal{V}_j$ is non-empty.

The next result gives a formula to compute the gradient for every vehicle.

Lemma 6.4.6 (Gradient computation) *For all vehicle configurations such that no two vehicles are at coincident locations, the gradient of the expected time with respect to vehicle location $\mathbf{p}_i$ is*

$$\frac{\partial T_{\text{exp}}}{\partial \mathbf{p}_i} = \int_{\mathcal{V}_i} \frac{\partial T}{\partial \mathbf{p}_i}(\mathbf{p}_i, x)\phi(x)dx.$$

Proof: We have,

$$\frac{\partial T_{\text{exp}}}{\partial \mathbf{p}_i} = \frac{\partial}{\partial \mathbf{p}_i} \int_{\mathcal{V}_i} T(\mathbf{p}_i, x)\phi(x)dx + \sum_{j \text{ neigh } i} \frac{\partial}{\partial \mathbf{p}_i} \int_{\mathcal{V}_j} T(\mathbf{p}_j, x)\phi(x)dx,$$

Now, let $\mathcal{V}_i = \bigcup_{l=1,\dots,n_i} [a_l, b_l]$, for some finite integer n_i. By Leibnitz's Rule[1],

$$\frac{\partial}{\partial \mathbf{p}_i} \int_{\mathcal{V}_i} T(\mathbf{p}_i, x)\phi(x)dx = \int_{\mathcal{V}_i} \frac{\partial T}{\partial \mathbf{p}_i}(\mathbf{p}_i, x)\phi(x)dx + \sum_{l=1}^{n_i} T(\mathbf{p}_i, b_l)\frac{\partial b_l}{\partial \mathbf{p}_i} - T(\mathbf{p}_i, a_l)\frac{\partial a_l}{\partial \mathbf{p}_i}.$$

Unless $a_1 = 0$, or $b_{n_i} = W$ (in which case the partial derivatives with respect to $\mathbf{p}_i$ are zero), for every $l \in \{1, \dots, n_i\}$, there exist some $j \in \text{neigh}(i)$ and some $k \in \text{neigh}(i)$, such that

$$\begin{aligned}
&\frac{\partial}{\partial \mathbf{p}_i} \int_{\mathcal{V}_j} T(\mathbf{p}_j, x)\phi(x)dx = -T(\mathbf{p}_j, b_l)\frac{\partial b_l}{\partial \mathbf{p}_i}, \qquad \text{and,} \\
&\frac{\partial}{\partial \mathbf{p}_i} \int_{\mathcal{V}_k} T(\mathbf{p}_k, x)\phi(x)dx = T(\mathbf{p}_k, a_l)\frac{\partial a_l}{\partial \mathbf{p}_i},
\end{aligned}$$

where we have made use of Leibnitz's Rule. Due to the continuity of T at the boundary points, we obtain

$$T(\mathbf{p}_j, b_l) = T(\mathbf{p}_i, b_l), \quad T(\mathbf{p}_k, a_l) = T(\mathbf{p}_i, a_l),$$

and on summation,

$$\sum_{j \text{ neigh } i} \frac{\partial}{\partial \mathbf{p}_i} \int_{\mathcal{V}_j} T(\mathbf{p}_j, x)\phi(x)dx + \sum_{l=1}^{n_i} T(\mathbf{p}_i, b_l)\frac{\partial b_l}{\partial \mathbf{p}_i} - T(\mathbf{p}_i, a_l)\frac{\partial a_l}{\partial \mathbf{p}_i} = 0.$$

This completes the proof. ■

For $\mathbf{z} \in \mathbb{R}^2$, define the function sat : $\mathbb{R}^2 \to \mathbb{R}^2$ as

$$\text{sat}(\mathbf{z}) := \begin{cases} \mathbf{z}, & \text{if } \|\mathbf{z}\| \leq 1, \\ \mathbf{z}/\|\mathbf{z}\|, & \text{otherwise.} \end{cases}$$

Algorithm 7 presents a *discrete-time Lloyd* algorithm.

---

[1]Leibnitz's Rule:

$$\frac{d}{dz}\int_a^b f(z,x)dx = \int_a^b \frac{df(z,x)}{dz}dx + f(z,b)\frac{db}{dz} - f(z,a)\frac{da}{dz}.$$

Algorithm 7: **Lloyd descent for vehicle** i

Assumes: Distinct initial locations $\{\mathbf{p}_1, \ldots, \mathbf{p}_m\} \in \mathcal{E}^m$

```
foreach time t ∈ ℕ do
    Compute 𝒱_i(t) by Algorithm 6 as a function of {p_1(t), ..., p_m(t)}
    if 𝒱_i(t) is empty, then
        Move in unit time to (X_i, Y_i − min{1, Y_i})
    else
        For τ ∈ [t, t+1], move according to
```

$$\dot{\mathbf{p}}_i(\tau) = -\operatorname{sat}\Big(\int_{\mathcal{V}_i(t)} \frac{\partial}{\partial \mathbf{p}_i} T(\mathbf{p}_i(\tau), x)\phi(x)dx\Big)$$

We now define the following vehicle configuration.

Definition 6.4.7 (Critical dominance region configuration) *A set of locations $\{\mathbf{p}_1, \ldots, \mathbf{p}_m\}$ is a* critical dominance region configuration *if, for all $i \in \{1, \ldots, m\}$,*

$$\mathbf{p}_i = \operatorname{argmin}_{\mathbf{z} \in \mathcal{E}} \int_{\mathcal{V}_i} T(\mathbf{z}, x)\phi(x)dx,$$

where $\{\mathcal{V}_1, \ldots, \mathcal{V}_m\}$ is the dominance region partition induced by $\{\mathbf{p}_1, \ldots, \mathbf{p}_m\}$.

A critical dominance region configuration is *unstable* under the action of the discrete-time Lloyd descent if there exists a direction in which a small displacement of a vehicle location leads to a trajectory for the vehicle that makes the vehicle move away from the critical location.

The next result gives a simple condition to identify unstable critical dominance region configuration.

Lemma 6.4.8 (Disconnected partitions are unstable) *A critical dominance region configuration in which a vehicle has a disconnected dominance region partition* *is unstable.*

Proof: We first prove the result for the case of two vehicles. Let $\{\mathbf{p}_1^*, \mathbf{p}_2^*\}$ be a critical dominance region configuration in which $\mathbf{p}_1$ has its dominance region disconnected. Let the dominance region partitions be

$$\mathcal{V}_1 = [A, B], \qquad \mathcal{V}_2 = [0, A] \cup [B, W].$$

Perturb $\mathbf{p}_1$ by a small distance δXin the positive X direction, as shown in Figure 6.8. It can be shown by geometry that the dominance region partitions are given by

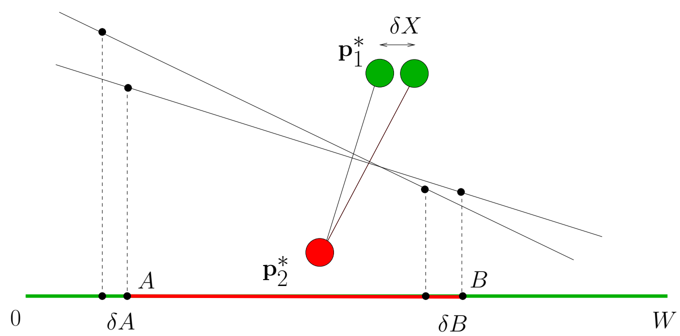

Figure 6.8. Illustrating instability of critical dominance region configuration having a disconnected dominance region.

$$\mathcal{V}_1 = [A - \delta A, B - \delta B], \qquad \mathcal{V}_2 = [0, A - \delta A] \cup [B - \delta B, W],$$

where δA and δB are both positive and sufficiently small. Evaluating the partial derivatives in X for $\mathbf{p}_2$,

$$(1 - v^2)\frac{\partial}{\partial X}T_2 = \int_{A-\delta A}^{B-\delta B} I_2 dx,$$

where $I_2(x, X_2, Y_2) := (X_2 - x)\phi(x)/\sqrt{(1 - v^2)(X_2 - x)^2 + Y_2^2}$. This can be further simplified as follows.

$$\begin{aligned}
(1 - v^2)\frac{\partial T_2}{\partial X} &= \int_{A-\delta A}^{A} I_2 dx + \int_{A}^{B} I_2 dx - \int_{B-\delta B}^{b} I_2 dx \\
&= \int_{A-\delta A}^{A} I_2 dx - \int_{B-\delta B}^{B} I_2 dx, \qquad (6.9)
\end{aligned}$$

as the sum of the first two terms is zero from the necessary condition for $\mathbf{p}_2^*$ to be a minimum. For sufficiently small δX, there exist δA and δB such that $I_2 > 0$ on the interval $[0, A - \delta A]$ and $I_2 < 0$ on the interval $[B - \delta B, B]$, since $X_2 - x > 0$ and $X_2 - x < 0$ respectively on the two intervals. Thus, $\partial T_2 / \partial X > 0$ when $\mathbf{p}_1$ is displaced to $(X_1 + \delta X, Y_1)$, which implies the direction of gradient descent in X is the negative X direction for $\mathbf{p}_2$, and similarly is the positive X direction for $\mathbf{p}_1$. Thus, this critical configuration is unstable.

In the case of $m > 2$ vehicles, let the dominance regions of $\mathbf{p}_1$ and $\mathbf{p}_2$ share at least one point. Since both terms on the right hand side of equation (6.9) are positive, the direction of gradient descent in X is the negative direction for $\mathbf{p}_2$ independent of the fact whether the dominance regions of $\mathbf{p}_1$ and $\mathbf{p}_2$ share one or two common points.

■

We now state the main result of this section.

Theorem 6.4.9 (Convergence of Lloyd descent) *Let $\gamma : \mathbb{N} \to \mathbb{R}^{2m}$ be the evolution of the m vehicles according to Algorithm 7 and assume that no two vehicle locations become coincident in finite time or asymptotically. The following statements hold:*

1. *the expected travel time $t \mapsto T_{\exp}(\gamma(t))$ is a non-increasing function of time;*
2. *if the dominance region $\mathcal{V}_i$ of any vehicle i is empty at some time, then $\mathcal{V}_i$ will be non-empty within a finite time; and*
3. *if there exists a time t such that every dominance region is non-empty for all times subsequent to t, then the vehicle locations converge to the set of critical dominance region configurations.*

Proof: In every iteration of Algorithm 7, step **2:** does not increase the expected time T_{exp} due to the optimality of the dominance region partition, by Proposition 6.4.4. Step **4:** does not change the T_{exp} as the associated dominance region is empty. Finally, step **6:** does not increase T_{exp} as the vehicle is moving along the gradient descent flow of T_{exp}. Thus, the expected time is non-increasing under Algorithm 7.

Part (ii) follows from the fact that whenever $\mathcal{V}_i = \emptyset$ for vehicle i, due to step **4:**, vehicle i reaches the generator after finite time and therefore has a non-empty $\mathcal{V}_i$.

To show part (iii), consider the discrete-time dynamical system given by the tuple $(\mathcal{X}, \mathcal{X}_0, \mathcal{A})$, where $\mathcal{X} = \mathcal{E}^m$ and $\mathcal{X}_0 \in \mathcal{E}^m$ is the set of initial vehicle positions. For non-empty $\mathcal{V}_i$, let $\mathcal{A} : \mathcal{X} \times \mathcal{P}([0, W]) \to \mathcal{X}$, be the flow map of the differential equation at step **6:** from time t to time $t + 1$.

We now apply the discrete-time LaSalle Invariance Principle (Theorem 1.19 in [26]), for which we verify the four assumptions as follows.

1. Existence of a positively invariant set: In our case, such a set is $\mathcal{X}$ itself since every vehicle remains in $\mathcal{E}$. This is because under the action of $\mathcal{A}$, every vehicle performs gradient descent over its partition, and since the cost function is convex, gradient descent keeps each vehicle in $\mathcal{E}$.

2. Existence of a non-increasing function along $\mathcal{A}$: In our case, such a function is T_{exp} which is non-increasing along $\mathcal{A}$, by part (i) of this theorem. Note that

3. All evolutions of $(\mathcal{X}, \mathcal{X}_0, \mathcal{A})$ are bounded: Since gradient descent keeps the X coordinates bounded in $[0, W]$, it remains to show that the Y-coordinates of all vehicles remain bounded. Let us suppose the contrary. Then, there are two cases: (a) at least one vehicle has its location bounded and at least one other vehicle, say vehicle k moves so that Y_k grows unbounded; or (b) all of the vehicles move so that their Y-coordinates grow unbounded. In case (a), after finite time, the dominance region

$\mathcal{V}_k$ becomes empty, thus contradicting the assumption of part (iii) of this theorem. If case (b) occurs, then T_{exp} grows unbounded, thus contradicting part (i) of this theorem. Thus, all evolutions of $(\mathcal{X}, \mathcal{X}_0, \mathcal{A})$ are bounded.

4. T_{exp} and $\mathcal{A}$ are continuous: Continuity of T_{exp} follows from Eq.s (6.1) and (6.8). To verify continuity of $\mathcal{A}$, note that whenever $\mathcal{V}_i$ is non-empty, by Proposition 6.4.5, $\mathcal{V}_i$ is continuous with respect to vehicle locations. Thus, as long as $\mathcal{V}_i$ is non-empty, $\mathcal{A}$ is continuous as the integrand is continuous with respect to vehicle locations, and so is the region of integration $\mathcal{V}_i$.

By LaSalle Invariance Principle, we obtain that the evolutions of $(\mathcal{X}, \mathcal{X}_0, \mathcal{A})$ converge to a set of the form $T_{\text{exp}}^{-1}(\kappa) \cap \mathcal{M}$, where κ is a real constant and $\mathcal{M}$ is the largest positively invariant set in $\{x \in \mathcal{X} \mid T_{\text{exp}}(\mathcal{A}(x)) = T_{\text{exp}}(x)\}$. Since T_{exp} remains constant under action of $\mathcal{A}$ for the set of critical dominance region configurations, it is contained in a set of the form $T_{\text{exp}}^{-1}(\kappa) \cap \mathcal{M}$. If a set of vehicle positions is not critical, then T_{exp} strictly decreases under the action $\mathcal{A}$, and therefore the set of vehicle positions is not contained in a set of $T_{\text{exp}}^{-1}(\kappa) \cap \mathcal{M}$. Thus, the vehicle locations converge to the set of critical dominance region configurations. ■

6.4.3 Simulations

We now present some simulations of Algorithm 7.

Examples of critical locations

We consider two vehicles, and a uniform probability density of target arrival, i.e., $\phi(x) = 1/W$. From initial locations such as in the leftmost of Figure 6.9 wherein both vehicles having the same X-coordinate of $W/2$, but different Y-coordinates, the vehicles asymptotically approach a set of locations shown in the center figure.

However, a small perturbation to the positions leads the vehicles to positions in the rightmost figure. From most initial conditions, the vehicles converged to a critical configuration as in the rightmost figure.

Non-uniform probability distribution

We consider three vehicles and the arrival probability density function,

$$\phi(x) = \begin{cases} \frac{8}{W^2}x, & \text{if } x \in [0, W/4], \\ \frac{2}{W} - \frac{8}{3W^2}(x - \frac{W}{4}), & \text{if } x \in]W/4, W]. \end{cases}$$

From most initial conditions, the vehicles converged to a critical configuration as in right-most part of Figure 6.10.

6.5 Adversarial Target: An Insight

We now provide some insight into the case of multiple vehicles wherein the target possesses adversarial motion, i.e., the goal of the target is to maximize a cost function such as the vertical distance (or the intercept time). The underlying pursuit game is similar to the classic *two-cutter* game [51].

Consider only two vehicles $\mathbf{p}_1$ and $\mathbf{p}_2$, and suppose the target arrives at $\mathbf{q}$. In order to maximize the vertical distance (resp. intercept time), the optimal strategy for the target is as follows [51].

1. Compute the multiplicative Voronoi partitions (MVP) (cf. Section 6.2.3) with respect to the pursuer locations $\mathbf{p}_1$ and $\mathbf{p}_2$.

2. Move towards the point with highest Y coordinate (resp. furthest point) in the intersection of the MVPs of the evader with respect to both the pursuers.

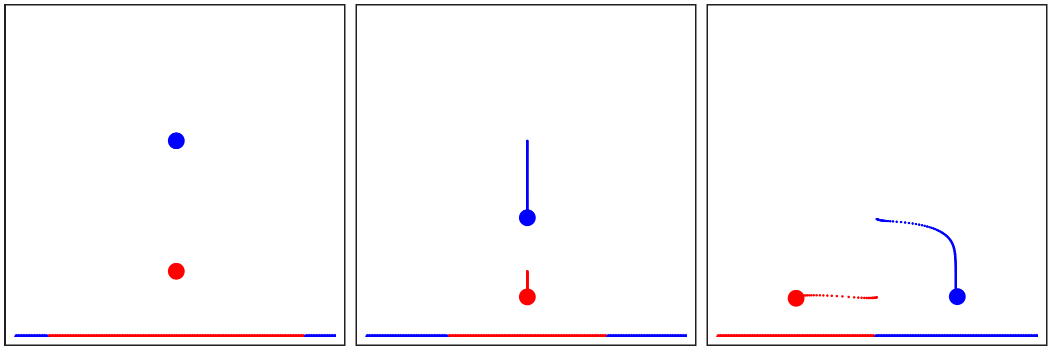

Figure 6.9. Evolution of two vehicles under the discrete-time Lloyd descent algorithm, for uniform arrival density. The vehicles first tend to an critical dominance region configuration in the center figure. A perturbation to their positions makes them move to a stable configuration as in the third figure.

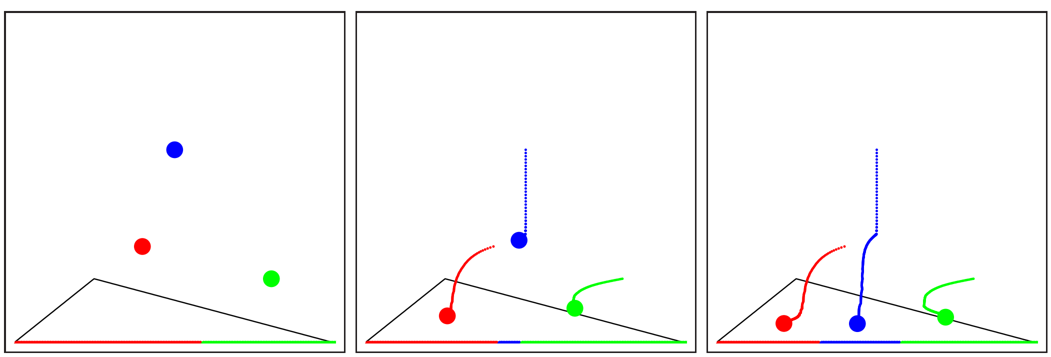

Figure 6.10. Evolution of three vehicles under the discrete-time Lloyd descent algorithm, for non-uniform arrival density as shown by the black triangle. Notice that the blue vehicle has no dominance region to begin with. The vehicles tend to a stable configuration.

The strategy is illustrated in Figure 6.11. We partition the generator into three regions:

- $\mathcal{V}_1$ (resp. $\mathcal{V}_2$): Set of all locations $\mathbf{q}$ for which the MVP of the target with respect to pursuer $\mathbf{p}_1$ (resp. $\mathbf{p}_2$) is entirely contained in the MVP with respect to pursuer $\mathbf{p}_2$ (resp. $\mathbf{p}_1$).
- $\mathcal{V}_{1,2} := G \setminus (\mathcal{V}_1 \cup \mathcal{V}_2)$.

Figure 6.11 shows examples when the arrival location is in either $\mathcal{V}_1$ or in $\mathcal{V}_{1,2}$. In

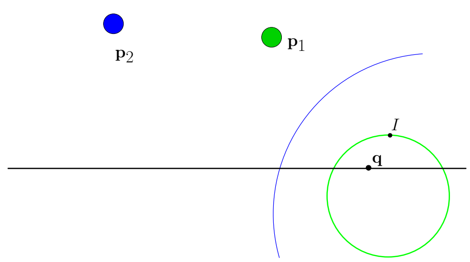

(a) This figure illustrates $\mathbf{q} \in \mathcal{V}_1$. The optimal strategies with respect to the vertical distance as the cost is for the target at $\mathbf{q}$ and the vehicle $\mathbf{p}_1$ to move towards I. Vehicle $\mathbf{p}_2$ need not move.

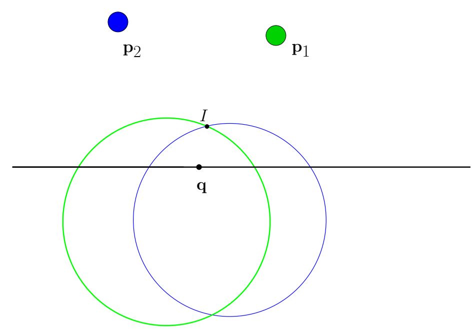

(b) This figure illustrates $\mathbf{q} \in \mathcal{V}_{1,2}$. The optimal strategies with respect to the vertical distance as the cost is for the target at $\mathbf{q}$ and both the vehicles to move towards I.

Figure 6.11. The partition of the generator for catching an adversarial target.

other words, the optimal pursuer strategy is to move pursuer $\mathbf{p}_i$ as per the constant bearing control if the target is in $\mathcal{V}_i$, for some $i \in \{1, 2\}$, and to move both pursuers if the target is in $\mathcal{V}_{1,2}$. Therefore, the average cost $C_{\text{exp}}(\mathbf{p}_1, \mathbf{p}_2)$, such as the intercept time or the vertical distance can be written as

$$C_{\text{exp}} = \sum_{i=1}^{2} \int_{\mathcal{V}_i} C(\mathbf{p}_i, x)\phi(x)dx + \int_{\mathcal{V}_{1,2}} C(\mathbf{p}_1, \mathbf{p}_2, x)\phi(x)dx. \tag{6.10}$$

The main difference between equation (6.10) and equation (6.8) is the extra term $C(\mathbf{p}_1, \mathbf{p}_2, x)$. The gradient of the first term in equation (6.10) is similar to that in Lemma 6.4.6. However, the second term $C(\mathbf{p}_1, \mathbf{p}_2, x)$ is difficult to characterize in the form of an analytical expression. The complexity of the calculation of terms such as $C(\mathbf{p}_1, \mathbf{p}_2, x)$ is expected to increase considerably as the number of vehicles is increased. Thus, the problem with adversarial targets involving multiple vehicles is presently open, and is a challenging future direction.

Summary

We addressed the problem of optimally placing vehicles having simple motion in order to intercept a mobile target that arrives stochastically on a line segment. The optimality of a vehicle placement is measured through a cost function, associated with intercepting the target. For the single vehicle case, we determined optimal placements when target motion was either constrained, i.e., with fixed speed and direction, or adversarial. The cost functions considered were the vertical distance from the line and the intercept time. For all the cases, we showed that the associated cost function is convex, sufficiently smooth and has a unique global minima, which the vehicle can reach by using a gradient-based optimization technique. For the multiple vehicle scenario and with constrained motion targets, we presented a partition and gradient based algorithm that takes the vehicles asymptotically to a set of critical locations of the cost function.

Acknowledgments: The authors would like to thank Prof. Jorge Cortés from University of California, San Diego for insightful discussions that lead to the proof of Lemma 6.3.3.

Algorithm 5: Pairwise dominance region

Assumes: Distinct $\mathbf{p}_i = (X_i, Y_i)$, $\mathbf{p}_j = (X_j, Y_j)$.

if $Y_i = Y_j$, **then**

$$U_{ij} := \begin{cases} [0, (X_i + X_j)/2], & \text{if } X_i < X_j \\ [(X_i + X_j)/2, W], & \text{if } X_i > X_j \end{cases}$$

else

$\theta := \arctan_2(Y_i - Y_j, X_i - X_j) + \pi/2$

$\ell_{1,2} :=$ two roots of $0 = 4(\sin^2(\theta) - v^2)\ell^2$

$+4(Y_i + Y_j)\sin(\theta)\ell + (Y_i + Y_j)^2 - v^2\|\mathbf{p}_i - \mathbf{p}_j\|^2$

$y_{1,2} := (Y_i + Y_j)/2 + \sin(\theta)\ell_{1,2}$

if $y_1 > 0$ and $y_2 > 0$ **then**

$x_{1,2} := (X_i + X_j)/2 + \cos(\theta)\ell_{1,2}$

$$U_{ij} := \begin{cases} [0, W] \cap [x_1, x_2], & \text{if } Y_i < Y_j \\ [0, W] \setminus]x_1, x_2[, & \text{if } Y_i \geq Y_j. \end{cases}$$

else

$k :=$ index in $\{1, 2\}$ for which $y_k > 0$

$x := (X_i + X_j)/2 + \ell_k \cos(\theta)$

$$U_{ij} := \begin{cases} [0, W] \cap]-\infty, x], & \text{if } X_i < X_j \\ [0, W] \cap [x, +\infty[, & \text{if } X_i \geq X_j \end{cases}$$

Chapter 7

Conclusions and Future Directions

We have addressed pursuit strategies for (i) a single adversarial target, and (ii) multiple, sequentially-arriving translating targets. For an adversarially moving target and under various constraints on sensing and motion, we gave sufficient conditions on parameters in every problem for which our strategies were provably effective. For multiple, sequentially arriving translating targets, our strategies were also provably efficient in terms of being close to fundamental limits of performance.

This thesis has focussed upon problem formulations that assume no noise in the measurements or in the motion of the players. It is essential to know that under ideal conditions, what strategies turn out to be effective and efficient. However, uncertainties are part of every physical system and therefore need to be accounted for in the analysis. For some problems, we have provided simulation-based studies for certain commonly observed sensor noise models. To provide analytical rigor would be an interesting direction of research. It is possible to extend the analysis for some problems under assumptions such as *bounded-but-unknown* noise, which would be a part of short term future goals.

Specifically, the following are detailed short-term future goals for the various problems addressed in this thesis.

1. For pursuit under sensing limitations, it would be worthwhile to provide a better upper bound on the time complexity of both the single as well as the multiple pursuer problems. The effects of communication losses or errors in the multiple pursuer problem, seem a promising direction. Another interesting direction would be to consider alternate sensing models such as probabilistic detection, or sensors with false alarms for the players.

2. For pursuit with minimalist sensing, the Grow-Intersect idea might prove to be an effective tool to solve the continuous-time problem of pursuit with only distance measurements. Simulation results definitely provide a positive indication.

3. For pursuit with motion constraints, it would be of interest to design decentralized pursuit strategies in which all pursuer play identical roles. Also of interest would be the optimal number of pursuers for such strategies.

4. For pursuing multiple and sequentially arriving translating targets, an interesting future direction is to have on-site service times for the demands. For the case in which the on-site service times are independent and identically distributed with a known expected value, and the vehicle is permitted to move with the demand upon reaching it, the results in this chapter could be extended using similar analysis. More recently, in [90], we have addressed a version of the present problem in which the goal for the vehicle is to maximize the fraction of demands served before they reach a deadline, which is at a given distance from the generator.

5. The placement problem for multiple pursuers to reach translating targets is a natural extension of the previous problem. Variations of this problem such as allowing the target to pick a direction and move, or actively evader a pursuer are within the scope of short-term future goals.

As part of long term goals, we envision addressing the general problem of pursuing multiple, sequentially arriving targets that have partially predictable motion. Akin to the approach presented in [62], we propose an heirarchical structure that comprises of (i) solving a dynamically changing combinatorial assignment problem at a higher level, and (ii) utilization of our set of pursuit strategies for engagement at the lower level. The partial predictability in the motion of the targets can be exploited to improve the solutions at both levels. The spatial arrival distribution of the targets may not be known and thus, there needs to be a phase in which the pursuers learn this distribution. This would lead to the fusion of tools from learning theory to this heirarchical control structure.

Bibliography

[1] M. Adler, H. Räcke, N. Sivadasan, C. Sohler, and B. Vöcking. Randomized pursuit-evasion in graphs. *Combinatorics, Probability and Computing*, 12:225–244, 2003.

[2] M. Aigner and M. Fromme. A game of cops and robbers. *Discrete Applied Mathematics*, 8:1–12, 1984.

[3] S. Alexander, R. Bishop, and R. Ghrist. Pursuit and evasion in non-convex domains of arbitrary dimension. In G. S. Sukhatme, S. Schaal, W. Burgard, and D. Fox, editors, *Robotics: Science and Systems II (Philadelphia PA)*. MIT Press, 2007.

[4] S. Alexander, R. Bishop, and R. Ghrist. Capture pursuit games on unbounded domains. *L'Enseignement Mathématique*, 55:127–137, 2009.

[5] L. Alonso, A. S. Goldstein, and E. M. Reingold. Lion and Man: Upper and lower bounds. *ORSA Journal of Computing*, 4(4):447–452, 1992.

[6] S. Alpern and S. Gal. *The theory of search games and rendezvous*, volume 55 of *International Series in Operations Research and Management*. Springer, 2003.

[7] Y. Asahiro, E. Miyano, and S. Shimoirisa. Grasp and delivery for moving objects on broken lines. *Theory of Computing Systems*, 42(3):289–305, 2008.

[8] T. Başar and G. J. Olsder. *Dynamic Noncooperative Game Theory*. SIAM, 2 edition, 1999.

[9] R. W. Beard, G. N. Saridis, and J. T. Wen. Approximate solutions to the time-invariant Hamilton-Jacobi-Bellman equation. *Journal of Optimization Theory & Applications*, 96(3):589–626, March 1998.

[10] J. Beardwood, J. Halton, and J. Hammersly. The shortest path through many points. In *Proceedings of the Cambridge Philosophy Society*, volume 55, pages 299–327, 1959.

[11] F. Belkhouche, B. Belkhouche, and P. Rastgoufard. Multi-robot hunting behavior. In *IEEE Int. Conference on Systems, Man and Cybernetics*, pages 2299–2304, Waikoloa, HI, October 2005.

[12] K. J. Benoit-Bird and W. W. L. Au. Cooperative prey herding by the pelagic dolphin, stenella longirostris. *Journal of Acoustical Society of America*, pages 125–137, January 2009.

[13] D. J. Bertsimas and G. J. van Ryzin. A stochastic and dynamic vehicle routing problem in the Euclidean plane. *Operations Research*, 39:601–615, 1991.

[14] D. J. Bertsimas and G. J. van Ryzin. Stochastic and dynamic vehicle routing in the Euclidean plane with multiple capacitated vehicles. *Operations Research*, 41(1):60–76, 1993.

[15] S. Bhattacharya, S. Hutchinson, and T. Basar. Game-theoretic analysis of a visibility-based pursuit-evasion game in presence of obstacles. In *American Control Conference*, pages 373–378, St. Louis, MO, USA, June 2009.

[16] S. D. Bopardikar, F. Bullo, and J. P. Hespanha. A cooperative Homicidal Chauffeur game. In *IEEE Conf. on Decision and Control*, pages 4857–4862, New Orleans, LA, December 2007.

[17] S. D. Bopardikar, F. Bullo, and J. P. Hespanha. Cooperative pursuit with sensing limitations. In *American Control Conference*, pages 5394–5399, New York, July 2007.

[18] S. D. Bopardikar, F. Bullo, and J. P. Hespanha. Sensing limitations in the Lion and Man problem. In *American Control Conference*, pages 5958–5963, New York, July 2007.

[19] S. D. Bopardikar, F. Bullo, and J. P. Hespanha. On discrete-time pursuit-evasion games with sensing limitations. *IEEE Transactions on Robotics*, 24(6):1429–1439, 2008.

[20] S. D. Bopardikar, F. Bullo, and J. P. Hespanha. A pursuit game with range-only measurements. In *IEEE Conf. on Decision and Control*, pages 4233–4238, Cancún, México, December 2008.

[21] S. D. Bopardikar, F. Bullo, and J. P. Hespanha. A cooperative Homicidal Chauffeur game. *Automatica*, 45(7):1771–1777, 2009.

[22] S. D. Bopardikar, S. L. Smith, and F. Bullo. Vehicle placement to intercept moving targets. In *American Control Conference*, Baltimore, MD, June 2010. Submitted.

[23] S. D. Bopardikar, S. L. Smith, F. Bullo, and J. P. Hespanha. Dynamic vehicle routing with moving demands – Part I: Low speed demands and high arrival rates. In *American Control Conference*, pages 1454–1459, St. Louis, MO, June 2009.

[24] S. D. Bopardikar, S. L. Smith, F. Bullo, and J. P. Hespanha. Dynamic vehicle routing for translating demands: Stability analysis and receding-horizon policies. *IEEE Transactions on Automatic Control*, January 2010. (Submitted, Mar 2009) to appear.

[25] S. Boyd and L. Vandenberghe. *Convex Optimization*. Cambridge University Press, 2004.

[26] F. Bullo, J. Cortés, and S. Martínez. *Distributed Control of Robotic Networks*. Applied Mathematics Series. Princeton University Press, 2009. Available at http://www.coordinationbook.info.

[27] Z. Cao, M. Tan, L. Li, N. Gu, and S. Wang. Cooperative hunting by distributed mobile robots based on local interaction. *IEEE Transactions on Robotics*, 22(2):403–407, 2006.

[28] T. Caraco and L. L. Wolf. Ecological determinants of group sizes of foraging lions. *The American Naturalist*, 109(967):343–352, May-June 1975.

[29] P. Chalasani and R. Motwani. Approximating capacitated routing and delivery problems. *SIAM Journal on Computing*, 28(6):2133–2149, 1999.

[30] C. F. Chung. *Reachable sets analysis in the cooperative control of pursuer vehicles*. PhD thesis, University of New South Wales, 2008.

[31] J. Cortés, S. Martínez, T. Karatas, and F. Bullo. Coverage control for mobile sensing networks. *IEEE Transactions on Robotics and Automation*, 20(2):243–255, 2004.

[32] C. Detweiler, J. Leonard, D. Rus, and S. Teller. Passive mobile robot localization within a fixed beacon field. In *Workshop on Algorithmic Foundations of Robotics*, New York, July 2006.

[33] Z. Drezner, editor. *Facility Location: A Survey of Applications and Methods*. Series in Operations Research. Springer, 1995.

[34] L. E. Dubins. On curves of minimal length with a constraint on average curva-

ture and with prescribed initial and terminal positions and tangents. *American Journal of Mathematics*, 79:497–516, 1957.

[35] S. P. Fekete, J. S. B. Mitchell, and K. Beurer. On the continuous Fermat–Weber problem. *Operations Research*, 53(1):61 – 76, 2005.

[36] L. Few. The shortest path and the shortest road through n points in a region. *Mathematika*, 2:141–144, 1955.

[37] Y. Gabriely and E. Rimon. Spanning-tree based coverage of continuous areas by a mobile robot. *Annals of Mathematics and Artificial Intelligence*, 31(1-4):77–98, 2001.

[38] S. K. Gazda, R. C. Connor, R. K. Edgar, and F. Cox. A division of labour with role specialization in group-hunting bottlenose dolphins (Tursiops truncatus) off Cedar Key, Florida. *Journal of the Royal Statistical Society. B: Biological Sciences*, 272(1559):135–140, 2005.

[39] B. P. Gerkey, S. Thrun, and G. Gordon. Visibility-based pursuit-evasion with limited field of view. In *National Conference on Artificial Intelligence*, pages 20–27, San Jose, CA, July 2004.

[40] B. P. Gerkey, S. Thrun, and G. Gordon. Visibility-based pursuit-evasion with limited field of view. *International Journal of Robotics Research*, 25(4):299–315, 2006.

[41] W. M. Getz and M. Pachter. Two-target pursuit-evasion differential games in the plane. *Journal of Optimization Theory & Applications*, 34(3):383–403, 1981.

[42] V. Y. Glizer. Homicidal chauffeur game with target set in the shape of a circular angular sector: Conditions for existence of a closed barrier. *Journal of Optimization Theory & Applications*, 101(3):581–598, 1999.

[43] D. Griffiths. Foraging costs and relative prey size. *The American Naturalist*, 116(5):743–752, 1980.

[44] L. Grüne. An adaptive grid scheme for the discrete Hamilton-Jacobi-Bellman equation. *Numerische Mathematik*, 75(3):319–327, January 1997.

[45] M. Guelman. A qualitative study of proportional navigation. *IEEE Transactions on Aerospace and Electronic Systems*, 7(4):637–643, 1971.

[46] L. J. Guibas, J. C. Latombe, S. M. LaValle, D. Lin, and R. Motwani. A visibility-based pursuit-evasion problem. *International Journal of Computational Geometry & Applications*, 9(4-5):471–493, 1999.

[47] M. Hammar and B. J. Nilsson. Approximation results for kinetic variants of TSP. *Discrete and Computational Geometry*, 27(4):635–651, 2002.

[48] C. S. Helvig, G. Robins, and A. Zelikovsky. The moving-target traveling salesman problem. *Journal of Algorithms*, 49(1):153–174, 2003.

[49] J. P. Hespanha, H. J. Kim, and S. S. Sastry. Multiple-agent probabilistic pursuit-evasion games. Technical report, Electrical Engineering and Computer Science, University of California at Berkeley, August 1999. Available at `http://www.ece.ucsb.edu/ hespanha/published`.

[50] Y. Ho, A. E. Bryson, and S. Baron. Differential games and optimal pursuit-evasion strategies. *IEEE Transactions on Automatic Control*, 10(4):385–389, 1965.

[51] R. Isaacs. *Differential Games*. Wiley, 1965.

[52] V. Isler, S. Kannan, and S. Khanna. Randomized pursuit-evasion in a polygonal environment. *IEEE Transactions on Robotics*, 5(21):875–884, 2005.

[53] V. Isler, S. Kannan, and S. Khanna. Randomized pursuit-evasion with local visibility. *SIAM Journal on Discrete Mathematics*, 1(20):26–41, 2006.

[54] N. Karnad and V. Isler. Bearing-only pursuit. In *IEEE Int. Conf. on Robotics and Automation*, pages 2665–2670, Pasadena, CA, USA, May 2008.

[55] T. Kim and T. Sugie. Cooperative control for target-capturing task based on cyclic pursuit strategy. *Automatica*, 43(8):1426–1431, 2007.

[56] L. Kleinrock. *Queueing Systems. Volume I: Theory*. Wiley, 1975.

[57] S. Kopparty and C. V. Ravishankar. A framework for pursuit evasion games in $\mathbb{R}^n$. *Information Processing Letters*, 96(3):114–122, 2005.

[58] B. Korte and J. Vygen. *Combinatorial Optimization: Theory and Algorithms*, volume 21 of *Algorithmics and Combinatorics*. Springer, 3 edition, 2005.

[59] V. M. Kuntsevic and A. V. Kuntsevich. Optimal control over the approach of conflicting moving objects under uncertainty. *Cybernetics and Systems Analysis*, 38(2):230–237, 2002.

[60] A. Kwok and S. Martínez. A coverage algorithm for drifters in a river environment. In *American Control Conference*, Baltimore, MD, USA, 2010. Submitted.

[61] S. M. LaValle and J. Hinrichsen. Visibility-based pursuit-evasion: The case of curved environments. *IEEE Transactions on Robotics and Automation*, 17(2):196–201, 2001.

[62] D. Li. *Multi-player pursuit-evasion differential games*. PhD thesis, Ohio State University, 2006.

[63] S.-H. Lim, T. Furukawa, G. Dissanayake, and H. F. Durrant-Whyte. A time-optimal control strategy for pursuit-evasion games problems. In *IEEE Int. Conf. on Robotics and Automation*, pages 3962–3967, New Orleans, LA, April 2004.

[64] J. E. Littlewood. *Littlewood's Miscellany.* Cambridge University Press, 1986.

[65] T. G. McGee and J. K. Hedrick. Guaranteed strategies to search for mobile evaders in the plane. In *American Control Conference*, pages 2819–2824, Minneapolis, MN, June 2006.

[66] T. W. McLain, P. R. Chandler, S. Rasmussen, and M. Pachter. Cooperative control of UAV rendezvous. In *American Control Conference*, pages 2309–2314, Arlington, VA, June 2001.

[67] N. Megiddo and K. J. Supowit. On the complexity of some common geometric location problems. *SIAM Journal on Computing*, 13(1):182–196, 1984.

[68] I. Mitchell and C. J. Tomlin. Overapproximating reachable sets by Hamilton-Jacobi projections. *Journal of Scienfic Computing*, 19(1-3):323–346, 2003.

[69] J. N. Newman. Approximations for the Bessel and Struve functions. *Mathematics of Computation*, 43(168):551–556, 1984.

[70] A. Okabe, B. Boots, K. Sugihara, and S. N. Chiu. *Spatial Tessellations: Concepts and Applications of Voronoi Diagrams.* Wiley Series in Probability and Statistics. Wiley, 2 edition, 2000.

[71] M. Pachter. Simple motion pursuit-evasion in the half-plane. *Computers and Mathematics with Applications*, 13(1-3):69–82, 1987.

[72] M. Pachter. Simple motion pursuit-evasion differential games. In *Mediterranean Conf. on Control and Automation*, Lisbon, Portugal, July 2002. Electronic Proceedings.

[73] M. Pachter and Y. Yavin. A stochastic homicidal chauffeur pursuit-evasion differential game. *Journal of Optimization Theory & Applications*, 34(3):405–424, 1981.

[74] C. Packer and L. Ruttan. The evolution of cooperative hunting. *The American Naturalist*, 132(2):159–198, 1988.

[75] J. D. Papastavrou. A stochastic and dynamic routing policy using branching processes with state dependent immigration. *European Journal of Operational Research*, 95:167–177, 1996.

[76] T. D. Parsons. Pursuit-evasion in a graph. In Y. Alavi and D. Lick, editors, *Theory and Applications of Graphs*, volume 642 of *Lecture Notes in Mathematics*, pages 426–441. Springer, 1978.

[77] B. L. Partridge and T. J. Pitcher. The sensory basis of fish schools: Relative roles of lateral line and vision. *Journal of Comparative Physiology A*, 135(4):315–325, 1980.

[78] M. Pavone, N. Bisnik, E. Frazzoli, and V. Isler. A stochastic and dynamic vehicle routing problem with time windows and customer impatience. *ACM/Springer Journal of Mobile Networks and Applications*, 14(3):350–364, 2009.

[79] M. Pavone, E. Frazzoli, and F. Bullo. Distributed policies for equitable partitioning: Theory and applications. In *IEEE Conf. on Decision and Control*, pages 4191–4197, Cancún, México, December 2008.

[80] A. G. Percus and O. C. Martin. Finite size and dimensional dependence of the Euclidean traveling salesman problem. *Physical Review Letters*, 76(8):1188–1191, 1996.

[81] R. L. Pitman, S. O'Sullivan, and B. Mase. Killer whales (Ornicus orca) attack a school of pantropical spotted dolphins (Stenella attenuata) in Gulf of Mexico. *Aquatic Mammals*, 29(3):321–324, 2003.

[82] M. M. Polycarpou, Y. Yang, and K. M. Passino. A cooperative search framework

for distributed agents. In *IEEE Int. Symposium on Intelligent Control*, pages 1–6, Mexico City, Mexico, September 2001.

[83] B. N. Pshenichnyi. Special pursuit and evasion problem with incomplete information. *Cybernetics and Systems Analysis*, 31(2):246–251, 1995.

[84] G. Rote. Pursuit-evasion with imprecise target location. In *ACM-SIAM Symposium on Discrete Algorithms*, pages 747–753, Baltimore, MA, January 2003.

[85] H. Ruser, A. V. Jena, V. Mágori, and H. R. Tränkler. A low cost ultrasonic microwave multisensor for robust sensing of velocity and range. In *Proceedings of Sensor '99*, Nürnberg, May 1999.

[86] M. Schwager, J. McLurkin, and D. Rus. Distributed coverage control with sensory feedback for networked robots. In Burgard Sukhatme, Schaal and Fox, editors, *Robotics Science and Systems*, pages 49–56, Philadelphia, PA, 2006.

[87] F. C. Schweppe. Recursive state estimation: Unknown but bounded errors and system inputs. *IEEE Transactions on Automatic Control*, 13(1):22–28, 1968.

[88] J. Sgall. A solution of David Gale's lion and man problem. *Theoretical Computational Science*, 259((1-2)):663–670, 2001.

[89] I. Shevchenko. Successive pursuit with a bounded detection domain. *Journal of Optimization Theory & Applications*, 95(1):25–48, 1997.

[90] S. L. Smith, S. D. Bopardikar, and F. Bullo. A dynamic boundary guarding problem with translating demands. In *IEEE Conf. on Decision and Control*, pages 8543–8548, Shanghai, China, December 2009.

[91] S. L. Smith, S. D. Bopardikar, F. Bullo, and J. P. Hespanha. Dynamic vehicle routing with moving demands – Part II: High speed demands or low arrival

rates. In *American Control Conference*, pages 1466–1471, St. Louis, MO, June 2009.

[92] S. L. Smith and F. Bullo. The dynamic team forming problem: Throughput and delay for unbiased policies. *Systems & Control Letters*, 58(10-11):709–715, 2009.

[93] S. L. Smith, M. Pavone, F. Bullo, and E. Frazzoli. Dynamic vehicle routing with priority classes of stochastic demands. *SIAM Journal on Control and Optimization*, 2009. (submitted Feb 2009) to appear.

[94] T. L. Song. Observability of target tracking with range-only measurements. *IEEE Journal of Ocean Engineering*, 24(3):383–387, 1999.

[95] L. D. Stone. *Theory of Optimal Search*. Operations Research Society of America, 1975.

[96] S. Suri, E. Vicari, and P. Widmayer. Simple robots with minimal sensing: From local visibility to global geometry. *International Journal of Robotics Research*, 27(9):1055–1067, 2008.

[97] I. Suzuki and M. Yamashita. Searching for a mobile intruder in a polygonal region. *SIAM Journal on Computing*, 21(5):863–888, 1992.

[98] I. Suzuki and P. Żyliński. Capturing an evader in a building: Randomized and deterministic algorithms for mobile robots. *IEEE Robotics and Automation magazine*, 15(2):16–26, 2008.

[99] Z. Tang and Ü. Özgüner. On non-escape search for a moving target by multiple mobile sensor agents. In *American Control Conference*, pages 3525–3530, Minneapolis, MN, June 2006.

[100] R. Vidal, O. Shakernia, H. Kim, D. H. Shim, and S. Sastry. Probabilistic pursuit-evasion games: Theory, implementation and experimental evaluation. *IEEE Transactions on Robotics and Automation*, 18(2):662–669, 2002.

[101] R. E. Walpole, R. H. Myers, and S. L. Myers. *Probability and Statistics for Engineers and Scientists*. Prentice Hall, New Jersey, USA, sixth edition, 1998.

[102] A. Yershova, B. Tovar, R. Ghrist, and S. M. LaValle. Bitbots: Simple robots solving complex tasks. In *AIAA Conference on Artifical Intelligence*, pages 1336–1341, Pittsburgh, PA, USA, 2005.

[103] E. Zemel. Probabilistic analysis of geometric location problems. *SIAM Journal on Algebraic and Discrete Methods*, 6(2):189–200, 1984.

[104] K. X. Zhou and S. I. Roumeliotis. Optimal motion strategies for range-only distributed target tracking. In *American Control Conference*, pages 5195–5200, Minneapolis, MN, June 2006.